SYNTHESIS AND CHARACTERIZATION OF NOVEL D-π-A TYPE ORGANIC DYES

PALITA KOCHPRADIST

A THESIS SUBMITTED IN PARTIAL FULFILLMENT OF THE REQUIREMENTS FOR

THE DEGREE OF DOCTOR OF PHILOSOPHY

MAJOR IN CHEMISTRY

FACULTY OF SCIENCE

UBON RATCHATHANI UNIVERSITY

YEAR 2013

THESIS APPROVAL

UBON RATCHATHANI UNIVERSITY

DOCTOR OF PHILOSOPHY

MAJOR IN CHEMISTRY FACULTY OF SCIENCE

TITLE SYNTHESIS AND CHARACTERIZATION OF NOVEL D-π -A TYPE ORGANIC DYES

NAME MS.PALITA KOCHPRADIST

THIS THESIS HAS BEEN ACCEPTED BY

..... CHAIR

(DR.TINNAGON KEAWIN)

..... COMMITTEE

(ASST.PROF.DR.BOOSAYARAT TOMAPATANAGET)

..... COMMITTEE

(ASSOC.PROF.DR.VINICH PROMARAK)

..... COMMITTEE

(ASST.PROF.DR.TAWEESAK SUDYOADSUK)

..... DEAN

(ASST.PROF.DR.JANPEN INTARAPRASERT)

APPROVAL BY UBON RATCHATHANI UNIVERSITY

.....

(ASSOC.PROF.DR.UTITH INPRASIT)

VICE PRESIDENT FOR ACADEMIC AFFAIRS

FOR THE PRESIDENT OF UBON RATCHATHANI UNIVERSITY

ACADEMIC YEAR 2013

ACKNOWLEDGMENTS

I wish to express my admiration and appreciation to Assoc.Prof.Dr.Vinich Promarak and Dr.Tinnagon Keawin, my advisor, for his excellent suggestions, supervision, and understanding throughout my study.

I would also like to thank the many people who contributed their time, instrumentation, and advice to my project. In particular, Asst.Prof.Dr.Taweesak Sudyoadsuk for devices, Asst.Prof.Dr.Siriporn Jungsuttiwong for molecular orbital calculation, Assoc.Prof.Dr.Sayant Saengsuwan for TGA and DSC data. Moreover, I would like to thank all of the staff at the Center of Scientific and Technological Equipment at Suranaree University of Technology for their excellent service and helpful suggestions for use of UV-Vis, Fluorescence, IR, NMR, MALDI-TOF, TGA and DSC techniques.

I wish to acknowledge Asst.Prof.Dr.Boosayarat Tomapatanaget for constructive comments and suggestion.

Thanks so much to Center of Excellence for Innovation in Chemistry (PERCH-CIC), Ubon Ratchathani University, Precise Green Technology & Service Co., Ltd. and Science Park Ubon Ratchathani University for financial support. Gratitude is expressed to all my teachers for showing me a different line in life, as a Chemistry graduate student. My sincere thankful is also express to the Department of Chemistry and Excellent Center for Innovation in Chemistry, Faculty of Science, Ubon Ratchathani University for providing a wonderful academic environment during the course work.

My appreciation is extended to all the staff of the Department of Chemistry. Furthermore, I feel thankful to my friends, sisters, brothers here in Center for Organic Electronic and Alternative Energy.

Most of all, I feel appreciate and grateful to my beloved family for their inculcation and encouragement that found me to be a fortitude person.

Palita Kochpradist

(Miss Palita Kochpradist)

Researcher

บทคัดย่อ

ชื่อเรื่อง : การสังเคราะห์และพิสูจน์เอกลักษณ์ของโมเลกุลสีย้อมไวแสงอินทรีย์แบบ D-π-A ชนิดใหม่

โดย : ปาลิดา คชประดิษฐ์

ชื่อปริญญา : ปรัชญาดุษฎีบัณฑิต

สาขาวิชา : เคมี

ประธานกรรมการที่ปรึกษา : ดร.พินกร แก้วอินทร์

ศัพท์สำคัญ : หมู่ให้ หมู่รับ ไพ-คอนจูเกต เซลล์แสงอาทิตย์ชนิดสีย้อมไวแสง ไดโอดเรืองแสงสารอินทรีย์ อุปกรณ์ออปโตอิเล็กทรอนิก

ในงานวิจัยนี้รายงานการสังเคราะห์และพิสูจน์เอกลักษณ์ของสารอินทรีย์ที่ประกอบด้วยหมู่ให้อิเล็กตรอน ไพ-คอนจูเกต และหมู่รับอิเล็กตรอน (D-π-A) ชนิดใหม่ โดยสามารถสังเคราะห์สารอินทรีย์ D-π-A ชนิดใหม่ (1-20) ซึ่งมีหมู่ให้อิเล็คตรอน และหมู่เชื่อมโยงที่แตกต่างกัน เพื่อใช้เป็นสีย้อมไวแสงในเซลล์แสงอาทิตย์ชนิดสีย้อมไวแสง (DSCs) ซึ่งโมเลกุลเป้าหมายที่สังเคราะห์ได้พิสูจน์เอกลักษณ์โดยใช้เทคนิค ^{1}H-NMR ^{13}C-NMR FT-IR และ MALDI-TOF MS เมื่อศึกษาสมบัติทางแสงด้วยเทคนิคยูวีและวิสิบิลสเปคโตรสโคปีพบว่า โมเลกุลที่ออกแบบไว้ดูดกลืนแสงในช่วงความยาวคลื่นแสงของยูวีและวิสิเบิล และยังพบว่าโมเลกุลสารเป้าหมายมีความเสถียรทางความร้อนด้วย นอกจากนี้ยังได้นำสีย้อมที่ออกแบบไว้ไปคำนวณด้วยทฤษฎีฟังก์ชันความหนาแน่น (DFT) พบว่าเกิดการกระจายของอิเล็กตรอนจากหมู่ให้อิเล็กตรอนไปยังหมู่รับอิเล็กตรอนระหว่างการกระตุ้น HOMO-LUMO ส่วนการพิสูจน์ประสิทธิภาพทางโฟโตโวลตาอิกของเซลล์แสงอาทิตย์ชนิดสีย้อมไวแสงเมื่อใช้โมเลกุลที่ออกแบบไว้เป็นสีย้อมจะรายงานต่อไปในอนาคต สุดท้ายนี้ในงานวิจัยยังได้สังเคราะห์และพิสูจน์เอกลักษณ์คาร์บาโซลที่มีหมู่แทนที่เป็นไตรฟีนิลเอมีนที่หลากหลาย (T2C T3C และ T4C) สำหรับใช้เป็นชั้นสารส่งผ่านประจุบวกในไดโอดเรืองแสงอินทรีย์ (OLEDs) โดยพบว่าเมื่อเพิ่มจำนวนของหมู่แทนที่ไตรฟีนิลเอมีนเข้าไปในโมเลกุล ทำให้โมเลกุลมีความเสถียรทางความร้อน ทางไฟฟ้าเคมี และมีความเป็นอสัณฐานเพิ่มขึ้น และยังพบว่าสาร T2C T3C และ T4C มีคุณสมบัติการส่งผ่านประจุบวกที่ดีสำหรับไดโอดเรืองแสงอินทรีย์สีเขียวที่ใช้ Alq3 ซึ่งได้รับประสิทธิภาพในการเรืองแสงอยู่ในช่วง 4.97-5.07 cd/A

ABSTRACT

TITLE : SYNTHESIS AND CHARACTERIZATION OF NOVEL D-π-A TYPE ORGANIC DYES

BY : PALITA KOCHPRADIST

DEGREE : DOCTOR OF PHILOSOPHY

MAJOR : CHEMISTRY

CHAIR : TINNAGON KEAWIN, Ph.D.

KEYWORDS : DONOR / ACCEPTOR / π-CONJUGATE / DYE SOLAR CELLS / ORGANIC LIGHT-EMITTING DIODES / OPTOELECTRONIC DEVICES

This thesis deals with synthesis and characterization of novel donor π-conjugated acceptor (D-π-A) organic materials. Novel D-π-A organic materials (**1-20**) containing different donor and linker units for using as dye molecules in dye solar cells (DSCs) were successfully synthesized. The target molecules were characterized by ^{1}H-NMR, ^{13}C-NMR, FT-IR, and MALDI-TOF MS techniques. The optical study by UV-Vis spectroscopy indicated that designed molecules exhibit an adsorption band cover UV and visible region. All compounds show good thermal properties. Moreover, Density functional theory (DFT) calculations have been performed on the dyes and the results show that electron distribution from the electron donors to the electron acceptors occurred during the HOMO-LUMO excitation. The photovoltaic performance of DSCs using these materials as dyes is under investigation and will be reported in the future. Finally, the multi-triphenylamine-substituted carbazoles (**T2C**, **T3C** and **T4C**) for using as hole-transporting layer in organic light-emitting diodes (OLEDs) were successfully synthesized and characterized. The thermal and electrochemical stability and formation of an amorphous form in the material was improved by increasing number of triphenylmine substituents in the molecule. **T2C**, **T3C** and **T4C** compounds show excellent hole-transporting property for Alq3-based green OLED with device's luminance efficiency in the range of 4.97-5.07 cd/A.

CONTENTS

CONTENTS (CONTINUED)

CONTENTS (CONTINUED)

CONTENTS (CONTINUED)

LIST OF TABLES

LIST OF FIGURES

LIST OF FIGURES (CONTINUED)

LIST OF FIGURES (CONTINUED)

LIST OF FIGURES (CONTINUED)

LIST OF FIGURES (CONTINUED)

LIST OF FIGURES (CONTINUED)

LIST OF ABBREVIATIONS

ABBREVIATION	FULL WORD
CH_2Cl_2	Dichloromethane
DCM	Dichloromethane
DMF	Dimethylformamide
EtOH	Ethanol
THF	Tetrahydrofuran
DMSO	Dimethylsulphoxide
KI	Potassium iodide
KIO_3	Potassium iodate
AcOH	Acetic acid
RT	Room temperature
d	Doublet
dd	Doublet of doublets
td	Triplet of doublets
ε	Molar absorption
eV	Electron volt
h	Hour/hours
HOMO	Highest occupied molecular orbital
LUMO	Lowest unoccupied molecular orbital
IPCE	Incident photon to current efficiency
η	Overall light-to-electric power conversion efficiency
ITO	Indium-tin oxide
FT-IR	Fourier transform Infrared
J	Coupling constant
M	Molar concentration
MHz	Megahertz
min	Minutes
μA	Microamperes

LIST OF ABBREVIATIONS (CONTINUED)

ABBREVIATION	FULL WORD
μm	Micrometers
mol	Moles
mmol	Milimoles
m	unresolved multiple
N	Normal concentration
nm	Nanometers
NMR	Nuclear magnetic resonance
δ	Chemical shift in ppm relative to tetramethylsilane
ppm	Parts per million
s	Singlet
t	Triplet
TLC	Thin-layer chromatography
UV	Ultra-violet
n-Bu_4NPF_6	Tetrabutylammonium hexafluorophosphate
TD-DFT	Time-dependent density functional theory
GBL	Gamma-butyrolactone
NMP	*N*-methyl-2-pyrrolidone
S^*	Excited dye
S^o	Original state
TiO_2	Titanium dioxide
AM1.5 G	Air Mass 1.5 Global
K	Kilo
W	Watt
V	Voltage (V)
s	second
I	Current (amp)
V_{oc}	Open circuit voltage

LIST OF ABBREVIATIONS (CONTINUED)

ABBREVIATION	FULL WORD
J_{sc}	Short circuit current
ff	Fill factor
J-V	Current density-voltage

CHAPTER 1

INTRODUCTION

1.1 Introduction

Donor π-conjugated acceptor (D-π-A) organic molecules are among the most important conjugated organic materials, and have attracted much academic and technological research interest [1]. In these compounds the electron-donating and electron-accepting groups are connected through a π-conjugated linker. Tuning different donor moiety or π-conjugated linker moiety in a D-π-A molecule would modify its physical and chemical properties. The molecules with D-π-A structures have attracted increasing attention since they can serve as electroactive and photoactive materials in molecular electronics, such as dye solar cells (DSCs) [2], organic light emitting diodes (OLEDs) [3], and etc [4].

1.2 Dye solar cells (DSCs)

The quality of human life is to a large extent dependent on the availability of energy sources. The present annual worldwide energy consumption has already reached a level of over 4×10^{18} *J* and is predicted to increase rapidly with the increasing world population and the rising demand of energy in the developing countries [5]. By meeting this energy demand with further depletion of fossil fuel reserves, the environmental damages followed by the enhanced green house effect, caused by the combustion of fossil fuels, could get out of hand. If, on other hand, this energy demand could be met by the use of renewable energy sources the environmental cost could be decreased. The sun could annually supply the earth with 3×10^{24} *J*, which is about 750000 times more than the global population currently consumes [6]. The dream to capture the sunlight and turn it into electric power or to generate chemical fuels, such as hydrogen, has in the last couple of decades become reality. Colloids and nanocrystalline films of several semiconductor systems have been employed in the direct conversion of solar energy into chemical or electrical energy [7]. The conventional photovoltaics, based on the solid-state junction devices, such as crystalline or amorphous silicon, has exceptional solar energy conversion to electricity

efficiencies of approximately 20%. [8]. However, the fabrication of these photovoltaics is expensive, using energy intensive high temperature and high vacuum processes. In 1991 O'Regan and Grätzel published a breakthrough of an alternative solar harvesting device, yielding a solar energy conversion to electricity of 7%, based on a mesoscopic inorganic semiconductor. Until then, an energy efficiency of 2.5% had been reached in this research field, in which a semiconductor surface such as TiO_2 or ZnO is sensitized with an optical absorbing chromophore with charge separation properties that can harvest the solar light and in its excited state inject electrons into the semiconductor [9].

1.2.1 Principle of DSCs

The DSCs, or the Grätzel cell, is a complex system where three different components, the semiconductor, the chromophore and the electrolyte are brought together to generate electric power from light without suffering any permanent chemical transformation (Figure 1.1) [10].

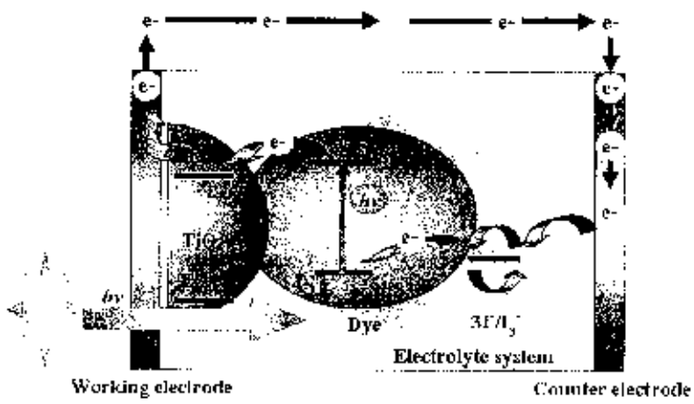

Figure 1.1 Schematic picture of the dye solar cells.

The nanocrystalline semiconductor is usually TiO_2, although alternative wide band gap oxides such as ZnO can be used. A monolayer of the chromophore, i.e. the sensitizer, is attached to the surface of the semiconductor. Photoexcitation of the chromophore results in the injection of an electron into the conduction band of the semiconductor (Figure 1.2). The chromophore is regenerated by the electrolyte, usually an organic solvent containing a redox

couple, such as iodide/triiodide. The electron donation to the chromophore by iodide is compensated by the reduction of triiodide at the counter electrode and the circuit is completed by electron migration through the external load. The overall voltage generated corresponds to the difference between the Fermi level of the semiconductor and the redox potential of the electrolyte.

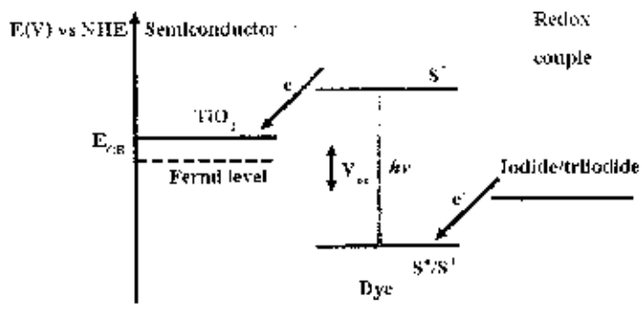

Figure 1.2 Schematic picture of the electron flow in the DSCs.

The performance of the solar cell can be quantified with parameters such as incident photon to current efficiency (IPCE), open circuit photovoltage (V_{oc}) and the overall efficiency of the photovoltaic cell (η_{cell}). The efficiency of the DSCs is related to a large number of parameters. This thesis will only focus on the development of efficient sensitizers and their synthesis, even so, it is important to have the general concepts in mind.

1.2.2 Overall efficiency of the photovoltaic cell (η_{cell})

The solar energy to electricity conversion efficiency under white-light irradiation (e.g., AM 1.5G) can be obtained from the following equation:

$$\eta_{cell} = \frac{J_{sc} \cdot V_{oc} \cdot ff}{I_0} \quad (1)$$

Where I_0 (mW/cm^2) is the photon flux (e.g., ca. 100 mW/cm^2 for AM 1.5 G), J_{sc} (mW/cm^2) is the short-circuit current density under irradiation, V_{oc} (V) is the open-circuit voltage, ff represents the cell fill factor. The fill factor is defined by the ratio of the current and the voltage at the maximum power point to the short circuit current and the open circuit voltage. The fill factor measures the squareness of the I-V curve (Figure 1.3).

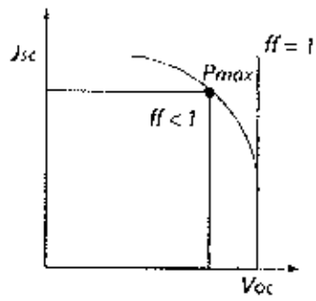

Figure 1.3 I-V curve.

1.2.3 Sensitizers

The efficiencies of the sensitizers are related to some basic criteria. The HOMO potential of the dye should be sufficiently positive compared to the electrolyte redox potential for efficient dye regeneration.10 The LUMO potential of the dye should be sufficiently negative to match the potential of the conduction band edge of the TiO_2 and the light absorption in the visible region should be efficient. However, by broadening the absorption spectra the difference in the potentials of the HOMO and the LUMO energy levels is decreased. If the HOMO and LUMO energy levels are too close in potential, the driving force for electron injection into the semiconductor or regeneration of the dye from the electrolyte could be hindered. The sensitizer should also exhibit small reorganization energy for excited- and ground-state redox processes, in order to minimize free energy losses in primary and secondary electron transfer steps [11].

1.2.3.1 Ruthenium sensitizers

Sensitizers of ruthenium complexes such as the N3, N719 and black dyes have been intensively investigated and show record solar energy-to-electricity conversion efficiencies (η) of 10, 11.2 and 10.8%, respectively (Figure 1.4) [12].

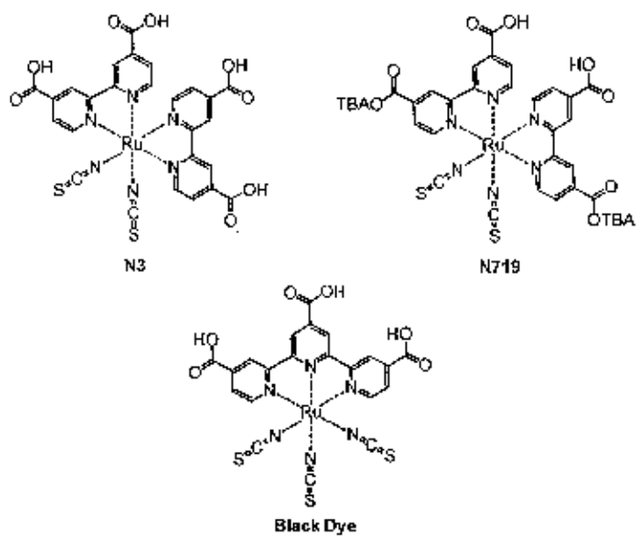

Figure 1.4 Chemical structures of **N3**, **N719** and black dyes.

A large number of different ruthenium based sensitizers have been investigated in order to improve the photovoltaic performance and stability of the DSCs. Amongst them especially four (**K19**, **K73**, **K77** and **Ru-1** [13]) have shown interesting properties in that they are competing in efficiency and have higher molar extinction coefficients than the three former. The enhanced absorption observed is expected from the extended conjugated system.

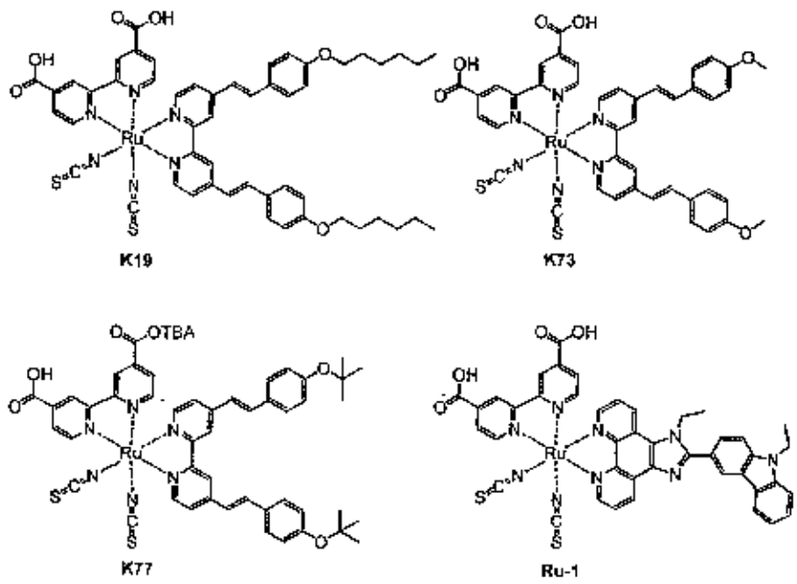

Figure 1.5 Chemical structures of **K19**, **K73**, **K77** and **Ru-1** dyes.

1.2.3.2 Organic sensitizers

Recently, performances of DSCs based on metal-free organic dyes have been remarkably improved by several groups. The first transient studies on a coumarin dye in DSCs was performed in 1996, when Gratzel et al. found injection rates of 200 fs from **C343** into the conduction band of TiO_2. Since **C343** has a narrow absorption spectrum, the conversion efficiency of this specific compound was low. By introduction of a methine unit, the π-system could be expanded and in 2001 a respectable efficiency of 5.6% was obtained with **NKX-2311** [14]. Adding more methine units (up to three) and introducing bulky substituents to prevent dye-aggregation could push the efficiency to 6.7% in 2005 **(NKX-2753)**. Currently other building blocks like thiophene are tested, which are believed to give a higher stability. First results of 7.4% for **NKX-2677** are encouraging [15].

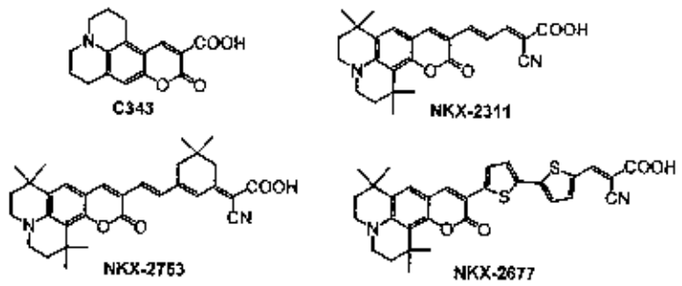

Figure 1.6 Chemical structures of **C343, NKX-2311, NKX-2753** and **NKX-2677** dyes

In 2003, an indoline dyes **(D102** and **D149)** discovered by Ito et al. These indoline dyes gave solar-to-electrical energy conversion efficiency of 6.1 and 9%, respectively, in full sunlight. A highest efficiency for organic dyes has been achieved by an indoline dye **(D149)** [16].

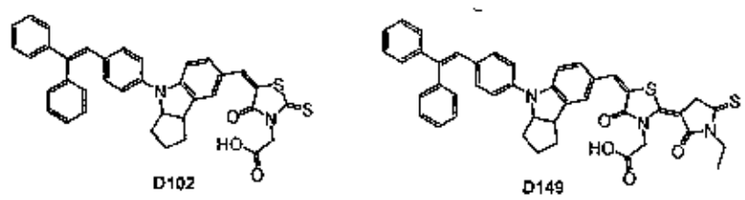

Figure 1.7 Chemical structures of **D102** and **D149** dyes.

In 2006, Nagatoshi Koumura et al. investigated that the organic dyes (**MK-1** and **MK-3**) containing carbazole as electron donor and cyanoacrylic acid as electron acceptor bridged by 4-hexylthiophene or thiophene units, gave an overall conversion efficiency (η) of 4.46-4.97% [17].

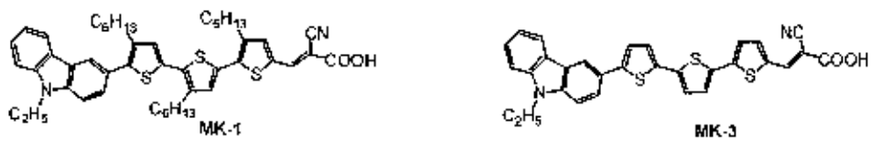

Figure 1.8 Chemical structures of **MK-1** and **MK-3** dyes.

In 2007, Duckhyun Kim et al. [18] investigated that the organic dyes (**JK-24**, **JK-25**, and **JK-28**) containing *N*-(9,9-dimethylfluoren-2-yl)carbazole or *N*-(4-(2,2-diphenylvinyl)phenyl)carbazole as electron donor and cyanoacrylic acid as electron acceptor bridged by thiophene units, gave an overall conversion efficiency (η) of 3.87-5.15%. Although many structure frameworks such as coumarin, aniline, and indoline have been employed as good electron donor unit, the small molecular organic dyes containing the *N*-substituted carbazole structural motif have been little explored for DSCs.

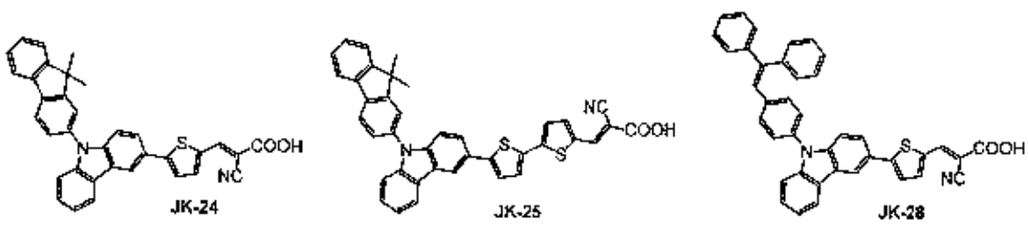

Figure 1.9 Chemical structures of **JK-24**, **JK-25** and **JK-28** dyes.

In 2009, Yuan Jay Chang et al. [19] reported that the highly efficient and stable organic dyes (**1P-PSP** and **1N-PSP**) composed of triphenylamine or *N*,*N*-diphenylnaphthalen-1-amine moiety as the electron donor and cyanoacrylic acid moiety as the electron acceptor with an overall conversion efficiency of 5.25-7.08%.

Figure 1.10 Chemical structures of **1P-PSP** and **1N-PSP** dyes.

In 2012, Zhongquan Wanet al. [20] investigated that the organic dyes (**CBZ, WD-5**, and **DTA**) containing carbazole, Phenothiazine or diphenylamine as electron donor and cyanoacrylic acid as electron acceptor bridged by phenyl units, gave an overall conversion efficiency (η) of 1.77-2.03%.

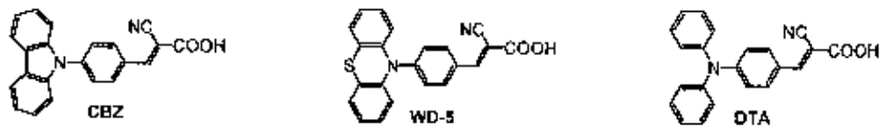

Figure 1.11 Chemical structures of **CBZ, WD-5**, and **DTA** dyes.

Most of the dyes employed in DSCs have carboxylic acid groups to anchor on the TiO_2-surface. The binding is reversible with high binding equilibrium constants (K = 10^5 M^{-1}). At a pH > 9 the equilibrium is typically shifted to the reactant side and the dye molecules desorb. This somewhat fragile linkage triggered the development of dyes with different anchoring groups. In general the binding strength to a metal oxide surface decreases in the order phosphonic acid > carboxylic acid > ester > acid chloride > carboxylate salts > amides [21] due to its strong electronic withdrawing properties, the most widely used and successful to date being the carboxylic acid and phosphonic acid functionalities. The carboxylic acid groups, while ensuring efficient adsorption of the dye on the surface also promote electronic coupling between the donor levels of the excited chromophores and the acceptor levels of the TiO_2 semiconductor. Some of the possible modes of chelation/derivatization, ranging from chemical bonding (chelating or bridging mode) to H-bonding, are shown in Figure 1.12 [22].

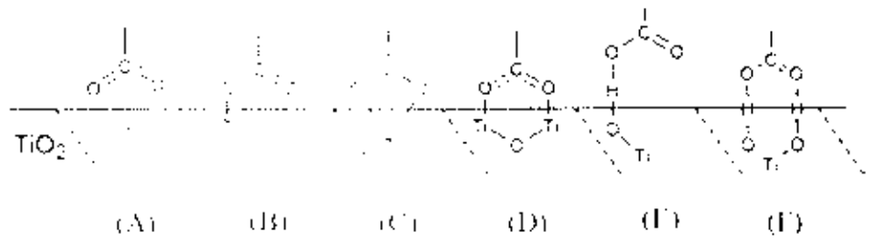

Figure 1.12 Possible binding modes for carboxylic acid groups on TiO_2.

1.3 Organic light emitting diodes (OLEDs)

Organic light emitting diodes (OLEDs) have recently received a great deal of attention because of their application for a wide range of display applications. OLEDs are attractive because of low voltage driving, high brightness, capability of multicolour emission by the selection of emitting materials, easy fabrication of large-area and thin-film devices, as no additional backlight is required for illumination of the screen. Following the reports on OLEDs using single crystals of anthracene [23], recent pioneering works on OLEDs using low molecular-weight organic materials and a conjugated polymer have triggered extensive research and development within this field. Recent years have witnessed significant progress with regard to brightness, multi- or full-colour emission, and durability and thermal stability of OLEDs. OLEDs fall into two competing technologies based on the materials used: small molecule devices are fabricated using vacuum evaporation techniques, whereas polymer structures can be applied using spin-casting or ink-jet techniques. The screen-printing technique has recently been introduced and is presumed to be applicable to both polymer and small molecule devices.

1.3.1 Principle of OLEDs

A single layer device architecture is the simplest OLED structure. In this case the organic emitter is deposited between two metal electrodes. In a single layer setup the organic semiconductor acts as emitter and charge transport material (holes and electrons) at the same time. As material for the anode indium-tin-oxide (ITO) is used in most cases. A thin, semitransparent ITO layer is sputtered onto a glass substrate. Afterwards, the emitting layer is deposited either by liquid phase or evaporation techniques onto the ITO anode. Finally, an electropositive metal like Al, Ca and Mg is evaporated on top of the OLED substrate as cathode. A suitable cathode material

has a low work function in order to ensure efficient electron injection into the organic semiconductor. A typical single layer OLED setup is shown in Figure 1.13.

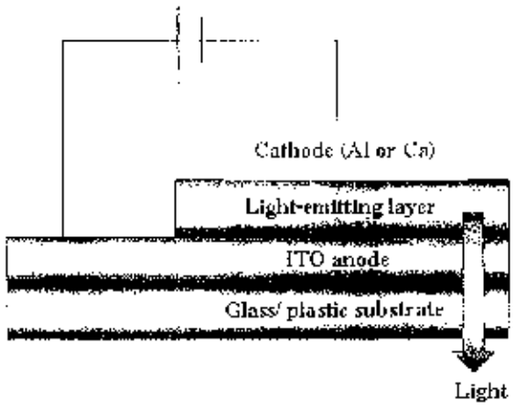

Figure 1.13 Schematic of a single layer OLED setup.

If a voltage is applied to the electrodes of an OLED device as depicted in Figure 1.13, electrons from the cathode and holes from the anode are injected into the organic semiconductor. Due to the electric field between the two electrodes, the positive and negative charge carriers move through the organic layer. As soon as they recombine in the emitting material, light is generated. The energy level diagram of a single layer OLED is shown in Figure 1.14.

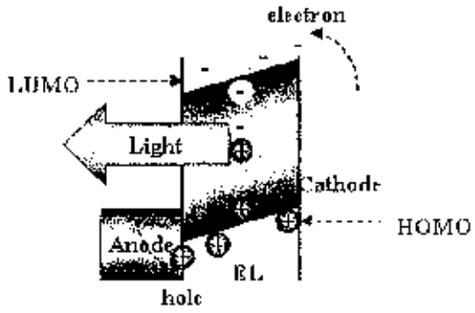

Figure 1.14 Energy level diagram of a single layer OLED device architecture.

The efficiency of an OLED is determined by the number of charge carriers that are injected and the number of holes and electrons that actually recombine under emission of light. The materials used in single layer devices are usually better hole than electron conductors. As the holes are moving faster through the emitting layer than the electrons, the recombination zone is shifted towards the cathode what usually leads to a non-radiative loss of energy [24]. Consequently, the efficiency of the device decreases [25].

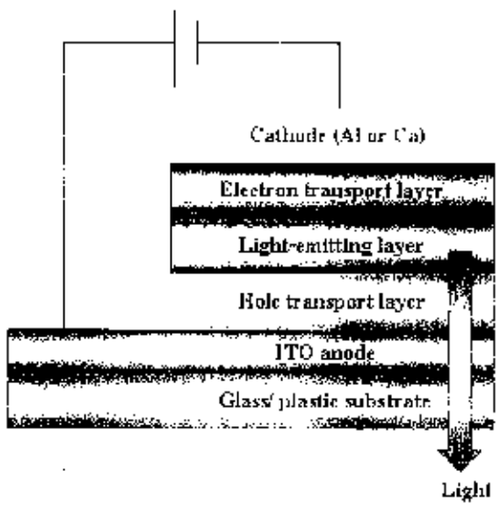

Figure 1.15 Schematic of a multi layer OLED setup.

In order to improve device efficiency, the multi layer OLED architecture was introduced as shown in Figure 1.15. Additional hole (HTL) and electron transport layers (ETL) are introduced in order to balance the different charge carrier mobilities. By varying transport properties and thickness of those supporting layers, the recombination zone can be shifted towards the emission layer. The advantages concerning a multi layer device setup, is the possibility to adapt the HOMO and LUMO levels of the used materials. A good overlap of the corresponding energy levels is essential to obtain a maximum carrier injection into the different layers [26].

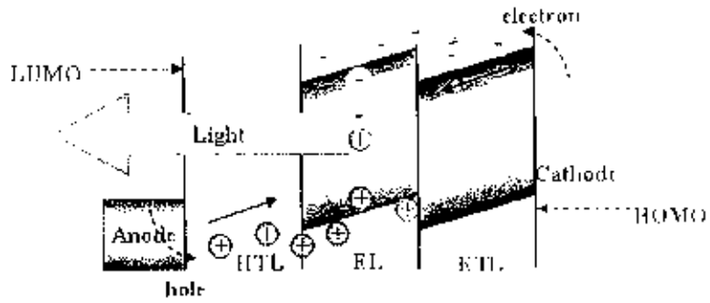

Figure 1.16 Energy level diagram of a multiple layer OLED device architecture.

1.3.2 Materials for OLED applications

Organic materials in OLEDs have to fulfil a variety of requirements. First of all they have to emit light with suitable color coordinates of the CIE-system (Commission International de L' Eclairage) and have to ensure a sufficient transport of charge carriers. A good chemical and electrochemical stability as well as a high thermal stability are also important prerequisites for OLED materials. Furthermore the compounds should exhibit good film forming properties. Crystallization of the thin films may lead to a decrease of charge carrier mobilities and finally to a short in the device [27, 28]. For this issue small molecules with bulky side groups are well suited. From low molar mass compounds homogeneous thin films can be prepared by vacuum deposition. As the bulky substituents prevent crystallization, molecular glasses are formed by these non-polymeric compounds [29]. Materials used as HTL have to exhibit HOMO levels in the order of -5.3 eV and therefore low ionization potentials. Aromatic amines like **NPD**, **CBP** and **TCTA** (Figure 1.17) are typical hole conductor materials for OLED applications [30]. Substances used for electron transport are often metal complexes like tris(8-hydroxyquinoline) aluminium **(AlQ3)** and bis-(2-dimethyl-8 quinoxalato)-4-(phenyl-phenoxalto) aluminium(III) **(BAlQ)** or electron poor heterocycles like 4,7-diphenyl-[1,10]phenanthroline **(BPhen)** [31] (Figure 1.17).

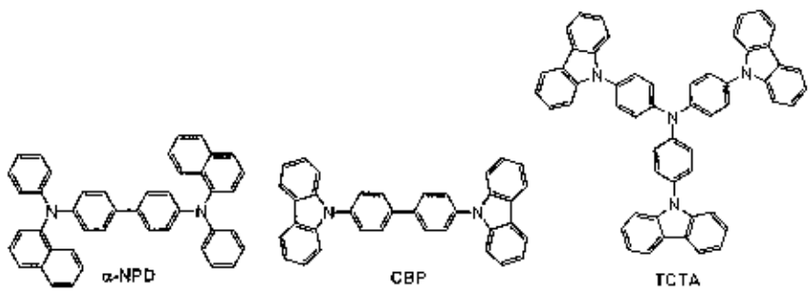

Figure 1.17 Typical aromatic amines that are used for hole transport in OLED devices: **α-NPD, CBP** and **TCTA.**

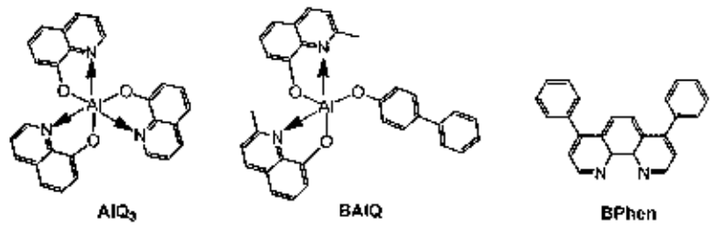

Figure 1.18 Typical examples for ETL materials: **AlQ_3, BAlQ** and **BPhen.**

The electroluminescence of polymers was first described by D.D.C. Bradley and co-workers [32]. They overcame the drawback of expensive and technologically inconvenient vapour deposition of fluorescent dyes by using the highly fluorescent conjugated polymer poly(*p*-phenylene-vinylene) (PPV) as active material in a single layer OLED. The structure are shown in Figure 1.19.

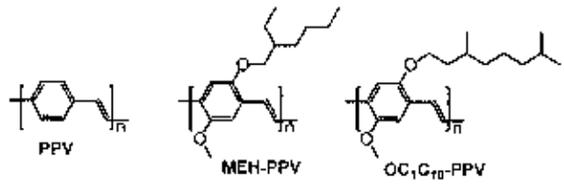

Figure 1.19 Chemical structure of **PPV** and its soluble derivatives.

In 2012, a highly fluorescent bis(4-diphenylaminophenyl) carbazole end-capped fluorene was synthesized and characterized by D. Meunmart and co-workers. This material showed greater ability as a solutionprocessed blue emitter and hole-transporter for OLEDs than

commonly used NPB. High-efficiency deep-blue and Alq3-based green devices with luminance efficiencies and CIE coordinates of 0.93 cd/A, (0.16, 0.09), and 3.78 cd/A and (0.29, 0.45) were achieved, respectively. The use of the triphenylamine-carbazole substituent might be an effective method to prepare amorphous molecules with excellent electrochemical, thermal, and morphological stabilities for OLEDs by forming dendritic structures with other fluorescent or non-fluorescent core units [33].

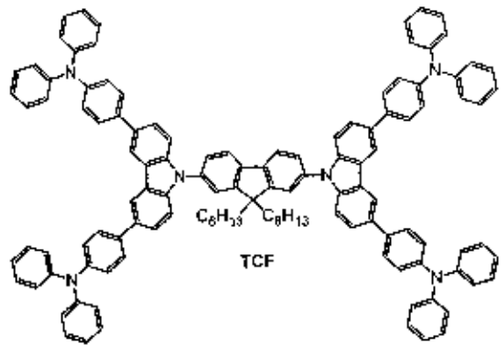

Figure 1.20 Chemical structure of TCF.

1.4 Aim of the thesis

In recent years, the development of novel organic materials for optoelectronic applications has attracted a lot of interest both in industry and academics. Especially in the area of dye solar cells (DSCs) and organic light emitting diodes (OLEDs) huge progress has been made. One of the main technological attractions of organic electronics is that the active layers can be deposited at low temperatures by liquid phase techniques. This makes organic semiconductors ideal candidates for low-cost, large-area electronic applications on flexible substrates.

The aims of this work as follows:

(1) To synthesize a novel donor π-conjugated acceptor (D-π-A) organic material based on triphenylamine and carbazole as the donor group. Chemically, carbazole can be easily functionalized at its 3,6-positions with a bulky group of *tert*-butyl moiety to protect the oxidation coupling at the 3,6-positions of the peripheral carbazole moiety. A thiophene as π-conjugated linker and a cyanoacrylic acid moiety as acceptor/anchor group for using as dye molecules in dye solar cells as show Figure 1.21.

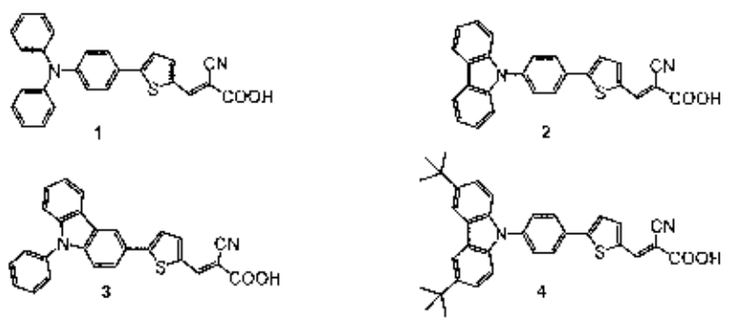

Figure 1.21 Chemical structures of novel D-π-A organic material (1-4).

(2) To synthesize novel donor π-conjugated acceptor (D-π-A) organic materials with different donor units. The *n*-hexyl substituents were introduced on the C-9 position of fluorene ring to increase the solubility. Chemically, carbazole and phenothiazine can be easily functionalized at its *N* positions with a bulky group of dodecyl moiety to increase the solubility, with a thiophene as π-conjugated linker and a cyanoacrylic acid moiety as acceptor/anchor group for using as dye molecules in dye solar cells as show in Figure 1.22.

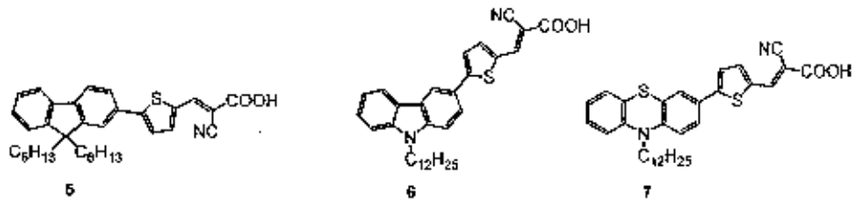

Figure 1.22 Chemical structures of novel D-π-A organic material (5-7).

(3) To synthesize novel donor π-conjugated acceptor (D-π-A) organic materials with different numbers of electron spacers are 4-hexylthiophene moieties for using as dye molecules in optoelectronic devices as show in Figure 1.23. The D-π-A containing carbazole as electron donor and cyanoacrylic acid as electron acceptor/anchoring group bridged by thiophene units. Carbazole and thiophene bearing alkyl groups at the *N* and C-4 position, respectively, to increase the solubility property and to prevent the recombination of the electrons from the semiconductor to the electrolyte. Different numbers of electron spacers are 4-hexylthiophene moieties, which are considered to be the ideal constructional unit in dye sensitizer engineering, adopted for expansion

of the π-conjugating backbone and adjusting the absorption spectra and HOMO/LUMO levels of the dyes.

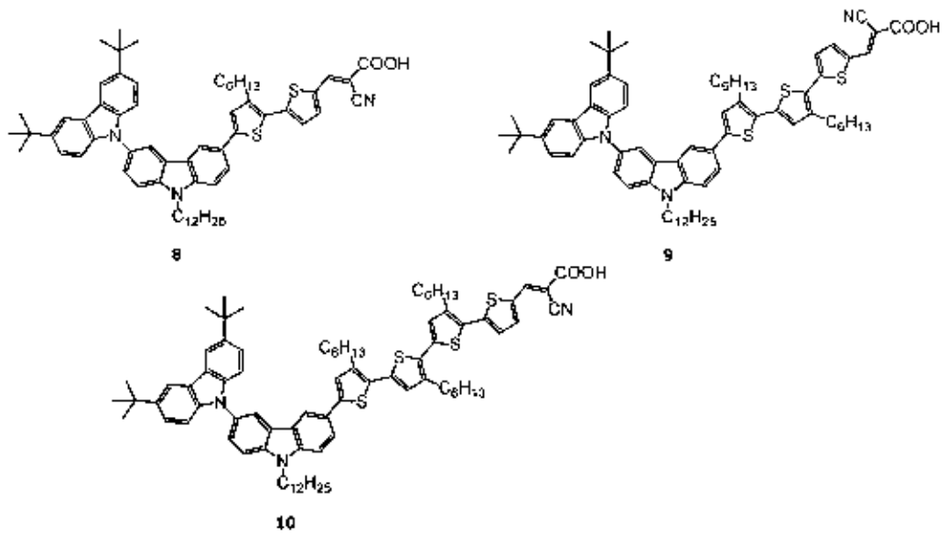

Figure 1.23 Chemical structures of novel D-π-A organic materials (**8-10**) with different numbers of electron spacers.

(4) To synthesize novel donor π-conjugated acceptor (D-π-A) organic materials with different linker units for using as dye molecules in optoelectronic devices as show in Figure 1.24. The D-π-A containing carbazole as electron donor and cyanoacrylic acid as electron acceptor/anchoring group bridged by thiophene units. Chemically, carbazole can be easily functionalized at its 3,6-positions with a bulky group of *tert*-butyl moiety to protect the oxidation coupling at the 3,6-positions of the peripheral carbazole moiety and *N* positions with a bulky group of dodecyl moiety to increase the solubility. The carbazole was functionalized with *tert*-butyl group to investigate if a bulky substituent would enhance the solar cell performance by suppressing aggregation. Different types of electron spacers containing thiophene moiety, which is considered to be the ideal constructional unit in dye sensitizer engineering, are adopted for expansion of the π-conjugating backbone and adjusting the absorption spectra and HOMO/LUMO levels of the dyes.

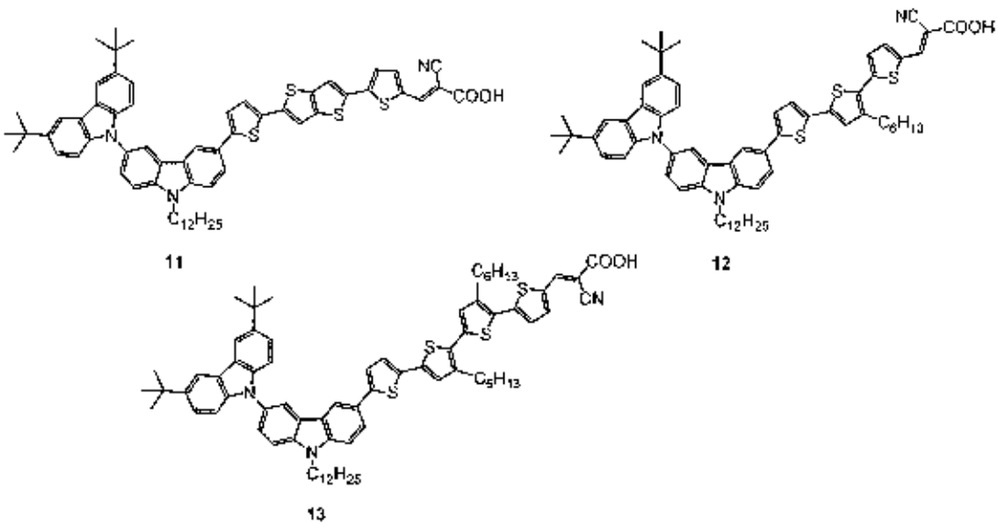

Figure 1.24 Chemical structures of novel D-π-A organic materials (**11-13**) with different linker units.

(5) To synthesize novel donor π-conjugated acceptor (D-π-A) organic materials with different numbers of electron spacers are thiophene moieties and different types of electron spacers containing furan, thiophene and phenyl moieties for using as dye molecules in optoelectronic devices as show in Figure 1.25. The D-π-A containing carbazole as electron donor and cyanoacrylic acid as electron acceptor/anchoring group bridged by thiophene and furan units. Carbazole bearing alkyl groups at the *N* position, to increase the solubility property and to prevent the recombination of the electrons from the semiconductor to the electrolyte. Different numbers of electron spacers are thiophene moieties and different types of electron spacers containing furan, thiophene and phenyl moieties, which are considered to be the ideal constructional unit in dye sensitizer engineering, adopted for expansion of the π-conjugating backbone and adjusting the absorption spectra and HOMO/LUMO levels of the dyes.

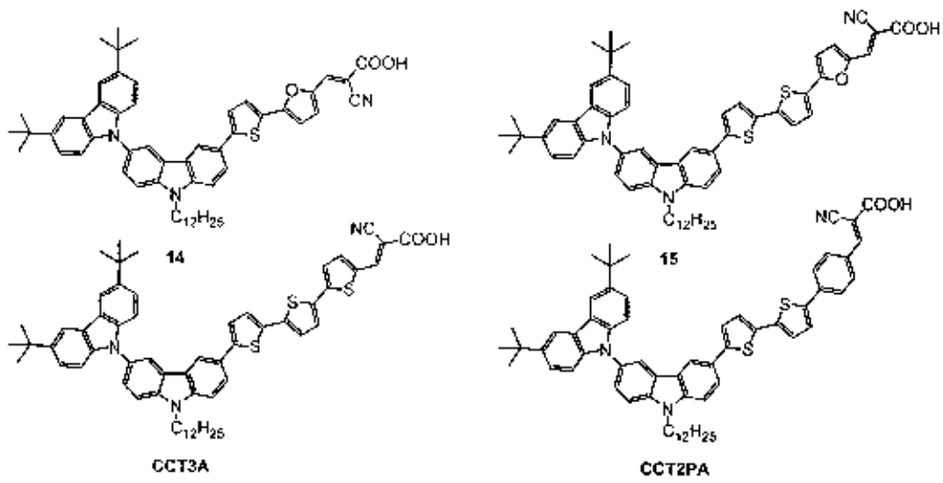

Figure 1.25 Chemical structures of novel D-π-A organic materials (**14, 15, CCT3A** [34] and **CCT2PA** [34]) with different numbers and types of electron spacers.

(6) To synthesize a novel donor π-conjugated acceptor (D-π-A) organic material based on carbazole as the donor group, with a fluorine, thiophene and phenyl as linker group and a cyanoacrylic acid moiety as acceptor/anchor group that would be an interesting starting point for further modifications as show in Figure 1.26. Chemically, carbazole can be easily functionalized at its 3,6-positions with a bulky group of *tert*-butyl moiety to protect the oxidation coupling at the 3,6-positions of the peripheral carbazole moiety. Fluorene, carbazole and phenothiazine were introduced on *N*-9 of carbazole as electron transport moiety.

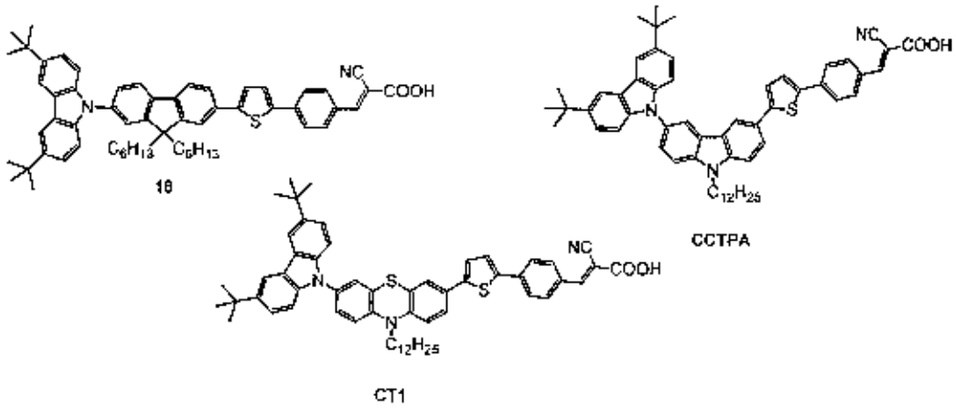

Figure 1.26 Chemical structures of novel D-π-A organic materials (**16, CCTPA** [34] and **CT1** [35])

(7) To synthesize novel donor π-conjugated acceptor (D-π-A) organic materials with different donor units for using as dye molecules in optoelectronic devices as show in Figure 1.27. The D-π-A containing *N*-phenylnaphthalen-1-amine as electron donor and cyanoacrylic acid as electron acceptor/anchoring group bridged by thiophene and furan units. Different types of substitute group at *N* position of *N*-phenylnaphthalen-1-amine moiety, which is considered to be the ideal constructional unit in dye sensitizer engineering, are adopted for expansion of the π-conjugating backbone and adjusting the absorption spectra and HOMO/LUMO levels of the dyes.

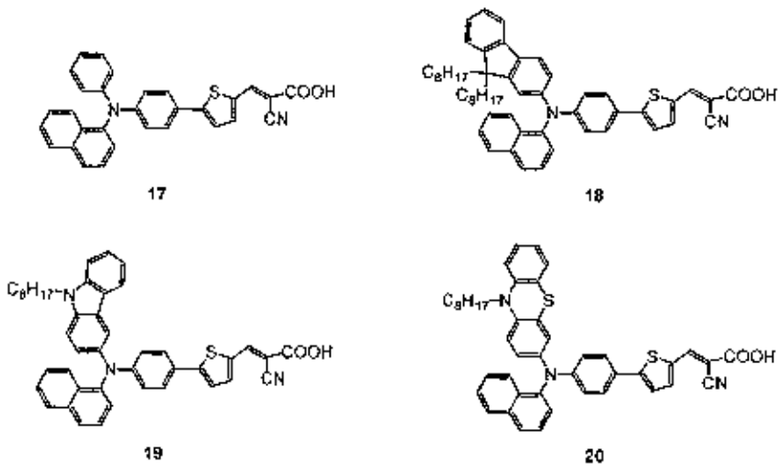

Figure 1.27 Chemical structures of novel D-π-A organic materials (**17-20**) with different donor units.

(8) To synthesize novel organic materials with carbazole as core and different number of triphenylamine substituents for using as hole-transporting layer in Alq3-based organic light emitting diode (OLED) as show in Figure 1.28. The carbazole group can be easily functionalized at the 1-, 3-, 6-, 8- or 9-position and covalently linked to other molecular groups. The *n*-dodecyl substituents were introduced on the *N*-9 position of carbazole ring to increasethe solubility, and triphenylamine as hole-transporting materials

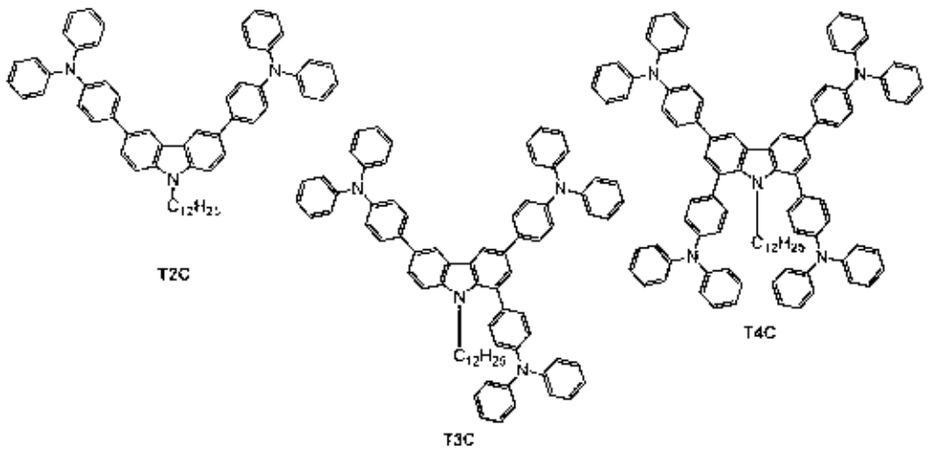

Figure 1.28 Chemical structures of novel hole-transporting materials (**TnC** (n = 2-4)).

(9) To characterize and to study the electronic, photophysical, electrochemical and thermal properties of the target molecules.

(10) To investigate their potential application as both dye sensitizer and hole-transporting layer for optoelectronic devices.

CHAPTER 2

SYNTHESIS AND CHARACTERIZATION OF NOVEL π-CONJUGATED ORGANIC MATERIALS BASED ON ARYLAMINE AS THE DONOR GROUP FOR DYE SOLAR CELLS

2.1 Introduction

Organic sensitizers were divided into three parts; donor, linker and acceptor. This is a convenient method to systematise the sensitizers. There are several basic criteria that an efficient sensitizer should fulfill, and these criteria can be used when designing a new organic sensitizer. First of all, light excitation should be associated with vectorial electron flow from the light harvesting moiety of the dye, i.e. the donor and the linker, towards the proximity of the semiconductor, i.e. the acceptor/anchoring group of the dye. This can be seen as the HOMO is located over the donor and the linker, while the LUMO is located over the acceptor, i.e. a pronounced push-pull effect. Second, the HOMO potential of the dye should be sufficiently positive compared to the electrolyte redox potential for efficient dye regeneration [36]. Third, the LUMO potential of the dye should be sufficiently negative to match the potential of the conduction band edge of the TiO_2. Fourth, a strong conjugation and electronic coupling across the donor and the acceptor to ensure high electron transfer rates. Finally, to obtain a dye with efficient photocurrent generation, π-stacked aggregation on the semiconductor should be avoided [37]. Aggregation may lead to intermolecular quenching or molecules residing in the system not functionally attached to the semiconductor surface and thus acting as filters.

2.1.1 Arylamine as donor

Due to the photophysical and redox properties of arylamine, they have been widely used as hole transporting materials for a number of applications, such as dye solar cell [38], organic light emitting diodes [39], and etc. In photovoltaic cells the interest of using arylamine based sensitizers has increased in recent years. Studies of the ruthenium complex Ru-1 containing a arylamine group showed especially improved photophysical properties (red-shifted metal-to-ligand charge-transfer transition absorptions and enhanced molar extinction coefficients)

and interesting electrochemical properties, resulting in its improved open circuit potential and high overall light-to-electric power conversion efficiency of 5.3% (AM1.5 G, 75 mW/cm^2) [40].

2.1.2 Thiophene as π-conjugated linker

Expansion of the π-conjugated backbone to extend the absorption spectrum and broaden it to the red region, is one way to decrease the HOMO/LUMO energy level differences and thereby increase the solar cell performance. This would, however, complicate the synthetic procedure and affect the stability of the dye due to photoinduced *trans* to *cis* isomerisation. The introduction of different π-conjugated ring moieties, benzene is an elegant way of extending the π-conjugated system without affecting the stability of the dye [41].

2.1.3 Acceptor and anchoring group

Anchoring to TiO_2 has been achieved through a number of functional groups. In general the binding strength to a metal oxide surface decreases in the order phosphonic acid > carboxylic acid > ester > acid chloride > carboxylate salts > amides [21] due to its strong electronic withdrawing properties.

2.2 Aim of the study

We designed four novel donor π-conjugated acceptor (D-π-A) organic materials based on arylamine as the different electron donor groups, with a thiophene linker and a cyanoacrylic acid as acceptor/anchor group that would be an interesting starting point for further modifications. The synthetic strategy included well-known methodology, such as Ullmann coupling, Suzuki coupling and Knoevenagel condensation reaction.

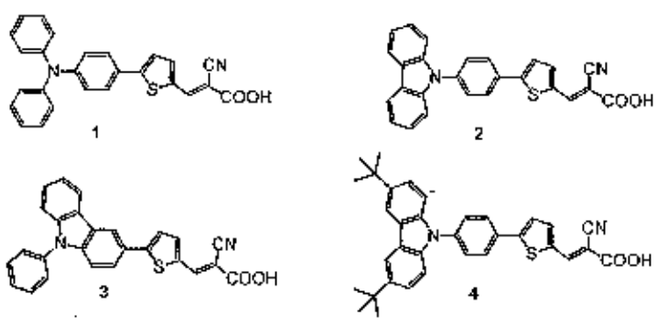

Figure 2.1 Chemical structure of dye (1-4).

2.3 Results and Discussion

2.3.1 Synthesis

For the synthesis of (*E*)-2-cyano-3-(5-(4-(diphenylamino)phenyl)thiophen-2-yl)acrylic acid, first 5-(4-(diphenylamino)phenyl)thiophene-2-carbaldehyde was prepared from (4-(diphenylamino)phenyl)boronic acid precursor **(21)** and commercially available 5-bromothiophene-2-carbaldehyde under Suzuki coupling reaction in the presence of $Pd(PPh_3)_4$ as a catalyst and Na_2CO_3 as a base in THF as a solvent at reflux. The desired 5-(4-(diphenylamino)phenyl)thiophene-2-carbaldehyde **(22)** was isolated by silica-gel column chromatography as brown solid in 99% yield. The successful introduction of aldehyde functional group was clearly confirmed by NMR and IR spectra. The singlet signal of aldehyde proton (measured in $CDCl_3$) was located at chemical shift 9.85 for aldehyde proton of **22**. The signal of the aldehyde carbon atom was located at chemical shift 182.90 for aldehyde carbon of **22**. The dominant IR peaks of C=O stretching of aldehyde was also observed at wavenumber 1658 cm^{-1} for **22**. The dye with cyanoacrylic acid as an acceptor was synthesized. Knoevenagel condensation reaction of **22** with cyanoacetic acid in the presence of piperidine as a base and catalyst in $CHCl_3$ as solvent at reflux for 6 h gave the target (*E*)-2-cyano-3-(5-(4-(diphenylamino)phenyl)thiophen-2-yl)acrylic acid **(1)** as light green solid in 50% yield as shown in Figure 2.2. The chemical structure of **1** was confirmed by NMR and IR analysis. The ^{1}H-NMR spectrum of the final product **1** shows a singlet signal at chemical shift 8.34 ppm (1H) assigning as the proton of double bond indicating that **1** excises as *E* isomer which has higher photostability properties. The ^{13}C-NMR spectrum of **1** shows a single peak for chemically carbon atom of carbonyl group at 169.86 ppm and a single peak for carbon atom of cyano group at 118.87 ppm. Furthermore IR spectrum reveals the adsorption at 3421 cm^{-1} which is consistent with the presence of hydroxy group and at 2212 cm^{-1} which is consistent with the presence of cyano group.

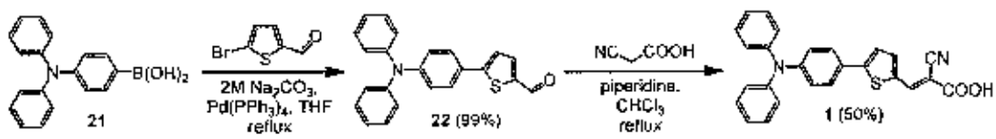

Figure 2.2 Synthesis of target (*E*)-2-cyano-3-(5-(4-(diphenylamino)phenyl) thiophen-2-yl)acrylic acid **(1)**.

The reaction follows a three-step mechanism cycle, oxidative addition, transmetallation and reductive elimination as described in Figure 2.3.

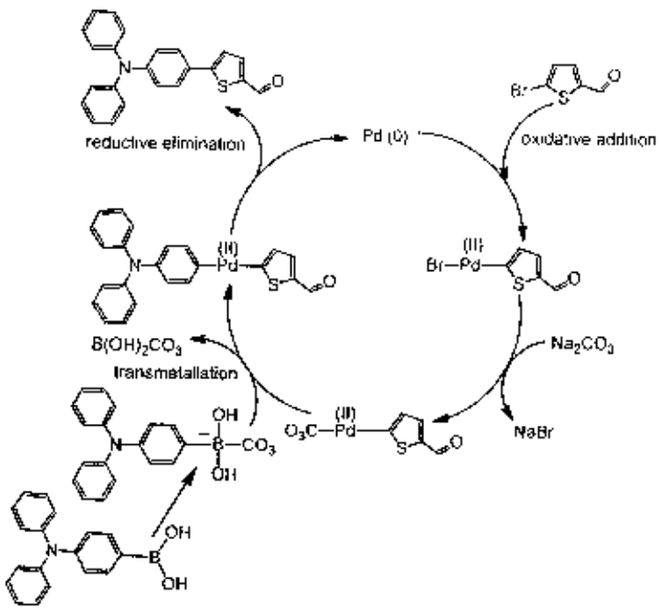

Figure 2.3 The proposed mechanism of Suzuki coupling reaction

Knoevenagel condensation mechanism involves the corresponding enolate anion as nucliophile and the corresponding iminium intermediate as electrophile and is shown in Figure 2.4.

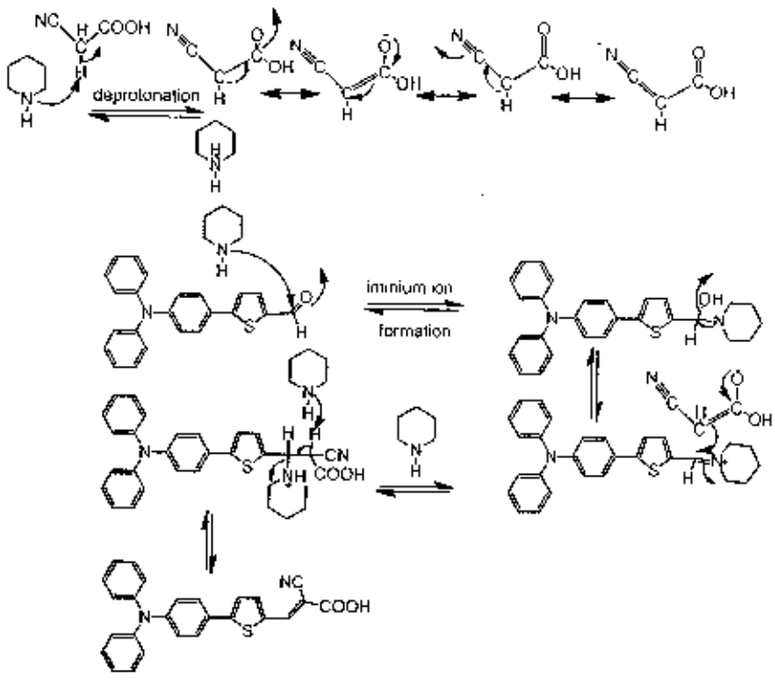

Figure 2.4 The proposed mechanism of Knoevenagel condensation reaction.

For the synthesis of (*E*)-3-(5-(4-(carbazol-9-yl)phenyl)thiophen-2-yl)-2-cyanoacrylic acid, first 5-(4-(carbazol-9-yl)phenyl)thiophene-2-carbaldehyde (**24**) was prepared according to the procedure described for **22** and obtained as green solid in 30% yield. The successful introduction of aldehyde functional group was clearly confirmed by NMR and IR spectra. The singlet signal of aldehyde proton (measured in $CDCl_3$) was located at chemical shift 9.94 ppm for aldehyde proton of **24**. The signal of the aldehyde carbon atom was located at chemical shift 182.77 ppm for aldehyde carbon of **24**.The dominant IR peaks of C=O stretching of aldehyde was also observed at wavenumber 1670 cm^{-1} for **24**. The dye having the cyanoacrylic acid as an acceptor was synthesized according to the procedure described for **1** and obtained as light green solid in 70% yield as shown in Figure 2.5. The chemical structure of **2** was confirmed by NMR and IR analysis. The ^{1}H-NMR spectrum of the final product (**2**) shows a singlet signal at chemical shift 8.50 ppm (H1) assigning as the proton of vinyl double bond indicating **2** exists as *E* isomer which has higher photostability properties. The ^{13}C-NMR spectrum of **2** shows a single peak for chemically carbon atom of carbonyl group at 168.83 ppm and a single peak for carbon atom of cyano group at 120.40 ppm. Furthermore IR spectrum reveals the adsorption at 3420 cm^{-1}

which is consistent with the presence of hydroxy group and at 2207 cm^{-1} which is consistent with the presence of cyano group.

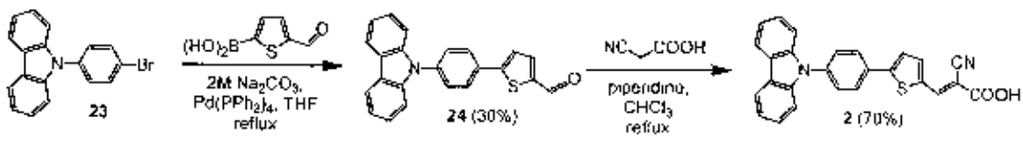

Figure 2.5 Synthesis of (*E*)-3-(5-(4-(carbazol-9-yl)phenyl)thiophen-2-yl)-2-cyanoacrylic acid (**2**).

For the synthesis of (*E*)-2-cyano-3-(5-(9-phenylcarbazol-3-yl)thiophen-2-yl)acrylic acid, first 3-iodocarbazole was prepared from carbazole precursor (**25**) under iodination in the presence of KI (0.65 equiv.) and KIO_3 (0.50 equiv.) in AcOH at reflux. The desired 3-iodocarbazole (**26**) was isolated by silica-gel column chromatography as brown solid in 84% yield. Subsequently, the key intermediate was synthesized by using Ullmann coupling reaction of **7** with iodobenzene in the presence of copper iodide as a catalyst, (±)-*trans*-1,2-diaminocyclohexane as a co-catalyst, and potassium *tert*-butoxide as a base in toluene as a solvent at reflux for 24 h led to 3-iodo-9-phenylcarbazole (**27**) as light yellow viscous in 93% yield. Then 5-(9-phenylcarbazol-3-yl)thiophene-2-carbaldehyde (**28**) was prepared according to the procedure described for **22** and obtained as green solid in 48% yield. The successful introduction of aldehyde functional group was clearly confirmed by NMR and IR spectra. The singlet signal of aldehyde proton (measured in $CDCl_3$) was located at chemical shift 9.89 ppm for aldehyde proton of **28**. The signal of the aldehyde carbon atom was located at chemical shift 182.62 ppm for aldehyde carbon of **28**. The dominant IR peaks of C=O stretching of aldehyde was also observed at wavenumber 1661 cm^{-1} for **28**. And (*E*)-2-cyano-3-(5-(9-phenylcarbazol-3-yl)thiophen-2-yl)acrylic acid (**3**) dye having the cyanoacrylic acid as an acceptor was synthesized according to the procedure described for **1** and obtained as light green solid in 68% yield. The chemical structure of **3** was confirmed by NMR and IR analysis. The ^{1}H-NMR spectrum of the final product (**3**) shows a singlet signal at chemical shift 8.42 ppm (1H) assigning as the proton of vinyl double bond indicating **3** exists as *E* isomer which has higher photostability properties. The ^{13}C-NMR spectrum of **3** shows a single peak for chemically carbon atom of carbonyl group at 167.96

ppm and a single peak for carbon atom of cyano group at 120.53 ppm. Furthermore IR spectrum reveals the adsorption at 3411 cm^{-1} which is consistent with the presence of hydroxy group and at 2219 cm^{-1} which is consistent with the presence of cyano group.

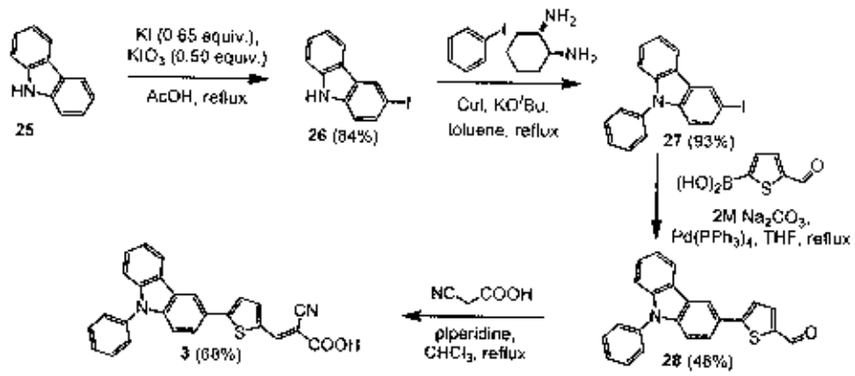

Figure 2.6 Synthesis of (*E*)-2-cyano-3-(5-(9-phenylcarbazol-3-yl)thiophen-2-yl) acrylic acid (**3**).

Ullmann coupling mechanism is shown in Figure 2.7. The active species is a copper (I) iodide which undergoes oxidative addition with the second equivalent of halide, followed by reductive elimination and the formation of the phenyl-carbazole carbon bond.

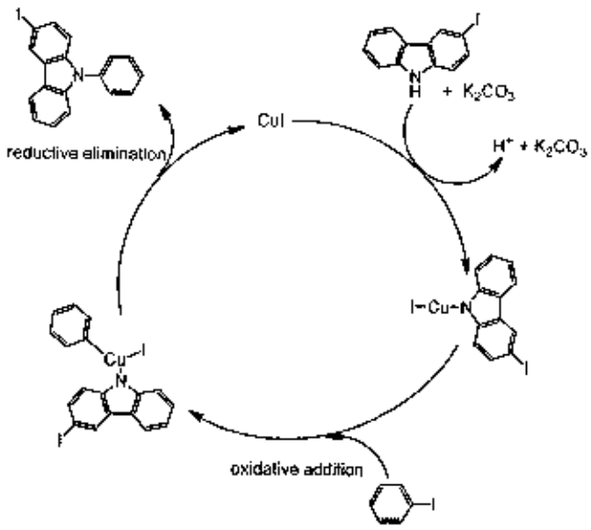

Figure 2.7 The proposed mechanism of Ullmann coupling reetion.

For The synthesis of (*E*)-2-cyano-3-(5-(4-(3,6-di-*tert*-butylcarbazol-9-yl)phenyl)thiophen-2-yl)acrylic acid (**4**) as shown in Figure 2.8, first, the key intermediate was synthesized by using Ullmann coupling reaction of 3,6-di-*tert*-butylcarbazole (**29**) with iodobenzene in the presence of copper iodide as a catalyst, (±)-*trans*-1,2-diaminocyclohexane as a co-catalyst, and potassium *tert*-butoxide as a base in toluene as a solvent at reflux for 24 h led to 3,6-di-*tert*-butyl-9-phenylcarbazole (**30**) as light yellow viscous in 99% yield. Then 3,6-di-*tert*-butyl-9-(4-iodophenyl) carbazole (**31**) was prepared from **30** under iodination in the presence of I_2 and KIO_3 in the mixture of AcOH and 20%H_2SO_4 at reflux. The desired 3,6-di-*tert*-butyl-9-(4-iodophenyl) carbazole (**31**) was isolated by silica-gel column chromatography as brown solid in 80% yield. Next 5-(4-(3,6-di-*tert*-butylcarbazol-9-yl)phenyl)thiophene-2-carbaldehyde (**32**) was prepared according to the procedure described for **22** and obtained as green solid in 60% yield. The successful introduction of aldehyde functional group was clearly confirmed by NMR and IR spectra. The singlet signal of aldehyde proton (measured in $CDCl_3$) was located at chemical shift 9.73 ppm for aldehyde proton of **32**. The signal of the aldehyde carbon atom was located at chemical shift 182.98 ppm for aldehyde carbon of **32**.The dominant IR peaks of C=O stretching of aldehyde was also observed at wavenumber 1603 cm^{-1} for **32**. And (*E*)-2-cyano-3-(5-(4-(3,6-di-*tert*-butylcarbazol-9-yl)phenyl)thiophen-2-yl)acrylic acid (**4**) dye having the cyanoacrylic acid as an acceptor was synthesized according to the procedure described for **1** and obtained as light green solid in 65% yield. The chemical structure of **4** was confirmed by NMR and IR analysis. The ^{1}H-NMR spectrum of the final product (**4**) shows a singlet signal at chemical shift 7.91 ppm (1H) assigning as the proton of vinyl double bond indicating **4** exists as *E* isomer which has higher photostability properties and a singlet signal at chemical shift 8.19 (1H) and 8.15 (1H) ppm assigning of unequivalent 4-H and 5-H protons of 3,6-di-*tert*-butylcarbazole. The ^{13}C-NMR spectrum of **4** shows a single peak for chemically carbon atom of carbonyl group at 165.18 ppm and a single peak for carbon atom of cyano group at 116.62 ppm. Furthermore IR spectrum reveals the adsorption at 3424 cm^{-1} which is consistent with the presence of hydroxy group and at 2207 cm^{-1} which is consistent with the presence of cyano group.

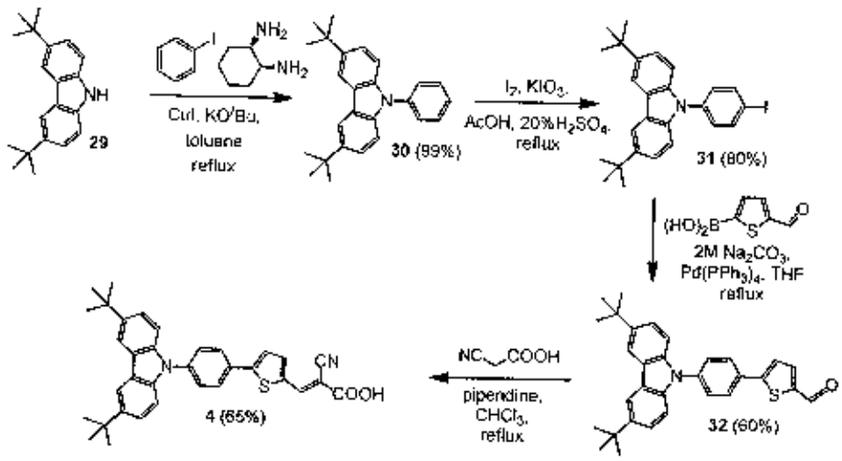

Figure 2.8 Synthesis of (*E*)-2-cyano-3-(5-(4-(3,6-di-*tert*-butylcarbazol-9-yl)phenyl)thiophen-2-yl)acrylic acid (**4**).

2.3.2 Optical properties

The influence of different arylamine electron donors on the light harvest capacity of a dye molecule was first evaluated by recording the UV-vis absorption spectra of the dyes dissolved in tetrahydrofuran (Figure 2.9), and the selected parameters were collected in Table 2.1. **1-4** showed the maximum absorption wavelength (λ_{max}) 427 nm (molar absorption coefficient (ε) = 39,000 M^{-1} cm^{-1}), 384 nm (ε = 31,069 M^{-1} cm^{-1}), 417 nm (ε = 24,506 M^{-1} cm^{-1}) and 355 nm (ε = 13,151 M^{-1} cm^{-1}), respectively, which were corresponding to HOMO (highest occupied molecular orbital) -> LUMO (lowest unoccupied molecular orbital) transition. Amongst these photosensitizers, due to strong electron donating ability of the diphenylamine unit, the **1** dye with the diphenylamine electron donor presents the longest maximum absorption wavelength, with the highest molar absorption coefficient, which is an advantageous spectral property for light harvesting of the solar spectrum. Figure 2.10 shows the absorption spectra of **1-4** on the TiO_2 films after 24 h adsorption. Upon dye adsorption onto the TiO_2 surface, the maximum absorption respectively hypsochromic shifted or blue shifted for **1-4** as compared to the spectra in solution. The broadening of the dyes adsorption on the surface of the TiO_2 films and blue shift of the peak maxima is believed to result from the formation of partial H-aggregates [39]. We observed that the **1-4** dyes exhibited strong luminescence maxima of 466-544 nm when it is excited within its π-π^* band in solution at room temperature showed the emission peak located in the blue-green region.

The energy band gaps of the **1-4** dyes were estimated to be 2.50, 2.56, 2.79, and 2.76 eV, respectively, from the absorption edge of the solution spectra.

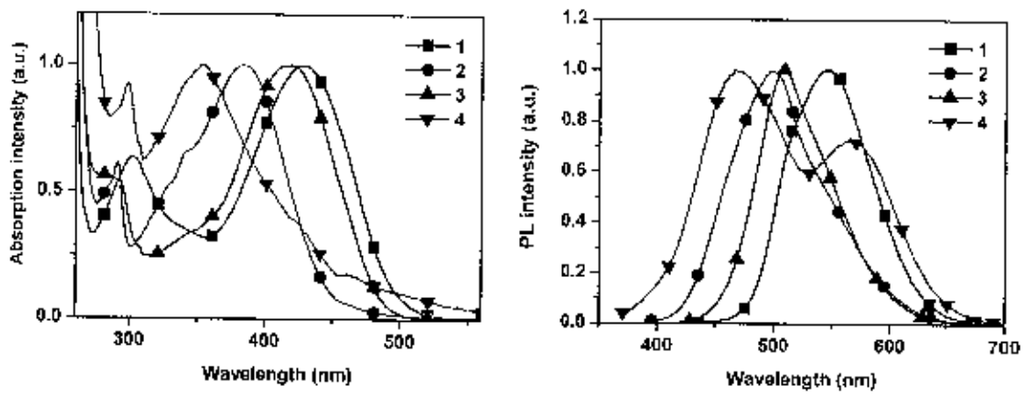

Figure 2.9 Absorption (left) and emission (right) spectra of **1-4** recorded in tetrahydrofuran.

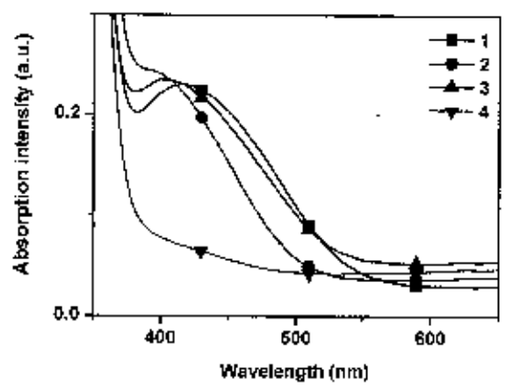

Figure 2.10 Absorption spectra of TiO_2 films sensitized by **1-4**.

Table 2.1 The absorption and fluorescence data of **1-4**

Compound	λ_{max}^{abs} (εx 10^4); (nm (M^{-1} cm^{-1}))[a]	λ_{max} on TiO_2 (nm)[b]	λ_{max}^{em} (nm)[a,c]	λ_{onset}^{abs} (nm)[a]	E_g (eV)[d]
1	427 (3.90), 302 (2.48)	418	544	495	2.50
2	384 (3.11), 291 (1.92)	-	498	485	2.56
3	417 (2.45)	403	507	445	2.79
4	355 (1.31), 298 (1.22)	-	466	450	2.76

[a] measured in dichloromethane solution at room temperature.

[b] measured dyes adsorbed on TiO_2 film.

[c] excited at maximum absorption in solution.

[d] estimated from the onset of absorption ($E_g = 1240/\lambda_{onset}$).

The effect of solvent polarity on the absorption spectra of **3** dye was also studied (Figure 2.11 and Table 2.2). The absorption was measured in five different solvents dimethylformamide (DMF), dimethylsulfoxide (DMSO), ethanol (EtOH), tetrahydrofurane (THF) and dichloromethane (DCM)). We assigned the absorption bands at 282 nm as **B1** and at 398-440 nm as **B2**, respectively. There is only **B2** band that be effected by solvent polarity change. These **B2** bands therefore are assigned as ICT bands of donor-accepter molecule which can be generally observed in most sensitizer. The absorption spectra show blue shift when the polarities of solvents are increasing. **3** in DMF exhibited lowest maximum absorption at 398 nm (4.99×10^{-19} *J*), whereas **3** in dichloromethane exhibited the highest at 440 nm (4.52×10^{-19} *J*). These results can be considered as the negative solvatochromism-physical intermolecular solute-solvent interaction forces which tend to alter the energy difference between ground and excited state of chromophore of the dyes [42]. The polar solvents are good supporting solvent to the excited state dye species more than non-polar solvents resulting in close molecular orbital, which tends to absorb light at high energy region (low wavelength). This effect was also found in the other molecules (**1**, **2** and **4**).

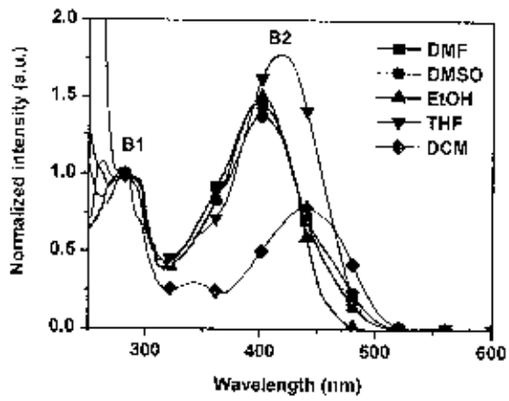

Figure 2.11 The absorption spectra of **3** dye in various solvents.

Table 2.2 Maximum absorption of **3** measured in various solvents.

solvent	DMF	DMSO	EtOH	THF	DCM
λ_{max} (nm)	398	400	402	417	440
E^a (10^{-19} J)	4.99	4.97	4.94	4.77	4.52

[a] calculated from $E = h\nu/\lambda$

2.3.3 Thermal properties

For optoelectronic applications, the thermal stability of organic materials is crucial for device stability and lifetime. The degradation of organic optoelectronic devices depends on morphological changes resulting from the thermal stability of the amorphous organic materials [43]. Figure 2.12 and Table 2.3 show TGA thermograms and temperature at 5% weight loss (T_{5d}) of **1-4** dyes investigated by TGA analysis under nitrogen atmospheric condition. Those results suggested that the dyes were thermally stable materials with T_{5d} well over 111 °C. The better thermal stability of the dye is important for the lifetime of the solar cells.

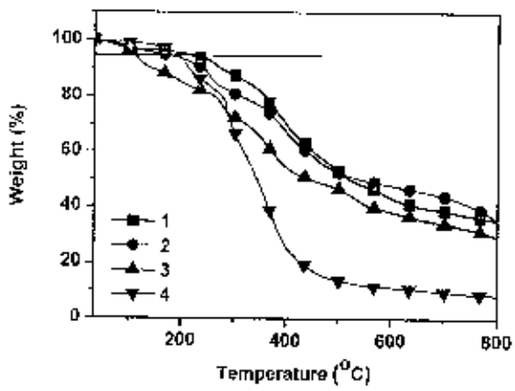

Figure 2.12 TGA thermograms of **1-4** dyes.

Table 2.3 Thermal properties of **1-4**

Compound	T_{5d} (°C)
1	211
2	162
3	111
4	192

2.3.4 Molecular orbital calculation

To get an insight into the molecular structure and electron distribution of the organic dye, the **1-4** dyes geometries have been optimized using DFT calculations with Gaussian 03 program. The calculations were performed with the BTLYP exchange correlation functional under 6-31G(d,p) basis set. Computed HOMO and LUMO distribution of **1-4** are depicted in Figure 2.13. The general characters of the orbitals are independent of the different electron donor. The HOMO is of π-characteristics and is delocalized over the entire molecule, including the arylamine groups. In the LUMO, which also has π-character, there is essentially no contribution from the arylamine groups, and the electron density has been shifted towards the acceptor group of the sensitizer. This supports the supposed push-pull characteristics of these sensitizers (Figure 2.13). In addition, the optimized geometry of **1-4** indicates that the arylamine moiety at the end of the molecule are in 3-D spatial arrangement, which makes the molecular structure nonplanar due to the twist conformation around the arylamine-phenyl C-C bond.

The nonplanar molecular structure of **1-4** could be beneficial to solution-processability to form amorphous film. **1-4** are soluble in common organic solvents such as THF, MeOH, CH_2Cl_2, $CHCl_3$ and acetone. High-quality amorphous film can be obtained by spin-coating its solution.

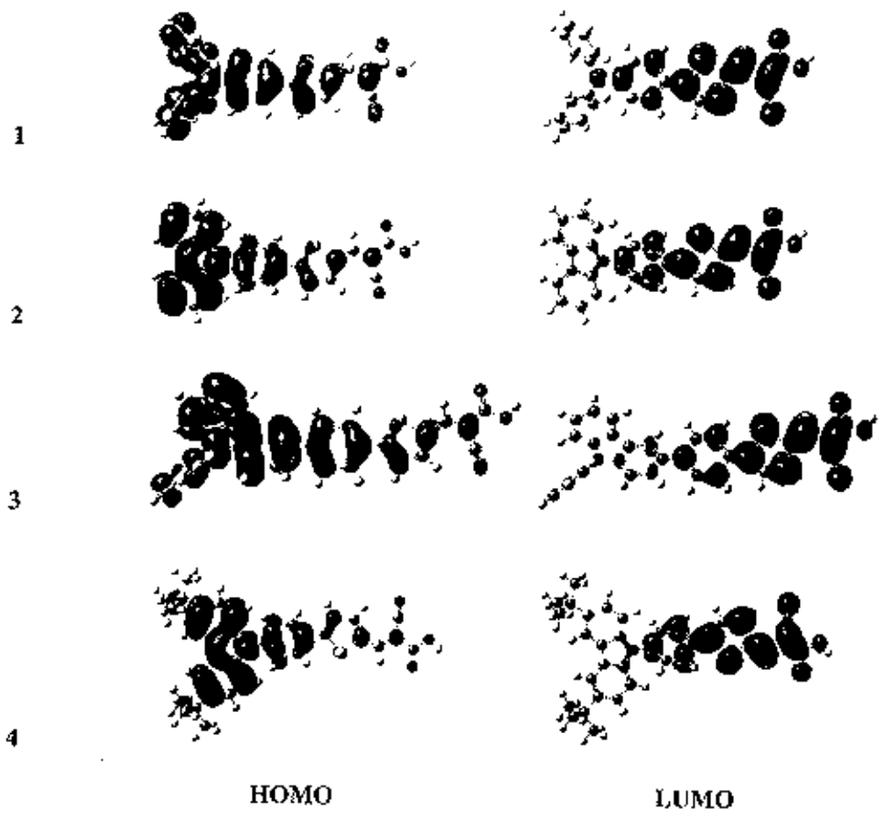

Figure 2.13 HOMO and LUMO distribution of the **1-4** dyes calculated with DFT on a BTLYP/6-31G(d,p) level.

2.4 Conclusions

Novel D-π-A organic dyes, **1-4**, have synthesized as photosensitizers for DSCs applications by using Ullmann coupling, Suzuki coupling and Knoevenagel condensation reaction. Different arylamine moieties are introduced to the molecules and serve as electron donor group. The electron-withdrawing part is cyanoacrylic acid group. The target molecules were characterized by using NMR, IR, UV-vis and fluorescence techniques. The target molecules exhibit an adsorption band cover UV and visible region. Fluorescence spectra of the target

molecules show emission peak at blue-green region, excited at λ_{max} of each molecule. **1-4** show a good thermal properties. DFT calculations have been performed on the dyes, and the results show that electron distribution from the whole molecules to the anchoring moieties occurred during the HOMO-LUMO excitation.

CHAPTER 3

SYNTHESIS AND CHARACTERIZATION OF NOVEL ORGANIC DYES WITH DIFFERENT DONOR UNIT FOR DYE SOLAR CELLS

3.1 Introduction

In 2010, Tzi-Yi Wu et al. investigated the organic dyes comprising carbazole, iminodibenzyl, or phenothiazine moieties, respectively, as the electron donors, and cyanoacetic acid or acrylic acid moieties as the electron acceptors/anchoring groups were synthesized and characterized. The influence of heteroatoms on carbazole, iminodibenzyl and phenothiazine donors, and cyano-substitution on the acid acceptor is evidenced by spectral, electrochemical, photovoltaic experiments, and density functional theory calculations. The phenothiazine dyes show solar-energy-to-electricity conversion efficiency (η) of 3.46-5.53%, whereas carbazole and iminodibenzyl dyes show η of 2.43% and 3.49%, respectively [4].

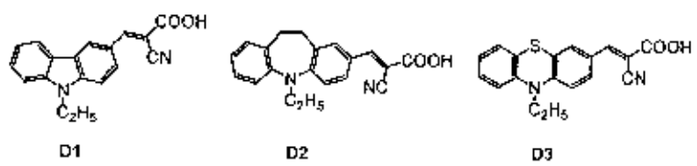

D1 D2 D3

Figure 3.1 Chemical structures of Carbazole, Iminodibenzyl, and Phenothiazine-containing Dyes **(D1-D3).**

3.2 Aim of the Study

We synthesized three novel donor π-conjugated acceptor (D-π-A) organic materials with different donor units for using as dye molecules in DSCs. D-π-A organic dyes based on fluorene, carbazole and phenothiazine as the donor group, with a thiophene linker and a cyanoacrylic acid as acceptor/anchor group. Fluorene, carbazole and phenothiazine bearing alkyl

groups at the C-9, *N* and *N* position, respectively, to increase the solubility property and to prevent the recombination of the electrons from the semiconductor to the electrolyte.

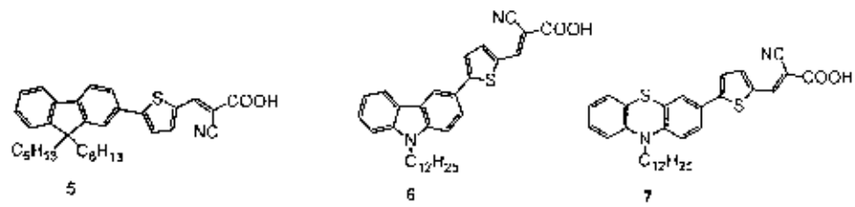

Figure 3.2 Chemical structures of D-π-A organic dyes (**5-7**).

3.3 Results and Discussion

3.3.1 Synthesis

The synthesis of The synthesis of fluorene donor part starting with fluorene starting material (**33**) was iodinated in the mixture of potassium iodide and potassium iodate in acetic acid at 80 °C resulting in 2-iodofluorene (**34**) in 41% yield (Figure 3.3). The structure of iodinated product (**34**) was confirmed by ^{1}H-NMR spectra (measured in $CDCl_3$) which exhibit very clear singlet signal of aromatic proton of C-1 fluorene at chemical shift at 7.89 ppm. Dialkylation at the C-9 position to increase the solubility of the resultant compound (**34**) was accomplished by generation of the fluorenyl anion with an aqueous NaOH solution in DMSO and subsequent dihexylation with 1-bromohexane in the presence of n-$Bu_4N^+Br^-$ as phase transfer catalyst at room temperature. The desired 9,9-dihexyl-2-iodofluorene (**1a**) was isolated by silica-gel column chromatography as brown solid in 89% yield.The Alkyl peaks were observed in ^{1}H-NMR spectrum of **1a** to confirm successful introduction of alkyl group to C-9 position of fluorene. The extended carboxaldehyde functionalized thiophene intermediate (**2a**) was achieved by Suzuki condition as well. The coupling reaction between corresponding aryl halide (**1a**) and 5-formyl-2-thiopheneboronic acid yielded the aldehyde (**2a**) in 40, 60 and 55%, respectively. This moderate yield are commonly observed in Suzuki coupling of 5-formyl-2-thiopheneboronic acid due to its unstable thiophene carboxaldehyde intermediate. The successful introduction of aldehyde functional group was confirmed by NMR and IR spectra. The singlet signal of aldehyde proton in $CDCl_3$ was located at chemical shift 9.90 ppm for aldehyde proton of **2a**. The signal of

the aldehyde carbon atom was located at chemical shift 182.93 ppm for aldehyde carbon of **2a**. Finally the **5** dye were obtained by Knoevenagel reaction of corresponding aldehyde (**2a**) with cyanoacetic acid. The **5** dye were obtained as yellow amorphous solid. The solubility of dye in common organic solvent is pretty excellent owing to the long alkyl chain attached to C-9 position of fluorene. The chemical structure of **5** was confirmed by NMR and IR analysis. The ^{1}H-NMR spectrum of the final product (**5**) show a singlet signal at chemical shift 8.29 (1H) ppm assigning as the proton of double bond indicating that **5** excises as *E* isomer which has higher photostability properties. The ^{13}C-NMR spectrum of **5** show a single peak for chemically carbon atom of carbonyl group at 165.30 ppm , respectively, and a single peak for carbon atom of cyano group at 116.95 ppm , respectively. Furthermore IR spectrum reveals the adsorption at 3420 cm^{-1} which is consistent with the presence of hydroxy group for **5**, respectively, and at 2211 cm^{-1} which is consistent with the presence of cyano group for **5**.

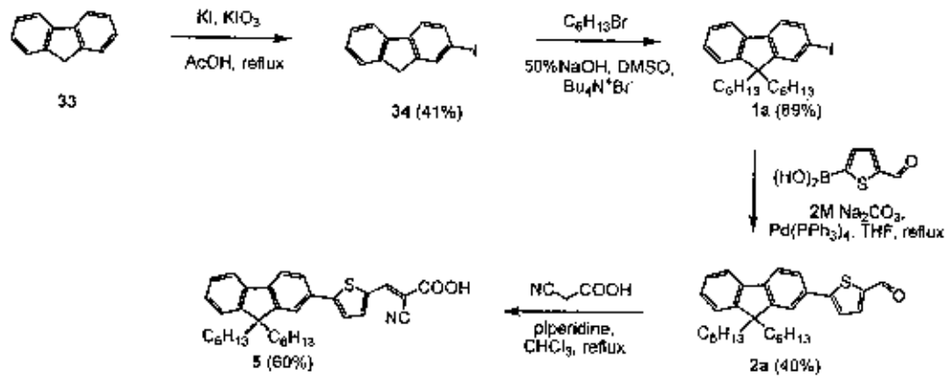

Figure 3.3 Synthesis of (*E*)-2-Cyano-3-(5-(9,9-dihexylfluoren-2-yl)thiophen-2-yl)acrylic acid (**5**).

The mechanism of alkylation with phase transfer catalyst to explain the critical role of tetraalkylammonium salts (Q^+X^-) in the reactions between two substances located in different immiscible phase is shown in Figure 3.4. Key to this tremendous enhancement in reactivity is the generation of a quaternary ammonium hydroxide, which makes the hydroxide anion soluble in organic solvents and sufficiently nucleophilic. The high rate of displacement is mainly due to two of the three characteristic features of the pairing cation (Q^+): high lipophilicity and the large ionic radius [44].

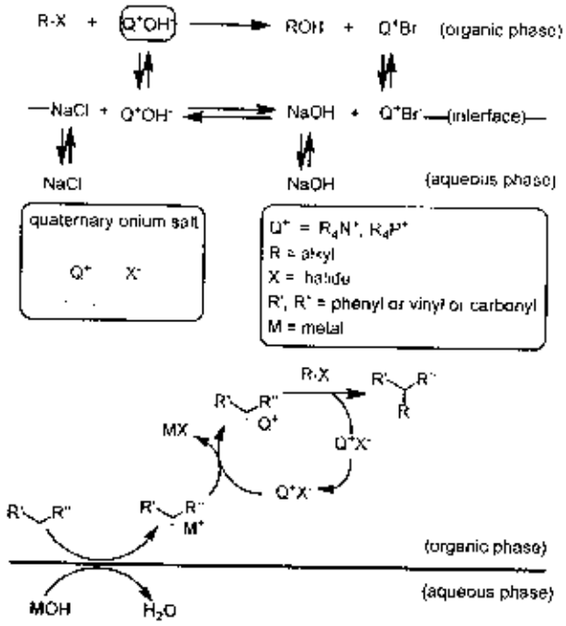

Figure 3.4 The proposed mechanism of alkylation.

For The synthesis of carbazole donor part starting with carbazole starting material (**25**) was iodinated in the mixture of KI (0.65 equiv.) and KIO_3 (0.50 equiv.) in AcOH at 80°C resulting in 3-iodocarbazole (**26**) in 84% yield (Figure 3.5). The structure of iodinated product (**26**) was confirmed by ^{1}H-NMR spectra (measured in $CDCl_3$) which exhibit very clear singlet signal of aromatic proton of C-4 carbazole at chemical shift at 8.33 ppm. Alkylation of **26** with 1-bromododecane in the presence of sodium hydride in DMF at room temperature gave 9-dodecyl-3-iodocarbazole (**1b**) in excellent yield. The Alkyl peaks were observed in ^{1}H-NMR spectrum of **1b** to confirm successful introduction of alkyl group to *N* position of carbazole. The extended carboxaldehyde functionalized thiophene intermediate (**2b**) was achieved by Suzuki condition as well. The coupling reaction between corresponding aryl halide (**1b**) and 5-formyl-2-thiopheneboronic acid yielded the aldehyde (**2b**) in 60%. This moderate yield are commonly observed in Suzuki coupling of 5-formyl-2-thiopheneboronic acid due to its unstable thiophene carboxaldehyde intermediate. The successful introduction of aldehyde functional group was confirmed by NMR and IR spectra. The singlet signal of aldehyde proton in $CDCl_3$ was located at chemical shift 9.88 ppm for aldehyde proton of **2b**. The signal of the aldehyde carbon atom was located at chemical shift 156.42 ppm for aldehyde carbon of **2b**. Finally the 6 dye was obtained by

Knoevenagel reaction of corresponding aldehyde (**2b**) with cyanoacetic acid. The **6** dye was obtained as orange amorphous solid. The solubility of dye in common organic solvent is pretty excellent owing to the long alkyl chain attached to *N* position of arylamine. The chemical structure of **6** was confirmed by NMR and IR analysis. The ^{1}H-NMR spectrum of the final product (**6**) show a singlet signal at chemical shift 8.50 (**1H**) ppm assigning as the proton of double bond indicating that **6** excises as *E* isomer which has higher photostability properties. The ^{13}C-NMR spectrum of **6** shows a single peak for chemically carbon atom of carbonyl group at 169.31 ppm and a single peak for carbon atom of cyano group at 117.74 ppm. Furthermore IR spectrum reveals the adsorption at 3420 cm^{-1} which is consistent with the presence of hydroxy group for **6** and at 2215 cm^{-1} which is consistent with the presence of cyano group for **6**.

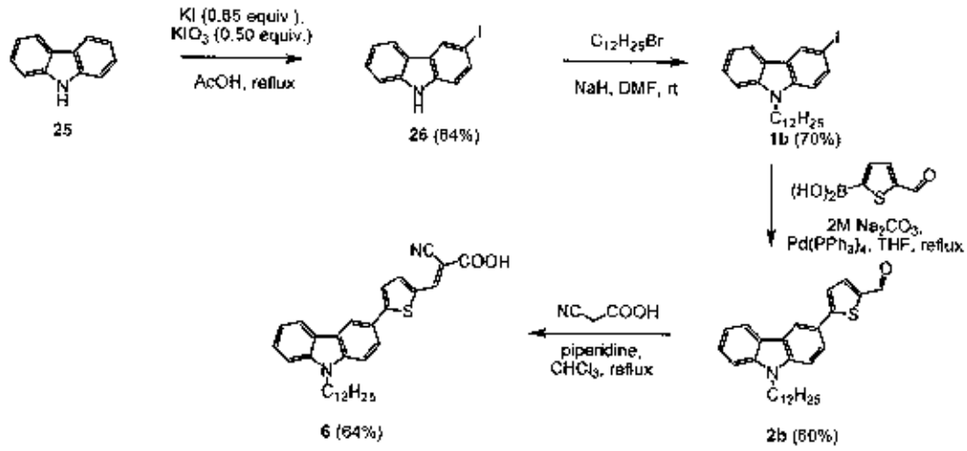

Figure 3.5 Synthesis of (*E*)-2-Cyano-3-(5-(9-dodecylcarbazol-3-yl)thiophen-2-yl)acrylic acid (**6**).

For The synthesis of phenothiazine donor part starting (Figure 3.6), start with alkylation of phenothiazine (**35**) with 1-bromododecane in the presence of sodium hydride in DMF at room temperature gave 10-dodecylphenothiazine (**36**) in excellent yield. The Alkyl peaks were observed in ^{1}H-NMR spectrum of **36** to confirm successful introduction of alkyl group to *N* position of phenothiazine. NBS bromination of the resultant thiophene intermediate in THF at room temperature afforded 3-bromo-10-dodecylphenothiazine (**1c**) in 80% yield. The structure of brominated product (**1c**) was confirmed by ^{1}H-NMR spectra (measured in $CDCl_3$) which exhibit very clear singlet signal of aromatic proton of C-4 phenothiazine at chemical shift at 7.29 ppm.

The extended carboxaldehyde functionalized thiophene intermediate (**2c**) was achieved by Suzuki condition as well. The coupling reaction between corresponding aryl halide (**1c**) and 5-formyl-2-thiopheneboronic acid yielded the aldehyde (**2c**) in 55%. This moderate yield are commonly observed in Suzuki coupling of 5-formyl-2-thiopheneboronic acid due to its unstable thiophene carboxaldehyde intermediate. The successful introduction of aldehyde functional group was confirmed by NMR and IR spectra. The singlet signal of aldehyde proton in $CDCl_3$ was located at chemical shift 9.84 ppm for aldehyde proton of **2c**. The signal of the aldehyde carbon atom was located at chemical shift 182.77 ppm for aldehyde carbon of **2c**. Finally the **7** dye was obtained by Knoevenagel reaction of corresponding aldehyde (**2c**) with cyanoacetic acid. The **7** dye was obtained as black amorphous solid. The solubility of dye in common organic solvent is pretty excellent owing to the long alkyl chain attached to *N* position of phenothiazine. The chemical structure of **7** was confirmed by NMR and IR analysis. The ^{1}H-NMR spectrum of the final product (**7**) show a singlet signal at chemical shift 8.23 (1H) ppm assigning as the proton of double bond indicating that **7** exeises as *E* isomer which has higher photostability properties. The ^{13}C-NMR spectrum of **7** show a single peak for chemically carbon atom of carbonyl group at 164.81 ppm and a single peak for carbon atom of cyano group at 116.97 ppm. Furthermore IR spectrum reveals the adsorption at 3442 cm^{-1} which is consistent with the presence of hydroxy group for **7** and at 2215 cm^{-1} which is consistent with the presence of cyano group for **7**.

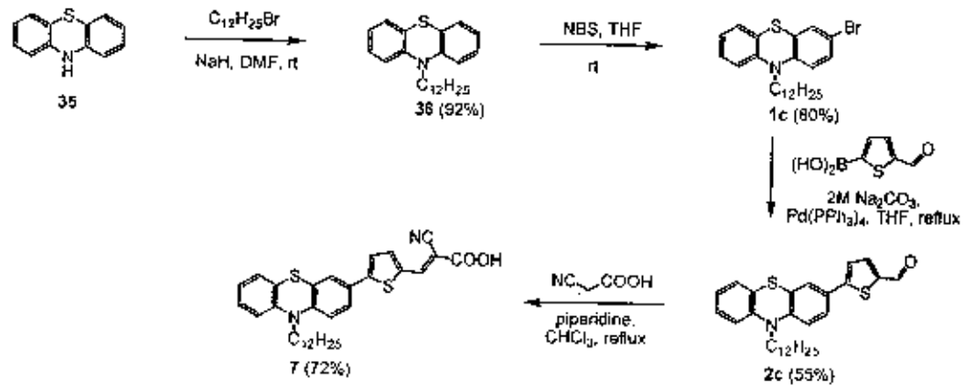

Figure 3.6 Synthesis of (*E*)-2-Cyano-3-(5-(10-dodecylphenothiazin-3-yl)thiophen-2-yl) acrylic acid (**7**).

3.3.2 Optical properties

The influence of different electron donors on the light harvest capacity of a dye molecule was first evaluated by recording the UV-vis absorption spectra of the dyes dissolved in dichloromethane (Figure 3.7), and the selected parameters were collected in Table 3.1. **5-7** showed the maximum absorption wavelength (λ_{max}) 425 nm (ε – 18,391 M^{-1} cm^{-1}), 422 nm (ε = 36,476 M^{-1} cm^{-1}) and 470 nm (ε = 16,326 M^{-1} cm^{-1}), respectively, which were corresponding to HOMO (highest occupied molecular orbital) -> LUMO (lowest unoccupied molecular orbital) transition. Amongst these photosensitizers, due to strong electron donating ability of the phenothiazine unit, the **7** dye with the phenothiazine electron donor presents the longest maximum absorption wavelength, which is an advantageous spectral property for light harvesting of the solar spectrum. We observed that the **5-7** dyes exhibited strong luminescence maxima of 531-587 nm when it is excited within its π-π^* band in solution at room temperature showed the emission peak located in the green-yellow region. The energy band gaps of the **5-7** dyes were estimated to be 2.54, 2.41, and 2.20 eV, respectively, from the absorption edge of the solution spectra.

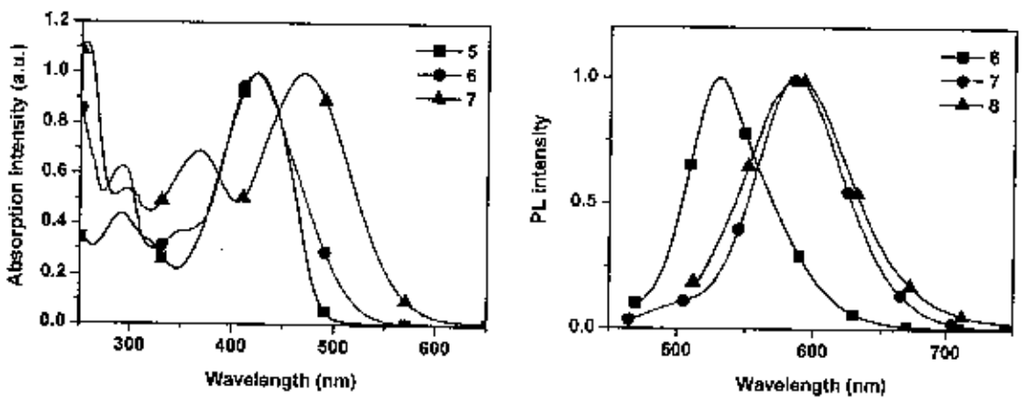

Figure 3.7 Absorption (left) and emission (right) spectra of **5-7** recorded in dichloromethane.

Table 3.1 The absorption and fluorescence data of **5-7**

Compound	λ_{max}^{abs} (εx 10^4); (nm (M^{-1} cm^{-1}))[a]	λ_{max}^{em} (nm)[a, b]	λ_{onset}^{abs} (nm)[a]	E_g (eV)[c]
5	425 (1.84), 291 (0.80)	531	488	2.54
6	422 (3.65), 291 (2.28)	587	515	2.41
7	470 (1.63), 368 (1.13), 297 (0.88)	587	564	2.20

[a] measured in dichloromethane solution at room temperature.

[b] excited at maximum absorption in solution.

[c] estimated from the onset of absorption (E_g =1240/λ_{onset}).

The effect of solvent polarity on the absorption spectra of **6** dye was also studied (Figure 3.8 and Table 3.2). The absorption was measured in five different solvents dimethylformamide (DMF), dimethylsulfoxide (DMSO), ethanol (EtOH), tetrahydrofurane (THF) and dichloromethane (DCM)). We assigned the absorption bands at 291 nm as **B1** and at 398-422 nm as **B2**, respectively. There is only **B2** band that be effected by solvent polarity change. These **B2** bands therefore are assigned as ICT bands of donor-accepter molecule which can be generally observed in most sensitizer. The absorption spectra show blue shift when the polarity of solvents are increasing. **6** in DMF exhibited lowest maximum absorption at 398 nm (4.99 x 10^{-19} *J*), whereas **6** in dichloromethane exhibited the highest at 422 nm (4.71 x 10^{-19} *J*). These results can be considered as the negative solvatochromism-physical intermolecular solute-solvent interaction forces which tend to alter the energy difference between ground and excited state of chromophore of the dyes [42]. The polar solvents are good supporting solvent to the excited state dye species more than non-polar solvents resulting in close molecular orbital, which tends to absorb light at high energy region (low wavelength). This effect was also found in the other molecules (**5** and **7**).

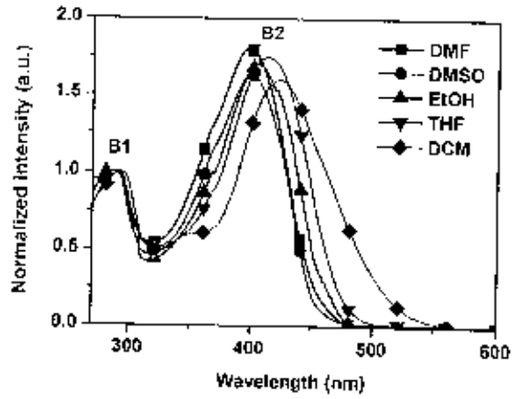

Figure 3.8 The absorption spectra of **6** dye in various solvents.

Table 3.2 Maximum absorption of **6** measured in various solvents

solvent	DMF	DMSO	EtOH	THF	DCM
λ_{max} (nm)	398	399	405	412	422
E^a (10^{-19} J)	4.99	4.98	4.91	4.82	4.71

[a] calculated from $E = h\nu/\lambda$.

3.3.3 Thermal properties

The thermal degradation of **5-7** were studied by thermogravimetric analysis under nitrogen atmospheric condition. TGA thermograms of the dyes are displayed in Figure 3.9 and $T_{5\%}$ are listed in Table 3.3. The dyes exhibit 5% weight loss at 228, 240 and 245 °C suggested that the dyes were thermally stable materials with temperature over 228 °C which is good for long term stability of DSCs devices.

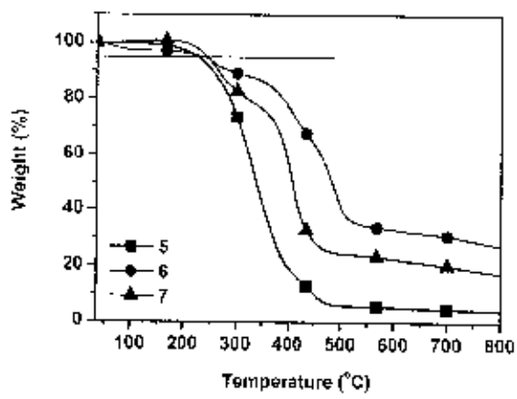

Figure 3.9 TGA thermograms of 5-7 dyes.

Table 3.3 Thermal properties of 5-7

Compound	$T_{5\%}$ (°C)
5	228
6	240
7	245

3.3.4 Molecular orbital calculation

To get further insight into the effect of molecular structures and electron distributions of the three dyes on the performances of DSCs, their geometries and energies were optimized by density functional theory (DFT) calculations. The HOMO is mainly located on the electron donating group and π-spacer, and the LUMO is mainly located in electron withdrawing groups through the π-spacer. It reveals that the thiophene π-spacer is essentially coplanar with cyanoacetic acid group. There are effective electron separations between HOMO and LUMO of these dyes induced by light irradiation. . This supports the supposed push-pull characteristics of these sensitizers (Figure 3.10). In addition, the optimized geometry of 5-7 indicates that the arylamine moiety at the end of the molecule are in 3-D spatial arrangement, which makes the molecular structure nonplanar due to the twist conformation around the aryl or arylamine-thiophene C-C bond. The nonplanar molecular structure of 5-7 could be beneficial to solution-processability to form amorphous film. 5-7 are soluble in common organic solvents such

as THF, CH_2Cl_2, $CHCl_3$ and acetone. High-quality amorphous film can be obtained by spin-coating its solution.

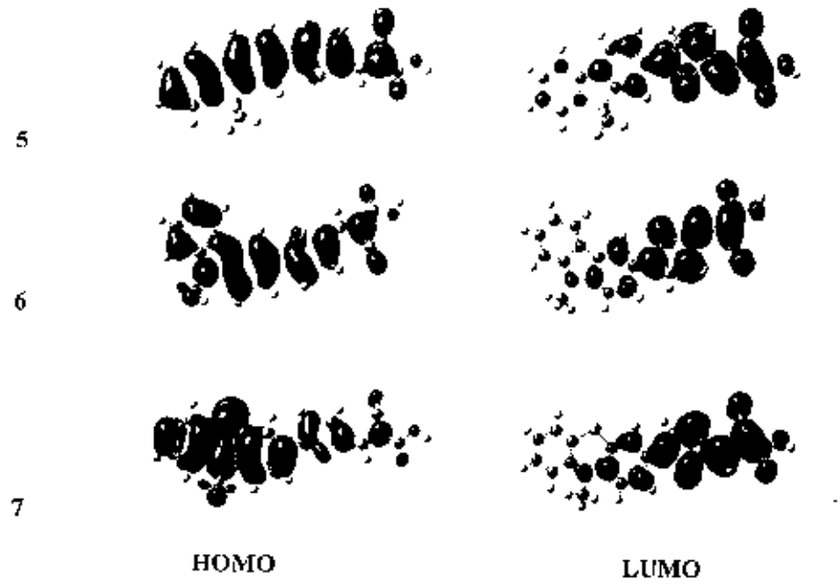

Figure 3.10 HOMO and LUMO distribution of the **5-7** dyes calculated with DFT on a BTLYP/6-31G(d,p) level.

3.4 Conclusions

Novel D-π-A organic dyes, **5-7**, have synthesized as photosensitizers for DSCs applications by using alkylation, halogenation, Suzuki coupling and Knoevenagel condensation reaction. Different arylamine moieties are introduced to the molecules and serve as electron donor group. The electron-withdrawing part is cyanoacrylic acid group. The target molecules were characterized by using NMR, IR, UV-vis and fluorescence techniques. The target molecules exhibit a adsorption band cover UV and visible region. Fluorescence spectra of the target molecules show emission peak at green-yellow region, excited at λ_{max} of each molecule. **5-7** show a good thermal properties. DFT calculations have been performed on the dyes, and the results show that electron distribution from the whole molecules to the anchoring moieties occurred during the HOMO-LUMO excitation.

CHAPTER 4

SYNTHESIS AND CHARACTERIZATION OF NOVEL BISCARBOZOLE WITH OLIGO-4-HEXYLTHIOPHENE FOR DYE SOLAR CELLS

4.1 Introduction

In 2013, Taweesak Sudyoadsuk et al. [53] reported that the highly efficient and stable organic dyes (CCTA) composed of *N*-dodecyl-3-(3,6-di-tert-butylcarbazol-*N*-yl)carbazol-6-yl as the electron donor, thiophene as π-spacer and cyanoacrylic acid moiety as the electron acceptor. The CCTA-sensitized solar cell produces higher device performance with an overall conversion efficiency of 5.69% [a short circuit current (J_{sc}) = 11.31 mA cm^{-2}, an open-circuit voltage (V_{oc}) = 0.71 V, and a field factor (ff) = 0.71] reaching >96% of the reference N719-based device (overall conversion efficiency = 5.92%).

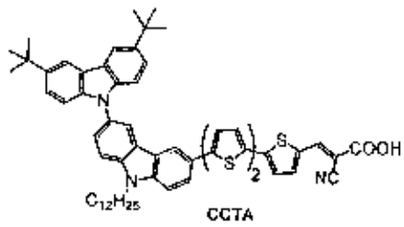

CCTA

Figure 4.1 Chemical structures of CCTA.

One way to increase the efficiency of the DSCs is to prevent recombination of electrons from the semiconductor to the electrolyte. This can be achieved by introducing alkyl chains in the linker part of the dye, forming an insulating layer yielding an increased electron lifetime in the DSCs (Figure 4.2, **MK-1**) [45,46]. The alkyl chains are also believed to prevent aggregate formation on the surface of the TiO_2. However, in 2007 Kim et al. reported a negative influence of the efficiency when introducing alkyl chains in the linker part of the dye (Figure 4.2, **JK-43**) [47].

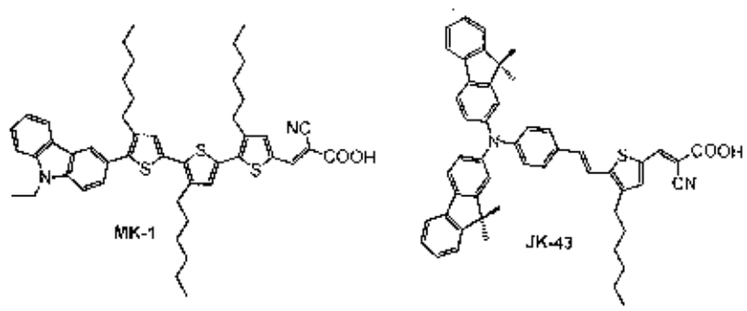

Figure 4.2 Examples of dyes (**MK-1** and **JK-43**)with alkyl chains on the linker.

4.2 Aim of the Study

In this work, we synthesized three carbazole-encabed with 3,6-di-*tert*-butylcarbazole based D-π-A organic dyes for DSCs application. It is well known that changes in molecular structure and conjugation system can induce very different optical and physical properties of the D-π-A compounds (see Figure 4.3). These compounds have been constructed based on the electron-donating moiety, substituted carbazole with 3,6-positions of carbazole being substituted with t-butyl group to prevent oxidative coupling. Carbazole bearing alkyl groups at the *N* position, to increase the solubility property and to prevent the recombination of the electrons from the semiconductor to the electrolyte. Different numbers of electron spacers are 4-hexylthiophene moieties, which are considered to be the ideal constructional unit in dye sensitizer engineering, adopted for expansion of the π-conjugating backbone and adjusting the absorption spectra and HOMO/LUMO levels of the dyes. The dyes have a cyanoacrylic acid group as electron-withdrawing part and for anchoring onto the TiO_2 surface.

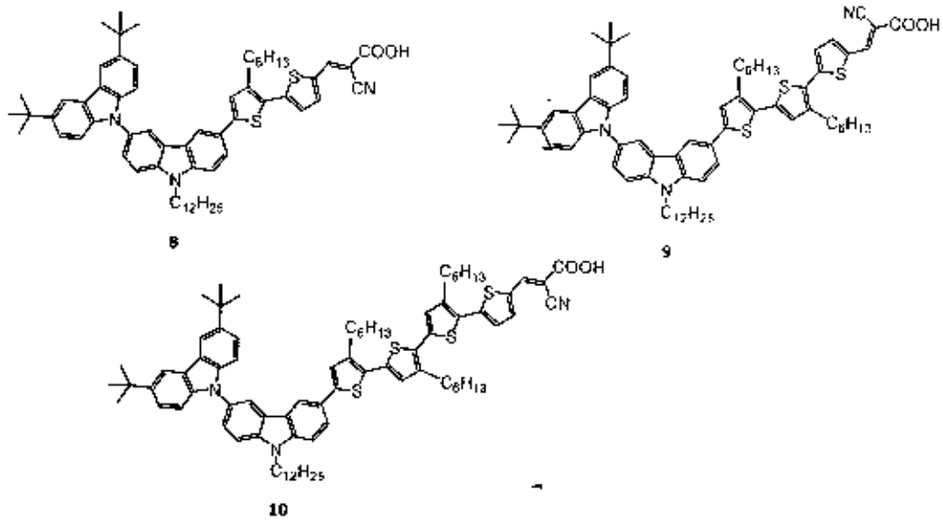

Figure 4.3 Chemical structures of D-π-A organic dyes (**8-10**).

4.3 Results and Discussion

4.3.1 Synthesis

The synthesis of carbazole donor part starting with carbazole starting material (**25**) was iodinated in the mixture of KI (1.30 equiv.) and KIO_3 (1.00 equiv.) in AcOH at 80 °C resulting in 3,6-diiodocarbazole (**37**) in 95% yield (Figure 4.4). The structure of iodinated product was confirmed by The ^{1}H-NMR spectrum of the **37** (measured in $CDCl_3$) shows a singlet signals at chemical shift 8.32 ppm (2H) assigning of 4-H and 5-H protons of carbazole adduct, a singlet signal at chemical shift 8.08 ppm (1 H) assigning as 9-H of carbazole unit. The *N*-H starching of free amine was also observed in IR spectrum at wavenumber 3413 cm^{-1} of **37**. Alkylation of **37** with 1-bromododecane in the presence of sodium hydride in DMF at room temperature gave 9-dodecyl-3,6-diiodocarbazole (**38**) in 56% yield. The chemical structure of **38** was confirmed by ^{1}H-NMR analysis. The ^{1}H-NMR of the alkylated product shows singlet signal at chemical shift 8.30 ppm (2H) ppm assigning as proton of carbazole ring at C-4 and C-5 position, triplet signal at chemical shift 4.18 ppm (2H, J = 6.7 Hz) assigning as proton of alkyl group of *N*-CH_2 of carbazole adduct.

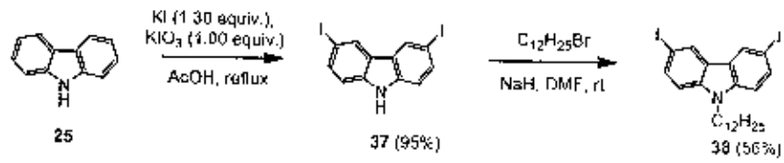

Figure 4.4 Synthesis of 9-dodecyl-3,6-diiodocarbazole (**38**).

The 3,6-di-*tert*-butylcarbazole-endcapped-carbazole donor part was prepared by Ullmann coupling reaction between 3,6-di-*tert*-butylcarbazole and excess amount of alkylated diiododicarbazole (**38**) yielded mono-substituted carbazole (**39**) as product. The tertiary butyl groups at position 3 sand 6 of carbazole were introduced in purpose of steric hindrance and oxidative coupling protection which is commonly observed in arylamine materials. The successful coupling between 9-dodecyl-3,6-diiodocarbazole and 3,6-di-*tert*-butylcarbazole was confirmed by ^{1}H-NMR spectrum. The singlet signal at chemical shift 8.34 (1H), 8.18 (2H) and 8.15 (1H) ppm was observed which contribute to the proton at position 4 and 5 of carbazole moiety.

To elongate the conjugation of the molecules, mono, di and tri(4-hexylthiophene) was introduced to donor using combination reaction of Suzuki coupling and bromination. Suzuki coupling reaction of 2-(4-hexylthiophen-2-yl)-4,4,5,5-tetramethyl-1,3,2-dioxaborolane and the corresponding halide-compound employed in order to increase the number of 4-hexylthiophene units in the molecules. The 4-hexylthiophene intermediates were prepared by using $Pd(PPh_3)_4$ as catalyst in the presence of aqueous sodium carbonate solution in THF at refluxing temperature afforded the 4-hexylthiophene adduct (**40-42**) in range 69-99 % yield. The bromination reaction was carried out in THF as solvent with NBS. The reaction mixture was stirred at room temperature for 30 min to directly yield bromo compound (**43-45**).

The extended carboxaldehyde functionalized thiophene intermediate (**46-48**) were achieved by Suzuki condition as well. The coupling reaction between corresponding aryl halide (**43, 44 and 45**) and 5-formyl-2-thiopheneboronic acid (Figure 4.5) yielded the aldehyde (**46**, **47** and **48**) in 70, 76 and 63%, respectively. This moderate yield are commonly observed in Suzuki coupling of 5-formyl-2-thiopheneboronic acid due to its unstable thiophene carboxaldehyde intermediate. The successful introduction of aldehyde functional group was confirmed by NMR and IR spectra. The singlet signal of aldehyde proton in $CDCl_3$ was located at chemical shift 9.85, 9.88 and 9.80 for aldehyde protons of **46**, **47** and **48**, respectively. The signal

of the aldehyde carbon atom was located at chemical shift 182.60, 182.60 and 182.59 ppm for aldehyde carbon of **46, 47** and **48**, respectively. The IR peaks of C=O stretching of aldehyde was also observed at wavenumber 1668, 1657 and 1647 cm^{-1} of **46**, **47** and **48**, respectively. Finally the dyes were obtained by Knoevenagel reaction of corresponding aldehyde (**46-48**) with cyanoacetic acid. All dyes (**8-10**) were obtained as orange, red and dark red amorphous solid. The solubility of dyes in common organic solvent is pretty excellent owing to the long alkyl chain attached to *N* position of carbazole and 4 position of thiophene. The chemical structure of **8-10** was confirmed by NMR and IR analysis. The ^{1}H-NMR spectrum of the final products (**8-10**) show a singlet signal at chemical shift 8.18 (1H), 8.19 (1H), and 8.15 (1H) ppm assigning as the proton of double bond indicating that **8-10** excises as *E* isomer which has higher photostability properties. The ^{13}C-NMR spectra of **8-10** shows a single peak for chemically carbon atom of carbonyl group at 169.43, 169.37, and 164.85 ppm , respectively, and a single peak for carbon atom of cyano group at 116.40, 116.39, and 116.60 ppm , respectively. Furthermore IR spectrum reveals the adsorption at 3421, 3416, and 3411 cm^{-1} which is consistent with the presence of hydroxy group for **8-10**, respectively, and at 2213, 2211, and 2207 cm^{-1} which is consistent with the presence of cyano group for **8-10**, respectively.

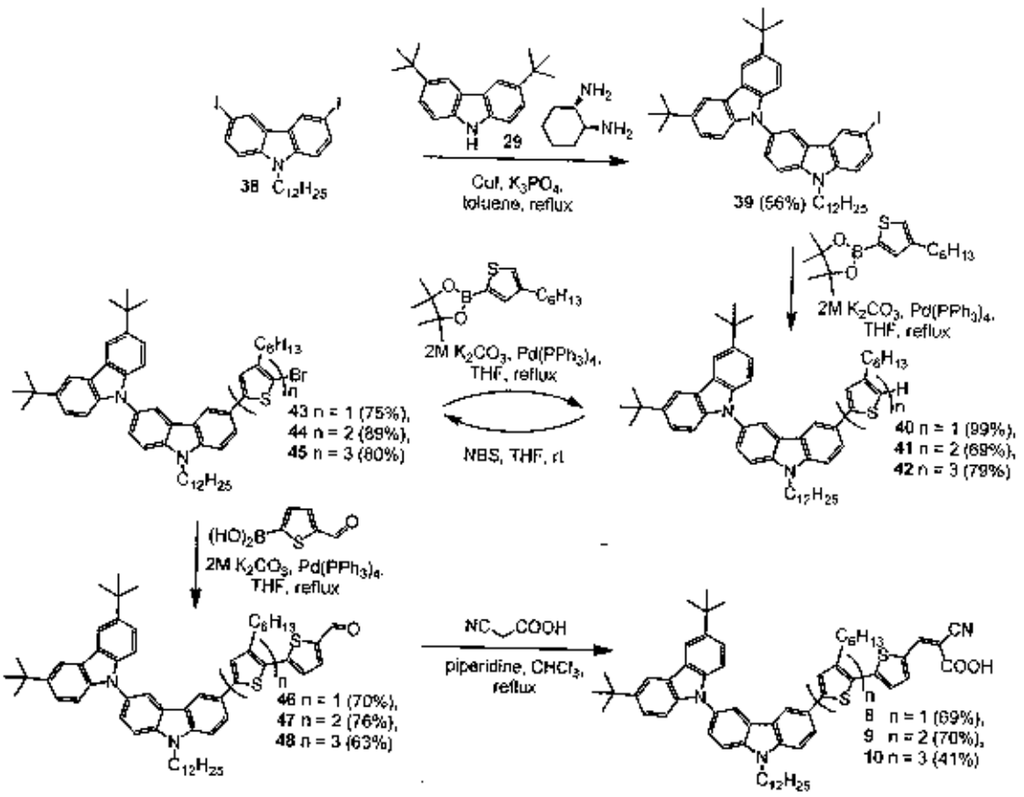

Figure 4.5 Synthesis of D-π-A organic dyes (**8-10**).

4.3.2 Optical properties

The UV-vis and fluorescence spectra of dyes in CH_2Cl_2 are shown in Figure 4.6 and listed in Table 4.1. In solution, all three dyes show similar characteristic of donor-accepter arylamine dyes which show strong absorption bands around 290-400 nm corresponds to π-π^* transition and broad absorption bands around 420-600 nm corresponds to Inframolecular Charge transfer Transition (ICT) of donor-accepter compound [48]. The bathochromic shifted (red shifted) absorption spectra and larger molar extinction coefficient (ε) were observed when more 4-hexylthiophene units were introduced. The red shift in absorption can be attributed to the extended conjugation system of the entire structure. The fluorescence emission spectra showed a red-shift upon increased number of 4-hexylthiophene units in the molecule, which is roughly parallel to the trend of the absorption spectra (Figure 4.6 (left)) due to the elongation of the conjugation in molecules. We observed that the **8-10** dyes exhibited strong luminescence maxima of 614-620 nm when it is excited within its π-π^* band in solution at room temperature

showed the emission peak located in the orange region. The energy band gaps of the **8-10** dyes were estimated to be 2.20, 2.09, and 2.16 eV, respectively, from the absorption edge of the solution spectra.

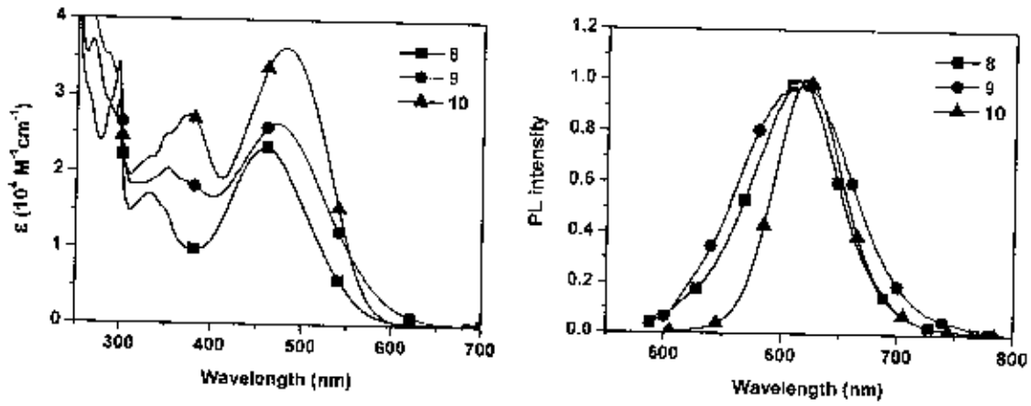

Figure 4.6 Absorption (left) and emission (right) spectra of **8-10** recorded in dichloromethane.

Table 4.1 The absorption and fluorescence data of **8-10**

Compound	λ_{max}^{abs} (εx 10^4); (nm (M^{-1} cm^{-1}))[a]	λ_{max}^{em} (nm)[a,b]	λ_{onset}^{abs} (nm)[a]	E_g (eV)[c]
8	460 (2.33), 332 (1.71), 297 (2.91)	614	563	2.20
9	472 (2.64), 351 (2.04), 297 (3.43)	616	593	2.09
10	480 (3.64), 375 (2.75), 296 (3.39)	620	573	2.16

[a] measured in dichloromethane solution at room temperature.

[b] excited at maximum absorption in solution.

[c] estimated from the onset of absorption ($E_g = 1240/\lambda_{onset}$).

The effect of solvent polarity on the absorption spectra of **8** dye was also studied (Figure 4.7 and Table 4.2). The absorption was measured in five different solvents dimethylformamide (DMF), ethanol (EtOH), dimethylsulfoxide (DMSO), tetrahydrofurane (THF) and dichloromethane (DCM)). We assigned the absorption bands at 297 nm as **B1**, at 332 nm as

B2 and at 423-460 nm as **B3**, respectively. There is only **B3** band that be effected by solvent polarity change. These **B3** bands therefore are assigned as ICT bands of donor-accepter molecule which can be generally observed in most sensitizer. The absorption spectra show blue shift when the polarities of solvents are increasing. **8** in DMF exhibited lowest maximum absorption at 423 nm (4.70×10^{-19} *J*), whereas **8** in dichloromethane exhibited the highest at 460 nm (4.32×10^{-19} *J*). These results can be considered as the negative solvatochromism-physical intermolecular solute-solvent interaction forces which tend to alter the energy difference between ground and excited state of chromophore of the dyes [42]. The polar solvents are good supporting solvent to the excited state dye species more than non-polar solvents resulting in close molecular orbital, which tends to absorb light at high energy region (low wavelength). This effect was also found in the other molecules (**9** and **10**).

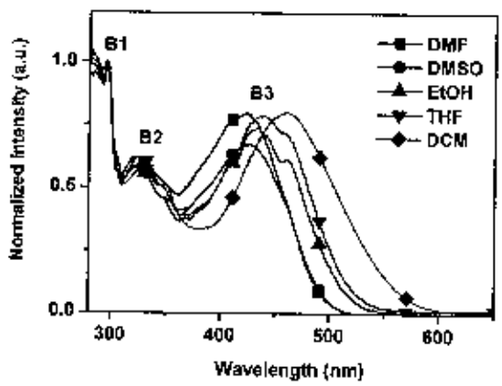

Figure 4.7 The absorption spectra of **8** dye in various solvents.

Table 4.2 Maximum absorption of **8** measured in various solvents

solvent	DMF	DMSO	EtOH	THF	DCM
λ_{max} (nm)	423	425	435	440	460
E^a (10^{-19} *J*)	4.70	4.68	4.57	4.52	4.32

[a] calculated from $E = h\nu/\lambda$

4.3.3 Thermal properties

The thermal decomposition of **8-10** dyes was studied by thermogravimetric analysis under nitrogen atmospheric condition. TGA thermograms of the dyes are displayed in

Figure 4.8 and T_{5d} are listed in Table 4.3. The dyes exhibit 5% weight loss between 226 and 257 °C suggested that the dyes were thermally stable materials with temperature over 226 °C which is good for long term stability of DSCs devices.

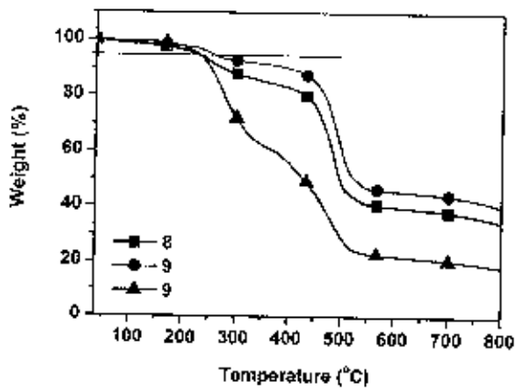

Figure 4.8 TGA thermograms of **8-10** dyes.

Table 4.3 Thermal properties of **8-10**

Compound	T_{5d} (°C)
8	226
9	257
10	229

4.3.4 Molecular orbital calculation

To get an insight into the molecular structure and electron distribution of the organic dye, the **8-10** dyes geometries have been optimized using DFT calculations with Gaussian 03 program. The calculations were performed with the BTLYP exchange correlation functional under 6-31G(d,p) basis set. Computed HOMO and LUMO distribution of **8-10** are depicted in Figure 4.9. The general characters of the orbitals are independent of the linker length and different electron acceptor. The HOMO is of π-characteristics and is delocalized over the entire molecule, including the carbazole groups. In the LUMO, which also has π-character, there is essentially no contribution from the carbazole groups, and the electron density has been shifted towards the acceptor group of the sensitizer. This supports the supposed push-pull

characteristics of these sensitizers. In addition, the optimized geometry of **8-10** indicates that the carbazole moiety at the end of the molecule are in 3-D spatial arrangement, which makes the molecular structure nonplanar due to the twist conformation around the carbazole-carbazole C-*N* bond. The nonplanar molecular structure of **8-10** could be beneficial to solution-processability to form amorphous film. **8-10** are soluble in common organic solvents such as THF, CH_2Cl_2, $CHCl_3$ and acetone. High-quality amorphous film can be obtained by spin-coating its solution.

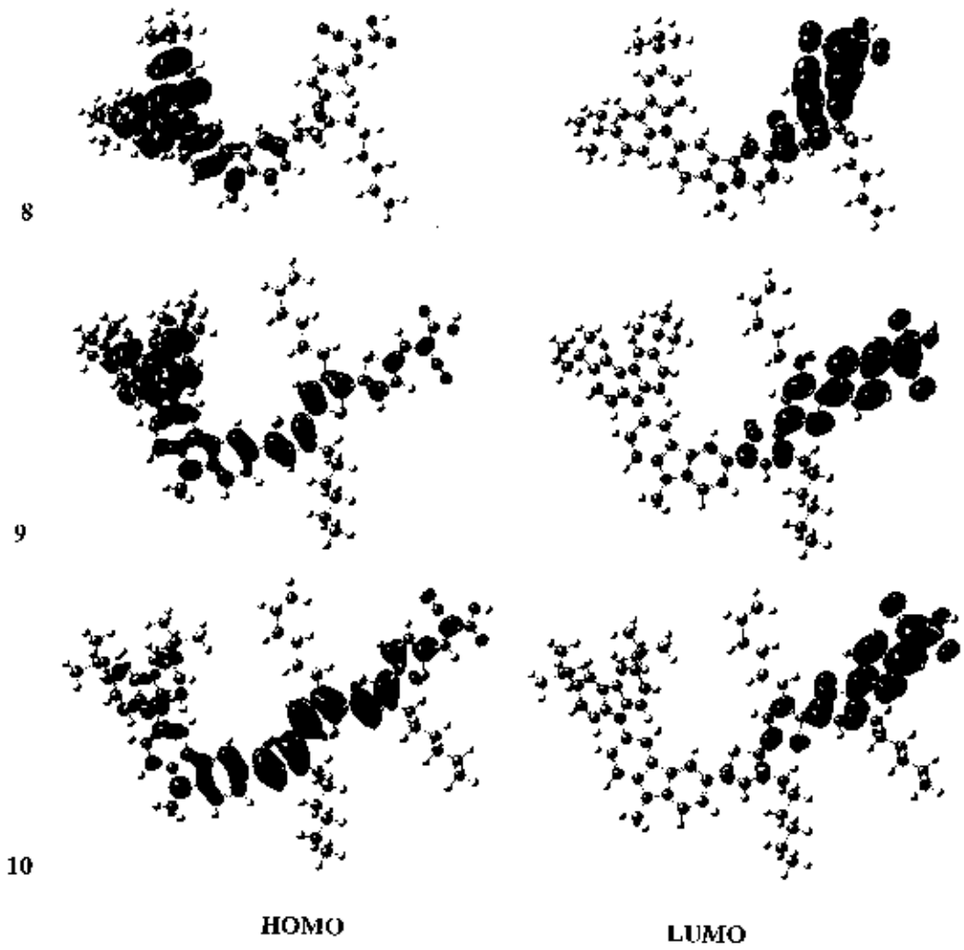

Figure 4.9 HOMO and LUMO distribution of the **8-10** dyes calculated with DFT on a BTLYP/6-31G(d,p) level.

4.4 Conclusions

Novel D-π-A organic dyes, **8-10**, have been synthesized as photosensitizers for DSCs applications by using Ullmann coupling, Suzuki coupling and Knoevenagel condensation reaction. Different number of 4-hexylthiophene moieties is introduced to the molecules and serve as linker. The electron-withdrawing parts are cyanoacrylic acid groups. The target molecules were characterized by using NMR, IR, UV-vis and fluorescence techniques. The target molecules exhibit a adsorption band cover UV and visible region. Fluorescence spectra of the target molecules show emission peak at orange region, excited at λ_{max} of each molecule. **8-10** show a good thermal properties. DFT calculations have been performed on the dyes, and the results show that electron distribution from the whole molecules to the anchoring moieties occurred during the HOMO-LUMO excitation.

CHAPTER 5

SYNTHESIS AND CHARACTERIZATION OF NOVEL BISCARBOZOLE WITH DIFFERENT π-SPACER UNITS FOR DYE SOLAR CELLS

5.1 Introduction

In 2011, Dan Deng et al. [49] investigated that the TPA-containing linear D-A-D molecules with benzothiadiazole (**BT**) as acceptor unit and TPA-(4-hexyl)thiophene (**TPA-HT**) and TPA-(4-hexyl)thieno[3,2-b]thiophene (**TPA-HTT**) as donor units, **TPA-HT-BT** and **TPA-HTT-BT**, gave an overall conversion efficiency (η) of 1.44%. The design of the molecular structure was from the following consider-ations:

(1) the D-A-D structure of the molecules is to reduce the band gap of the materials for improving the absorption;

(2) (4-hexyl)thieno[3,2-b]thiophene is introduced in **TPA-HTT-BT** for enhancing the hole mobility and improving absorption of the compounds, because fused thiophenes usually show larger pconjugation and higher hole mobility.

TPA-HT-BT and **TPA-HTT-BT** films show broad absorption band in the range of 350--700 nm, lower band gap and good thermal stability. The solution processed bulk-heterojunction OSC devices based on the blend of **TPA-HT-BT** or **TPA-HTT-BT** as donor and PC70BM as acceptor (the weight ratio of donor/acceptor is 1:3), reached 1.44% under the illumination of AM1.5 G, 100 mW/cm^2, which indicates that **TPA-HT-BT** and **TPAHTT-BT** are promising organic donor photovoltaic materials.

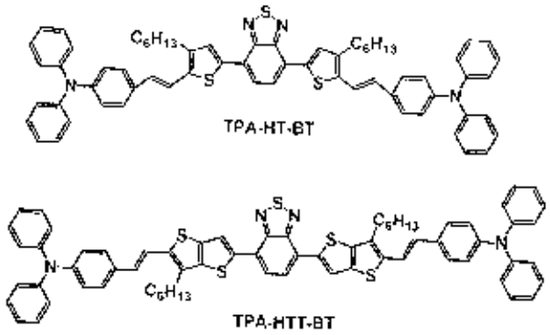

Figure 5.1 Chemical structures of **TPA-HT-BT** and **TPA-HTT-BT**.

5.2 Aim of the Study

In this work, we synthesized three biscarbazole based D-π-A organic dyes for DSCs application. It is well known that changes in molecular structure and conjugation system can induce very different optical and physical properties of the D-π-A compounds (see Figure 5.2). These compounds have been constructed based on the electron-donating moiety, substituted carbazole with 3,6-positions of carbazole being substituted with t-butyl group to prevent oxidative coupling. Carbazole bearing alkyl groups at the *N* position, to increase the solubility property and to prevent the recombination of the electrons from the semiconductor to the electrolyte. Different types of electron spacers containing thiophene moiety, which are considered to be the ideal constructional unit in dye sensitizer engineering, adopted for expansion of the π-conjugating backbone and adjusting the absorption spectra and HOMO/LUMO levels of the dyes. The dyes have a cyanoacrylic acid group as electron-withdrawing part and for anchoring onto the TiO_2 surface.

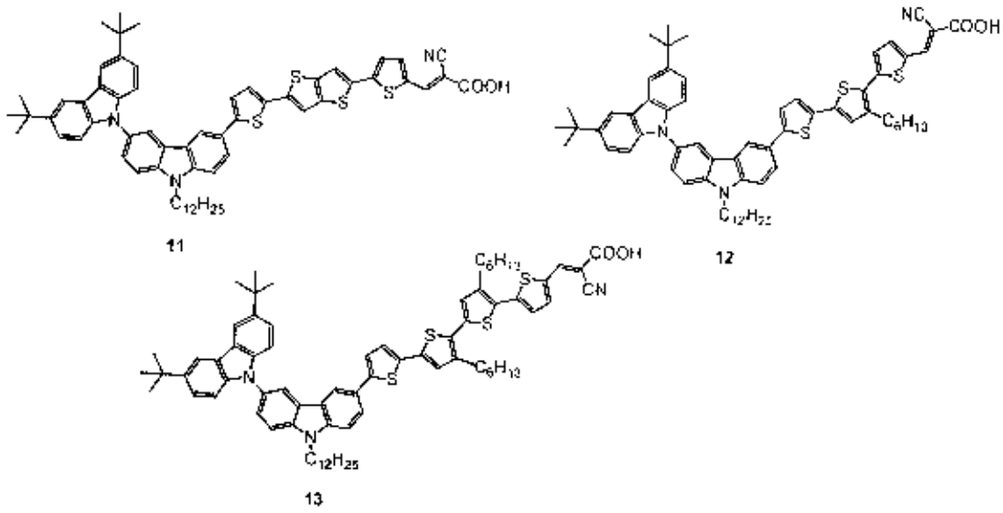

Figure 5.2 Chemical structures of **11-13.**

5.3 Results and Discussion

5.3.1 Synthesis

For the synthesis of bicarbazole based dye having the 4-hexylthiophene and thieno[3,2-b]thiophene as different types of electron spacers used a combination of Suzuki coupling, bromination and Knoevanegel reaction as depicted in Figure 5.3 and 5.4.

To elongate the conjugation of the molecules, mono thiophene was introduced to donor using combination reaction of Suzuki coupling and bromination. Monothiophene intermediate (**49**) was prepared by coupling reaction between donor (**39**) and 2-thiopheneboronic acid using tetrakis(triphenylphosphine)palladium(0) as catalyst, sodium carbonate as base in THF/H_2O at reflux and obtained in good yield. NBS bromination of the resultant thiophene intermediate in THF at room temperature afforded bromothiophene intermediate (**50**) in moderate yield.

Suzuki coupling reaction of bromothiophene intermediate (**50**) and thieno[3,2-b]thiophen-2-ylboronic acid (**1d**) or 2-(4-hexylthiophen-2-yl)-4,4,5,5-tetramethyl-1,3,2-dioxaborolane (**1e**) employed in order to increase the different types of electron spacers units in the molecules. The 4-hexylthiophene and thieno[3,2-b]thiophene intermediates were prepared according to the procedure described for **40** (Chapter 4) and obtained as yellow solid in 48 and 93

% yield, respectively. The bromination reaction was carried out according to the procedure described for **50** and obtained as yellow solid in 55 and 99% yield, respectively.

The extended carboxaldehyde functionalized thiophene intermediate (**4d** and **4e**) were achieved by Suzuki condition as well. The coupling reaction between corresponding aryl halide (**3d** and **3e**) and 5-formyl-2-thiopheneboronic acid yielded the aldehyde (**4d** and **4e**) in 44 and 99%, respectively. This moderate yield are commonly observed in Suzuki coupling of 5-formyl-2-thiopheneboronic acid due to its unstable thiophene carboxaldehyde intermediate. The successful introduction of aldehyde functional group was confirmed by NMR and IR spectra. The singlet signal of aldehyde proton in $CDCl_3$ was located at chemical shift 9.86 and 9.88 ppm for aldehyde protons of **4d** and **4e**, respectively. The signal of the aldehyde carbon atom was located at chemical shift 182.86 and 182.50 ppm for aldehyde carbon of **4d** and **4e**, respectively. Finally the dyes were obtained by Knoevenagel reaction of corresponding aldehyde (**4d** and **4e**) with cyanoacetic acid. All dyes were obtained as orange, red and dark red amorphous solid.

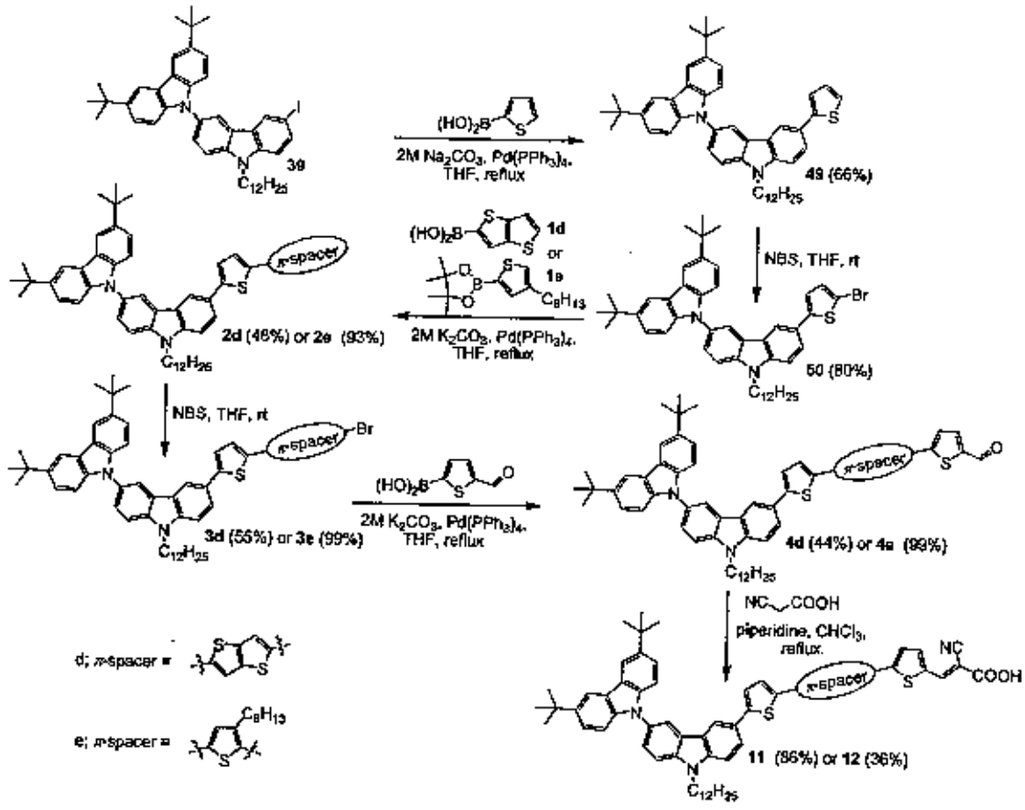

Figure 5.3 Synthesis of D-π-A organic dyes (**11** and **12**).

For the synthesis of bicarbazole based dye having the bi(4-hexylthiophene) as electron spacers was prepared from Suzuki coupling, Bromination and Knoevanegel reaction according to the procedure described above and obtained as dark red solid in 45% yield (Figure 5.4). The successful introduction of aldehyde functional group was confirmed by ^{1}H-NMR, ^{13}C-NMR and IR spectra. The singlet signal of aldehyde proton in $CDCl_3$ was located at chemical shift 9.80 for aldehyde protons of **53**, respectively. The signal of the aldehyde carbon atom was located at chemical shift 182.87 ppm for aldehyde carbon of **53**. The IR peak of C=O stretching of aldehyde was also observed at wavenumber 1655 cm^{-1}.

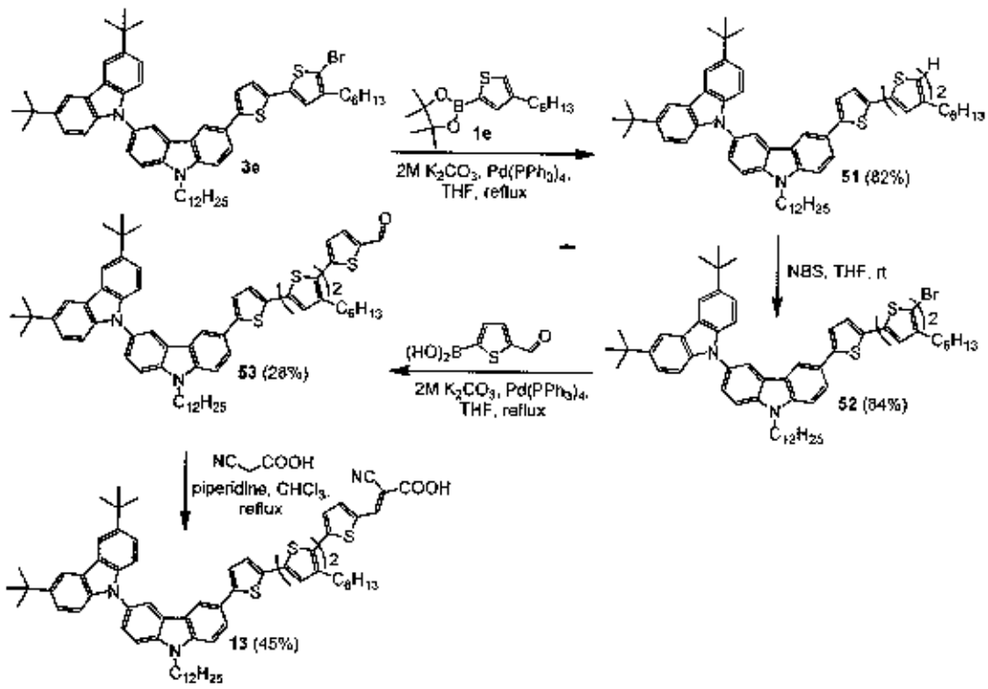

Figure 5.4 Synthesis of D-π-A organic dye (**13**).

5.3.2 Optical properties

The UV-vis and fluorescence spectra of dyes in CH_2Cl_2 are shown in Figure 5.5 and listed in Table 5.1, together with the UV-vis spectra of the corresponding dyes absorbed on TiO_2 film. In solution, all three dyes show similar characteristic of donor-accepter arylamine dyes which show strong absorption bands around 290-400 nm corresponds to π-π^* transition and broad absorption bands around 420-600 nm corresponds to Intramolecular Charge transfer Transition

(ICT) of donor-accepter compound [48]. The **12** dye have mono(4-hexylthiophene) unit as π-spacer. This dye is larger molar extinction coefficients (ε) and red shifted as compared to that **11** dye have thieno[3,2-b]thiophene unit as π-spacer. This results indicates the presence of mono(4-hexylthiophene) unit in photosensitizer could increase the light harvesting efficiency and increased the extension of π system due mono(4-hexylthiophene) is larger π-conjugating system. In addition, **13** dye have di(4-hexylthiophene) unit as π-spacer. This dye is smaller molar extinction coefficients (ε) and blue shifted as compared to that **12** dye. This is due to arrangement of di(4-hexylthiophene) unit can induce the non-planar structure. We observed that the **11-13** dyes exhibited strong luminescence maxima of 500-604 nm when they are excited within their π–π^* bands in solution at room temperature showed the emission peak located in the cyan-orange region. The energy band gaps of the **11-13** dyes were estimated to be 2.34, 2.11 and 2.08 eV, respectively, from the absorption edge of the solution spectra.

When the dyes are attached to TiO_2 surface, the absorption spectra of these dyes are broadened and blue-shifted more or less as compared to that in solutions (Figure 5.6), indicating strong interactions between the dyes and the semiconductor surface. Also, the strong interaction between the surface and the absorbed molecules often lead to aggregation effect. The red shifted and blue shifted values of different dyes are changed obviously depending on the different electron spacer. These values may be results of J and H-type aggregation of the dyes on TiO_2 surface. 4-hexylthiophene and thieno[3,2-b]thiophene as different types of electron spacers in the molecules could increase the different type aggregation effect of adsorbed dyes. One can find that the red-shift values of **11** dye adsorbed onto TiO_2 surface is 44 nm, indicating that **11** dye have a more tendency to J-aggregate on TiO_2. On the other hand, the maximum absorption respectively blue shifted by 25 and 11 nm for **12** and **13** dyes as compared to the spectra in solution, indicating that **12** and **13** dyes have a more tendency to H-aggregate on TiO_2. Additionally, Many research results have indicated that monolayer dyes anchoring onto TiO_2 surface are necessary for higher efficiency of DSCs.

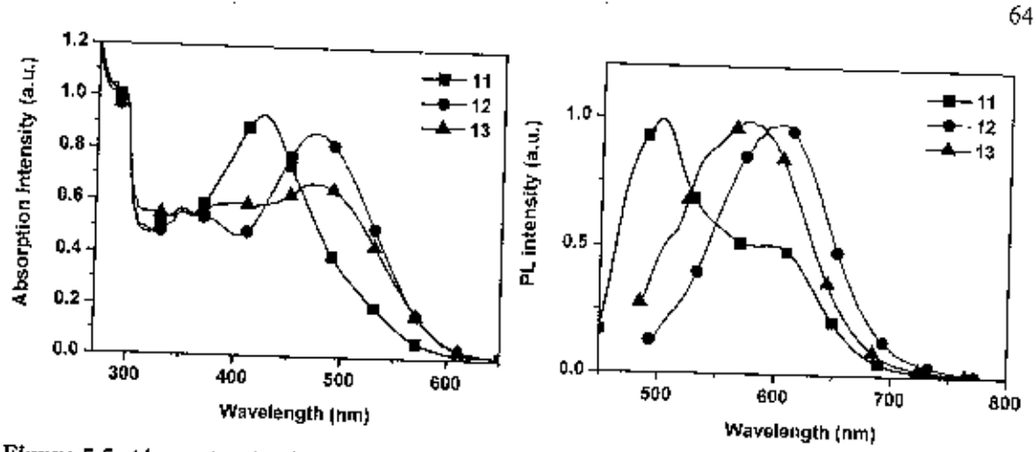

Figure 5.5 Absorption (left) and emission (right) spectra of **11-13** recorded in dichloromethane.

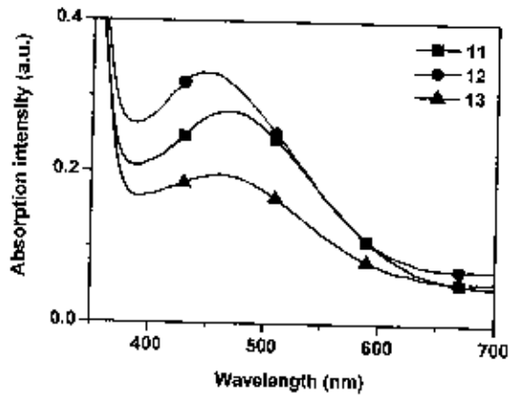

Figure 5.6 Absorption spectra of TiO_2 films sensitized by **11-13**.

Table 5.1 The absorption and fluorescence data of **11-13**

Compound	λ_{max}^{abs} (εx 10^4); (nm (M^{-1} cm^{-1}))[a]	λ_{max} on TiO_2 (nm)[b]	λ_{max}^{em} (nm)[a,c]	λ_{onset}^{abs} (nm)[a]	E_g (eV)[d]
11	424 (1.22), 350 (0.74), 297 (1.31)	468	500	530	2.34
12	475 (4.47), 353 (2.89), 297 (5.13)	450	604	587	2.11
13	471 (1.03), 297 (1.53)	460	575	595	2.08

[a] measured in dichloromethane solution at room temperature.

[b] measured dyes adsorbed on TiO_2 film.

[c] excited at maximum absorption in solution.

[d] estimated from the onset of absorption (E_g =1240/λ_{onset}).

The effect of solvent polarity on the absorption spectra of **12** dye was also studied (Figure 5.7 and Table 5.2). The absorption was measured in five different solvents dimethylformamide (DMF), dimethylsulfoxide (DMSO), ethanol (EtOH), tetrahydrofurane (THF) and dichloromethane (DCM)). We assigned the absorption bands at 297 nm as **B1**, at 353 nm as **B2** and at 432-475 nm as **B3**, respectively. There is only **B3** band that be effected by solvent polarity change. These **B3** bands therefore are assigned as ICT bands of donor-accepter molecule which can be generally observed in most sensitizer. The absorption spectra show blue shift when the polarity of solvents are increasing. **12** in DMF exhibited lowest maximum absorption at 432 nm (4.60 x 10^{-19} *J*), whereas **12** in dichloromethane exhibited the highest at 475 nm (4.18 x 10^{-19} *J*). These results can be considered as the negative solvatochromism-physical intermolecular solute-solvent interaction forces which tend to alter the energy difference between ground and excited state of chromophore of the dyes [42]. The polar solvents are good supporting solvent to the excited state dye species more than non-polar solvents resulting in close molecular orbital, which tends to absorb light at high energy region (low wavelength). This effect was also found in the other molecules (**11** and **13**).

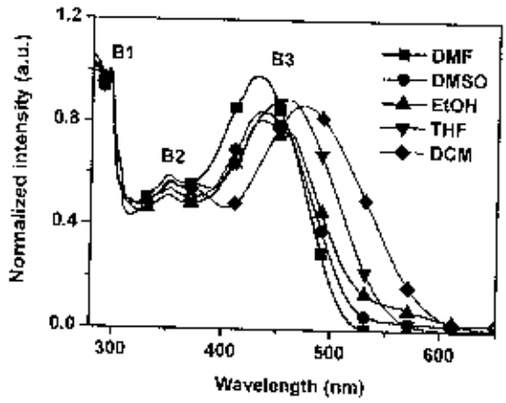

Figure 5.7 The absorption spectra of **12** dye in various solvents.

Table 5.2 Maximum absorption of **12** measured in various solvents

solvent	DMF	DMSO	EtOH	THF	DCM
λ_{max} (nm)	432	434	435	461	475
E^a (10^{-19} J)	4.60	4.58	4.57	4.31	4.18

[a] calculated from $E = h\nu/\lambda$

5.3.3 Thermal properties

For DSC applications, the thermal stability of organic materials is crucial for device stability and lifetime. The degradation of organic optoelectronic devices depends on morphological changes resulting from the thermal stability of the amorphous organic materials. Figure 5.8 and Table 5.3 show TGA thermograms and temperature at 5% weight loss (T_{5d}) of **11-13** dyes investigated by TGA analysis under nitrogen atmospheric condition. The dyes exhibit 5% weight loss at 263, 228 and 216 °C, respectively. Those results suggested that the dyes were thermally stable materials with T_{5d} well over 216 °C. The better thermal stability of the dye is important for the lifetime of the solar cells.

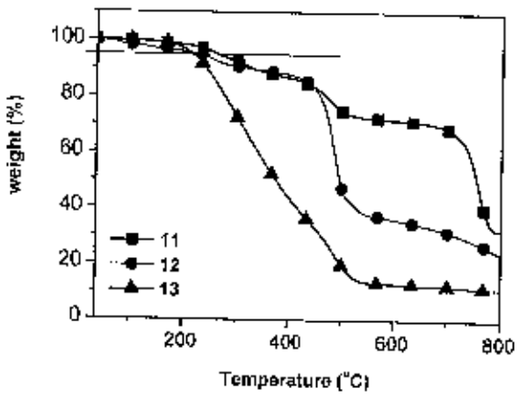

Figure 5.8 TGA thermograms of **11-13** dyes.

Table 5.3 Thermal properties of **11-13**

Compound	T_{5d} (°C)
11	263
12	228
13	216

5.3.4 Molecular orbital calculation

To get an insight into the molecular structure and electron distribution of the organic dye, the **11-13** dyes geometries have been optimized using DFT calculations with Gaussian 03 program. The calculations were performed with the BTLYP exchange correlation functional under 6-31G(d,p) basis set. Computed HOMO and LUMO distribution of **11-13** are depicted in Figure 5.9. The general characters of the orbitals are independent of the linker length and different electron acceptor. The HOMO is of π-characteristics and is delocalized over the entire molecule, including the carbazole groups. In the LUMO, which also has π-character, there is essentially no contribution from the carbazole groups, and the electron density has been shifted towards the acceptor group of the sensitizer. This supports the supposed push-pull characteristics of these sensitizers. In addition, the optimized geometry of **11-13** indicates that the carbazole moiety at the end of the molecule are in 3-D spatial arrangement, which makes the molecular structure nonplanar due to the twist conformation around the carbazole-carbazole C-*N* bond. The nonplanar molecular structure of **11-13** could be beneficial to solution-

processability to form amorphous film. **11-13** are soluble in common organic solvents such as THF, CH_2Cl_2, $CHCl_3$ and acetone. High-quality amorphous film can be obtained by spin-coating its solution.

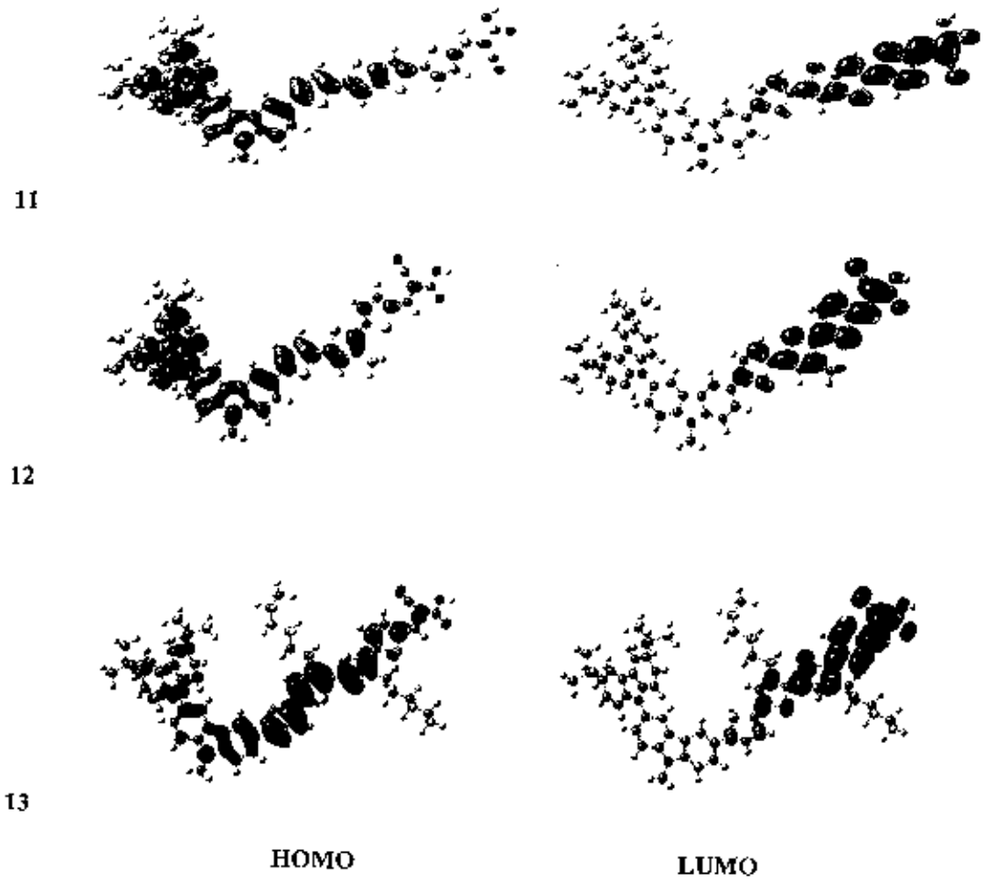

Figure 5.9 HOMO and LUMO distribution of the **11-13** dyes calculated with DFT on a BTLYP/6-31G(d,p) level.

5.4 Conclusions

Novel D-π-A organic dyes, **11-13**, have synthesized as photosensitizers for DSCs applications by using Ullmann coupling, Suzuki coupling and Knoevenagel condensation reaction. Different types of electron spacers containing thiophene moiety is introduced to the molecules and

serve as linker. The electron-withdrawing parts are cyanoacrylic acid groups. The target molecules were characterized by using NMR, IR, UV-vis and fluorescence techniques. The target molecules exhibit a adsorption band cover UV and visible region. Fluorescence spectra of the target molecules show emission peak at cyan-orange region, excited at λ_{max} of each molecule. **11-13** show a good thermal properties. DFT calculations have been performed on the dyes, and the results show that electron distribution from the whole molecules to the anchoring moieties occurred during the HOMO-LUMO excitation.

CHAPTER 6

SYNTHESIS AND CHARACTERIZATION OF NOVEL BISCARBOZOLE WITH DIFFERENT π-CONJUGATED BRIDGES FOR DYE SOLAR CELLS

6.1 Introduction

Increased conjugation by linker modifications is one way to broaden the absorption spectra and hence decreasing the HOMO and LUMO energy level gap. However, there is a limit where the energy level potential of the HOMO becomes too low and the regeneration from the electrolyte, i.e. iodide/triiodide, is hindered. The limit for the LUMO energy level is not of the same importance since the conduction band potential of the semiconductor can be tuned by additives in the electrolyte [50].

A series of novel D-π-A hydrazone dyes (**HB**, **HF** and **HT**) containing an *N,N*-diphenylhydrazone donor and 2-cyanoacetic acid acceptor linked by a different aromatic bridge (benzene, furan, and thiophene) have been designed and synthesized to evaluate the aromatic bridge effects on the photophysical, electrochemical and the photovoltaic properties of the hydrazone-sensitized TiO_2 solar cells. All the dyes exhibit two distinct absorption bands: one absorption band is in the UV region (280–350 nm) corresponding to the π-π^* electron transitions of the conjugated molecules; and the other is in the visible region (380-550 nm) that can be assigned to an intramolecular charge transfer (ICT) between the *N,N*-diphenylhydrazone donating unit and the cyanoacrylic acid acceptor moiety [51]. It can be seen that the maximum absorption (λ_{max}) of the visible region red-shifts from 425 nm to 452 nm, and 465 nm for **HB**, **HF**, and **HT**, respectively. This red-shifted phenomenon may be ascribed to the different aromatic ability of the two five-membered heteroaromatic bridges. The aromatic ability of furan is larger than that of thiophene due to the stronger electronegative of oxygen element than that of nitrogen and sulphur elements. We can see that the λ_{max} values in the visible region shift to a lower energy with the decreased electronegativity of heteroatoms [52].

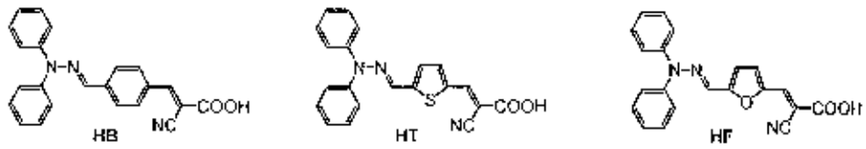

Figure 6.1 Chemical structures of **HB**, **HF** and **HT** dyes.

6.2 Aim of the study

In this work, we synthesized novel donor π-conjugate acceptor (D-π-A) organic materials with different numbers of electron spacers are thiophene moieties moieties and different types of electron spacers containing furan, thiophene and phenyl moieties for using as dye molecules in optoelectronic devices as show in Figure 6.2. The D-π-A containing carbazole as electron donor and cyanoacrylic acid as electron acceptor/anchoring group bridged by thiophene and furan units. Carbazole bearing alkyl groups at the *N* position, to increase the solubility property and to prevent the recombination of the electrons from the semiconductor to the electrolyte. Different numbers of electron spacers are thiophene moieties moieties and different types of electron spacers containing furan, thiophene and phenyl moieties, which are considered to be the ideal constructional unit in dye sensitizer engineering, adopted for expansion of the π-conjugating backbone and adjusting the absorption spectra and HOMO/LUMO levels of the dyes.

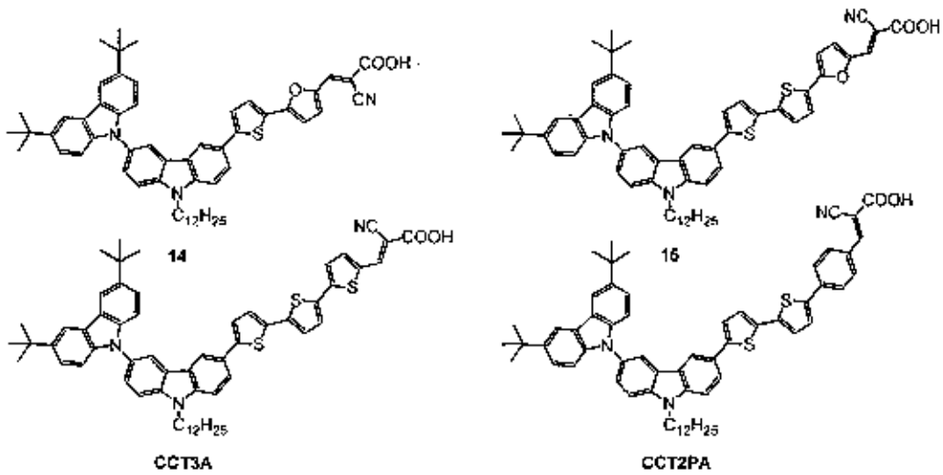

Figure 6.2 Chemical structures of dyes (**14**, **15**, **CCT3A** [34] and **CCT2PA** [34]).

6.3 Results and Discussion

6.3.1 Synthesis

For the synthesis of bicarbazole based dye having the 4-hexylthiophene and thieno[3,2-b]thiophene as different numbers of electron spacers used a combination of Suzuki coupling, Bromination and Knoevanegel reaction as depicted in Figure 6.3 and 6.4.

To elongate the conjugation of the molecules, mono thiophene was introduced to donor using combination reaction of Suzuki coupling and bromination. Bithiophene intermediate (**54**) was prepared by coupling reaction between monothiophene intermediate (**50**) and 2-thiopheneboronic acid using tetrakis(triphenylphosphine)palladium(0) as a catalyst, sodium carbonate as base in THF/H_2O at reflux and obtained in good yield. NBS bromination of the resultant thiophene intermediate in THF at room temperature afforded bromothiophene intermediate (**55**) in 79% yield.

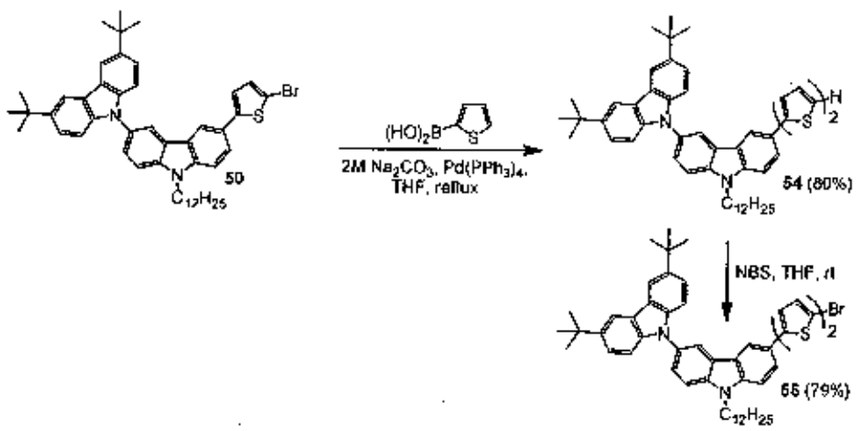

Figure 6.3 Synthesis of oligothiophene intermediate.

The extended carboxaldehyde functionalized furan intermediate (**56** and **57**) were achieved by Suzuki condition as well. The coupling reaction between corresponding bromothiophene intermediate (**50** and **55**) and (5-formylfuran-2-yl)boronic acid yielded the aldehyde (**56** and **57**) in 63 and 71%, respectively. This moderate yield are commonly observed in Suzuki coupling of (5-formylfuran-2-yl)boronic acid due to its unstable furan carboxaldehyde intermediate. The successful introduction of aldehyde functional group was confirmed by NMR and IR spectra. The singlet signal of aldehyde proton in $CDCl_3$ was located at

chemical shift 9.60 and 9.70 ppm for aldehyde protons of **56** and **57**, respectively. The signal of the aldehyde carbon atom was located at chemical shift 176.92 and 176.71 ppm for aldehyde carbon of **56** and **57**, respectively. The IR peaks of C=O stretching of aldehyde was also observed at wavenumber 1662 and 1665 cm^{-1} of **56** and **57**, respectively. Finally the dyes were obtained by Knoevenagel reaction of corresponding aldehyde (**56** and **57**) with cyanoacetic acid. All dyes were obtained as red and dark red amorphous solid. The chemical structure of **14** and **15** was confirmed by NMR and IR analysis. The ^{1}H-NMR spectrum of the final products (**14** and **15**) show a singlet signal at chemical shift 7.89 (1H) and 7.82 (1H) ppm assigning as the proton of double bond indicating that **14** and **15** excises as *E* isomer which has higher photostability properties. The ^{13}C-NMR spectra of **14** and **15** shows a single peak for chemically carbon atom of carbonyl group at 176.44 and 167.63 ppm , respectively, and a single peak for carbon atom of cyano group at 116.49 and 116.49 ppm , respectively. Furthermore IR spectrum reveals the adsorption at 3411 and 3420 cm^{-1} which is consistent with the presence of hydroxy group for **14** and **15**, respectively, and at 2219 and 2219 cm^{-1} which is consistent with the presence of cyano group for **14** and **15**, respectively.

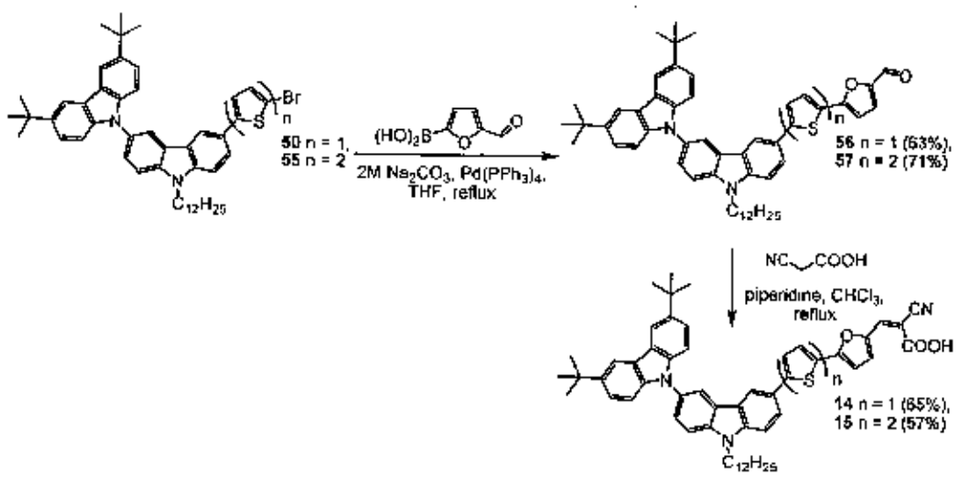

Figure 6.4 Synthesis of D-π-A organic dyes (**14** and **15**).

6.3.2 Optical properties

The UV-vis and fluorescence spectra of dyes in CH_2Cl_2 are shown in Figure 6.5 and listed in Table 6.1. In solution, all three dyes show similar characteristic of donor-accepter arylamine dyes which show strong absorption bands around 290-400 nm corresponds to π-π^* transition and broad absorption bands around 420-600 nm corresponds to Intramolecular Charge transfer Transition (ICT) of donor-accepter compound. The bathochromic shifted (red shifted) absorption spectra were observed when thiophene units were introduced. The red shift in absorption can be attributed to the extended conjugation system of the entire structure. The fluorescence emission spectra showed a red-shift upon increased number of thiophene units in the molecule, which is roughly parallel to the trend of the absorption spectra (Figure 6.5 (left)) due to the elongation of the conjugation in molecules. Comparition between the **15**, **CCT3A** and **CCT2PA** dyes, which has the same electron donor and acceptor moiety, but different π-conjugating systems. It can be seen that the maximum absorption (λ_{max}) of the visible region red-shifts from 414 nm to 464 nm, and 485 nm for **CCT2PA**, **CCT3A**, and **15**, respectively. This red-shifted phenomenon may be ascribed to the different aromatic ability of the one six-membered and two five-membered heteroaromatic bridges. The aromatic ability of furan is larger than that of thiophene and phenyl due to the stronger electronegative of oxygen element than that of sulphur and carbon elements. We observed that the **14**, **15**, **CCT3A** and **CCT2PA** dyes exhibited strong luminescence maxima of 580-615 nm when it is excited within its π-π^* band in solution at room temperature showed the emission peak located in the yellow-orange region. The energy band gaps of the **14**, **15**, **CCT3A** and **CCT2PA** dyes were estimated to be 2.23, 2.17, 2.11 and 2.12 eV, respectively, from the absorption edge of the solution spectra.

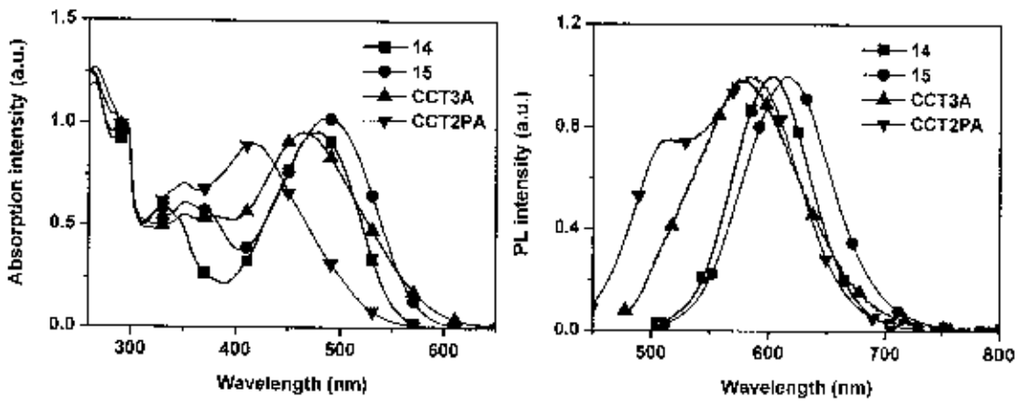

Figure 6.5 Absorption (left) and emission (right) spectra of **14**, **15**, **CCT3A** and **CCT2PA** recorded in dichloromethane.

Table 6.1 The absorption and fluorescence data of **14**, **15**, **CCT3A** and **CCT2PA**

Compound	λ_{max}^{abs} (εx 10^4); (nm (M^{-1} cm^{-1}))[a]	λ_{max}^{em} (nm)[a, b]	λ_{onset}^{abs} (nm)[a]	E_g (eV)[c]
14	480 (2.88), 332 (1.77), 297 (2.99)	604	555	2.23
15	488 (6.92), 353 (4.13), 297 (6.72)	615	572	2.17
CCT3A	464 (3.47), 382 (1.94), 352 (2.00), 297 (3.62)	580	587	2.11
CCT2PA	414 (3.55), 351 (2.80), 297 (3.95)	584	525	2.12

[a] measured in dichloromethane solution at room temperature.

[b] excited at maximum absorption in solution.

[c] estimated from the onset of absorption ($E_g = 1240/\lambda_{onset}$).

The effect of solvent polarity on the absorption spectra of **14** dye was also studied (Figure 6.6 and Table 6.2). The absorption was measured in five different solvents dimethylformamide (DMF), dimethylsulfoxide (DMSO), ethanol (EtOH), tetrahydrofurane (THF) and dichloromethane (DCM)). We assigned the absorption bands at 297 nm as **B1**, at 332 nm as **B2** and at 433-476 nm as **B3**, respectively. There is only **B3** band that be effected by solvent polarity change. These **B3** bands therefore are assigned as ICT bands of donor-accepter molecule which can be generally observed in most sensitizer. The absorption spectra show blue shift when

the polarity of solvents are increasing. **14** in DMF exhibited lowest maximum absorption at 433 nm (4.59×10^{-19} *J*), whereas **14** in dichloromethane exhibited the highest at 476 nm (4.18×10^{-19} *J*). These results can be considered as the negative solvatochromism-physical intermolecular solute-solvent interaction forces which tend to alter the energy difference between ground and excited state of chromophore of the dyes. The polar solvents are good supporting solvent to the excited state dye species more than non-polar solvents resulting in close molecular orbital, which tends to absorb light at high energy region (low wavelength). This effect was also found in the other molecules (**15**, **CCT3A** and **CCT2PA**).

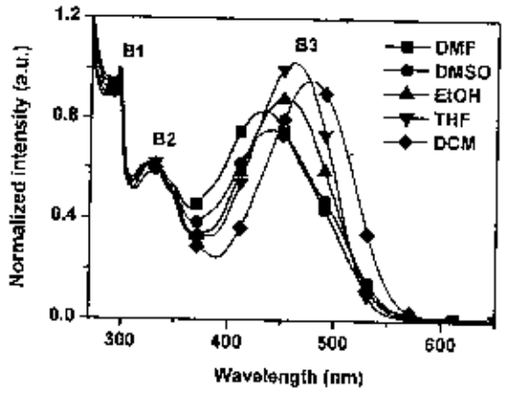

Figure 6.6 The absorption spectra of **14** dye in various solvents.

Table 6.2 Maximum absorption of **14** measured in various solvents

solvent	**DMF**	**DMSO**	**EtOH**	**THF**	**DCM**
λ_{max} (nm)	433	441	451	462	476
E^a (10^{-19} *J*)	4.59	4.51	4.41	4.30	4.18

[a] calculated from $E = h\nu/\lambda$

6.3.3 Thermal properties

The thermal decomposition of **14**, **15**, **CCT3A** and **CCT2PA** dyes was studied by thermogravimetric analysis under nitrogen atmospheric condition. TGA thermograms of the dyes are displayed in Figure 6.7 and T_{5d} are listed in Table 6.3. The dyes exhibit 5% weight

loss between 227 and 359 °C suggested that the dyes were thermally stable materials with temperature over 227 °C which is good for long term stability of DSCs devices.

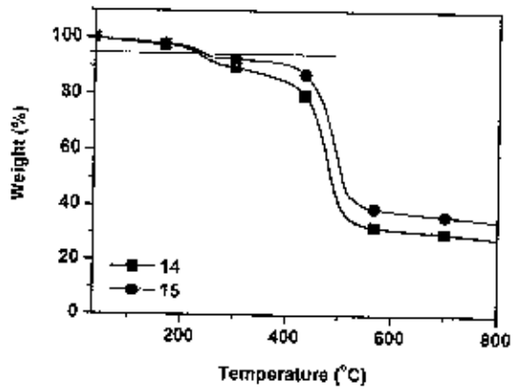

Figure 6.7 TGA thermograms of **14** and **15** dyes.

Table 6.3 Thermal properties of **14**, **15**, **CCT3A** and **CCT2PA**

Compound	T_{5d} (°C)
14	227
15	238
CCT3A	255
CCT2PA	359

6.3.4 Molecular orbital calculation

To get an insight into the molecular structure and electron distribution of the organic dye, the **14**, **15**, **CCT3A** and **CCT2PA** dyes geometries have been optimized using DFT calculations with Gaussian 03 program. The calculations were performed with the BTLYP exchange correlation functional under 6-31G(d,p) basis set. Computed HOMO and LUMO distribution of **14**, **15**, **CCT3A** and **CCT2PA** are depicted in Figure 6.8 and 6.9. The general characters of the orbitals are independent of the linker length and different electron acceptor. The HOMO is of π-characteristics and is delocalized over the entire molecule, including the carbazole groups. In the LUMO, which also has π-character, there is essentially no contribution from the carbazole groups, and the electron density has been shifted towards

the acceptor group of the sensitizer. This supports the supposed push-pull characteristics of these sensitizers. In addition, the optimized geometry of **14**, **15**, **CCT3A** and **CCT2PA** indicates that the carbazole moiety at the end of the molecule are in 3-D spatial arrangement, which makes the molecular structure nonplanar due to the twist conformation around the carbazole-carbazole C-*N* bond. The nonplanar molecular structure of **14**, **15**, **CCT3A** and **CCT2PA** could be beneficial to solution-processability to form amorphous film. **14**, **15**, **CCT3A** and **CCT2PA** are soluble in common organic solvents such as THF, CH_2Cl_2, $CHCl_3$ and acetone. High-quality amorphous film can be obtained by spin-coating its solution.

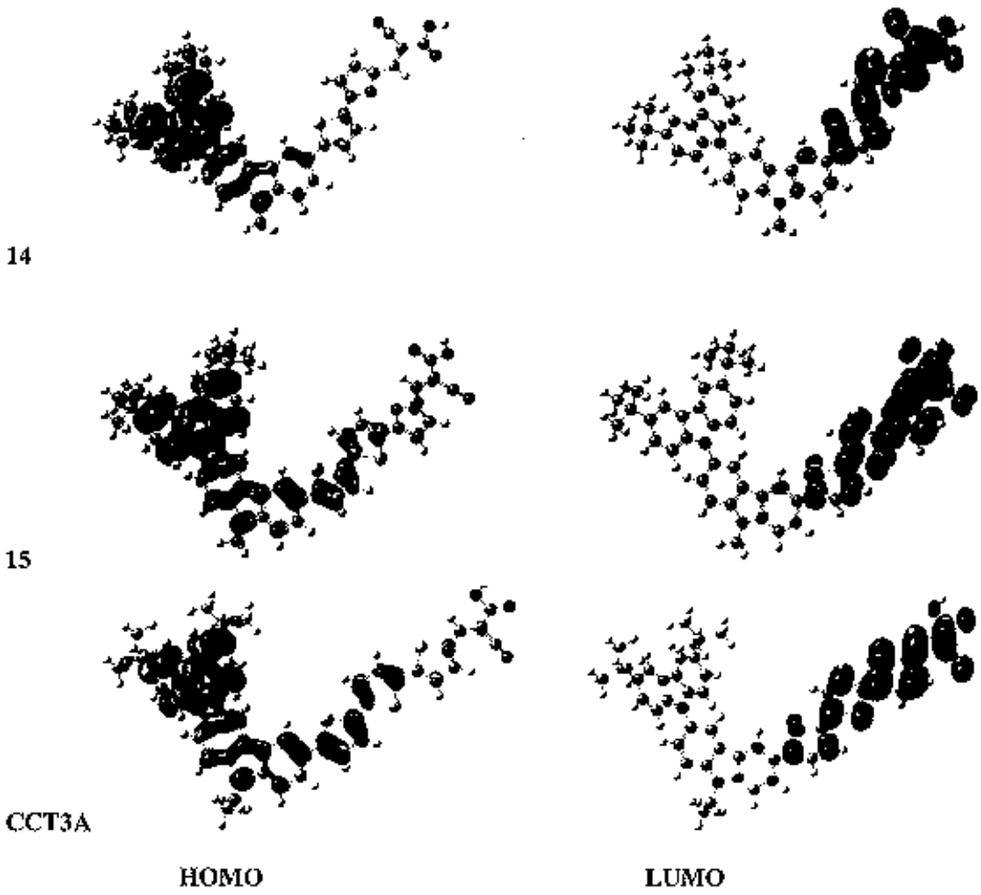

Figure 6.8 HOMO and LUMO distribution of the **14**, **15** and **CCT3A** dyes calculated with DFT on a BTLYP/6-31G(d,p) level.

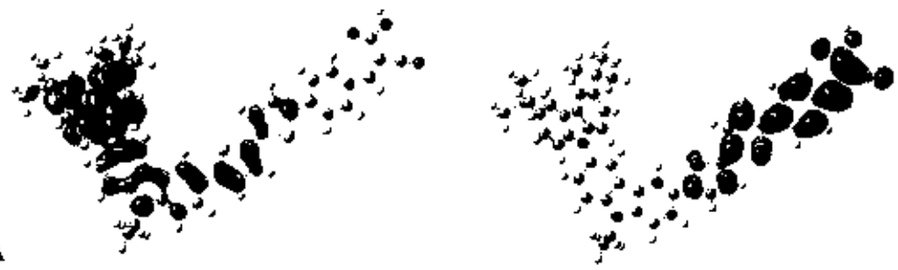

CCT2PA

HOMO LUMO

Figure 6.9 HOMO and LUMO distribution of the **CCT2PA** dye calculated with DFT on a BTLYP/6-31G(d,p) level.

6.4 Conclusions

Novel D-π-A organic dyes, **14**, **15**, **CCT3A** and **CCT2PA**, have been synthesized as photosensitizers for DSCs applications by using Suzuki coupling and Knoevenagel condensation reaction. Different numbers of electron spacers containing thiophene moiety is introduced to the molecules and serve as linker. The electron-withdrawing parts are cyanoacrylic acid groups. The target molecules were characterized by using NMR, IR, UV-vis and fluorescence techniques. The target molecules exhibit a adsorption band cover UV and visible region. Fluorescence spectra of the target molecules show emission peak at yellow-orange region, excited at λ_{max} of each molecule. **14**, **15**, **CCT3A** and **CCT2PA** show a good thermal properties. DFT calculations have been performed on the dyes, and the results show that electron distribution from the whole molecules to the anchoring moieties occurred during the HOMO-LUMO excitation.

CHAPTER 7

SYNTHESIS AND CHARACTERIZATION OF NOVEL CARBAZOLE DERIVATIVES AS DONOR MOIETIES FOR DYE SOLAR CELLS

7.1 Introduction

New organic dyes, namely **CCTA** and **CFTA** using *N*-dodecyl-3-(3,6-di-*tert*-butylcarbazol-*N*-yl)carbazol-6-yl and 2-(3,6-di-*tert*-butylcarbazol-*N*-yl)-9,9-bishexylfluoren-7-yl as donor moieties, respectively, were synthesized, characterized, and employed as a dye sensitizer in dye solar cells (DSCs). Both dyes in solution show donor–acceptor characteristic absorption spectra. The broad absorption bands at 445-460 nm were attributed to intramolecular charge-transfer transitions (ICT) from the D–D to A moieties, exhibited a hypsochromic shift in more polar solvents, while the positions of other peaks at lower wavelengths were nearly independent of the solvent polarity. **CCTA** shows a broader and increased molar extinction coefficient (ε) (~1.17 fold) ICT band compared to that of **CFTA**, which is desirable for harvesting more solar light. This mainly stems from the stronger electron-donating ability of the *N*-dodecyl-3-(3,6-di-*tert*-butylcarbazol-*N*-yl)carbazol-6-yl donor in **CCTA** than that of the 2-(3,6-di-*tert*-butylcarbazol-*N*-yl)-9,9-bishexylfluoren-7-yl donor in **CFTA**. Moreover, the ε value (27938 M^{-1} cm^{-1}) of **CCTA** is also considerably larger than that of the standard Ru dye, N719 (14400 M^{-1} cm^{-1}), indicating excellent light harvesting ability. The **CCTA**-sensitized solar cell produces higher device performance with an overall conversion efficiency of 5.69% [a short circuit current (J_{sc}) = 11.31 mA cm^{-2}, an open-circuit voltage (V_{oc}) = 0.71 V, and a field factor (ff) = 0.71] reaching >96% of the reference N719-based device (overall conversion efficiency = 5.92%) [53].

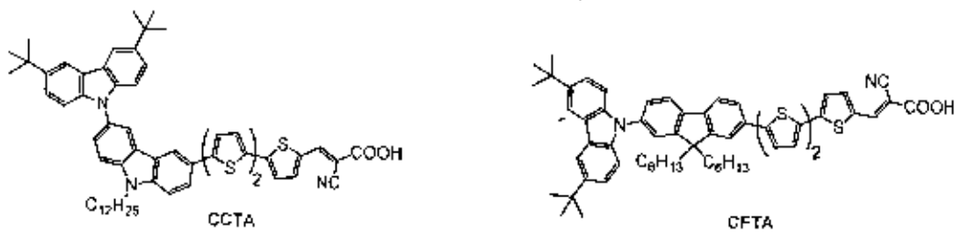

Figure 7.1 Chemical structures of **CCTA** and **CFTA.**

7.2 Aim of the Study

In this work, we synthesized carbazole derivatives based D-π-A organic dye for DSCs application. The dye had been constructed based on the electron-donating moiety, substituted carbazole with 3,6-positions of carbazole being substituted with t-butyl group to prevent oxidative coupling. Fluorene, carbazole and phenothiazine bearing alkyl groups at the C-9, *N*-9, and *N*-9 position, to increase the solubility property and to prevent the recombination of the electrons from the semiconductor to the electrolyte. Electron spacers are thiophene and phenyl moieties, which are considered to be the ideal constructional unit in dye sensitizer engineering, adopted for expansion of the π-conjugating backbone and adjusting the absorption spectra and HOMO/LUMO levels of the dyes. The dyes had a cyanoacrylic acid group as electron-withdrawing part and for anchoring onto the TiO_2 surface.

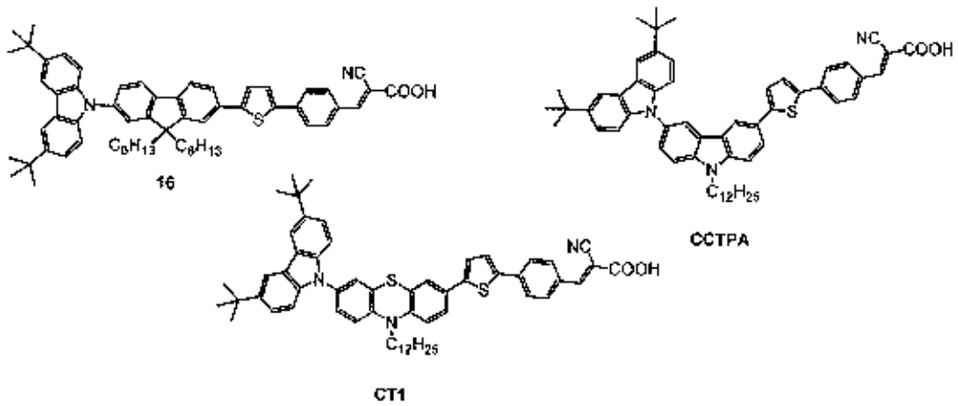

Figure 7.2 Chemical structures of **16**, **CCTPA** and **CT1**

7.3 Results and Discussion

7.3.1 Synthesis

The synthesis of **16** (Figure 7.3), first, NBS bromination of the resultant thiophene intermediate in THF at room temperature afforded bromothiophene intermediate **(59)** in 94% yield. The extended carboxaldehyde functionalized thiophene intermediate **(60)** were achieved by Suzuki condition as well. The coupling reaction between corresponding aryl halide **(59)** and 5-formyl-2-thiopheneboronic acid yielded the aldehyde 53%, respectively. The successful introduction of aldehyde functional group was confirmed by NMR and IR spectra. The singlet signal of aldehyde proton in $CDCl_3$ was located at chemical shift 10.02 ppm for aldehyde protons of **60**. The signal of the aldehyde carbon atom was located at chemical shift 191.36 ppm for aldehyde carbon of **60**. The IR peaks of C=O stretching of aldehyde was also observed at wavenumber 1697 cm^{-1} of **60**. And (*E*)-2-cyano-3-(4-(5-(7-(3,6-di-*tert*-butylcarbazol-9-yl)-9,9-dihexylfluoren-2-yl)thiophen-2-yl)phenyl)acrylic acid dye **(16)** having the cyanoacrylic acid as an acceptor was synthesized according to the procedure described for **1** and obtained as light orange solid in 42% yield. The chemical structure of **16** was confirmed by NMR and IR analysis. The ^{13}C-NMR spectrum of **16** shows a single peak for chemically carbon atom of carbonyl group at 164.06 ppm and a single peak for carbon atom of cyano group at 116.16 ppm. Furthermore IR spectrum reveals the adsorption at 3415 cm^{-1} which is consistent with the presence of hydroxy group and at 2224 cm^{-1} which is consistent with the presence of cyano group.

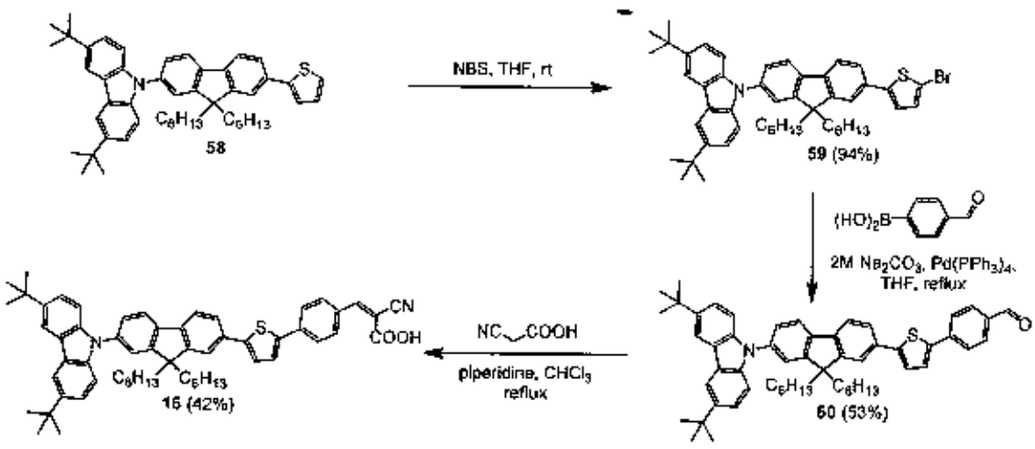

Figure 7.3 Synthesis of D-π-A organic dye (**16**).

7.3.2 Optical properties

The UV-vis and fluorescence spectra of dyes in CH_2Cl_2 are shown in Figure 7.4 and listed in Table 7.1. When a carbazole-fluorene group is introduced to the molecule as electron donor (**16**), comparing the **CCTPA** dye with a carbazole-carbazole group as electron donor, the maximum absorption peak is blue-shifted and the ε value is decreased. This is due to the twist conformation around the carbazole-carbazole *N*-C bond. Comparing the carbazole-carbazole based D-π-A organic dye (**CCTPA**) to the carbazole-phenothiazine based D-π-A organic dye (**CT1**), which has the same π-conjugating system, but different electron donor moieties, the maximum absorption peak is red-shifted but the ε value is decreased. This is due to the electron-donating property. We observed that the **16**, **CCTPA** and **CT1** dyes exhibited strong luminescence maxima of 506-569 nm when they are excited within their π–π^* bands in solution at room temperature showed the emission peak located in the cyan-yellow region. The energy band gaps of the **16**, **CCTPA** and **CT1** dyes were estimated to be 2.48, 2.40, and 2.37 eV, respectively, from the absorption edge of the solution spectra.

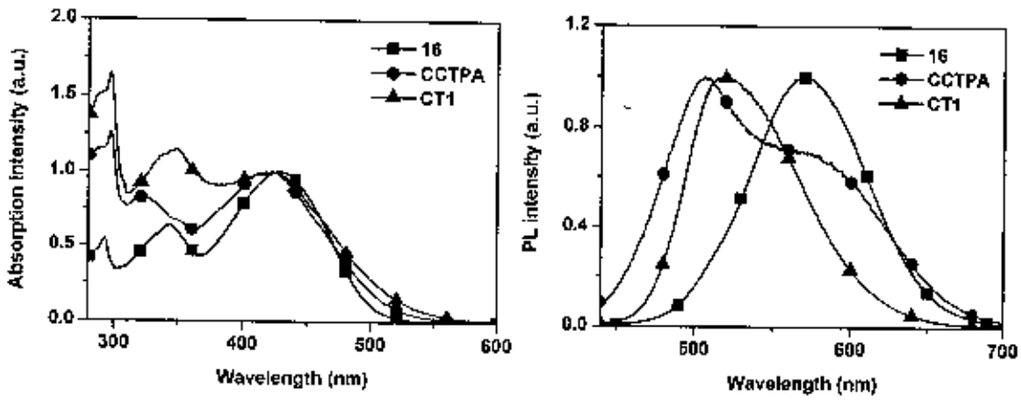

Figure 7.4 Absorption (left) and emission (right) spectra of **16**, **CCTPA** and **CT1** recorded in dichloromethane.

Table 7.1 The absorption and fluorescence data of **16**, **CCTPA** and **CT1**

Compound	λ_{max}^{abs} (εx 10^{-4}); (nm (M^{-1} cm^{-1}))[a]	λ_{max}^{em} (nm)[a, b]	λ_{onset}^{abs} (nm)[a]	E_g (eV)[c]
16	428 (5.02), 343 (3.19), 293 (5.74)	569	500	2.48
CCTPA	421 (2.99), 323 (2.47), 297 (3.75)	506	517	2.40
CT1	424 (2.15), 348 (2.46), 297 (3.54)	519	524	2.37

[a] measured in dichloromethane solution at room temperature.

[b] excited at maximum absorption in solution.

[c] estimated from the onset of absorption (E_g =1240/λ_{onset}).

The effect of solvent polarity on the absorption spectra of **16** dye was also studied (Figure 7.5 and Table 7.2). The absorption was measured in five different solvents dimethylformamide (DMF), dimethylsulfoxide (DMSO), ethanol (EtOH), tetrahydrofurane (THF) and dichloromethane (DCM)). We assigned the absorption bands at 293 nm as **B1**, at 343 nm as **B2** and at 394-428 nm as **B3**, respectively. There is only **B3** band that be effected by solvent polarity change. These **B3** bands therefore are assigned as ICT bands of donor-accepter molecule which can be generally observed in most sensitizer. The absorption spectra show blue shift when the polarity of solvents are increasing. **16** in DMF exhibited lowest maximum absorption at 394 nm (5.05 x 10^{-19} *J*), whereas **16** in dichloromethane exhibited the highest at 428 nm (4.64 x 10^{-19} *J*). These results can be considered as the negative solvatochromism-physical intermolecular solute-solvent interaction forces which tend to alter the energy difference between ground and excited state of chromophore of the dyes. The polar solvents are good supporting solvent to the excited state dye species more than non-polar solvents resulting in close molecular orbital, which tends to absorb light at high energy region (low wavelength). This effect was also found in the other molecules (**CCTPA** and **CT1**).

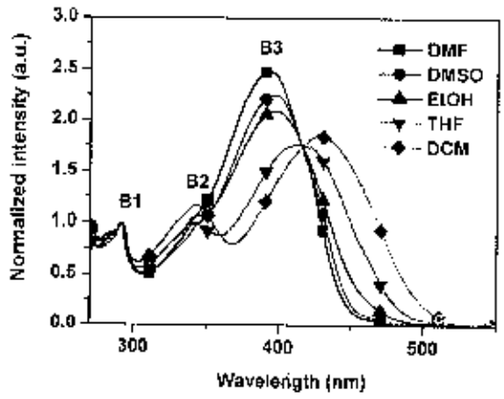

Figure 7.5 The absorption spectra of **16** dye in various solvents.

Table 7.2 Maximum absorption of **16** measured in various solvents

solvent	DMF	DMSO	EtOH	THF	DCM
λ_{max} (nm)	394	397	398	413	428
E^a (10^{-19} J)	5.05	5.01	4.99	4.81	4.64

[a] calculated from $E = h\nu/\lambda$

7.3.3 Thermal properties

For optoelectronic applications, the thermal stability of organic materials is crucial for device stability and lifetime. The degradation of organic optoelectronic devices depends on morphological changes resulting from the thermal stability of the amorphous organic materials. Figure 7.6 and Table 7.3 show TGA thermograms and temperature at 5% weight loss (T_{5d}) of **16**, **CCTPA** and **CT1** dyes investigated by TGA analysis under nitrogen atmospheric condition. Those results suggested that the dyes were thermally stable materials with T_{5d} well over 232 °C. The better thermal stability of the dye is important for the lifetime of the solar cells.

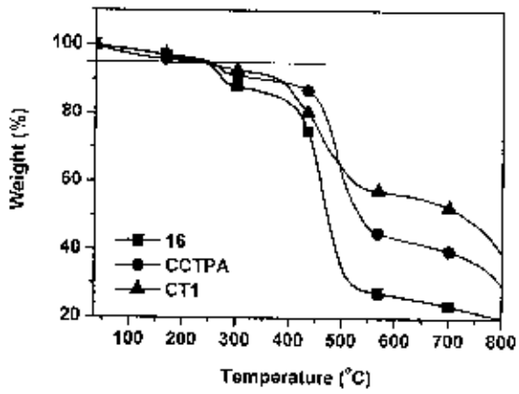

Figure 7.6 TGA thermograms of **16**, **CCTPA** and **CT1** dyes.

Table 7.3 Thermal properties of **16**, **CCTPA** and **CT1**

Compound	T_{5d} (°C)
16	237
CCTPA	232
CT1	250

7.3.4 Molecular orbital calculation

To get further insight into the effect of molecular structures and electron distributions of the three dyes on the performances of DSCs, their geometries and energies were optimized by density functional theory (DFT) calculations. The HOMO is mainly located on the electron donating group and π-spacer, and the LUMO is mainly located in electron withdrawing groups through the π-spacer. It reveals that the thiophene π-spacer is essentially coplanar with cyanoacetic acid group. There are effective electron separations between HOMO and LUMO of these dyes induced by light irradiation. This supports the supposed push-pull characteristics of these sensitizers (Figure 7.7). In addition, the optimized geometry of **16**, **CCTPA** and **CT1** indicates that the carbazole moiety at the end of the molecule are in 3-D spatial arrangement, which makes the molecular structure nonplanar due to the twist conformation around the carbazole-fluorene, carbazole-carbazole, and carbazole-phenothiazine *N*-C bond. The nonplanar molecular structure of **16**, **CCTPA** and **CT1** could be beneficial to solution-processability to form amorphous film. **16**, **CCTPA** and **CT1** are soluble in common organic

solvents such as THF, CH_2Cl_2, $CHCl_3$ and acetone. High-quality amorphous film can be obtained by spin-coating its solution.

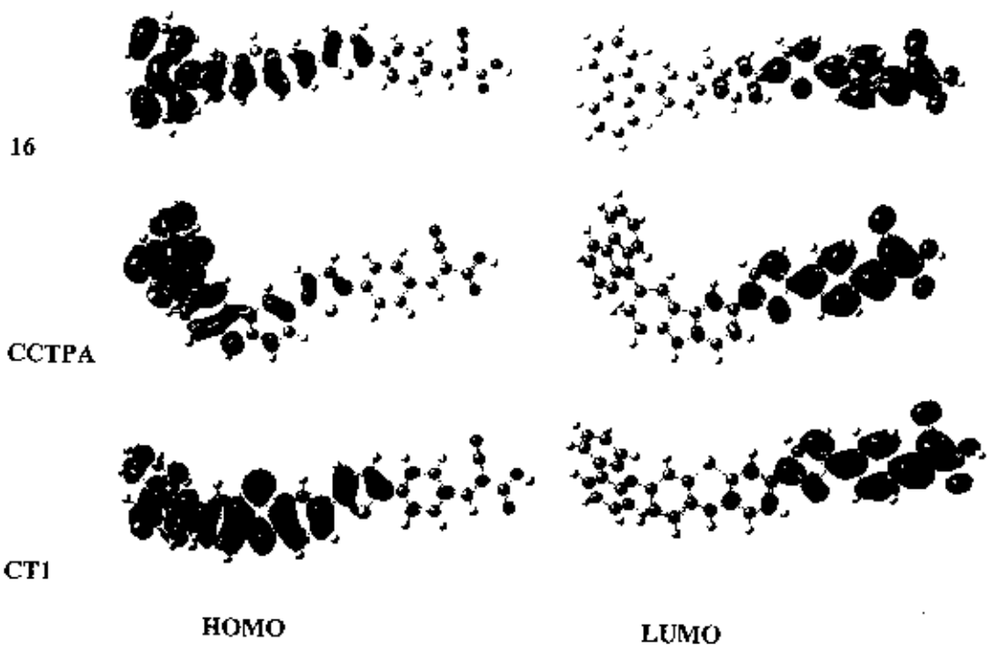

Figure 7.7 HOMO and LUMO distribution of the **16**, **CCTPA** and **CT1** dyes calculated with DFT on a BTLYP/6-31G(d,p) level.

7.4 Conclusions

Novel D-π-A organic dyes (**16**, **CCTPA** and **CT1**) have synthesized as photosensitizers for DSCs applications by using alkylation, halogenation, Suzuki coupling and Knoevenagel condensation reaction. Different types of electron donor moieties are introduced to the molecules. The electron-withdrawing part is cyanoacrylic acid group. The target molecules were characterized by using NMR, IR, UV-vis and fluorescence techniques. The target molecules exhibit a adsorption band cover UV and visible region. Fluorescence spectra of the target molecules show emission peak at cyan-yellow region, excited at λ_{max} of each molecule. **16**, **CCTPA** and **CT1** show a good thermal properties. DFT calculations have been performed on

the dyes, and the results show that electron distribution from the whole molecules to the anchoring moieties occurred during the HOMO-LUMO excitation.

CHAPTER 8

SYNTHESIS AND CHARACTERIZATION OF NOVEL *N*-PHENYLNAPHTHALEN-1-AMINE DERIVATIVES WITH DIFFERENT *N*-SUBSTITUTED UNITS FOR DYE SOLAR CELLS

8.1 Introduction

In 2009, Y. J. Chang et al. synthesized a series of organic dipolar compounds containing a donor (D), a bridge (B), and an acceptor (A), forming a D-B-A type of dyads for dyesensitized solar cells. The central bridges were made of three linearly connected arylene groups, i.e.,phenylenes or thiophenylenes. The donor groups were aromatic amines, i.e., either a diphenylamine or a naphthylphenylamine group. The acceptor group was a cyanoacrylic acid, which can be anchored onto the surface of TiO_2 in a photovoltaic device. These devices performed remarkably well, with a typical quantum efficiency of 5-7%, and optimal incident photon to current conversion efficiency (IPCE) exceeding 80%. The devices made with a naphthylphenylamine donor group performed slightly better than those made with a diphenylamine donor group. Compounds containing a phenylene–thiophenylene–phenylene bridge group performed better than those with other kinds of triarylene linkages [19].

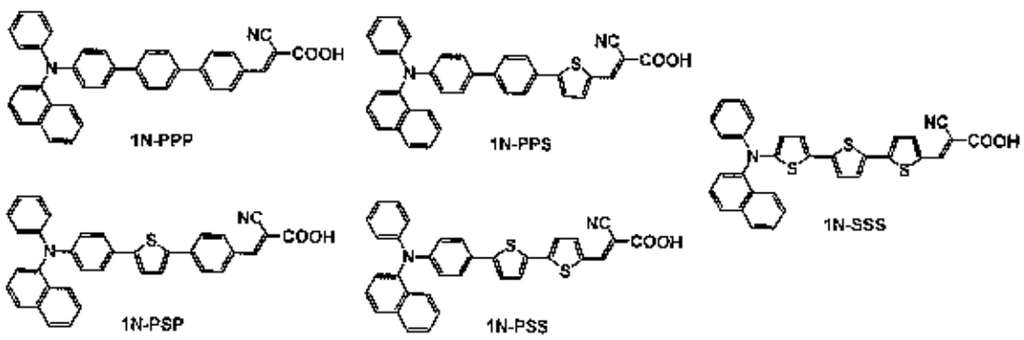

Figure 8.1 Organic dye structure of **1N** series.

8.2 Aim of the Study

We synthesized four novel donor π-conjugate acceptor (D-π-A) organic materials with different donor units for using as dye molecules in DSCs. D-π-A organic dyes based on phenyl, fluorene, carbazole and phenothiazine as the donor group, with a thiophene linker and a cyanoacrylic acid as acceptor/anchor group. Fluorene, carbazole and phenothiazine bearing alkyl groups at the C-9, *N*-9 and *N*-9 position, respectively, to increase the solubility property and to prevent the recombination of the electrons from the semiconductor to the electrolyte.

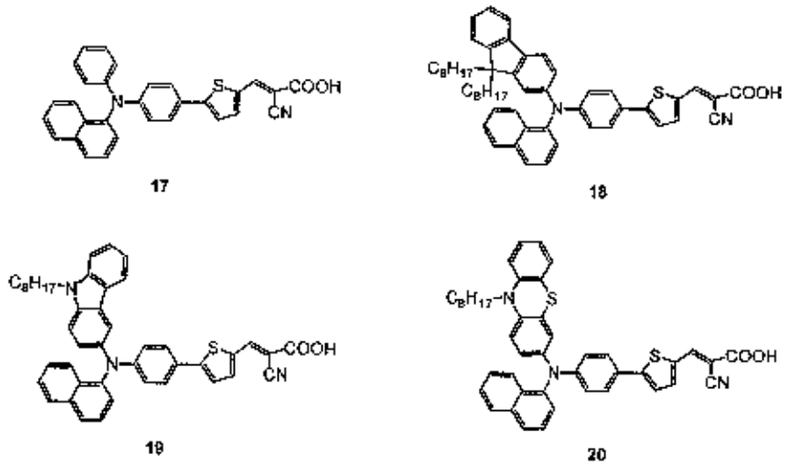

17 18 19 20

Figure 8.2 Chemical structures of **18-20**.

8.3 Results and Discussion

8.3.1 Synthesis

For the synthesis of (*E*)-2-cyano-3-(5-(9-phenylcarbazol-3-yl)thiophen-2-yl)acrylic acid, first *N*-(4-bromophenyl)-*N*-phenylnaphthalen-1-amine was prepared from *N*-phenylnaphthalen-1-amine precursor (**61**) and 1,4-dibromobenzene under Ullmann coupling reaction in the presence of $Pd(OAc)_2$ as a catalyst, PPh_3 as a co-catalyst, and Cs_2CO_3 as a base in toluene as a solvent at reflux for 24 h led to *N*-(4-bromophenyl)-*N*-phenylnaphthalen-1-amine (**62**) as light yellow viscous in 34% yield. Then 5-(4-(naphthalen-1-yl(phenyl)amino)phenyl) thiophene-2-carbaldehyde (**63**) was prepared according to the procedure described for **22** (Chapter 2) and obtained as green solid in 50% yield. The successful introduction of aldehyde functional

group was clearly confirmed by NMR and IR spectra. The singlet signal of aldehyde proton (measured in $CDCl_3$) was located at chemical shift 9.34 ppm for aldehyde proton of **63**. The signal of the aldehyde carbon atom was located at chemical shift 182.88 ppm for aldehyde carbon of **63**. And (*E*)-2-cyano-3-(5-(4-(naphthalen-1-yl(phenyl)amino)phenyl) thiophen-2-yl)acrylic acid (**17**) dye having the cyanoacrylic acid as an acceptor was synthesized according to the procedure described for **1** and obtained as light green solid in 45% yield. The chemical structure of **17** was confirmed by NMR and IR analysis. The ^{1}H-NMR spectrum of the final product (**17**) shows a singlet signal at chemical shift 8.25 ppm (1H) assigning as the proton of double bond indicating that **17** excises as *E* isomer which has higher photostability properties. The ^{13}C-NMR spectrum of **17** shows a single peak for chemically carbon atom of carbonyl group at 163.32 ppm and a single peak for carbon atom of cyano group at 118.70 ppm. Furthermore IR spectrum reveals the adsorption at 342 cm^{-1} which is consistent with the presence of hydroxy group and at 2211 cm^{-1} which is consistent with the presence of cyano group..

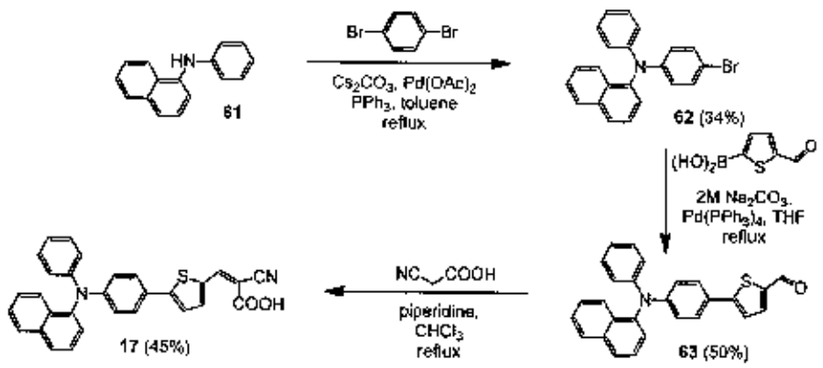

Figure 8.3 Synthesis of D-π-A organic dye (**17**).

The synthesis of The synthesis of fluorene donor part starting with fluorene starting material (**33**) was iodinated in the mixture of potassium iodide and potassium iodate in acetic acid at 80 °C resulting in 2-iodofluorene (**34**) in 41% yield (Figure 8.4). The structure of iodinated product (**34**) was confirmed by ^{1}H-NMR spectra (measured in $CDCl_3$) which exhibit very clear singlet signal of aromatic proton of C-1 fluorene at chemical shift at 7.89 ppm. Dialkylation at the C-9 position to increase the solubility of the resultant compound (**34**) was accomplished by generation of the fluorenyl anion with an aqueous NaOH solution in DMSO and

subsequent dihexylation with 1-bromooctane in the presence of n-$Bu_4N^+Br^-$ as phase transfer catalyst at room temperature. The desired 9,9-dioctyl-2-iodofluorene (**1f**) was isolated by silica-gel column chromatography as brown solid in 80% yield. The Alkyl peaks were observed in ^{1}H-NMR spectrum of **1f** to confirm successful introduction of alkyl group to C-9 position of fluorene.

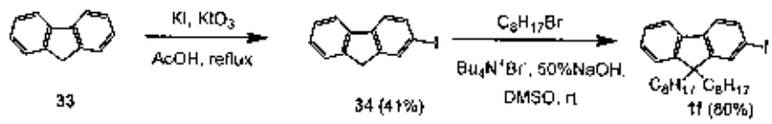

Figure 8.4 Synthesis of 9,9-dioctyl-2-iodofluorene (**1f**).

For The synthesis of carbazole donor part starting with carbazole starting material (**25**) was iodinated in the mixture of potassium iodide and potassium iodate in acetic acid at 80 °C resulting in 3-iodocarbazole (**26**) in 84% yield (Figure 8.5). The structure of iodinated product (**26**) was confirmed by ^{1}H-NMR spectra (measured in $CDCl_3$) which exhibit very clear singlet signal of aromatic proton of C-4 carbazole at chemical shift at 8.38 ppm. Alkylation of **26** with 1-bromooctane in the presence of sodium hydride in DMF at room temperature gave 9-octyl-3-iodocarbazole (**1g**) in excellent yield. The Alkyl peaks were observed in ^{1}H-NMR spectrum of compound **1g** to confirm successful introduction of alkyl group to *N* position of carbazole.

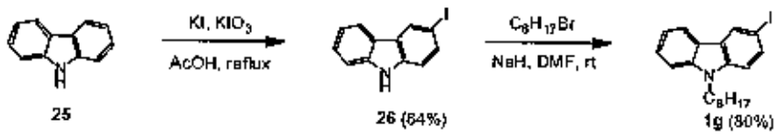

Figure 8.5 Synthesis of 9-octyl-3-iodocarbazole (**1g**).

For The synthesis of phenothiazine donor part starting (Figure 8.6), start with alkylation of phenothiazine (**35**) with 1-bromooctane in the presence of sodium hydride in DMF at room temperature gave 10-octylphenothiazine (**64**) in excellent yield. The Alkyl peaks were observed in ^{1}H-NMR spectrum of **64** to confirm successful introduction of alkyl group to *N* position of phenothiazine. 10-Octylphenothiazine (**64**) was iodinated in the mixture of periodic acid dehydrate and of iodine. A solution of H_2SO_4 conc. and 20% HOAc in acetic acid is added to this mixture. The resulting purple solution is heated at 65-70 °C. The desired 3-iodo-10-

octylphenothiazine (**1h**) was isolated by silica-gel column chromatography as brown solid in 60% yield. (Figure 8.6). The structure of iodinated product (**26**) was confirmed by ^{1}H-NMR spectra (measured in Acetone) which exhibit very clear singlet signal of aromatic proton of C-4 carbazole at chemical shift at 8.37 ppm.

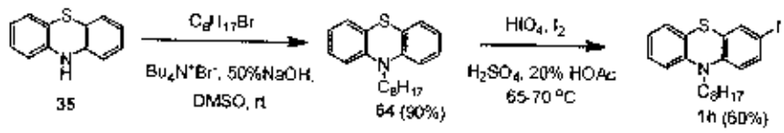

Figure 8.6 Synthesis of 3-iodo-10-octylphenothiazine (**1h**).

For the synthesis of (*E*)-2-cyano-3-(5-(4-(naphthalen-1-yl(aryl)amino)phenyl) thiophen-2-yl)acrylic acid dyes (**18, 19** or **20**), first *N*-aryl-*N*-phenylnaphthalen-1-amine was prepared from *N*-phenylnaphthalen-1-amine precursor (**61**) and aryl iodide (X-I, **1f, 1g** or **1h**) under Ullmann coupling reaction in the presence of copper iodide as a catalyst, (±)-trans-1,2-diaminocyclohexane as a co-catalyst, and potassium tert-butoxide as a base in toluene as a solvent at reflux for 24 h led to *N*-aryl-*N*-phenylnaphthalen-1-amine (**2f, 2g** or **2h**) as light yellow viscous in 65, 61 or 41% yield, respectively. NBS bromination of the resultant intermediate in THF at room temperature afforded *N*-(4-bromophenyl)-*N*-arylnaphthalen-1-amine (**3f, 3g** or **3h**) in 67, 63 or 65% yield, respectively. Then 5-(4-(naphthalen-1-yl(aryl)amino)phenyl)thiophene-2-carbaldehyde (**4f, 4g** or **4h**) was prepared according to the procedure described for **22** (Chapter 2) and obtained as green solid in 60, 62 or 30% yield, respectively. The successful introduction of aldehyde functional group was clearly confirmed by NMR and IR spectra. The singlet signals of aldehyde protons (measured in $CDCl_3$) were located at chemical shift 9.84, 9.97 and 9.94 ppm for aldehyde protons of **4f, 4g** or **4h**, respectively. And (*E*)-2-cyano-3-(5-(4-(naphthalen-1-yl(aryl)amino)phenyl)thiophen-2-yl)acrylic acid dyes (**18, 19** or **20**) having the cyanoacrylic acid as an acceptor was synthesized according to the procedure described for **1** and obtained as light dark orange solid in 56, 60 or 64% yield, respectively. The chemical structure of **18-20** was confirmed by NMR and IR analysis. The ^{1}H-NMR spectrum of the final products (**18-20**) show a singlet signal at chemical shift 8.47 (1H), 8.46 (1H), and 8.47 (1H) ppm assigning as the proton of double bond indicating that **18-20** excises as *E* isomer which has higher photostability

properties. The ^{13}C-NMR spectra of **18-20** shows a single peak for chemically carbon atom of carbonyl group at 166.82, 169.49, and 169.62 ppm , respectively, and a single peak for carbon atom of cyano group at 117.59, 116.92, and 118.80 **ppm** , respectively. Furthermore IR spectrum reveals the adsorption at 3428, 3421, and 3394 cm^{-1} which is consistent with the presence of hydroxy group for **18-20**, respectively, and at 2206, 2211, and 2213 cm^{-1} which is consistent with the presence of cyano group for **18-20**, respectively.

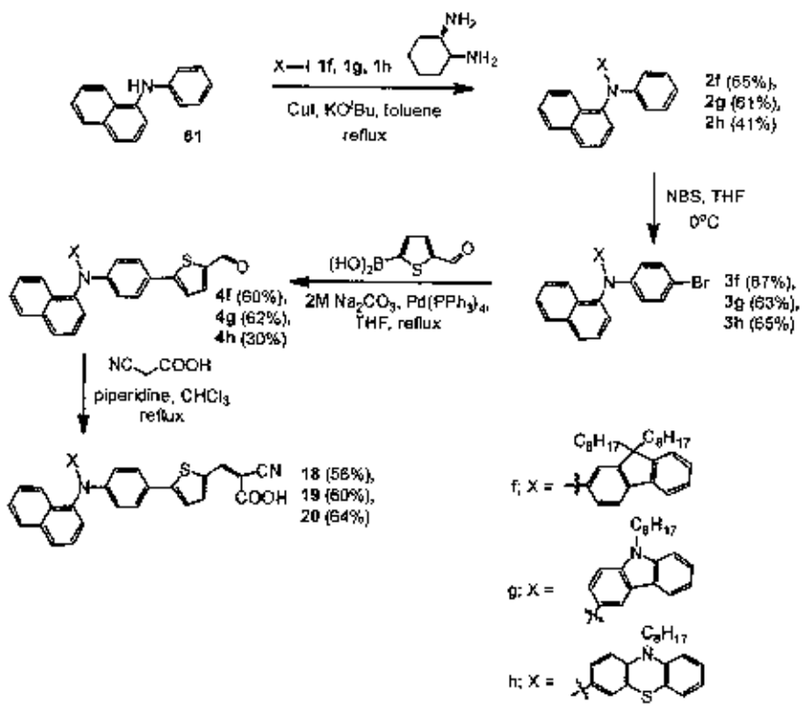

Figure 8.7 Synthesis of D-π-A organic dyes (**18-20**).

8.3.2 Optical properties

The influence of different electron donors on the light harvest capacity of a dye molecule was first evaluated by recording the UV-vis absorption spectra of the dyes dissolved in dichloromethane (Figure 8.8), and the selected parameters were collected in Table 8.1. **17-20** showed the maximum absorption wavelength (λ_{max}) 436 nm (ε = 15,700 M^{-1} cm^{-1}), 438 nm (ε = 16,100 M^{-1} cm^{-1}), 430 nm (ε = 5,900 M^{-1} cm^{-1}), and 459 nm (ε = 12,100 M^{-1} cm^{-1}), respectively, which were corresponding to HOMO (highest occupied molecular orbital) -> LUMO (lowest unoccupied molecular orbital) transition. Amongst these photosensitizers, due to strong electron

donating ability of the phenothiazine unit, the **20** dye with the phenothiazine electron donor presents the longest maximum absorption wavelength, which is an advantageous spectral property for light harvesting of the solar spectrum. We observed that the **17-20** dyes exhibited strong luminescence maxima of 437-599 nm when it is excited within its π–π^* band in solution at room temperature showed the emission peak located in the blue-orange region. The energy band gaps of the **17-20** dyes were estimated to be 2.28, 2.31, 2.23, and 2.23 eV, respectively, from the absorption edge of the solution spectra.

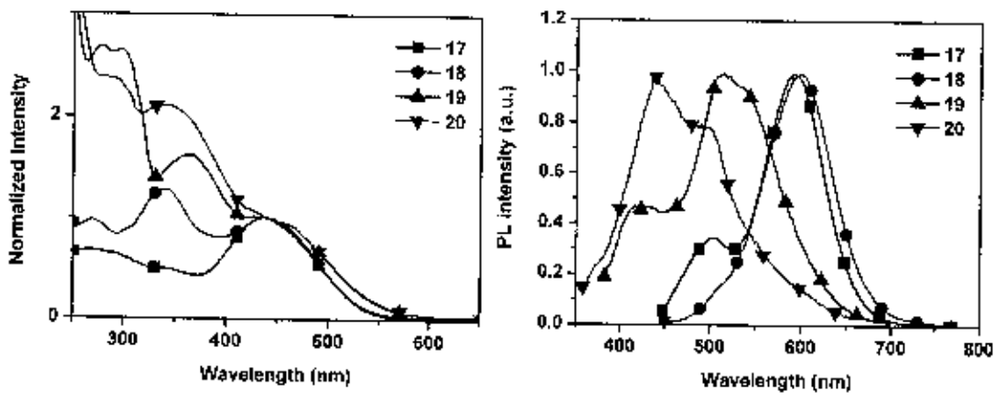

Figure 8.8 Absorption (left) and emission (right) spectra of **17-20** recorded in dichloromethane.

Table 8.1 The absorption and fluorescence data of **17-20**

Compound	λ_{max}^{abs} (εx 10^4); (nm (M^{-1} cm^{-1}))[a]	λ_{max}^{em} (nm)[a, b]	λ_{onset}^{abs} (nm)[a]	E_g (eV)[c]
17	436 (1.57)	592	544	2.28
18	438 (1.61), 341 (2.06)	599	537	2.31
19	430 (0.59), 362 (0.94), 298 (1.55)	516	556	2.23
20	459 (1.21), 339 (2.72)	437	556	2.23

[a] measured in dichloromethane solution at room temperature.

[b] excited at maximum absorption in solution.

[c] estimated from the onset of absorption ($E_g = 1240/\lambda_{onset}$).

The effect of solvent polarity on the absorption spectra of **17** dye was also studied (Figure 8.9 and Table 8.2). The absorption was measured in five different solvents dimethylformamide (DMF), dimethylsulfoxide (DMSO), ethanol (EtOH), tetrahydrofurane (THF) and dichloromethane (DCM)). We assigned the absorption bands at 280 nm as **B1** and at 408-436 nm as **B2**, respectively. There is only **B2** band that be effected by solvent polarity change. These **B2** bands therefore are assigned as ICT bands of donor-accepter molecule which can be generally observed in most sensitizer. The absorption spectra show blue shift when the polarity of solvents are increasing. **17** in DMF exhibited lowest maximum absorption at 408 nm (4.87×10^{-19} *J*), whereas **17** in dichloromethane exhibited the highest at 436 nm (4.56×10^{-19} *J*). These results can be considered as the negative solvatochromism-physical intermolecular solute-solvent interaction forces which tend to alter the energy difference between ground and excited state of chromophore of the dyes [40]. The polar solvents are good supporting solvent to the excited state dye species more than non-polar solvents resulting in close molecular orbital, which tends to absorb light at high energy region (low wavelength). This effect was also found in the other molecules (**18-20**).

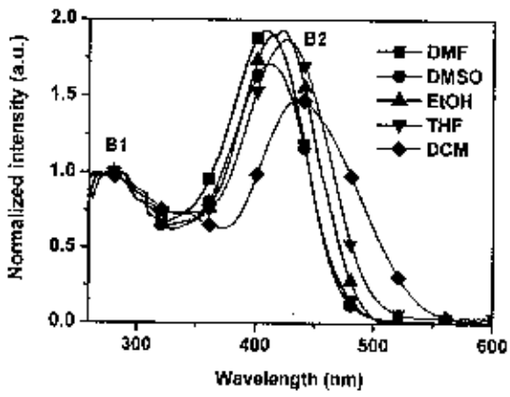

Figure 8.9 The absorption spectra of **17** dye in various solvents.

Table 8.2 Maximum absorption of **17** measured in various solvents

solvent	DMF	DMSO	EtOH	THF	DCM
λ_{max} (nm)	408	411	422	424	436
E^a (10^{-19} *J*)	4.87	4.84	4.71	4.69	4.56

[a] calculated from $E = h\nu/\lambda$

8.3.3 Thermal properties

The thermal decomposition of **17-20** dyes was studied by thermogravimetric analysis under nitrogen atmospheric condition. TGA thermograms of the dyes are displayed in Figure 8.10 and T_{5d} are listed in Table 8.3. The dyes exhibit 5% weight loss between 179 and 247 °C suggested that the dyes were thermally stable materials with temperature over 179 °C which is good for long term stability of DSCs devices.

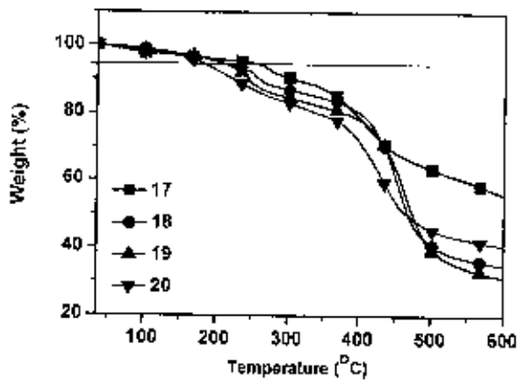

Figure 8.10 TGA thermograms of **17-20** dyes.

Table 8.3 Thermal properties of **17-20** dyes

Compound	T_{5d} (°C)
17	247
18	205
19	206
20	179

8.3.4 Molecular orbital calculation

To get an insight into the molecular structure and electron distribution of the organic dye, the **17-20** dyes geometries have been optimized using DFT calculations with Gaussian 03 program. The calculations were performed with the BTLYP exchange correlation functional under 6-31G(d,p) basis set. Computed HOMO and LUMO distribution of **17-20** are depicted in Figure 8.11 and 8.12. The general characters of the orbitals are independent of the linker length and different electron acceptor. The HOMO is of π-characteristics and is

delocalized over the entire molecule, including the *N*-aryl and *N*-phenylnaphthalen-1-amine groups. In the LUMO, which also has π-character, there is essentially no contribution from the *N*-aryl and *N*-phenylnaphthalen-1-amine groups, and the electron density has been shifted towards the acceptor group of the sensitizer. This supports the supposed push-pull characteristics of these sensitizers. In addition, the optimized geometry of **17-20** indicates that the *N*-aryl and *N*-phenylnaphthalen-1-amine moiety at the end of the molecule are in 3-D spatial arrangement, which makes the molecular structure nonplanar due to the twist conformation around the carbazole-carbazole C-*N* bond. The nonplanar molecular structure of **17-20** could be beneficial to solution-processability to form amorphous film. **17-20** are soluble in common organic solvents such as THF, CH_2Cl_2, $CHCl_3$ and acetone. High-quality amorphous film can be obtained by spin-coating its solution.

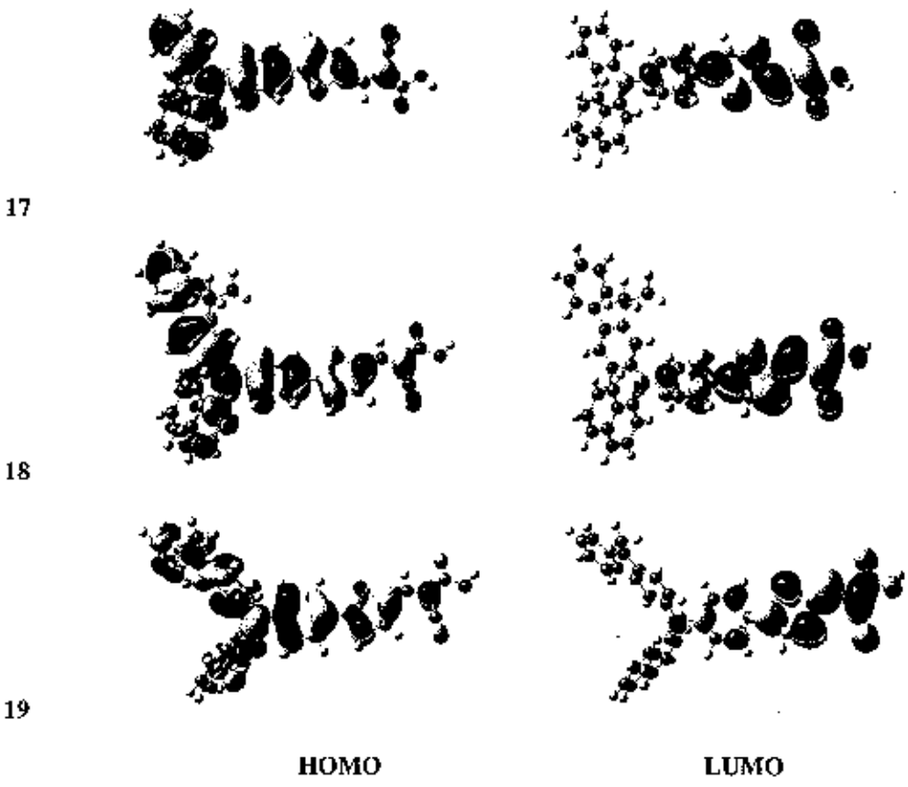

Figure 8.11 HOMO and LUMO distribution of the **17-19** dyes calculated with DFT on a BTLYP/6-31G(d,p) level.

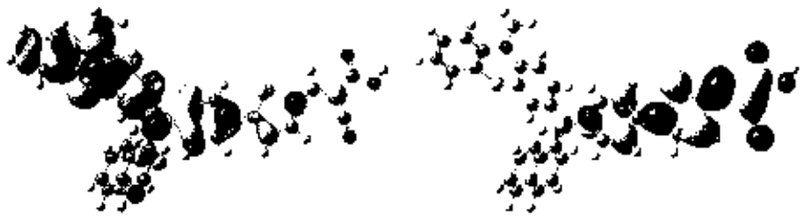

20

HOMO LUMO

Figure 8.12 HOMO and LUMO distribution of the **20** dye calculated with DFT on a BTLYP/6-31G(d,p) level.

8.4 Conclusions

Novel D-π-A organic dyes, **17-20**, have synthesized as photosensitizers for DSCs applications by using Ullmann coupling, Suzuki coupling and Knoevenagel condensation reaction. Different types of substitute group at *N* position of *N*-phenylnaphthalen-1-amine moiety are introduced to the molecules and serve as donor. The electron-withdrawing parts are cyanoacrylic acid groups. The target molecules were characterized by using NMR, IR, UV-vis and fluorescence techniques. The target molecules exhibit a adsorption band cover UV and visible region. Fluorescence spectra of the target molecules show emission peak at blue-orange region, excited at λ_{max} of each molecule. **17-20** show good thermal properties. DFT calculations have been performed on the dyes, and the results show that electron distribution from the whole molecules to the anchoring moieties occurred during the HOMO-LUMO excitation.

CHAPTER 9

SYNTHESIS, CHARACTERIZATION, PROPERTIES AND APPLICATION AS HOLE-TRANSPORTING MATERIAL OF MULTI-TRIPHENYLAMINE-SUBSTITUTED CARBAZOLE

9.1 Introduction

Since the pioneering works on the first organic light-emitting diodes (OLEDs) by Tang in 1987 [54], OLEDs have attracted massive attentions in the scientific community due to their potential for future flat-panel displays and lighting applications [55]. The past decade has seen great progress in both device fabrication techniques and materials development [56, 57]. One of the key developments is the use of hole-transporting layers (HTL) for hole injection from the anode into the light-emitting layer providing significant improvement in the performance of the device [58]. As a result, many new hole-transporting materials (HTM) have been developed. In particular, low-molecular weight amorphous materials have received interest as candidates for HTM due to their easy purification by vapor deposition or column chromatographic techniques, and uniformly thin films can be processed simply by coating techniques. The most commonly used amorphous hole-transporting materials (AHTM) are triarylamine derivatives such as *N*,*N*′-diphenyl-*N*,*N*′-bis(1-naphthyl)-(1,1′-biphenyl)-4,4′-diamine (NPB) and *N*,*N*′-bis(3-methylphenyl)-*N*,*N*′-bis(phenyl)benzidine (TPD) which have excellent hole-transporting properties. However, their low thermal and morphological stability usually lead to their degradation. In order to achieve highly efficient and long lifetime devices, an AHTM with high mobility, a high glass transition temperature (T_g), a stable amorphous state and good thin film formation is desirable. To optimize all these requirements, many efforts have been devoted to the synthesis of new AHTM. Carbazole derivatives containing peripheral diarylamine, additional carbazole, bis(4-*tert*-butylphenyl)carbazole units and dipyrenyl units were also reported to exhibit good thermal and morphological stability. Recently, we synthesized a series of aromatic compounds with peripheral triphenylamine-carbazole possessing high T_g (121-185 °C) values and found the OLED devices based on the resulting carbazole compounds to be promising in terms of

device performance and stability. Undoubtedly, it is very attractive to explore and develop new carbazole derivatives that meet the requirements as AHTM for OLEDs and which can be synthesized using simple and low-cost methods. Our design involved multiple substitution of the carbazole ring with triphenylamine moieties. With this molecular architecture, amorphous hole-transporting materials would be achieved [59].

9.2 Aim of the Study

Herein, we report on a simplistic synthesis of multi-triphenylamine substituted carbazole (**TnC** (n = 2-4)), and their physical and photophysical properties. Investigation on their abilities as hole-transporting layer in OLEDs is also reported.

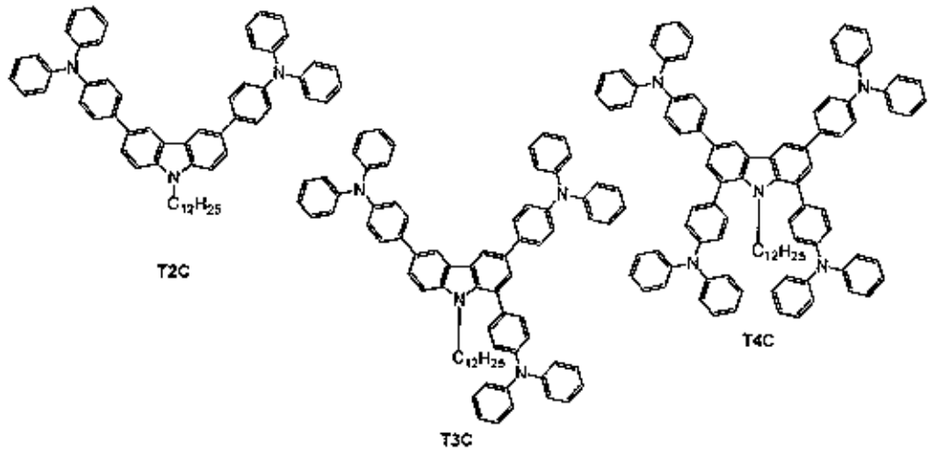

Figure 9.1 Chemical structures of **TnC** (n = 2-4).

9.3 Results and Discussion

9.3.1 Synthesis

Figure 9.2 outlines the synthesis of the triphenylamine functionalized carbazoles. We began with the synthesis of 3,6-dibromo-*N*-dodecylcarbazole (**66**), 1,3,6-tribromo-*N*-dodecyl carbazole (**67**) and 1,3,6,8-tetrabromo-*N*-dodecylcarbazole (**68**) by bromination of *N*-dodecylcarbazole (**65**) with NBS. A solution of **65** in THF was treated with NBS (2.1-15.0 equiv.) in small portions in the absence of light to yield **66-68** in moderate to good yields (75-

94%). Subsequently coupling of these multibromo-*N*-dodecylcarbazoles (**66**, **67** and **68**) with 4-(diphenylamino)phenylboronic acid (2.2-5.5 equiv.) in the presence of $Pd(PPh_3)_4$ as the catalyst and aqueous Na_2CO_3 as the base in THF at reflux afforded 3,6-bis(4-(diphenylamino)phenyl)-*N*-dodecylcarbazole (**T2C**), 1,3,6-tri(4-(diphenylamino)phenyl)-*N*-dodecylcarbazole (**T3C**) and 1,3,6,8-tetrakis(4-(diphenylamino)phenyl)-*N*-dodecyl carbazole (**T4C**) as white solids in good yields (75-92%). The structures of all molecules were characterized unambiguously with ^{1}H-NMR, ^{13}C-NMR spectroscopy as well as high resolution mass spectrometry. Noticeably, the ^{1}H-NMR spectra of **TnC** show the chemical shifts of the dodecyl protons being shifted to low frequency as the number of the triphenylamine substituents on a carbazole increased. This is due to a shielding effect resulting from a ring current produced by the surrounding 1- and 8- triphenylamine substituents. For example, the chemical shift of $-NCH_2-$ protons of **T2C** (4.34 ppm) shifts to 4.00 and 3.70 ppm in **T3C** and **T4C**, respectively. These compounds show good solubility in most organic solvents

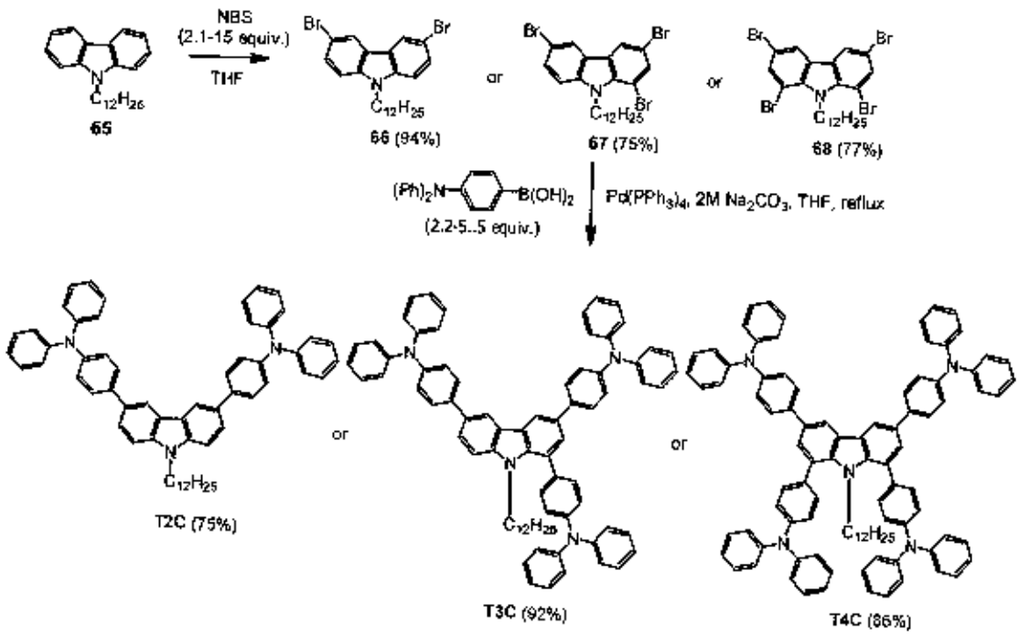

Figure 9.2 Synthesis of triphenylamine substituted carbazoles (**TnC** (n = 2-4)).

9.3.2 Optical properties

The solution UV-Vis absorption spectra of **TnC** show absorption band at 320–328 nm corresponding to the π–π^* electron transition of the π-conjugated 3,6-bis(4-(diphenylamino)phenyl)carbazole backbone (Figure 9.3). In cases of **T3C** and **T4C**, absorption band at lower wavelengths (284-296 nm) is observed, which is identical to the absorption peak of a triphenylamine chromophore. This absorption band can be assigned to the π–π^* electron transition of the isolated triphenylamine substituents at the 1- or 8-positions. The intensity of this peak is stronger in **T4C** as it has two triphenylamine moieties (1,8-positions). This outcome agrees with the quantum chemistry calculation results. The solution photoluminescence (PL) spectra of **TnC** display an emission band in the blue-purple region (λ_{max} = 415-419 nm). The PL spectra of their thin films are similar to those in solution with a ~10 nm red shift. This indicates the presence of certain intermolecular electronic interactions. Nevertheless, the degree of the red shift is considerably smaller than those observed with π-conjugated compounds that adopt face-to-face stacking. These materials show slight Stokes shifts (91-95 nm) suggesting reduced energy loss during the relaxation process.

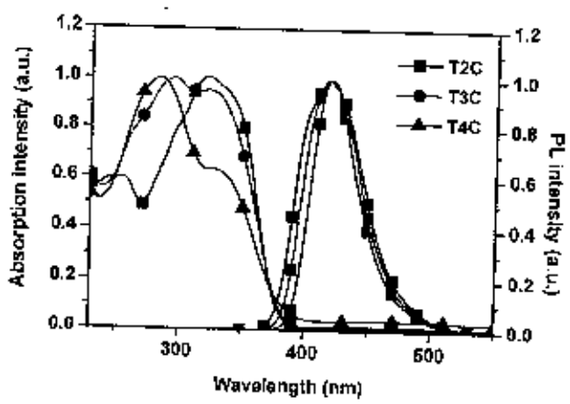

Figure 9.3 Absorption (left) and emission (right) spectra of **TnC** (n = 2-4) recorded in dichloromethane.

Table 9.1 The absorption and fluorescence data of TnC (n = 2-4)

Compound	λ_{max}^{abs} (nm)[a]	λ_{max}^{em} (nm)[a,b]	λ_{onset}^{abs} (nm)[a]	E_g (eV)[c]
T2C	320	415	496	2.50
T3C	325, 296	417	484	2.56
T4C	328, 284	419	449	2.76

[a] measured in dichloromethane solution at room temperature.

[b] excited at maximum absorption in solution.

[c] estimated from the onset of absorption ($E_g = 1240/\lambda_{onset}$).

9.3.3 Thermal properties

The thermal properties of **TnC** were determined by differential scanning calorimetry (DSC) and thermogravimetric analysis (TGA) and the results are shown in Figure 9.4 and Table 9.2. **T2C** is a crystalline material as its DSC trace reveals only an endothermic peak due to the melting point at 189 °C, while thermogram of **T4C** shows only an endothermic baseline shift due to glass transitions (T_g) at 122 °C, indicating amorphous material. When the crystalline sample of **T3C** was subjected to DSC heating scan, an endothermic baseline shift at 78 °C followed by an exothermic peak due to crystallization and endothermic melting peak at 163 and 207 °C, respectively, are observed, indicating semi-crystalline material. The T_g value of the amorphous T4C is higher than those of the most widely used HTMs, NPB (T_g = 100 °C) and TPD (T_g = 63 °C). The thermal stabilities of TnC were further confirmed by TGA measurements showing an increasing 5% weight loss temperatures (T_{5d}) from 334 °C for **T2C** to 415 °C for **T4C** as number the triphenylamine in the molecule increased. The results suggest that the presence of more triphenylamines in the molecule not only improve its thermal stability, but also induce the formation of an amorphous form in the material, which in turn could increase the service time in device operation and enhance the morphological stability of the thin film. Moreover, the ability to form a molecular glass with the possibility to prepare good thin films by both evaporation and solution casting processes is highly desirable for application in electroluminescent devices.

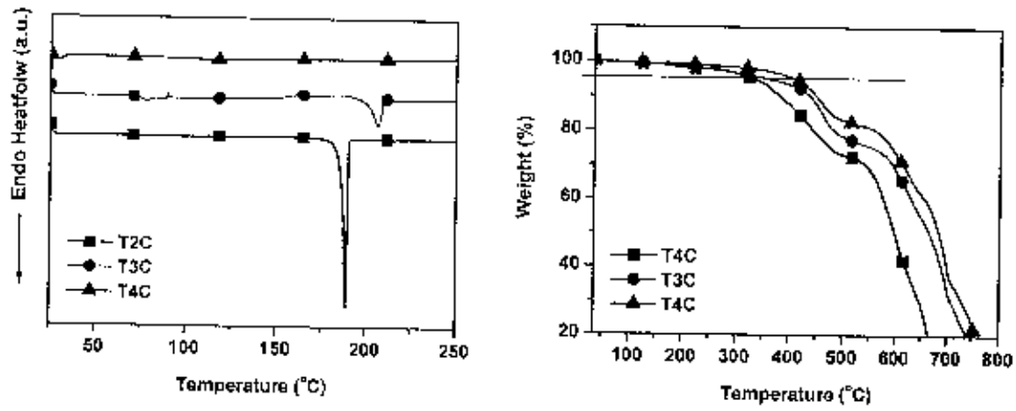

Figure 9.4 DSC and TGA curves measured with a heating rate of 10 °C/min under N_2.

Table 9.2 Thermal properties of **TnC** (n = 2-4)

Compound	T_g (°C)	T_m (°C)	T_{5d} (°C)
T2C	-	189	334
T3C	78	207	372
T4C	122	-	415

9.3.4 Electrochemical property

CV curves of **TnC** measured in CH_2Cl_2 containing n-Bu_4NF_6 as supporting electrolyte exhibit multiple quasireversible oxidation processes (Figure 9.5, Table 9.3). Under these experimental conditions, no reduction is observed in all cases. The first two oxidation waves at 0.78 and 0.89 V in all compounds appear at the same potential and can be assigned to the removal of electrons from the conjugated 3,6-bis(4-(diphenylamino)phenyl)carbazole backbone resulting in radical cation and dication, respectively. The oxidation waves at 1.03-1.07 V in both **T3C** and **T4C** match with the oxidation potential of a triphenylmine (E_{ox} = 0.98 V vs SCE) and therefore can be allocated to an oxidation of the isolated triphenylamine substituent at the 1,8-positions, consenting with both optical and the quantum chemistry calculation results. The oxidation waves at higher potential (1.20-1.29 V) of all cases correspond to the removal of electrons from the interior carbazole moiety. Multiple CV scans revealed identical CV curves with no additional peak at lower potentials on the cathodic scan (E_{pc}) being observed. This suggests no electrochemical coupling at both the carbazole and triphenylamine peripheries, indicating

electrochemically stable molecules. Usually, this type of electrochemical coupling reaction is detected in most triphenylamine derivatives with unsubstituted p-position of the phenyl ring such as in case of 7-(pyren-1-yl)-2,9,9-tris(4-diphenylaminophenyl)fluorene. The steric hindrance effect and stability by electron delocalization might play an important role in preventing the triphenylamine moieties to such electrochemical reaction in all compounds. The HOMO and LUMO energy levels of the **TnC** were calculated from the oxidation onset potentials (E_{onset}) and energy gaps (E_g) and the results are summarized in Table 9.3. All compounds have identical HOMO levels of -5.15 V, while their LUMO levels are varied from -1.86 to -1.91 V.

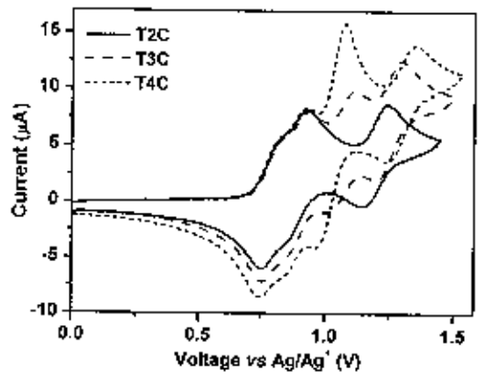

Figure 9.5 CV curves measured in CH_2Cl_2 at a scan rate of 50 mV/s.

Table 9.3 Electrochemical properties of **TnC** (n = 2-4)

compoud	$E_{1/2}^{ox}$ vs Ag/Ag^+ (V)[a]	E_g (eV)[b]	HOMO/LUMO (eV)[b]
T2C	0.78, 0.89, 1.20	3.29	-5.15/-1.86
T3C	0.78, 0.89, 1.07, 1.25	3.26	-5.16/-1.90
T4C	0.78, 0.89, 1.03, 1.29	3.24	-5.15/-1.91

[a] Measured by CV using glassy carbon working electrode, Pt counter electrode and Ag/Ag^+ reference electrode with 0.1 M *n*-Bu_4NPF_6 as supporting electrolyte in CH_2Cl_2 solution.

[b] Calculated by $E_g = 1240/\lambda_{onset}$; HOMO = $-(4.44 + E^{ox}_{onset})$; LUMO = E_g + HOMO.

9.3.5 Molecular orbital calculation

To gain insight into the geometrical and electronic properties of these multiple substituted carbazole, quantum chemistry calculation was performed using the TDDFT/B3LYP/6-31G(d) method. The optimized structures of **TnC** reveal that the phenyl rings attached to the carbazole of each triphenylamine twist out of plane of the carbazole forming bulky substituents around the carbazole especially in **T4C** (Figure 9.6 and 9.7). This would facilitate the formation amorphous materials. In all cases, π-electrons in the HOMO orbitals delocalize only over the carbazole and two triphenylamine substituents at the 3,6-positions (3,6-bis(4-(diphenylamino)phenyl)carbazole backbone), and no electrons at triphenylamine moieties at the 1,8-positions. In the LUMO orbitals, the excited electrons are delocalized over the carbazole plane and the phenyl ring of the triphenylamine substituents at the 1,8-positions. This suggests that substitution of a carbazole at the 1- or 8-positions with triphenylamine only has the effect on the LUMO of the molecule, while the HOMO remains nearly untouched.

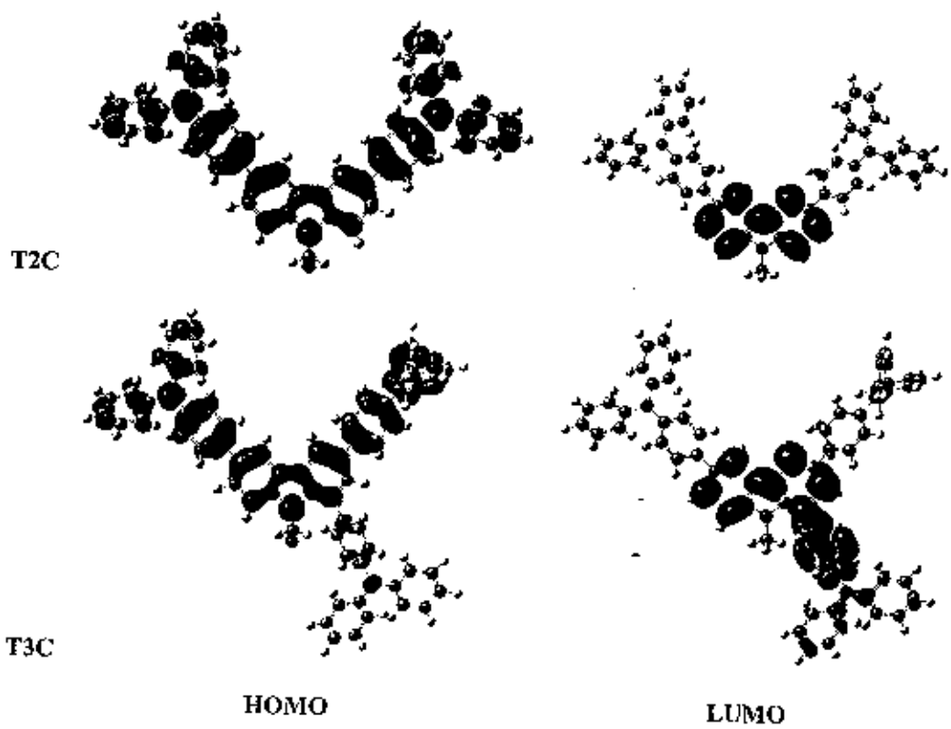

Figure 9.6 HOMO and LUMO orbitals of TnC (n = 2-3) calculated by TDDFT/B3LYP/6-31G(d).

Table 9.4 OLED device characteristics

compoud	V_{on}/V_{100} (V)[a]	λ_{em} (nm)	L_{max} (cd/m^2)	η (cd/A)	EQE (%)[b]
T2C	2.4/3.0	518	28781	4.97	0.24
T3C	2.4/3.4	518	25052	5.00	0.24
T4C	2.5/3.4	518	22411	5.07	0.25

[a] Voltage at luminance of 1 and 100 cd/m^2.

[b] External quantum efficiency.

9.4 Conclusions

In summary, we demonstrated the simple design strategy, synthesis and characterizations of multi-triphenylamine-substituted carbazole. By increasing number of triphenylmine substituents in the molecule not only improve its thermal stability, but also induce the formation of an amorphous form in the material. They are electrochemically and thermally stable materials with reasonable high glass transition temperatures. These materials show excellent hole-transporting property for Alq3-based green OLED with device's luminance efficiency as high as 5.07 cd/A being achieved.

CHAPTER 10

SUMMARY

Novel D-π-A organic materials (**1-20**) containing different donor and linker units for using as dye molecules in dye solar cells (DSCs) were successfully synthesized. The target molecules were characterized by ^{1}H-NMR, ^{13}C-NMR, FT-IR, and MALDI-TOF MS techniques. The optical study by UV-Vis spectroscopy indicated that designed molecules exhibit an adsorption band cover UV and visible region. All compounds show good thermal properties. Moreover, Density functional theory (DFT) calculations have been performed on the dyes and the results show that electron distribution from the electron donors to the electron acceptors occurred during the HOMO-LUMO excitation. The photovoltaic performance of DSCs using these materials as dyes is under investigation and will be reported in the future. Finally, the multi-triphenylamine-substituted carbazoles (**T2C**, **T3C** and **T4C**) for using as hole-transporting layer in organic light-emitting diodes (OLEDs) were successfully synthesized and characterized. The thermal and electrochemical stability and formation of an amorphous form in the material was improved by increasing number of triphenylmine substituents in the molecule. **T2C**, **T3C** and **T4C** compounds show excellent hole-transporting property for Alq3-based green OLED with device's luminance efficiency in the range of 4.97-5.07 cd/A.

CHAPTER 11

EXPERIMENT

11.1 General procedures and instruments

^{1}H-NMR spectra were recorded on Brüker AVANCE (300 and 500 MHz) and Varian Inova 300 MHz spectrometer. ^{13}C NMR spectra were recorded on Brüker AVANCE (75 and 125 MHz) and Varian Inova 75 MHz spectrometer and were fully decoupled. Chemical shifts (δ) are reported relative to the residual solvent peak in part per million (ppm). Coupling constants (J) are given in Hertz (Hz). Multiplicities are quoted as singlet (s), broad (br), doublet (d), triplet (t), quartet (q), AA′BB′ quartet system (AA′BB′), AB quartet (ABq) and multiplet (m).

The IR spectra were recorded on a Perkin-Elmer FT-IR spectroscopy as KBr disks or neat liquid between two NaCl plates. The absorption peaks are quoted in wavenumber (cm^{-1}). UV-visible spectra were measured in spectrometric grade dichloromethane and tetrahydrofuran on Perkin-Elmer UV Lambda 25 and Varian Cary 1E UV Visible spectrometer. The absorption peaks are reported as in wavelength (nm) (log ε /$dm^3mol^{-1}cm^{-1}$) and sh refers to shoulder. Fluorescence spectra were recorded as a dilute solution in spectroscopic grade dichloromethane on a Perkin-Elmer LS 50B Luminescence Spectrometer.

Dichloromethane was washed with conc. H_2SO_4 and distilled twice from calcium hydride. Tetrahydrofuran (THF) was heated at reflux under nitrogen over sodium wire and benzophenone until the solution became blue and freshly distilled before use. All reagents and solvents were purchased from Aldrich, Acros, Fluka or Thai Supplies and received unless otherwise stated.

Analytical thin-layer chromatography (TLC) was performed with Merck aluminium plates coated with silica gel 60 F_{254}. Column chromatography was carried out using gravity feed chromatography with Merck silica gel mesh, 60 Å. Where solvent mixtures are used, the portions are given by volume.

The electrochemistry was performed using a AUTOLAB spectrometer. All measurements were made at room temperature on sample dissolved in freshly distilled

dichloromethane, 0.1 M tetra-*n*-butylammonium hexafluorophosphate as electrolyte. The solutions were degassed by bubbling with argon. Dichloromethane was washed with concentrated sulfuric acid and distilled from calcium hydride. A glassy carbon working electrode, platinum wire counter electrode, and a Ag/AgCl/NaCl (Sat.) reference electrode were used. The ferrocenium/ferrocene couple was used as standard, and the ferrocene was purified by recrystallisation from ethanol and then dried under high vacuum and stored over P_2O_5.

Thermal gravimetric analysis (TGA) was performed on TG8120 thermoPlus, Rigaku, Japan thermal analyzer and TGA/DSC 1 thermogravimetric analyzer from Mettler Toledo. Samples were scanned from 25 °C to 800 °C using a heating rate of 10 °C/min and a cooling rate of 70 °C/min under a nitrogen flow.

Differential scanning carolimetry (DSC) analysis was performed on a METTLER DSC823e thermal analyzer using a heating rate of 10 °C/min and a cooling rate of 50 °C/min under a nitrogen flow. Samples were scanned from 25 to 350 °C and then rapidly cooled to 25 °C and scanned for the second time at the same heating rate to 350 °C.

Melting points was measured by Griffin Melting point apparatus in open capillary method and are uncorrected and reported in degree Celsius.

11.2 Synthesis and characterization

Chapter 2:

5-(4-(Diphenylamino)phenyl)thiophene-2-carbaldehyde (22)

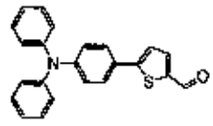

A mixture of (4-(diphenylamino)phenyl)boronic acid (**21**) (0.50 g, 1.73 mmol), 5-bromothiophene-2-carbaldehyde (0.33 g, 1.73 mmol), $Pd(PPh_3)_4$ (0.08 g, 0.07 mmol), and 2 M Na_2CO_3 aqueous solution (17 ml, 34 mmol) in THF (20 ml) was degassed with N_2 for 5 min. The reaction mixture was stirred at reflux under N_2 for 24 h. After being cooled to room temperature, water (30 ml) was added and extracted with CH_2Cl_2 (30 ml x 3). The combined organic phases were washed with water (30 ml) and brine solution (70 ml), dried over anhydrous

Na_2SO_4, filtered, and the solvents were removed to dryness. Purification by column chromatography over silica gel eluting with a mixture of CH_2Cl_2 and hexane (2:3) followed by recrystallization with a mixture of CH_2Cl_2 and methanol afforded 5-(4-(diphenylamino)phenyl)thiophene-2-carbaldehyde (0.61 g, 99%) as green solid $C_{23}H_{17}NOS$; ^{1}H-NMR (300 MHz, $CDCl_3$) δ 9.85 (1H, s), 7.71 (1H, d, J = 3.9 Hz), 7.52 (2H, d, J = 8.4 Hz), 7.33-7.27 (5H, m), and 7.16-7.05 (8H, m) ppm; ^{13}C-NMR (75 MHz, $CDCl_3$) δ 182.90, 147.24, 138.01, 129.76, 127.52, 125.45, 124.15, 123.13, and 122.64 ppm; FT-IR (KBr) 3033, 2923, 2800, 2743, 1658, 1595, 1444, 1322, 1284, 1228, 1020, 805, 756, and 696 cm^{-1}; MS (MALDI-TOF) m/z = 355.2590 $[M]^{+\bullet}$, 355.1031 calcd for $C_{23}H_{17}NOS$.

(*E*)-2-Cyano-3-(5-(4-(diphenylamino)phenyl)thiophen-2-yl)acrylic acid (1)

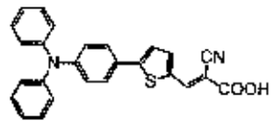

A mixture of **22** (0.20 g, 0.56 mmol) and cyanoacetic acid (0.24 g, 2.81 mmol) was vacuum-dried and added piperidine (0.33 ml, 3.94 mmol) in $CHCl_3$ (20 ml). The solution was refluxed for 6 h. After cooling the solution, the organic layer was removed in vacuo. The pure product was obtained by column chromatography over silica gel eluting with a mixture of MeOH and EtOAc (1:9) followed by recrystallization with a mixture of CH_2Cl_2 and methanol afforded **1** (0.12 g, 50%) as light orange solid; $C_{26}H_{18}N_2O_2S$; m.p. 254-255 °C; ^{1}H-NMR (300 MHz, $CDCl_3$) δ 8.34 (1H, s), 7.53 (1H, s), 7.19 (7H, s), 7.00 (7H, s), and 6.86 (2H, s) ppm; ^{13}C-NMR (75 MHz, $CDCl_3$) δ 169.86, 151.69, 148.45, 147.14, 145.31, 138.33, 135.14, 129.58, 127.17, 126.74, 125.10, 123.79, 123.13, 122.54, 118.87, and 103.54 ppm; FT-IR (KBr) 3422, 3064, 3024, 2919, 2853, 2212, 1590, 1489, 1442, 1392, 1314, 1271, 1239, 1193, 1061, 935, 802, 752, 695, and 617 cm^{-1}; MS (MALDI-TOF) m/z = 422.2762 $[M]^{+\bullet}$, 422.1089 calcd for $C_{26}H_{18}N_2O_2S$.

5-(4-(Carbazol-9-yl)phenyl)thiophene-2-carbaldehyde (24)

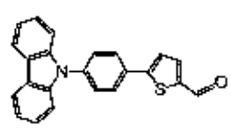

A mixture of 9-(4-bromophenyl)carbazole (**23**) (0.80 g, 2.48 mmol), (5-formylthiophen-2-yl)boronic acid (0.42 g, 2.68 mmol), $Pd(PPh_3)_4$ (0.11 g, 0.10 mmol), and 2 M Na_2CO_3 aqueous solution (25 ml, 50 mmol) in THF (40 ml) was degassed with N_2 for 5 min. The reaction mixture was stirred at reflux under N_2 for 24 h. After being cooled to room temperature, water (70 ml) was added and extracted with CH_2Cl_2 (70 ml x 3). The combined organic phases were washed with water (70 ml) and brine solution (70 ml), dried over anhydrous Na_2SO_4, filtered, and the solvents were removed to dryness. Purification by column chromatography over silica gel eluting with a mixture of CH_2Cl_2 and hexane (2:3) followed by recrystallization with a mixture of CH_2Cl_2 and methanol afforded 5-(4-(carbazol-9-yl)phenyl)thiophene-2-carbaldehyde (0.26 g, 30%) as green solid; $C_{23}H_{15}NOS$; ^{1}H-NMR (300 MHz, $CDCl_3$) δ 9.94 (1H, s), 8.16 (2H, d, J = 7.8 Hz), 7.91 (2H, d, J = 8.4 Hz), 7.80 (1H, d, J = 3.9 Hz), 7.67 (2H, d, J = 8.4 Hz), 7.51-7.41 (5H, m), and 7.35-7.29 (2H, m) ppm; ^{13}C-NMR (75 MHz, $CDCl_3$) δ 182.77, 153.07, 142.87, 140.51, 138.80, 137.43, 131.95, 127.89, 127.52, 126.13, 124.49, 123.67, 120.44, 120.37, and 109.73 ppm; FT-IR (KBr) 3090, 3061, 2926, 2848, 2734, 1670, 1478, 1452, 1416, 1364, 1337, 1231, 1117, 1017, 816, 753, and 725 cm^{-1}; MS (MALDI-TOF) m/z = 353.2087 $[M]^{+\cdot}$, 353.0874 calcd for $C_{23}H_{15}NOS$.

(*E*)-3-(5-(4-(Carbazol-9-yl)phenyl)thiophen-2-yl)-2-cyanoacrylic acid (2)

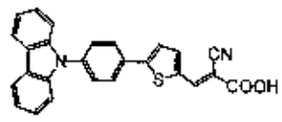

A mixture of **24** (0.30 g, 0.85 mmol) and cyanoacetic acid (0.36 g, 4.24 mmol) was vacuum-dried and added piperidine (0.59 ml, 5.94 mmol) in $CHCl_3$ (20 ml). The solution was refluxed for 6 h. After cooling the solution, the organic layer was removed in vacuo. The pure product was obtained by column chromatography over silica gel eluting with a mixture of MeOH and EtOAc (1:9) followed by recrystallization with a mixture of CH_2Cl_2 and methanol afforded **2** (0.25 g, 70%) as light yellow solid; $C_{26}H_{16}N_2O_2S$; m.p. 254-255 °C; ^{1}H-NMR (300 MHz, $CDCl_3$) δ 8.50 (1H, s, br), 8.03-8.02 (2H, m), 7.67 (2H, m), 7.40 (4H, m), and 7.24 (6H, m) ppm; ^{13}C-NMR (75 MHz, $CDCl_3$) δ 168.83, 140.38, 138.08, 132.04, 127.60, 127.19, 126.19, 123.60, 120.40, and

109.76 ppm; FT-IR (KBr) 3420, 3059, 3020, 2918, 2852, 2307, 1590, 1489, 1441, 1392, 1314, 1271, 1237, 1191, 1178, 1060, 891, 803, 752, and 696 cm^{-1}; MS (MALDI-TOF) m/z = 420.2902 $[M]^{+\cdot}$, 420.0932 calcd for $C_{26}H_{16}N_2O_2S$.

3-Iodocarbazole (26)

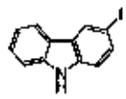

A mixture of carbazole (**25**) (5.00 g, 29.90 mmol), KI (3.23 g, 19.44 mmol), KIO_3 (3.20 g, 14.95 mmol) in glacial acetic acid (75 ml) was heated at 70 °C for 10 min. The temperature was cooled and DCM (200 ml) was added. The organic phase was thoroughly washed with water (200 ml x 4), 0.2 M aqueous Na_2SO_3 (70 ml x 2) and aqueous $NaHCO_3$ (200 ml), brine solution (200 ml), dried over anhydrous Na_2SO_4 and filtered. After solvent evaporation, the pure compound was obtained by recrystallization from DCM/hexane mixture as light gray solids (7.36 g, 84%): $C_{12}H_8IN$; m.p. 145-146 °C; ^{1}H-NMR (300 MHz, $CDCl_3$) δ 8.39 (1H, s), 8.08 (s, 1H, br), 8.02 (1H, d, J = 7.8 Hz), 7.66 (1H, dd, J = 9.0 Hz, J = 1.6 Hz), 7.48-7.41 (2H, m), and 7.30-7.21 (2H, m) ppm; ^{13}C-NMR (75 MHz, $CDCl_3$) δ 135.04, 134.30, 129.61, 129.46, 126.83, 120.72, 120.20, 112.94, 112.83, and 110.98 ppm; FT-IR (KBr) 3404, 3033, 1608, 1441, 1018, 928, 808, 746, and 569 cm^{-1}.

3-Iodo-9-phenylcarbazole (27)

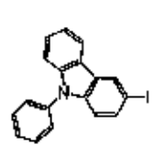

To a mixture of CuI (0.65 g, 3.41 mmol), KO^{t}Bu (1.91 g, 17.06 mmol), and iodobenzene (1.39 g, 6.82 mmol) in toluene (60 mL) were added 3-iodocarbazole (**26**) (2.00 g, 6.82 mmol) and (±)-*trans*-1,2-diaminocyclohexane (0.41 g, 3.41 mmol). The reaction mixture was stirred at 110 °C under nitrogen. After 24 h, water (50 ml) was added until the two phases mixed. The solution was extracted with CH_2Cl_2 (50 ml x 3), washed with water (50 ml), brine solution (50

ml) and dried with Na_2SO_4, filtered, and the solvents removed to dryness. After the solvent was evaporated. The crude product was purified by column chromatography on silica gel with hexane as eluent to yield 3-iodo-9-phenylcarbazole (**27**) (2.34 g, 93%) as light white viscous $C_{18}H_{12}IN$; ^{1}H-NMR (300 MHz, $CDCl_3$) δ 8.52, (1H, s), 8.13 (1H, d, J = 7.2 Hz), 7.71-7.62 (3H,m), 7.55-7.45 (5H, m), 7.35 (1H, t, J = 3.5 Hz), and 7.23-7.18 (1H, m) ppm; ^{13}C-NMR (75 MHz, $CDCl_3$) δ 134.15, 129.99, 129.16, 127.80, 127.07, 126.64, 120.43, 120.38, 111.83, and 109.94 ppm; MS (MALDI-TOF) m/z = 369.1355 $[M]^{+\cdot}$, 369.0014 calcd for $C_{18}H_{12}IN$.

5-(9-Phenylcarbazol-3-yl)thiophene-2-carbaldehyde (28)

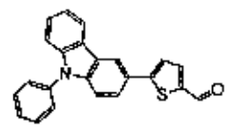

A mixture of **27** (0.75 g, 2.03 mmol), (5-formylthiophen-2-yl)boronic acid (0.34 g, 2.19 mmol), $Pd(PPh_3)_4$ (0.09 g, 0.08 mmol), and 2 M Na_2CO_3 aqueous solution (20 ml, 40 mmol) in THF (20 ml) was degassed with N_2 for 5 min. The reaction mixture was stirred at reflux under N_2 for 24 h. After being cooled to room temperature, water (30 ml) was added and extracted with CH_2Cl_2 (30 ml x 3). The combined organic phases were washed with water (30 ml) and brine solution (30 ml), dried over anhydrous Na_2SO_4, filtered, and the solvents were removed to dryness. Purification by column chromatography over silica gel eluting with a mixture of CH_2Cl_2 and hexane (2:3) followed by recrystallization with a mixture of CH_2Cl_2 and methanol afforded 5-(9-phenylcarbazol-3-yl)thiophene-2-carbaldehyde (**28**) (0.34 g, 48%) as yellow solid; $C_{23}H_{15}NOS$; m.p. 125-126 °C; ^{1}H-NMR (300 MHz, $CDCl_3$) δ 9.89 (1H, s), 8.44 (1H, s), 8.19 (1H, d, J = 7.8 Hz), 7.77-7.70 (2H, m), 7.66-7.61 (2H, m), 7.57-7.49 (3H, m), and 7.46-7.32 (5H, m) ppm; ^{13}C-NMR (75 MHz, $CDCl_3$) δ 182.62, 155.99, 141.46, 137.80, 137.15, 130.04, 127.92, 127.06, 126.74, 127.20, 124.67, 123.99, 123.12, 123.04, 120.61, 120.54, 118.48, 110.43, and 110.19 ppm; FT-IR (KBr) 3064, 2958, 2924, 2854, 2800, 1661, 1598, 1501, 1436, 1364, 1233, 1262, 1057, 1025, 879, 801, 747, and 699 cm^{-1}; MS (MALDI-TOF) m/z = 353.2273 $[M]^{+\cdot}$, 353.0874 calcd for $C_{23}H_{15}NOS$.

(*E*)-2-Cyano-3-(5-(9-phenylcarbazol-3-yl)thiophen-2-yl)acrylic acid (3)

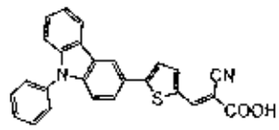

A mixture of **28** (0.30 g, 0.85 mmol) and cyanoacetic acid (0.36 g, 4.24 mmol) was vacuum-dried and added piperidine (0.51 ml, 5.94 mmol) in $CHCl_3$ (20 ml). The solution was refluxed for 6 h. After cooling the solution, the organic layer was removed in vacuo. The pure product was obtained by column chromatography over silica gel eluting with a mixture of MeOH and EtOAc (1:9) followed by recrystallization with a mixture of CH_2Cl_2 and methanol afforded **3** (0.24 g, 68%) as light orange solid; $C_{26}H_{16}N_2O_2S$; m.p. 260-261 °C; ^{1}H-NMR (300 MHz, $CDCl_3$) δ 8.42 (1H, s), 8.22 (1H, s), 8.01 (1H, d, J = 6.6 Hz), 7.70 (1H, s), 7.55 (1H, s), 7.48-7.47 (4H, m), 7.31-7.28 (4H, m), 7.20 (1H, d, J = 6.6 Hz), 7.10 (1H, m), and 6.96 (1H, s) ppm; ^{13}C-NMR (75 MHz, $CDCl_3$) δ 167.96, 153.62, 145.37, 141.18, 140.84, 138.56, 136.89, 136.67, 134.73, 129.96, 127.72, 126.68, 125.45, 125.18, 124.45, 123.71, 123.17, 122.94, 120.53, 118.41, 118.08, 110.09, and 110.00 ppm; FT-IR (KBr) 3411, 3055, 3037, 2956, 2910, 2861, 2219, 1684, 1567, 1500, 1414, 1235, 1062, 805, 760, and 698 cm^{-1}; MS (MALDI-TOF) m/z = 420.2049 $[M]^{+\cdot}$, 420.0932 calcd for $C_{26}H_{16}N_2O_2S$.

3,6-Di-*tert*-butyl-9-phenylcarbazole (30)

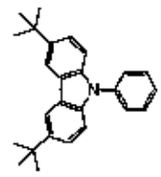

To a mixture of CuI (1.70 g, 8.95 mmol), KO^{t}Bu (5.02 g, 44.73 mmol), and iodobenzene (3.65 g, 17.89 mmol) in toluene (60 mL) were added 3,6-di-*tert*-butylcarbazole (**29**) (5 g, 17.89 mmol) and (±)-*trans*-1,2-diaminocyclohexane (1.02 g, 1.07 mmol). The reaction mixture was stirred at 110 °C under nitrogen. After 24 h, water (100 ml) was added until the two phases mixed. The solution was extracted with CH_2Cl_2 (100 ml x 3), washed with water (100 ml), brine solution (100 ml) and dried with Na_2SO_4, filtered, and the solvents removed to dryness. After

the solvent was evaporated. The crude product was purified by column chromatography on silica gel with hexane as eluent to yield 3,6-di-*tert*-butyl-9-phenylcarbazole (6.29 g, 99%) as light white solid; $C_{26}H_{29}N$; m.p. 150-151 °C; ^{1}H-NMR (300 MHz, $CDCl_3$) δ 8.14, (2H, s), 7.56-7.54 (4H,m), 7.46-7.32 (5H, m), and 1.46 (18H, s) ppm; ^{13}C-NMR (75 MHz, $CDCl_3$) δ 143.11, 139.61, 138.66, 130.03, 127.25, 127.09, 123.87, 123.66, 116.50, 109.50, 35.03, and 32.34 ppm; FT-IR (KBr) 3058, 3034, 3004, 2951, 2904, 2862, 1595, 1503, 1488, 1477, 1456, and 1361, cm^{-1}; MS (MALDI-TOF) m/z = 355.4462 $[M]^{+\cdot}$, 355.2300 calcd for $C_{26}H_{29}N$.

3,6-Di-*tert*-butyl-9-(4-iodophenyl)carbazole (31)

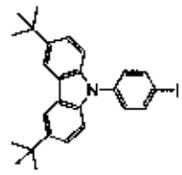

A mixture of 3,6-di-*tert*-butyl-9-phenylcarbazole (30) (4.36 g, 12.27 mmol), I_2 (1.56 g, 6.13 mmol), KIO_3 (0.52 g, 2.45 mmol) and 20%H_2SO_4 (50 ml) in glacial acetic acid (75 ml) was heated at 70 °C for 10 min. The temperature was cooled and DCM (100 ml) was added. The organic phase was thoroughly washed with water (100 ml x 4), 0.2 M aqueous Na_2SO_3 (100 ml x 2) and aqueous $NaHCO_3$ (100 ml), brine solution (100 ml), dried over anhydrous Na_2SO_4 and filtered. After solvent evaporation, the pure compound was obtained by recrystallization from DCM/hexane mixture as light white solids (4.27 g, 80%): $C_{26}H_{28}IN$; m.p. 271-272 °C; ^{1}H-NMR (300 MHz, $CDCl_3$) δ 8.10 (1H, s), 8.09 (1H, s), 7.93 (2H, s), 7.58-7.45 (6H, m), and 1.43 (18H, s) ppm; ^{13}C-NMR (75 MHz, $CDCl_3$) δ 145.19, 139.11, 137.99, 136.01, 135.43, 130.36, 128.38, 124.79, 116.31, 109.99, 73.44, 34.71, and 32.05 ppm; FT-IR (KBr) 3069, 3040, 3007, 2954, 2897, 2865, 1547, 1477, 1418, 1264, and 496 cm^{-1}; MS (MALDI-TOF) m/z = 481.3173 $[M]^{+\cdot}$, 481.1266 calcd for $C_{26}H_{28}IN$.

5-(4-(3,6-Di-*tert*-butylcarbazol-9-yl)phenyl)thiophene-2-carbaldehyde (32)

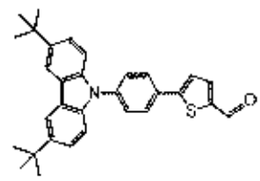

A mixture of **31** (2.50 g, 5.20 mmol), (5-formylthiophen-2-yl)boronic acid (0.87 g, 5.61 mmol), $Pd(PPh_3)_4$ (0.24 g, 0.21 mmol), and 2 M Na_2CO_3 aqueous solution (52 ml, 104 mmol) in THF (50 ml) was degassed with N_2 for 5 min. The reaction mixture was stirred at reflux under N_2 for 24 h. After being cooled to room temperature, water (70 ml) was added and extracted with CH_2Cl_2 (70 ml x 3). The combined organic phases were washed with water (70 ml) and brine solution (70 ml), dried over anhydrous Na_2SO_4, filtered, and the solvents were removed to dryness. Purification by column chromatography over silica gel eluting with a mixture of CH_2Cl_2 and hexane (2:3) followed by recrystallization with a mixture of CH_2Cl_2 and methanol afforded 5-(4-(3,6-di-*tert*-butylcarbazol-9-yl)phenyl)thiophene-2-carbaldehyde (**32**) (1.45 g, 60%) as yellow solid $C_{31}H_{31}NOS$; ^{1}H-NMR (300 MHz, $CDCl_3$) δ 9.73 (1H, s), 8.24 (1H, s), 8.16 (1H, s), 7.45-7.13 (7H, m), 6.45 (1H, d, J ≈ 24.6 Hz), and 1.48-0.86 (18H, m) ppm; ^{13}C-NMR (75 MHz, $CDCl_3$) δ 182.135.93, 129.11, 128.40, 127.38, 127.28, 116.32, 109.98, 37.37, 32.23, 32.17, 32.09, 29.95, 22.94, and 14.34 ppm; FT-IR (KBr) 2954, 2924, 2853, 1603, 1452, 1259, 1226, 1088, 878, and 805 cm^{-1}; MS (MALDI-TOF) m/z = 465.3744 $[M]^{+\cdot}$, 465.2126 calcd for $C_{31}H_{31}NOS$.

(*E*)-2-Cyano-3-(5-(4-(3,6-di-*tert*-butylcarbazol-9-yl)phenyl)thiophen-2-yl)acrylic acid (4)

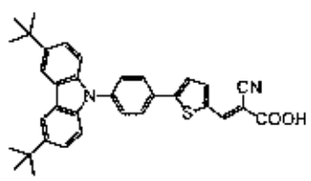

A mixture of **32** (0.30 g, 0.64mmol) and cyanoacetic acid (0.27 g, 3.22 mmol) was vacuum-dried and added piperidine (0.45 ml, 4.5 mmol) in $CHCl_3$ (20 ml). The solution was refluxed for 6 h. After cooling the solution, the organic layer was removed in vacuo. The pure

product was obtained by column chromatography over silica gel eluting with a mixture of MeOH and EtOAc (1:9) followed by recrystallization with a mixture of CH_2Cl_2 and methanol afforded **4** (0.22 g, 65%) as light yellow solid; $C_{34}H_{32}N_2O_2S$; 8.19-8.15 (2H, m), 7.91 (1H, s), 7.33-7.12 (9H, m), 6.41 (1H, s), and 1.45-1.26 (18H, m); ^{13}C-NMR (75 MHz, $CDCl_3$) δ 165.18, 146.61, 145.33, 142.86, 139.26, 138.11, 137.62, 136.74, 135.88, 132.26, 130.13, 128.95, 128.60, 128.48, 125.31, 124.05, 117.56, 116.62, 109.99, 42.94, 34.89, 34.73, 32.11, 32.07, 29.94, 29.59, 22.94, and 14.38 ppm; FT-IR (KBr) 3424, 3037, 2954, 2925, 2854, 2207, 1702, 1595, 1478, 1454, 1365, 1285, 1263, 1209, 1055, 1011, 875, 811, 731, and 695 cm^{-1}; MS (MALDI-TOF) m/z = 532.2700 $[M]^{+\cdot}$, 532.2184 calcd for $C_{34}H_{32}N_2O_2S$.

Chapter 3:

2-Iodofluorene (34)

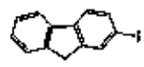

A mixture of fluorene (**33**) (1.00 g, 6.02 mmol), I_2 (0.83 g, 3.25 mmol), KIO_3 (0.26 g, 1.20 mmol) in glacial acetic acid (50 ml) was heated at 80 °C for 10 h. The temperature was cooled and DCM (50 ml) was added. The organic phase was thoroughly washed with water (50 ml x 4), 0.2 M aqueous Na_2SO_3 (50 ml x 2) and aqueous $NaHCO_3$ (50 ml), brine solution (50 ml), dried over anhydrous Na_2SO_4 and filtered. After solvent evaporation, the pure compound was obtained by recrystallization from DCM/hexane mixture as light yellow solids (0.72 g,41%): $C_{13}H_9I$; ^{1}H-NMR (300 MHz, $CDCl_3$) δ 7.82 (1H, s), 7.70-7.63 (2H, m), 7.49-7.43 (2H, m), 7.39-7.26 (2H, m), and 3.78 (2H, s) ppm; ^{13}C-NMR (75 MHz, $CDCl_3$) δ 145.75, 142.96, 141.61, 141.05, 136.25, 136.03, 134.44, 127.61,127.24, 125.29, 121.84, 121.78, 120.29, 92.16, and 36.93 ppm; FT-IR (KBr) 3049, 3028, 2993, 2889, 1595, 1562, 1465, 145, 1393, 1272, 997, 820, 762, 730, and 568 cm^{-1}.

9,9-Dihexyl-2-iodofluorene (1a)

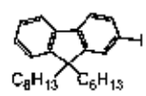

To a mixture of 2-iodofluorene (**34**) (10g, 34.23 mmol) and tetrabutyl ammonium bromide (1g) in DMSO (100 ml) was added an aqueous NaOH solution (50% W/V, 6 ml) follow by 1-bromohexane (14 ml). After being stirred at room temperature for 3 h, the reaction mixture was extracted with ethyl acetate (100 mlx3). The combined organic phase was washed with water (100 ml), HCl solution(1 M, 50 ml), brine solution(100 ml), dried over sodium sulfate anhydrous, filtered and the organic phase was removed in vacuum. Purification by column chromatography using siliga gel eluent with hexane gave 9,9-dihexyl-2-iodofluorene (**19**) (14 g, 89%) as colourless viscous $C_{25}H_{33}I$; ^{1}H-NMR (300 MHz, $CDCl_3$) δ 7.66 (3H, s), 7.44 (1H, d, J = 6 Hz), 7.26-7.34 (3H, m), 1.88-1.97 (4H, m), 1.04-1.06 (12H, m), 0.79 (6H, t, J = 6 Hz), and 0.58-0.63 (4H, m) ppm; ^{13}C-NMR (75 MHz, $CDCl_3$) δ 153.28, 150.12, 140.80, 136.07, 135.82, 132.07, 127.67, 126.93, 122.84, 121.42, 119.82, 92.54, 55.34, 40.31, 31.51, 29.69, 23.72, 22.62, and 14.07 ppm; FT-IR (KBr) 3053, 2924, 1597, 1462, 1443, 1398, 735, and 570 cm^{-1}.

5-(9,9-Dihexylfluoren-2-yl)thiophene-2-carbaldehyde (2a)

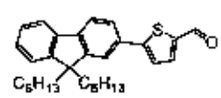

A mixture of **1a** (1.09 g, 2.38 mmol), (5-formylthiophen-2-yl)boronic acid (0.40 g, 2.57 mmol), $Pd(PPh_3)_4$ (0.11 g, 0.09 mmol), and 2 M Na_2CO_3 aqueous solution (24 ml, 47 mmol) in THF (30 ml) was degassed with N_2 for 5 min. The reaction mixture was stirred at reflux under N_2 for 24 h. After being cooled to room temperature, water (50 ml) was added and extracted with CH_2Cl_2 (50 ml x 3). The combined organic phases were washed with water (50 ml) and brine solution (70 ml), dried over anhydrous Na_2SO_4, filtered, and the solvents were removed to dryness. Purification by column chromatography over silica gel eluting with a mixture of CH_2Cl_2 and hexane (2:3) followed by recrystallization with a mixture of CH_2Cl_2 and methanol afforded 5-(9,9-dihexylfluoren-2-yl)thiophene-2-carbaldehyde (**2a**) (0.42 g, 40%) as yellow viscous; $C_{30}H_{36}OS$; ^{1}H-NMR (300 MHz, $CDCl_3$) δ 9.90 (1H, s), 7.76-7.75 (1H, m), 7.72-7.59 (5H, m), 7.47-7.44 (2H, m), 7.35-7.34 (1H, m), 2.02-1.94 (4H, m), 1.05-0.75 (16H, m), and 0.63 (6H, m) ppm; ^{13}C-NMR (75 MHz, $CDCl_3$) δ 182.93, 169.95, 151.40, 137.62, 136.40, 132.50, 125.92, 124.23, 124.04,

123.25, 121.99, 120.89, 120.74, 120.35, 40.56, 40.43, 31.67, 29.95, 29.81, 23.96, 22.79, 15.37, and 14.21 ppm; MS (MALDI-TOF) m/z = 444.3971 $[M]^{+\cdot}$, 444.2487 calcd for $C_{30}H_{36}OS$.

(*E*)-2-Cyano-3-(5-(9,9-dihexylfluoren-2-yl)thiophen-2-yl)acrylic acid (5)

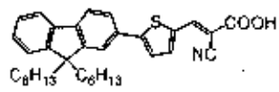

A mixture of **40** (0.12 g, 0.27 mmol) and cyanoacetic acid (0.11 g, 1.35 mmol) was vacuum-dried and added piperidine (0.19 ml, 1.89 mmol) in $CHCl_3$ (20 ml). The solution was refluxed for 6 h. After cooling the solution, the organic layer was removed in vacuo. The pure product was obtained by column chromatography over silica gel eluting with a mixture of MeOH and EtOAc (1:9) followed by recrystallization with a mixture of CH_2Cl_2 and methanol afforded **5** (0.08 g, 60%) as light yellow viscous; $C_{33}H_{37}NO_2S$; m.p. 139-140 °C; ^{1}H-NMR (300 MHz, $CDCl_3$/DMSO) δ 8.29 (1H, s), 7.72-7.60 (7H, m), 7.45-7.44 (2H, m), 7.34-7.31 (1H, m), 1.99-1.96 (4H, m), 1.06-0.84 (16H, m), and 0.80-0.72 (6H, m) ppm; ^{13}C-NMR (75 MHz, $CDCl_3$/DMSO) δ 165.30, 153.75, 151.57, 151.40, 146.03, 141.86, 140.04, 138.55, 136.35, 135.37, 132.47, 127.98, 127.19, 125.96, 125.77, 124.45, 124.27, 123.21, 121.92, 120.73, 120.50, 120.29, 116.95, 93.54, 37.67, 37.32, 32.99, 32.11, 31.61, 30.22, 29.88, 29.72, 29.53, 27.28, 23.93, 22.86, 22.69, 19.95, 14.25, and 14.12 ppm; FT-IR (KBr) 3420, 2954, 2928, 2951, 2215, 1739, 1684, 1573, 1507, 1464, 1413, 1375, 1275, 1220, 1062, 873, 804, 750, and 670 cm^{-1}.

9-Dodecyl-3-iodocarbazole (1b)

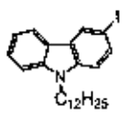

To a solution of 3-iodocarbazole (**26**) (0.98 g, 3.35 mmol) in DMF (10 ml) was added followed by NaH (0.16 g, 6.71). 1-Bromododecane (1.082 g, 4.36 mmol) was added. The reaction mixture was stirred at room temperature for 3 h. Water (50 ml) was added and the mixture was extracted with methylene chloride (50 ml x 3). The combined organic phases were washed with a dilute HCl solution (50 ml x 2), water (100 ml), and brine solution (50 ml), dried over anhydrous

Na_2SO_4, filtered and the solvents were removed to dryness. Purification by column chromatography over silica gel eluting with hexane gave **1b** (1.08 g, 70%) as white viscous oil; $C_{24}H_{32}IN$; ^{1}H-NMR (500 MHz, $CDCl_3$) δ 8.33 (1H, s), 7.96 (1H, d, J = 7.5 Hz), 7.63 (1H, dd, J =8.4 Hz, J = 1.6 Hz), 7.45-7.40 (1H, m), 7.31 (1H, d, J = 8.4 Hz), 7.21-7.16 (1H, m), 7.10-7.02 (1H, m), 4.13 (2H, t, J = 7.2 Hz), 1.75-1.73 (2H, m), 1.19 (18H, m), and 0.87 (3H, t, J = 6.6 Hz) ppm; ^{13}C-NMR (125 MHz, $CDCl_3$) δ 140.67, 139.82, 134.03, 129.44, 126.60, 120.80, 119.56, 111.03, 109.17, 81.49, 43.41, 32.28, 29.96, 29.92, 29.83, 29.70, 29.20, 27.59, 23.06, and 14.52 ppm; FT-IR (KBr) 3067, 3042, 2954, 2920, 2847, 1624, 1590, 1464, 1441, 1348, 1275, 1224, 1139, 1047, 866, 787, 747, 719, and 595 cm^{-1}; MS (MALDI-TOF) m/z = 461.3477 $[M]^{+\cdot}$, 461.1579 calcd for $C_{24}H_{32}IN$.

5-(9-Dodecylcarbazol-3-yl)thiophene-2-carbaldehyde (2b)

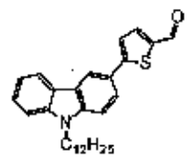

A mixture of **1b** (0.96 g, 2.08 mmol), (5-formylthiophen-2-yl)boronic acid (0.33 g, 2.14 mmol), $Pd(PPh_3)_4$ (0.10 g, 0.08 mmol), and 2 M Na_2CO_3 aqueous solution (21 ml, 41 mmol) in THF (50 ml) was degassed with N_2 for 5 min. The reaction mixture was stirred at reflux under N_2 for 24 h. After being cooled to room temperature, water (70 ml) was added and extracted with CH_2Cl_2 (70 ml x 3). The combined organic phases were washed with water (70 ml) and brine solution (70 ml), dried over anhydrous Na_2SO_4, filtered, and the solvents were removed to dryness. Purification by column chromatography over silica gel eluting with a mixture of CH_2Cl_2 and hexane (2:3) followed by recrystallization with a mixture of CH_2Cl_2 and methanol afforded 5-(9-dodecylcarbazol-3-yl)thiophene-2-carbaldehyde (**2b**) (0.56 g, 60%) as yellow solid; $C_{29}H_{35}NOS$; ^{1}H-NMR (500 MHz, $CDCl_3$) δ 9.88 (1H, s), 8.40 (1H, s), 8.14 (1H, d, J = 10.0 Hz),7.76-7.79 (2H, m), 7.51 (1H, t, J = 7.5 Hz),7.42-7.45 (3H, m), 7.28 (1H, t, J = 7.5 Hz), 4.31 (2H, t, J = 7.5 Hz), 1.88 (2H, quin, J = 7.5 Hz), 1.38-1.23 (18H, m), and 0.87 (3H, t, J = 5.0 Hz) ppm; ^{13}C-NMR (125 MHz, $CDCl_3$) δ 156.42, 141.22, 141.09, 141.04, 137.91, 126.43, 124.41, 124.06, 123.44, 122.86, 122.64, 120.62, 119.55, 118.56 109.30, 109.15, 43.33, 31.92, 29.61, 29.57, 29.50, 29.34, 28.99,

27.30, 22.70 and 14.14 ppm; FT-IR (KBr) 3090, 3051, 2948, 2919, 2847, 2791, 2743, 2664, 1660, 1595, 1440, 1381, 1274, 1234, 1056, 879, 792, 745, 723, and 626 cm^{-1}; MS (MALDI-TOF) m/z = 445.4209 $[M]^{+\cdot}$, 445.2439 calcd for $C_{29}H_{35}NOS$.

(*E*)-2-Cyano-3-(5-(9-dodecylcarbazol-3-yl)thiophen-2-yl)acrylic acid (6)

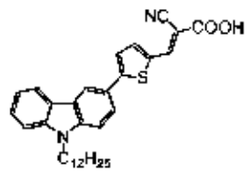

A mixture of **2a** (0.46 g, 1.03 mmol) and cyanoacetic acid (0.44 g, 5.18 mmol) was vacuum-dried and added piperidine (0.72 ml, 7.24 mmol) in $CHCl_3$ (20 ml). The solution was refluxed for 6 h. After cooling the solution, the organic layer was removed in vacuo. The pure product was obtained by column chromatography over silica gel eluting with a mixture of MeOH and EtOAc (1:9) followed by recrystallization with a mixture of CH_2Cl_2 and methanol afforded **6** (0.34 g, 64%) as light orange solid; $C_{32}H_{36}N_2O_2S$; m.p. 243-244 °C; ^{1}H-NMR (500 MHz, $CDCl_3$/DMSO-d6) δ 8.50 (1H, br), 7.97 (1H, br), 7.81 (1H, br), 7.67 (1H, br), 7.35 (2H, br), 7.18 (2H, br), 7.05 (1H, br), 6.89 (1H, br), 3.83 (2H, br), 1.57 (2H, br),7.67 (1H, br), 1.17 (6H, br), and 1.85 (5H, br) ppm; ^{13}C-NMR (125 MHz, $CDCl_3$/DMSO-d6) δ 169.31, 153.25, 144.92, 140.53, 140.24, 138.20, 134.57, 125.97, 123.93, 122.81, 122.58, 122.34, 120.46, 119.13, 117.74, 108.77, 103.28, 42.74, 31.83, 29.61, 29.53, 29.34, 29.26, 28.75, 27.08, 22.62, and 14.17 ppm; FT-IR (KBr) 3420, 3046, 2949, 2923, 2852, 2211, 1597, 1489, 1465, 1439, 1393, 1379, 1290, 1264, 1235, 746, 722, and 617 cm^{-1}; MS (MALDI-TOF) m/z = 512.2425 $[M]^{+\cdot}$, 512.2497 calcd for $C_{32}H_{36}N_2O_2S$.

10-Dodecylphenothiazine (36)

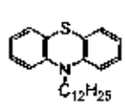

To a mixture of phenothiazine **(35)** (15 g, 75.27 mmol) and tetrabutyl ammonium bromide (1 g) in DMSO (130 ml) was added an aqueous NaOH solution (50% W/V, 12 ml)

follow by 1-bromododecane (20 ml). After being stirred at room temperature for 3 h, the reaction mixture was extracted with ethyl acetate (100 mlx3). The combined organic phase was washed with water (100 ml), HCl solution(1 M, 50 ml), brine solution(100 ml), dried over sodium sulfate anhydrous, filtered and the organic phase was removed in vacuum. Purification by column chromatography using siliga gel eluent with hexane gave 10-dodecylphenothiazine (**36**) (25 g, 92%) as colourless viscous; $C_{24}H_{33}NS$; ^{1}H-NMR (300 MHz, $CDCl_3$) δ 7.15-7.10 (4H, m), 6.91-6.83 (4H, m), 3.83 (2H, t, J = 6.3 Hz), 1.79 (2H, quin, J = 7.2 Hz), 1.42-1.24 (18H, m), and 0.88 (3H, t, J = 6.6 Hz) ppm; FT-IR (KBr) 3065, 2924, 2853, 1654, 1571, 1459, 1443, 1369, 1333, 1285, 1250, 1105, 1038, 926, 748, 727, and 670 cm^{-1}; MS (MALDI-TOF) m/z = 367.4178 $[M]^{+\cdot}$, 367.2334 calcd for $C_{24}H_{33}NS$.

3-bromo-10-dodecylphenothiazine (1c)

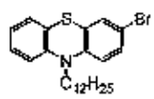

NBS (1.61 g, 9.07 mmol) was added in small portions to a stirred solution of 10-dodecylphenothiazine (3.18 g, 8.64 mmol) in THF (50 ml). After being stirred at room temperature for 30 min, water was added. The mixture was extracted with dichloromethane (30 ml x 3). The combined organic phase was washed with water (50 ml), brine solution (50 ml), dried over anhydrous sodium sulfate, filtered and the solvent was remove in vacuum. Purification by short column chromatography using silica gel eluting with dichloromethane : hexane, 5:95 gave **1c** as dark green viscous (3.09 g, 80%); $C_{24}H_{32}BrNS$; ^{1}H-NMR (500 MHz, C_3H_6O) δ 7.34 (1H, dd, J = 20.0 Hz, J = 10.0 Hz), 7.29 (1H, s), 7.23 (1H, t, J = 7.5 Hz), 7.16 (1H, d, J = 5.0 Hz), 7.00-6.97 (2H, m), 3.95 (2H, t, J = 5.0 Hz), 1.79 (2H, quin, J = 5.0 Hz), 1.31-1.27 (18H, m), and 0.89 (3H, t, J = 7.5 Hz) ppm; ^{13}C-NMR (125 MHz, $CDCl_3$) δ 144.98, 144.51, 144.17, 130.12, 129.82, 129.73, 129.63, 127.51, 127.44, 127.25, 126.50, 124.21, 122.66, 116.68, 116.54, 115.55, 114.77, 114.41, 47.54, 31.93, 29.63, 29.53, 29.46, 29.36, 29.21, 29.16, 28.80, 28.21, 26.88, 26.78, 26.64, 22.71, and 14.14 ppm; FT-IR (KBr) 3063, 2954, 2921, 2851, 1589, 1454, 1391, 1328, 1249, 1106, 864, 798, 747, and 541 cm^{-1}; MS (MALDI-TOF) m/z = 445.3432 $[M]^{+\cdot}$, 445.1439 calcd for $C_{24}H_{32}BrNS$.

5-(10-Dodecylphenothiazin-3-yl)thiophene-2-carbaldehyde (2c)

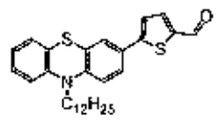

A mixture of **1c** (1.09 g, 2.46 mmol), (5-formylthiophen-2-yl)boronic acid (0.41 g, 2.65 mmol), $Pd(PPh_3)_4$ (0.11 g, 0.10 mmol), and 2 M Na_2CO_3 aqueous solution (25 ml, 49 mmol) in THF (50 ml) was degassed with N_2 for 5 min. The reaction mixture was stirred at reflux under N_2 for 24 h. After being cooled to room temperature, water (70 ml) was added and extracted with CH_2Cl_2 (70 ml x 3). The combined organic phases were washed with water (70 ml) and brine solution (70 ml), dried over anhydrous Na_2SO_4, filtered, and the solvents were removed to dryness. Purification by column chromatography over silica gel eluting with a mixture of CH_2Cl_2 and hexane (2:3) followed by recrystallization with a mixture of CH_2Cl_2 and methanol afforded 5-(10-dodecylphenothiazin-3-yl)thiophene-2-carbaldehyde (**2c**) (1.02 g, 87%) as yellow viscous; $C_{29}H_{35}NOS_2$; ^{1}H-NMR (300 MHz, $CDCl_3$) δ 9.84 (1H, s), 7.68 (1H, d, J = 4.2 Hz), 7.44-7.40 (2H, m), 7.27-7.26 (2H, m), 7.15-7.11 (1H, m), 6.95-6.83 (3H, m), 3.85 (2H, t, J = 6.6 Hz), 1.83-1.78 (2H, m), 1.43-1.24 (18H, m), and 0.87 (3H, t, J = 6.0 Hz) ppm; ^{13}C-NMR (75 MHz, $CDCl_3$) δ 182.78, 153.91, 146.63, 144.65, 141.88, 137.76, 127.75, 127.55, 125.84, 125.21, 124.11, 123.27, 123.15, 116.97, 115.83, 115.72, 47.93, 32.17, 29.87, 29.77, 29.59, 29.46, 27.13, 22.93, and 14.35 ppm; MS (MALDI-TOF) m/z = 477.4100 $[M]^{+\cdot}$, 477.2160 calcd for $C_{29}H_{35}NOS_2$.

(*E*)-2-Cyano-3-(5-(10-dodecylphenothiazin-3-yl)thiophen-2-yl)acrylic acid (7)

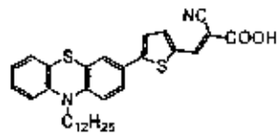

A mixture of **2c** (0.36 g, 0.75 mmol) and cyanoacetic acid (0.32 g, 3.75 mmol) was vacuum-dried and added piperidine (0.52 ml, 5.25 mmol) in $CHCl_3$ (20 ml). The solution was refluxed for 6 h. After cooling the solution, the organic layer was removed in vacuo. The pure product was obtained by column chromatography over silica gel eluting with a mixture of MeOH

and EtOAc (1:9) followed by recrystallization with a mixture of CH_2Cl_2 and methanol afforded 7 (0.29 g, 72%) as dark solid; $C_{32}H_{36}N_2O_2S_2$; m.p. 139-140 °C; ^{1}H-NMR (300 MHz, $CDCl_3$) δ 8.23 (1H, s), 7.67 (1H, d, J = 3.9 Hz), 7.46-7.37 (2H, m), 7.29 (1H, s), 7.26 (1H, d, J = 4.2 Hz), 7.17-7.09 (2H, m), 6.94-6.81 (3H, m), 3.85 (2H, t, J = 7.0 Hz), 1.80 (2H, quin, J = 6.7 Hz), 1.26-1.24 (18H, m), and 0.92-0.85 (3H, m); ^{13}C-NMR (75 MHz, $CDCl_3$) δ 164.81, 146.65, 146.25, 144.54, 138.86, 134.58, 127.70, 127.32, 125.95, 125.86, 125.08, 124.10, 123.44, 123.12, 115.84, 115.71, 47.92, 32.10, 29.80, 29.71, 29.51, 29.39, 27.06, 22.85, and 14.27 ppm; FT-IR (KBr) 3442, 3050, 2949, 2922, 2851, 2215, 1730, 1681, 1444, 1403, 1367, 1282, 1215, 1174, 1064, 927, 814, 790, 734, and 608 cm^{-1}; MS (MALDI-TOF) m/z = 544.2623 $[M]^{+\cdot}$, 544.2218 calcd for $C_{32}H_{36}N_2O_2S_2$.

Chapter 4:

3,6-Diiodocarbazole (37)

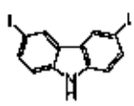

A mixture of carbazole (25) (5.00 g, 29.90 mmol), KI (6.45 g, 38.87 mmol), KIO_3 (6.40 g, 29.90 mmol) in glacial acetic acid (150 ml) was heated at 70 °C for 10 min. The temperature was cooled and DCM (200 ml) was added. The organic phase was thoroughly washed with water (200 ml x 4), 0.2 M aqueous Na_2SO_3 (200 ml x 2) and aqueous $NaHCO_3$ (200 ml), brine solution (200 ml), dried over anhydrous Na_2SO_4 and filtered. After solvent evaporation, the pure compound was obtained by recrystallization from DCM/hexane mixture as white solid (11.90 g, 95%): $C_{12}H_7I_2N$; m.p. 191-192 °C; ^{1}H-NMR (300 MHz, $CDCl_3$) δ 8.32 (1H, s), 8.08 (1H, s, br), 7.68 (2H, dd, J = 8.4 Hz, J = 1.8 Hz), and 7.20 (2H, d, J = 8.4 Hz) ppm; ^{13}C-NMR (75 MHz, $CDCl_3$) δ 135.11, 129.67, and 112.95 ppm; FT-IR (KBr) 3413, 2932, 1601, 1426, 1123, 1093, 1044, 1018, 893, 869, 804, and 565 cm^{-1}.

9-Dodecyl-3,6-diiodocarbazole (38)

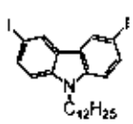

To a solution of 3,6-diiodocarbazole (**37**) (6.57 g, 15.69 mmol) in DMF (100 ml) was added followed by NaH (0.75 g, 31.38 mmol). 1-Bromododecane (5.06 g, 20.40 mmol) was added. The reaction mixture was stirred at room temperature for 3 h. Water (50 ml) was added and the mixture was extracted with methylene chloride (50 ml x 3). The combined organic phases were washed with a dilute HCl solution (50 ml x 2), water (100 ml), and brine solution (50 ml), dried over anhydrous Na_2SO_4, filtered and the solvents were removed to dryness. Purification by column chromatography over silica gel eluting with hexane gave a white viscous oil (56%): $C_{24}H_{31}I_2N$; m.p. 59-60 °C; ^{1}H-NMR (300 MHz, $CDCl_3$) δ 8.30 (2H, s), 7.69 (2H, d, J = 8.4 Hz), 7.14 (2H, d, J = 8.7 Hz), 4.18 (2H, t, J = 6.7 Hz), 1.79 (2H, s), and 1.23 (18H, s) ppm; ^{13}C-NMR (75 MHz, $CDCl_3$) δ 139.78, 134.77, 129.62, 124.26, 111.15, 81.89, 43.52, 32.17, 29.84, 29.77, 29.69, 29.58, 29.06, 27.45, 22.94, and 14.37 ppm; MS (MALDI-TOF) m/z = 587.2110 $[M]^{+\cdot}$, 587.0546 calcd for $C_{24}H_{31}I_2N$.

3',6'-Di-*tert*-butyl-9-dodecyl-6-iodo3,9'-bicarbazole (39)

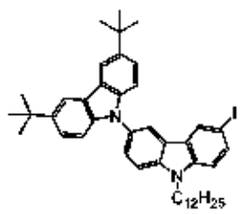

To a mixture of CuI (0.56 g, 2.92 mmol), K_3PO_4 (3.10 g, 14.60 mmol), and 9-dodecyl-3,6-diiodocarbazole (**38**) (10.18 g, 17.52 mmol) in toluene (30 mL) were added 3,6-di-*tert*-butylcarbazole (**29**) (1.29 g, 5.84 mmol), and (±)-*trans*-1,2-diaminocyclohexane (0.33 g, 2.92 mmol). The reaction mixture was stirred at 110 °C under nitrogen. After 24 h, water (50ml) was added until the two phases mixed. The solution was extracted with CH_2Cl_2 (50 ml x 3), washed with water (50 ml), brine solution (100 ml) and dried with Na_2SO_4, filtered, and the solvents removed to dryness. The crude product was purified by column chromatography on silica gel with hexane as eluent to yield 3',6'-di-*tert*-butyl-9-dodecyl-6-iodo-3,9'-bicarbazole (**39**) (2.42 g, 56%) as white solid: $C_{44}H_{55}IN_2$; m.p. 154-155 °C; ^{1}H-NMR (300 MHz, $CDCl_3$) δ 8.34 (1H, s), 8.18 (2H, s), 8.15 (1H, s), 7.71 (1H, d, J = 8.4 Hz), 7.58 (2H, d, J = 7.5 Hz), 7.50 (2H, d, J = 8.7 Hz), 7.44 (2H, d, J = 8.4 Hz), 7.29 (2H, d, J = 8.4 Hz), 7.20 (2H, d, J = 8.1 Hz), 4.28 (2H, t, J = 6.6 Hz),

1.89 (2H, m), 1.47-1.25 (36H, m), and 0.87 (3H, t, J = 6.3 Hz) ppm; ^{13}C-NMR (75 MHz, $CDCl_3$) δ 142.80, 140.48, 134.69, 129.72, 125.97, 123.79, 123.37, 119.57, 116.45, 109.38, 32.34, 28.88, 29.27 ppm; FT-IR (KBr) 3007, 2963, 2922, 2850, 1489, 1278, 1262, 1237, 870, 798, 750, and 611 cm^{-1}; MS (MALDI-TOF) m/z = 738.3863 $[M]^{+\cdot}$, 738.3410 calcd for $C_{44}H_{55}IN_2$.

3',6'-Di-*tert*-butyl-9-dodecyl-6-(4-hexylthiophen-2-yl)- 3,9'-bicarbazole (40)

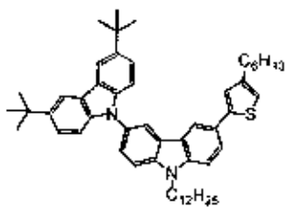

A mixture of **39** (0.40 g, 0.59 mmol), 2-(4-hexylthiophen-2-yl)-4,4,5,5-tetramethyl-1,3,2-dioxaborolane (0.17 g, 0.59 mmol), $Pd(PPh_3)_4$ (0.03 g, 0.02 mmol), and 2 M K_2CO_3 aqueous solution (6 ml, 12 mmol) in THF (30 ml) was degassed with N_2 for 5 min. The reaction mixture was stirred at reflux under N_2 for 24 h. After being cooled to room temperature, water (50 ml) was added and extracted with CH_2Cl_2 (50 ml x 3). The combined organic phases were washed with water (50 ml) and brine solution (50 ml), dried over anhydrous Na_2SO_4, filtered, and the solvents were removed to dryness. Purification by column chromatography over silica gel eluting with hexane followed by recrystallization with a mixture of CH_2Cl_2 and methanol afforded 3',6'-di-*tert*-butyl-9-dodecyl-6-(4-hexylthiophen-2-yl)-3,9'-bicarbazole (**40**) (0.45 g, 99%) as white solid; $C_{54}H_{70}N_2S$; m.p. 119-120 °C; ^{1}H-NMR (300 MHz, $CDCl_3$) δ 8.26 (1H, s), 8.21 (1H, s), 8.20 (2H, s), 7.76 (1H, dd, J = 8.7 Hz, J = 1.5 Hz), 7.63 (1H, dd, J = 9.3 Hz, J = 1.5 Hz), 7.57 (1H, d, J = 8.7 Hz), 7.50-7.45 (3H, m), 7.36 (2H, d, J = 8.4 Hz), 7.21 (1H, d, J = 3.9 Hz), 7.07 (1H, d, J = 3.9 Hz), 6.89 (1H, s), 4.39 (2H, t, J = 7.0 Hz), 2.54 (2H, t, J = 7.6 Hz), 1.97 (2H, quin, J = 6.6 Hz), 1.58 (4H, m), 1.50-1.27 (40H, m), and 0.88 (6H, t, J = 6.0 Hz) ppm; ^{13}C-NMR (75 MHz, $CDCl_3$) δ 144.57, 142.93, 142.48, 140.72, 140.26, 139.80, 137.08, 134.95, 129.78, 125.55, 125.42, 124.62, 124.47, 124.05, 123.61, 123.51, 123.09, 123.03, 122.66, 119.30, 117.76, 116.20, 109.84, 109.44, 109.18, 107.24, 43.55, 34.75, 32.08, 31.92, 31.62, 29.61, 29.54, 29.43, 29.35, 29.12, 28.91, 27.36, 22.59, 14.12, and 14.09 ppm; FT-IR (KBr) 3050, 2954, 2925, 2854, 1655, 1561, 1544, 1491,

1461, 1364, 1294, 1264, 1233, 1020, 873, 808, and 670 cm^{-1}; MS (MALDI-TOF) m/z = 778.5224 $[M]^{+\cdot}$, 778.5260 calcd for $C_{54}H_{70}N_2S$.

6-(5-Bromo-4-hexylthiophen-2-yl)-3',6'-di-*tert*-butyl-9-dodecyl-3,9'-bicarbazole (43)

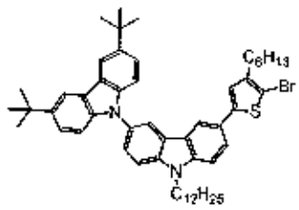

NBS (0.15 g, 0.19 mmol) was added in small portions to a stirred solution of 3',6'-di-*tert*-butyl-9-dodecyl-6-(4-hexylthiophen-2-yl)-3,9'-bicarbazole (**40**) (0.04 g, 0.20 mmol) in THF (20 ml). After being stirred at room temperature for 30 min, water was added. The mixture was extracted with dichloromethane (30 ml x 3). The combined organic phase was washed with water (30 ml), brine solution (30 ml), dried over anhydrous sodium sulfate, filtered and the solvent was remove in vacuum. Purification by short column chromatography using silica gel eluting with hexane gave 6-(5-bromo-4-hexylthiophen-2-yl)-3',6'-di-*tert*-butyl-9-dodecyl-3,9'-bicarbazole (**43**) as white solid (0.13 g, 75%); $C_{54}H_{69}BrN_2S$; m.p. 152-153 °C; ^{1}H-NMR (300 MHz, $CDCl_3$) δ 8.26 (1H, d, J = 1.2 Hz), 8.21 (1H, s), 8.20 (1H, s), 8.19 (1H, s), 7.69-7.56 (3H, m), 7.50-7.43 (3H, m), 7.36 (2H, d, J = 8.4 Hz), 7.04 (1H, s), 4.38 (2H, t, J = 7.0 Hz), 2.59 (2H, t, J = 7.6 Hz), 1.97 (2H, quin, J = 6.7 Hz), 1.67-1.27 (44H, m), and 0.89 (6H, t, J = 3.7 Hz) ppm; ^{13}C-NMR (75 MHz, $CDCl_3$) δ 144.71, 143.08, 142.49, 140.70, 140.27, 139.80, 129.76, 125.57, 125.41, 124.36, 123.60, 123.50, 123.10, 123.02, 123.00, 119.31, 117.54, 116.21, 109.82, 109.18, 34.75, 32.09, 31.66, 29.77, 29.73, 29.63, 29.60, 29.54, 29.43, 29.35, 29.11, 28.98, and 27.36 ppm; FT-IR (KBr) 3055, 2954, 2922, 2853, 1602, 1494, 1362, 1290, 1263, 1235, 1021, 8775, 801, 741, 722, 658, and 612 cm^{-1}; MS (MALDI-TOF) m/z = 856.3296 $[M]^{+\cdot}$, 856.4365 calcd for $C_{54}H_{69}BrN_2S$.

5'-(3',6'-Di-*tert*-butyl-9-dodecyl-[3,9'-bicarbazol]-6-yl)-3'-hexyl-[2,2'-bithiophene]-5-carbaldehyde (46)

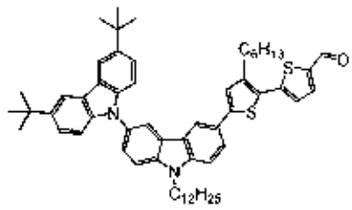

A mixture of **43** (0.65 g, 0.76 mmol), (5-formylthiophen-2-yl)boronic acid (0.13 g, 0.82 mmol), $Pd(PPh_3)_4$ (0.03 g, 0.03 mmol), and 2 M Na_2CO_3 aqueous solution (8 ml, 15.20 mmol) in THF (30 ml) was degassed with N_2 for 5 min. The reaction mixture was stirred at reflux under N_2 for 24 h. After being cooled to room temperature, water (50 ml) was added and extracted with CH_2Cl_2 (50 ml x 3). The combined organic phases were washed with water (50 ml) and brine solution (50 ml), dried over anhydrous Na_2SO_4, filtered, and the solvents were removed to dryness. Purification by column chromatography over silica gel eluting with a mixture of CH_2Cl_2 and hexane (1:4) followed by recrystallization with a mixture of CH_2Cl_2 and methanol afforded 5'-(3',6'-di-*tert*-butyl-9-dodecyl-3,9'-bicarbazol]-6-yl)-3'-hexyl-[2,2'-bithiophene]-5-carbaldehyde **(46)** (0.47 g, 70%) as yellow solid; $C_{59}H_{72}N_2OS_2$; m.p. 116-117 °C; ^{1}H-NMR (300 MHz, $CDCl_3$) δ 9.85 (1H, s), 8.26 (2H, s), 8.18 (1H, s), 8.17 (1H, s), 7.75-7.68 (2H, m), 7.61-7.56 (2H, m), 7.46 (3H, m), 7.34 (2H, m), 7.23-7.22 (2H, m), 4.37 (2H, s), 2.84 (2H, t, J = 3 Hz), 1.95 (2H, s), 1.71 (2H, s), 1.54-1.25 (42H, m), and 0.87 (6H, s) ppm; ^{13}C-NMR (75 MHz, $CDCl_3$) δ 182.60, 146.98, 145.50, 143.45, 142.53, 141.69, 140.98, 140.25 139.83, 137.03, 129.88, 127.99, 125.70, 125.51, 125.03, 124.52, 123,52, 123.11, 119.34, 117.88, 116.26, 109.93, 109.50, 109.17, 43.59, 32.10, 31.70, 30.31, 29.65, 29.56, 29.45, 29.36, 29.14, 27.38, 14.15, and 14.12 ppm; FT-IR (KBr) 3046, 2954, 2925, 2850, 2791, 2732, 1668, 1488, 1447, 1292, 1262, 1229, 1056, 875, 801, 752, and 611 cm^{-1}; MS (MALDI-TOF) m/z = 888.8062 $[M]^{+\cdot}$, 888.5086 calcd for $C_{59}H_{72}N_2OS_2$.

(*E*)-2-Cyano-3-(5'-(3',6'-di-*tert*-butyl-9-dodecyl-3,9'-bicarbazol]-6-yl)-3'-hexyl-[2,2'-bithiophen]-5-yl)acrylic acid (8)

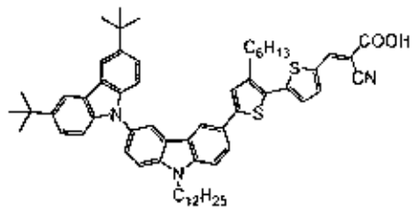

A mixture of **46** (0.26 g, 0.29 mmol) and cyanoacetic acid (0.12 g, 1.47 mmol) was vacuum-dried and added piperidine (0.20 ml, 2.06 mmol) in $CHCl_3$ (20 ml). The solution was refluxed for 6 h. After cooling the solution, the organic layer was removed in vacuo. The pure product was obtained by column chromatography over silica gel eluting with a mixture of MeOH and EtOAc (1:9) followed by recrystallization with a mixture of CH_2Cl_2 and methanol afforded **8** (0.19 g, 69%) as dark red solid; $C_{62}H_{73}N_3O_2S_2$; m.p. 194-195 °C; ^{1}H-NMR (300 MHz, $CDCl_3$/DMSO-d6) δ 8.31-8.04 (5H, m), 7.56-7.31 (8H, m), 7.10-6.99 (3H, m), 4.02 (2H, m), 3.59 (3H, m), 2.66 (2H, m), 1.75 (2H, m), 1.46-1.22 (41H, m), and 0.85-0.78 (6H, m) ppm; ^{13}C-NMR (75 MHz, $CDCl_3$/DMSO) δ 169.43, 144.71, 142.70, 140.72, 140.29, 139.73, 135.39, 129.82, 128.62, 125.30, 123.74, 123.28, 122.89, 119.19, 118.90, 117.34, 116.40, 109.31, 103.59, 43.40, 34.94, 32.33, 32.27, 31.87, 30.34, 29.80, 29.54, 29.19, 27.47, 22.88, 22.79, and 14.31 ppm; FT-IR (KBr) 3421, 3055, 3024, 2954, 2922, 2853, 2213, 1730, 1590, 1481, 1442, 1392, 1331, 1314, 1271, 1239, 1193, 1176, 1062, 937, 802, 752, 695, and 617 cm^{-1}; MS (MALDI-TOF) m/z = 955.4208 $[M]^{+\cdot}$, 955.5144 calcd for $C_{62}H_{73}N_3O_2S_2$.

3',6'-Di-*tert*-butyl-6-(3,4'-dihexyl-[2,2'-bithiophen]-5-yl)-9-dodecyl-3,9'-bicarbazole (41)

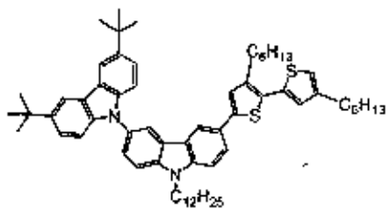

A mixture of **43** (0.59 g, 0.69 mmol), 2-(4-hexylthiophen-2-yl)-4,4,5,5-tetramethyl-1,3,2-dioxaborolane (0.20 g, 68 mmol), $Pd(PPh_3)_4$ (0.03 g, 0.03 mmol), and 2 M K_2CO_3 aqueous solution (7 ml, 13.71 mmol) in THF (30 ml) was degassed with N_2 for 5 min. The reaction mixture was stirred at reflux under N_2 for 24 h. After being cooled to room temperature, water (50 ml) was added and extracted with CH_2Cl_2 (50 ml x 3). The combined organic phases were washed with water (50 ml) and brine solution (50 ml), dried over anhydrous Na_2SO_4, filtered, and the solvents were removed to dryness. Purification by column chromatography over silica gel eluting with hexane followed by recrystallization with a mixture of CH_2Cl_2 and methanol afforded 3',6'-di-*tert*-butyl-6-(3,4'-dihexyl-[2,2'-bithiophen]-5-yl)-9-dodecyl-3,9'-bicarbazole (**41**) (0.45 g, 69%) as white solid: $C_{64}H_{84}N_2S_2$; ^{1}H-NMR (300 MHz, $CDCl_3$) δ 8.26 (2H, s), 8.19 (2H, s), 7.75 (1H, d, J = 8.4 Hz), 7.61 (1H, d, J = 8.7 Hz), 7.55 (1H, d, J = 8.4 Hz), 7.49-7.43 (3H, m), 7.35 (2H, d, J = 8.7 Hz), 7.16 (1H, s), 6.98 (1H, s), 6.87 (1H, s), 4.37 (2H, t, J = 6.0 Hz), 2.77 (2H, t, J = 7.5 Hz), 2.60 (2H, t, J = 7.3 Hz), 1.96 (2H, m), 1.69-1.59 (4H, m), 1.48-1.26 (48H, m), and 0.89-0.88 (9H, m) ppm; ^{13}C-NMR (75 MHz, $CDCl_3$) δ 143.87, 142.93, 142.72, 140.87, 140.57, 140.52, 104.34, 136.41, 129.94, 129.80, 127.12, 126.66, 126.09, 125.55, 125.29, 124.96, 124.72, 123.94, 123.78, 123.45, 123.25, 119.56, 118.71, 117.84, 116.47, 110.05, 109.61, 109.48, 43.82, 35.34, 32.37, 31.99, 30.93, 30.82, 30.69, 29.92, 29.84, 29.73, 29.64, 29.41, 29.32, 27.66, 22.99, 22.92, and 14.42 ppm; FT-IR (KBr) 3050, 2949, 2927, 2856, 1624, 1577, 1491, 1463, 1364, 1295, 1262, 1235, 1020, 876, 807, 737, 656, and 610 cm^{-1}; MS (MALDI-TOF) m/z = 944.3324 $[M]^{+\cdot}$, 944.6076 calcd for $C_{64}H_{84}N_2S_2$.

6-(5'-Bromo-3,4'-dihexyl-[2,2'-bithiophen]-5-yl)-3',6'-di-*tert*-butyl-9-dodecyl-3,9'-bicarbazole (44)

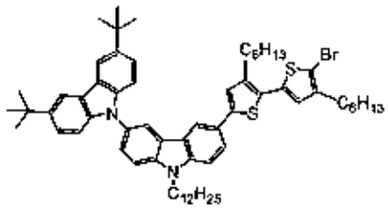

NBS (0.92 g, 0.97 mmol) was added in small portions to a stirred solution of 3',6'-di-*tert*-butyl-6-(3,4'-dihexyl-[2,2'-bithiophen]-5-yl)-9-dodecyl-3,9'-bicarbazole (**41**) (0.18 g, 1.02

Purification by column chromatography over silica gel eluting with a mixture of CH_2Cl_2 and hexane (2:3) followed by recrystallization with a mixture of CH_2Cl_2 and methanol afforded 5''-(3',6'-di-*tert*-butyl-9-dodecyl-[3,9'-bicarbazol]-6-yl)-3',3''-dihexyl-[2,2':5',2''-terthiophene]-5-carbaldehyde (**47**) (0.60 g, 76%) as orange solid; $C_{69}H_{86}N_2OS_3$; m.p. 140-141 °C; ^{1}H-NMR (300 MHz, $CDCl_3$) δ 9.88 (1H, s), 8.26 (2H, s), 8.19 (2H, s), 7.76 (1H, d, J = 6.0 Hz), 7.70 (1H, s), 7.62 (1H, d, J = 6.0 Hz), 7.57 (1H, d, J = 6.0 Hz), 7.47 (3H, d, J = 6.0 Hz), 7.35 (2H, d, J = 3.0 Hz), 7.26-7.23 (1H, m), 7.19 (1H, s), 7.02 (1H, s), 4.39 (2H, s), 2.84-2.81 (4H, m), 1.97 (2H, s), 1.72-1.70 (4H, m), 1.49-1.26 (48H, m), and 0.89-0.87 (9H, m) ppm; ^{13}C-NMR (75 MHz, $CDCl_3$) δ 182.60, 146.48, 143.71, 142.61, 142.50, 141.97, 141.45, 140.77, 140.23, 139.79, 136.90, 129.78, 128.82, 128.61, 128.30, 125.70, 125.45, 125.39, 125.33, 124.42, 123.63, 123.51, 123.10, 123.03, 119.29, 117.70, 116.23, 109.43.109.19, 43.58, 32.10, 31.94, 31.71, 31.68, 30.52, 30.23, 29.85, 29.82, 29.64, 29.62, 29.56, 29.45, 29.37, 29.35, 29.27, 29.14, 27.38, 22.71, 22.65, 22.62, 14.13, and 14.10 ppm; FT-IR (KBr) 3046, 2954, 2923, 2853, 2782, 2729, 1657, 1485, 1434, 1361, 1262, 1231, 1151, 1060, 873, 801, 752, 657, and 611 cm^{-1}; MS (MALDI-TOF) m/z = 1054.0910 $[M]^{+\cdot}$, 1054.5902 calcd for $C_{69}H_{86}N_2OS_3$.

(*E*)-2-Cyano-3-(5''-(3',6'-di-*tert*-butyl-9-dodecyl-3,9'-bicarbazol]-6-yl)-3',3''-dihexyl-[2,2':5',2''-terthiophen]-5-yl)acrylic acid (9)

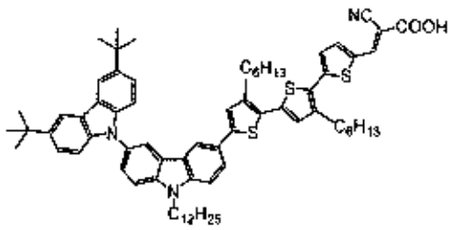

A mixture of **47** (0.32 g, 0.31 mmol) and cyanoacetic acid (0.13 g, 1.54 mmol) was vacuum-dried and added piperidine (0.21 ml, 2.16 mmol) in $CHCl_3$ (20 ml). The solution was refluxed for 6 h. After cooling the solution, the organic layer was removed in vacuo. The pure product was obtained by column chromatography over silica gel eluting with a mixture of MeOH and EtOAc (1:9) followed by recrystallization with a mixture of CH_2Cl_2 and methanol afforded **9** (0.24 g, 70%) as dark solid; $C_{72}H_{87}N_3O_2S_3$; m.p. 195-196 °C; ^{1}H-NMR (300 MHz, $CDCl_3$/DMSO-d6) δ 8.31-8.10 (5H, m), 7.56 (3H, s), 7.50-7.44 (3H, m), 7.36-7.33 (3H, m), 7.21 (1H, d, J = 7.5

Hz), 7.02 (2H, s), 6.86 (1H, s), 4.15 (2H, m), 3.16 (4H, m), 2.68 (4H, m), 1.83 (2H, m), 1.60-1.24 (48H, m), and 0.86-0.84 ppm; ^{13}C-NMR (75 MHz, $CDCl_3$/DMSO-d6) δ 169.37, 144.57, 144.02, 143.19, 142.69, 141.92, 141.10, 140.66, 140.33, 139.79, 136.89, 136.40, 135.75, 129.77, 129.34, 128.78, 128.32, 125.64, 125.28, 124.49, 123.73, 123.26, 122.96, 119.23, 118.86, 117.38, 116.39, 109.99, 109.40, 103.91, 34.93, 30.52, 30.31, 30.04, 29.80, 29.73, 29.59, 29.52, 29.44, 29.23, 27.49, 22.87, 22.80, and 14.33 ppm; FT-IR (KBr) 3416, 3055, 2954, 2924, 2853, 2211, 1715, 1605, 1575, 1490, 1453, 1375, 1323, 1295, 1261, 1235, 1169, 1150, 1055, 1031, 935, 876, 804, 741, and 612 cm^{-1}; MS (MALDI-TOF) m/z = 1121.5662 [M] $^{+\cdot}$, 1121.5960 calcd for $C_{72}H_{87}N_3O_2S_3$.

3',6'-Di-*tert*-butyl-9-dodecyl-6-(3,4',4''-trihexyl-[2,2':5',2''-terthiophen]-5-yl)-3,9'-bicarbazole (42)

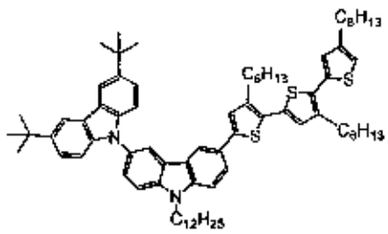

A mixture of **44** (0.37 g, 0.36 mmol), 2-(4-hexylthiophen-2-yl)-4,4,5,5-tetramethyl-1,3,2-dioxaborolane (0.06 g, 0.39 mmol), $Pd(PPh_3)_4$ (0.02 g, 0.01 mmol), and 2 M K_2CO_3 aqueous solution (4 ml, 7.23 mmol) in THF (30 ml) was degassed with N_2 for 5 min. The reaction mixture was stirred at reflux under N_2 for 24 h. After being cooled to room temperature, water (50 ml) was added and extracted with CH_2Cl_2 (50 ml x 3). The combined organic phases were washed with water (50 ml) and brine solution (50 ml), dried over anhydrous Na_2SO_4, filtered, and the solvents were removed to dryness. Purification by column chromatography over silica gel eluting with hexane followed by recrystallization with a mixture of CH_2Cl_2 and methanol afforded 3',6'-di-*tert*-butyl-9-dodecyl-6-(3,4',4''-trihexyl-[2,2':5',2''-terthiophen]-5-yl)-3,9'-bicarbazole (**42**) (0.32 g, 79%) as yellow solid; $C_{74}H_{98}N_2S_3$; m.p. 99-100 °C; ^{1}H-NMR (300 MHz, $CDCl_3$) δ 8.26 (2H, s), 8.19 (2H, s), 7.76 (1H, d, J = 8.4 Hz), 7.62 (1H, d, J = 8.7 Hz), 7.56 (1H, d, J = 8.7 Hz), 7.48-7.43 (3H, m), 7.35 (2H, d, J = 8.7 Hz), 7.25 (1H, s), 7.17 (1H, s), 6.97 (1H, s), 6.88 (1H, s), 4.38 (2H, t, J = 7.5 Hz), 2.77 (2H, quin, J = 8.1 Hz), 2.26 (2H, t, J = 7.6 Hz), 1.96 (2H, m), 1.71-1.11 (62H,

m), and 0.88 (12H, t, J = 2.8 Hz) ppm; ^{13}C-NMR (75 MHz, $CDCl_3$) δ 143.90, 143.00, 142.71, 140.89, 140.75, 140.49, 140.03, 139.82, 135.92, 134.38, 130.78, 129.94, 129.38, 128.41, 127.33, 125.99, 125.55, 125.42, 124.68, 123.92, 123.76, 123.33, 123.25, 120.14, 119.54, 117.84, 116.46, 110.05, 109.62, 109.46, 35.02, 32.35, 32.19, 31.97, 30.83, 30.79, 30.67, 29.98, 29.10, 29.81, 29.71, 29.62, 29.59, 29.52, 29.39, 29.29, 27.64, 22.96, 22.90, and 14.39 ppm; FT-IR (KBr) 3050, 2954, 2927, 2856, 1603, 1491, 1484, 1465, 1295, 1263, 1235, 1093, 1021, 873, 807, 740, and 613 cm^{-1}; MS (MALDI-TOF) m/z = 1110.0719 $[M]^{+\cdot}$, 1110.6892 calcd for $C_{74}H_{98}N_2S_3$.

6-(5''-Bromo-3,4',4''-trihexyl-[2,2':5',2''-terthiophen]-5-yl)-3',6'-di-*tert*-butyl-9-dodecyl-3,9'-bicarbazole (45)

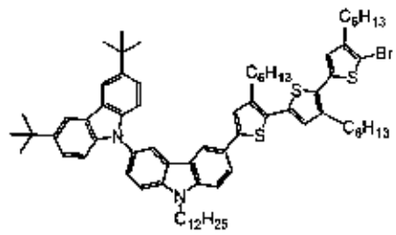

NBS (0.09 g, 0.49 mmol) was added in small portions to a stirred solution of 3',6'-di-*tert*-butyl-9-dodecyl-6-(3,4',4''-trihexyl-[2,2':5',2''-terthiophen]-5-yl)-3,9'-bicarbazole (**42**) (0.51 g, 0.47 mmol) in THF (20 ml). After being stirred at room temperature for 30 min, water was added. The mixture was extracted with dichloromethane (50 ml x 3). The combined organic phase was washed with water (50 ml), brine solution (50 ml), dried over anhydrous sodium sulfate, filtered and the solvent was remove in vacuum. Purification by short column chromatography using silica gel eluting with dichloromethane : hexane, 5:95 gave 6-(5''-bromo-3,4',4''-trihexyl-[2,2':5',2''-terthiophen]-5-yl)-3',6'-di-*tert*-butyl-9-dodecyl-3,9'-bicarbazole (**45**) as yellow solid (0.45 g, 80%); $C_{74}H_{97}BrN_2S_3$; ^{1}H-NMR (300 MHz, $CDCl_3$) δ 8.25 (2H, s), 8.19 (2H, s), 7.73 (1H, d, J = 8.4 Hz), 7.62-7.53 (3H, m), 7.48-7.41 (3H, m), 7.35 (2H, d, J = 9.0 Hz), 7.15 (1H, s), 6.83 (1H, s), 4.35 (2H, t, J = 5.7 Hz), 2.72 (2H, quin, J = 6.9 Hz), 2.55 (2H, t, J = 6.6 Hz), 1.95 (2H, m), 1.68-1.26 (65H, m), and 0.89 (9H, m) ppm; ^{13}C-NMR (75 MHz, $CDCl_3$) δ 143.52, 142.74, 142.65, 141.12, 140.95, 149.51, 140.04, 136.24, 129.99, 128.76, 126.58, 125.86, 125.60, 125.26, 124.71, 123.91, 123.78, 123.37, 123.27, 119.54, 117.89, 116.48, 110.08, 109.65, 109.47, 108.41, 43.80, 35.04, 32.37, 32.22, 32.08, 31.97, 31.93, 30.92, 29.93, 29.84, 29.72, 29.65, 29.58, 29.40, 29.21, 27.65,

22.99, 22.90, and 14.39 ppm; FT-IR (KBr) 3050, 2954, 2925, 2853, 1621, 1489, 1362, 1294, 1261, 1237, 1121, 1095, 1020, 878, 805, 665, and 615 cm^{-1}; MS (MALDI-TOF) m/z = 1188.8076 $[M]^{+\cdot}$, 1188.5997 calcd for $C_{74}H_{99}BrN_2S_3$.

5'''-(3',6'-Di-*tert*-butyl-9-dodecyl-3,9'-bicarbazol]-6-yl)-3',3'',3'''-trihexyl-[2,2':5',2'':5'',2'''-quaterthiophene]-5-carbaldehyde (48)

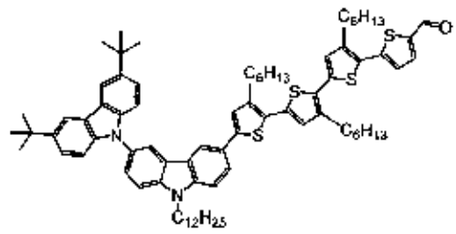

A mixture of **45** (0.43 g, 0.36 mmol), (5-formylthiophen-2-yl)boronic acid (0.06 g, 0.39 mmol), $Pd(PPh_3)_4$ (0.02 g, 0.01 mmol), and 2 M Na_2CO_3 aqueous solution (4 ml, 7.27 mmol) in THF (30 ml) was degassed with N_2 for 5 min. The reaction mixture was stirred at reflux under N_2 for 24 h. After being cooled to room temperature, water (50 ml) was added and extracted with CH_2Cl_2 (50 ml x 3). The combined organic phases were washed with water (50 ml) and brine solution (50 ml), dried over anhydrous Na_2SO_4, filtered, and the solvents were removed to dryness. Purification by column chromatography over silica gel eluting with a mixture of CH_2Cl_2 and hexane (2:3) followed by recrystallization with a mixture of CH_2Cl_2 and methanol afforded 5'''-(3',6'-di-*tert*-butyl-9-dodecyl-3,9'-bicarbazol]-6-yl)-3',3'',3'''-trihexyl-[2,2':5',2'':5'',2'''-quater thiophene]-5-carbaldehyde (**48**) (0.28 g, 63%) as orange viscous oil; $C_{79}H_{100}N_2OS_4$; ^{1}H-NMR (300 MHz, $CDCl_3$) δ 9.80 (1H, s), 8.37-8.21 (5H, m), 7.85-7.71 (1H, m), 7.59 (2H, s), 7.51-7.45 (3H, m), 7.37 (3H, m), 7.23 (1H, s), 7.16 (1H, s), 7.00 (1H, s), 4.29 (2H, m), 2.78-2.62 (4H, m), 1.91 (2H, m), 1.67 (6H, m), 1.49-1.25 (54H, m), and 0.89 (12H, m) ppm; ^{13}C-NMR (125 MHz, $CDCl_3$) 182.63, 146.13, 145.86, 144.53, 142.55, 142.51, 140.91, 140.83, 140.73, 140.32, 140.28, 139.81, 139.29, 136.88, 136.83, 136.68, 135.51, 134.29, 130.81, 130.12, 129.88, 129.79, 129.49, 129.36, 129.22, 129.08, 128.81, 128.34, 127.61, 126.68, 126.14, 125.90, 125.78, 125.68, 125.49, 125.35, 125.25, 124.66, 124.08, 123.98, 123.72, 123.56, 123.15, 123.04, 122.70, 121.61, 119.38, 119.29, 117.82, 116.25, 109.87, 109.42, 109.24, 109.05, 43.56, 34.79, 32.14, 32.07, 31.97, 31.69, 31.55, 30.53, 30.48, 30.28, 30.19, 30.03, 29.84, 29.80, 29.76, 29.69, 29.65, 29.60, 29.49, 29.41, 29.26,

29.26, 29.17, 27.43, 27.41, 22.75, 22.64, and 14.15 ppm; FT-IR (KBr) 3050, 2949, 2919, 2848, 2800, 1648, 1488, 1445, 1410, 1362, 1290, 1217, 1147, 1047, 1020, 895, 878, 805, 788, and 667 cm^{-1}; MS (MALDI-TOF) m/z = 1220.7742 $[M]^{+\cdot}$, 1220.6718 calcd for $C_{79}H_{100}N_2OS_4$.

(*E*)-2-Cyano-3-(5'''-(3',6'-di-*tert*-butyl-9-dodecyl-3,9'-bicarbazol]-6-yl)-3',3'',3'''-trihexyl-[2,2':5',2'':5'',2'''-quaterthiophen]-5-yl)acrylic acid (10)

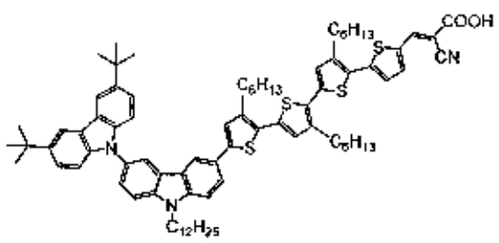

A mixture of **48** (0.25 g, 0.20 mmol) and cyanoacetic acid (0.09 g, 1.02 mmol) was vacuum-dried and added piperidine (0.01 ml, 1.40 mmol) in $CHCl_3$ (20 ml). The solution was refluxed for 6 h. After cooling the solution, the organic layer was removed in vacuo. The pure product was obtained by column chromatography over silica gel eluting with a mixture of MeOH and EtOAc (1:9) followed by recrystallization with a mixture of CH_2Cl_2 and methanol afforded **10** (0.10 g, 41%) as dark red solid; $C_{82}H_{101}N_3O_2S_4$; m.p. 204-205 °C; ^{1}H-NMR (300 MHz, $CDCl_3$/DMSO-d6) δ 8.25-8.15 (4H, m), 7.87-7.81 (2H, m), 7.72 (1H, s), 7.64 (1H, d, J = 7.8 Hz), 7.49-7.46 (3H, m), 7.35-7.29 (4H, m), 7.21 (2H, s), 7.08 (1H, s), 4.32 (2H, m), 3.1102.83 (10H, m), and 2.06-0.88 (70H, m) ppm; ^{13}C-NMR (75 MHz, $CDCl_3$/DMSO-d6) δ 164.85, 145.70, 143.48, 142.07, 139.50, 137.79, 137.47, 136.96, 136.19, 135.27, 132.38, 131.74, 130.46, 129.62, 128.56, 128.41, 127.41, 126.28, 125.71, 125.07, 124.61, 124.25, 124..05, 123.66, 117.55, 116.77, 116.60, 109.20, 48.80, 37.32, 35.00, 32.25, 32.15, 31.88, 30.45, 30.25, 29.92, 29.58, 29.45, 27.31, 27.12, 22.92, 22.82, and 14.37 ppm; FT-IR (KBr) 3411, 3055, 2949, 2921, 2850, 2207, 1713, 1582, 1478, 1451, 1433, 1358, 1294, 1236, 1202, 1059, 985, 876, 820, 787, 712, and 614 cm^{-1}.

Chapter 5:

3',6'-Di-*tert*-butyl-9-dodecyl-6-(thiophen-2-yl)-3,9'-bicarbazole (49)

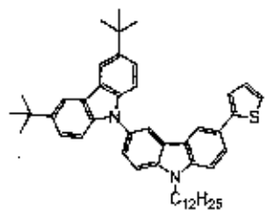

A mixture of **39** (0.80 g, 1.18 mmol), thiophen-2-ylboronic acid (0.15 g, 1.18 mmol), $Pd(PPh_3)_4$ (0.055 g, 0.47 mmol), and 2 M Na_2CO_3 aqueous solution (12 ml, 23.62 mmol) in THF (50 ml) was degassed with N_2 for 5 min. The reaction mixture was stirred at reflux under N_2 for 24 h. After being cooled to room temperature, water (50 ml) was added and extracted with CH_2Cl_2 (50 ml x 3). The combined organic phases were washed with water (50 ml) and brine solution (50 ml), dried over anhydrous Na_2SO_4, filtered, and the solvents were removed to dryness. Purification by column chromatography over silica gel with hexane as eluent followed by recrystallization with a mixture of CH_2Cl_2 and methanol afforded 3',6'-di-*tert*-butyl-9-dodecyl-6-(thiophen-2-yl)- 3,9'-bicarbazole (**49**) (0.54 g, 66%) as white solid; $C_{48}H_{58}N_2S$; mp: 132 °C, ^1H NMR (300 MHz, $CDCl_3$) δ 8.28 (2H, d, J = 4.80 Hz), 8.20 (2H, s), 7.79 (1H, d, J = 8.40 Hz), 7.59 (2H, q), 7.48 (3H, m), 7.35 (3H, m), 7.24 (2H, s), 7.10 (1H, t, J = 4.50 Hz), 4.39 (2H, t, J = 7.20 Hz), 1.97 (2H, t, J = 6.90 Hz), 1.56-1.27 (36H, m), and 0.87 (3H, t, J = 6.90 Hz) ppm; ^{13}C NMR (300 MHz, $CDCl_3$) δ 145.51, 142.44, 140.61, 140.31, 139.81, 129.64, 128.01, 126.09, 125.35, 124.88, 123.80, 123.68, 123.50, 123.07, 122.97, 122.14, 119.37, 118.05, 116.20, 109.77, 109.34, 109.19, 43.53, 34.76, 32.09, 31.93, 29.64, 29.55, 29.45, 29.36, 29.13, 27.37, 22.70, and 14.13 ppm; HRMS-ESI m/z = 695.4405 [MH^+], 694.4321 calcd for $C_{48}H_{58}N_2S$.

6-(5-Bromothiophen-2-yl)-3',6'-di-*tert*-butyl-9-dodecyl-3,9'-bicarbazole (50)

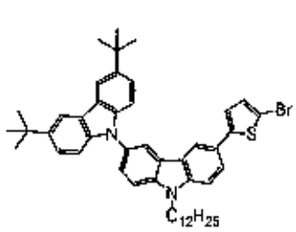

NBS (0.54 g, 3.02 mmol) was added in small portions to a stirred solution of 3',6'-di-*tert*-butyl-9-dodecyl-6-(thiophen-2-yl)- 3,9'-bicarbazole (**49**) (1.97 g, 2.88 mmol) in THF (20 ml). After being stirred at room temperature for 30 min, water was added. The mixture was extracted with dichloromethane (30 ml x 3). The combined organic phase was washed with water (50 ml), brine solution (50 ml), dried over anhydrous sodium sulfate, filtered and the solvent was remove in vacuum. Purification by short column chromatography using silica gel with hexane as eluent followed by recrystallization with a mixture of CH_2Cl_2 and methanol gave 6-(5-bromothiophen-2-yl)-3',6'-di-*tert*-butyl-9-dodecyl-3,9'-bicarbazole (**50**) as as white solid (1.78 g, 80%); $C_{48}H_{57}BrN_2S$; mp: 174 °C, ^{1}H NMR (300 MHz, $CDCl_3$): δ 8.26 (2H, s), 8.21 (2H, s), 7.69 (3H, d, J = 8.40 Hz), 7.61 (3H, d, J = 6.90 Hz), 7.50-7.46 (3H, m), 7.35 (2H, d, J = 8.70 Hz), 7.08-7.04 (2H, q), 4.40 (2H, t, J = 7.20 Hz), 1.98 (2H, t, J = 6.90 Hz), 1.57-1.27 (36H, m), and 0.89 (3H, t, J = 6.90 Hz) ppm; ^{13}C NMR (300 MHz, $CDCl_3$) δ 147.02, 142.48, 140.76, 140.26, 139.81, 130.82, 129.79, 125.50, 125.30, 124.49, 123.54, 123.50, 123.08, 123.00, 122.23, 119.34, 117.80, 116.21, 110.03, 109.85, 109.47, 109.15, 43.55, 34.75, 32.08, 31.92, 29.63, 29.60, 29.53, 29.43, 29.35, 29.10, 27.35, 22.69, and 14.12 ppm; HRMS-ESI m/z = 773.3482 [MH$^+$], 772.3426 calcd for $C_{48}H_{57}BrN_2S$.

3',6'-Di-*tert*-butyl-9-dodecyl-6-(5-(thieno[3,2-b]thiophen-2-yl)thiophen-2-yl)-3,9'-bicarbazole (2d)

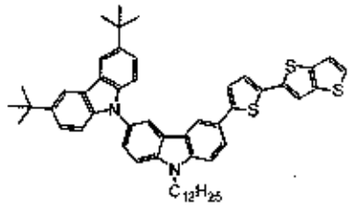

A mixture of **50** (0.50 g, 0.65 mmol), thieno[3,2-b]thiophen-2-ylboronic acid (0.12 g, 0.65 mmol), $Pd(PPh_3)_4$ (0.03 g, 0.03 mmol), and 2 M K_2CO_3 aqueous solution (6 ml, 13.02 mmol) in THF (30 ml) was degassed with N_2 for 5 min. The reaction mixture was stirred at reflux under N_2 for 24 h. After being cooled to room temperature, water (50 ml) was added and extracted with CH_2Cl_2 (50 ml x 3). The combined organic phases were washed with water (50 ml) and brine solution (50 ml), dried over anhydrous Na_2SO_4, filtered, and the solvents were removed to dryness.

Purification by column chromatography over silica gel with hexane as eluent followed by recrystallization with a mixture of CH_2Cl_2 and methanol afforded 3',6'-di-*tert*-butyl-9-dodecyl-6-(5-(thieno[3,2-b]thiophen-2-yl)thiophen-2-yl)-3,9'-bicarbazole (**2d**) (0.26 g, 48%) as yellow solid; $C_{54}H_{60}N_2S_3$; m.p. 226-227 °C; ^{1}H-NMR (300 MHz, $CDCl_3$) δ 8.28 (2H, s), 8.20 (1H, s), 8.19 (1H, s), 7.78 (1H, d, J = 7.8 Hz), 7.63 (1H, dd, J = 8.7 Hz, J = 1.5 Hz), 7.58 (1H, d, J = 8.7 Hz), 7.50-7.47 (3H, m), 7.37-7.33 (4H, m), 7.26-7.19 (3H, m), 4.39 (2H, t, J = 6.9 Hz), 1.97 (2H, quin, J = 6.6 Hz), 1.58-1.27 (33H, m), and 0.88-0.86 (6H, m) ppm; ^{13}C-NMR (75 MHz, $CDCl_3$) δ 144.83, 142.48, 140.74, 140.28, 139.62, 139.51, 137.79, 135.84, 129.78, 126.85, 125.57, 125.44, 124.88, 124.53, 123.63, 123.51, 123.09, 123.04, 122.47, 119.47, 119.36, 117.77, 116.20, 115.28, 109.83, 109.45, 109.18, 43.55, 34.75, 32.08, 31.92, 29.71, 29.63, 29.60, 29.54, 29.43, 29.35, 29.12, 27.37, 22.69, and 14.11 ppm; MS (MALDI-TOF) m/z = 832.0360 $[M]^{+\cdot}$, 832.3919 calcd for $C_{54}H_{60}N_2S_3$.

6-(5-(5-Bromothieno[3,2-b]thiophen-2-yl)thiophen-2-yl)-3',6'-di-*tert*-butyl-9-dodecyl-3,9'-bicarbazole (3d)

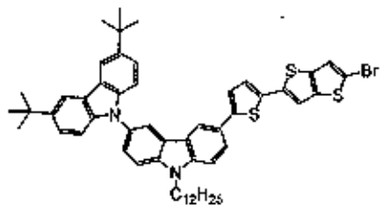

NBS (0.04 g, 0.21 mmol) was added in small portions to a stirred solution of 3',6'-di-*tert*-butyl-9-dodecyl-6-(5-(thieno[3,2-b]thiophen-2-yl)thiophen-2-yl)-3,9'-bicarbazole (**2d**) (0.17 g, 0.20 mmol) in THF (20 ml). After being stirred at room temperature for 30 min, water was added. The mixture was extracted with dichloromethane (30 ml x 3). The combined organic phase was washed with water (50 ml), brine solution (50 ml), dried over anhydrous sodium sulfate, filtered and the solvent was remove in vacuum. Purification by short column chromatography using silica gel eluting with hexane gave 6-(5-(5-bromothieno[3,2-b]thiophen-2-yl)thiophen-2-yl)-3',6'-di-*tert*-butyl-9-dodecyl-3,9'-bicarbazole (**3d**) as light yellow solid (0.10 g, 55%); $C_{54}H_{59}BrN_2S_3$; m.p. 165-166 °C; ^{1}H-NMR (300 MHz, $CDCl_3$) δ 8.30-8.27 (2H, m), 8.21-8.20 (2H, m), 7.81-7.75 (1H, m), 7.60 (1H, d, J = 8.1 Hz), 7.57 (1H, d, J = 8.7 Hz), 7.50-7.42 (4H, m), 7.37-7.29 (2H, m), 7.26-7.17 (3H, m), 4.39 (2H, t, J = 6.9 Hz), 1.97-1.95 (2H, m), 1.58-1.27 (36H, m), and 0.88 (3H, t, J = 6.4

Hz) ppm; ^{13}C-NMR (75 MHz, $CDCl_3$) δ 146.77, 145.13, 142.50, 140.87, 140.77, 140.29, 139.99, 139.82, 138.98, 136.41, 135.19, 129.81, 127.82, 125.47, 125.32, 125.09, 124.58, 124.51, 123.62, 123.52, 123.11, 122.83, 122.79, 122.55, 122.15, 119.36, 117.96, 117.78, 116.22, 114.78, 113.91, 112.88, 109.86, 109.47, 109.18, 43.56, 34.76, 32.09, 31.93, 29.71, 29.64, 29.55, 29.44, 25.35, 29.12, 27.37, 22.70, and 14.12 ppm; FT-IR (KBr) 3050, 2954, 2928, 2854, 1656, 1628, 1547, 1488, 1462, 1364, 1294, 1262, 1154, 1092, 1022, 876, 806, 733, 660, and 614 cm^{-1}; MS (MALDI-TOF) m/z = 910.0072 $[M]^{+\cdot}$, 910.3024 calcd for $C_{54}H_{59}BrN_2S_3$.

5-(5-(5-(3',6'-Di-*tert*-butyl-9-dodecyl-3,9'-bicarbazol]-6-yl)thiophen-2-yl)thieno[3,2-b]thiophen-2-yl)thiophene-2-carbaldehyde (4d)

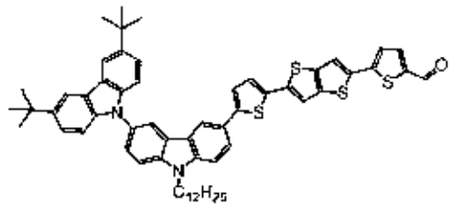

A mixture of **3d** (0.24 g, 0.26 mmol), (5-formylthiophen-2-yl)boronic acid (0.04 g, 0.28 mmol), $Pd(PPh_3)_4$ (0.01 g, 0.02 mmol), and 2 M Na_2CO_3 aqueous solution (3 ml, 5.28 mmol) in THF (20 ml) was degassed with N_2 for 5 min. The reaction mixture was stirred at reflux under N_2 for 24 h. After being cooled to room temperature, water (70 ml) was added and extracted with CH_2Cl_2 (70 ml x 3). The combined organic phases were washed with water (70 ml) and brine solution (70 ml), dried over anhydrous Na_2SO_4, filtered, and the solvents were removed to dryness. Purification by column chromatography over silica gel eluting with a mixture of CH_2Cl_2 and hexane (2:3) followed by recrystallization with a mixture of CH_2Cl_2 and methanol afforded 5-(5-(5-(3',6'-di-*tert*-butyl-9-dodecyl-[3,9'-bicarbazol]-6-yl)thiophen-2-yl)thieno[3,2-b]thiophen-2-yl)thiophene-2-carbaldehyde (**4d**) (0.10 g, 44%) as orange solid; $C_{59}H_{62}N_2OS_4$; m.p. 272-173 °C; ^{1}H-NMR (300 MHz, $CDCl_3$) δ 8.30-8.27 (2H, m), 8.19 (2H, s), 7.83-7.76 (1H, m), 7.68-7.56 (4H, m), 7.49-7.46 (5H, m), 7.36-7.32 (4H, m), 7.26 (1H, s), 4.39 (2H, m), 1.97 (2H, m), 1.55-1.26 (36H, m), and 0.87 (3H, m) ppm; ^{13}C-NMR (75 MHz, $CDCl_3$)183.86, 153.75, 142.76, 140.52, 130.08, 125.74, 124.82, 123.77, 123.34, 119.61, 118.29, 116.49, 115.26, 110.16, 109.43, 43.82,

35.02, 32.35, 32.19, 29.97, 29.89, 29.82, 29.38, 27.63, 25.64, 22.96, and 14.93 ppm; MS (MALDI-TOF) m/z = 942.1108 $[M]^{+\cdot}$, 942.3745 calcd for $C_{59}H_{62}N_2OS_4$.

(*E*)-2-Cyano-3-(5-(5-(5-(3',6'-di-*tert*-butyl-9-dodecyl-3,9'-bicarbazol]-6-yl)thiophen-2-yl)thieno[3,2-b]thiophen-2-yl)thiophen-2-yl)acrylic acid (11)

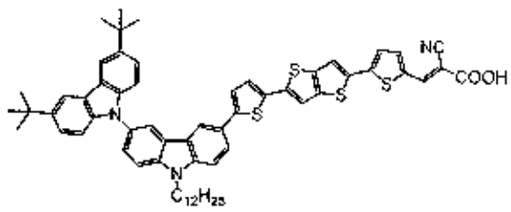

A mixture of **4d** (0.11 g, 0.11 mmol) and cyanoacetic acid (0.05 g, 0.58 mmol) was vacuum-dried and added piperidine (0.08 ml, 0.81 mmol) in $CHCl_3$ (20 ml). The solution was refluxed for 6 h. After cooling the solution, the organic layer was removed in vacuo. The pure product was obtained by column chromatography over silica gel eluting with a mixture of MeOH and EtOAc (1:9) followed by recrystallization with a mixture of CH_2Cl_2 and methanol afforded **11** (0.10 g, 86%) as light orange solid; $C_{62}H_{63}N_3O_2S_4$; m.p. 251-252 °C; ^{1}H-NMR (500 MHz, $CDCl_3$/DMSO-d6) δ 8.16 (5H, m), 7.44-7.29 (15H, m), 4.39 (2H, m), and 1.48-0.84 (41H, m) ppm; ^{13}C-NMR (75 MHz, $CDCl_3$/DMSO-d6) δ 142.48, 140.09, 123.51, 123.03, 116.15, 109.15, 59.50, 37.06, 32.71, 32.04, 31.89, 31.22, 30.00, 29.66, 29.32, 27.28, 27.05, 26.69, 22.43, 19.71, and 14.09 ppm; FT-IR (KBr) 3421, 3050, 2954, 2924, 2853, 2207, 1726, 1617, 1582, 1489, 1443, 1376, 1296, 1261, 1130, 877, 799, 763, 638, and 615 cm^{-1}; MS (MALDI-TOF) m/z = 1009.3901 $[M]^{+\cdot}$, 1009.3803 calcd for $C_{62}H_{63}N_3O_2S_4$.

3',6'-Di-*tert*-butyl-9-dodecyl-6-(4'-hexyl-[2,2'-bithiophen]-5-yl)-3,9'-bicarbazole (2e)

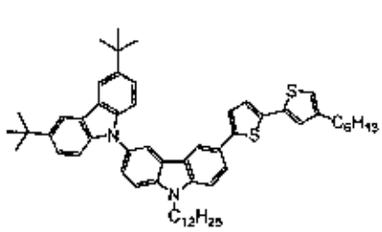

A mixture of **50** (0.44 g, 0.56 mmol), 2-(4-hexylthiophen-2-yl)-4,4,5,5-tetramethyl-1,3,2-dioxaborolane (0.17 g, 0.56 mmol), $Pd(PPh_3)_4$ (0.03 g, 0.02 mmol), and 2 M K_2CO_3 aqueous solution (6 ml, 11.30 mmol) in THF (30 ml) was degassed with N_2 for 5 min. The reaction mixture was stirred at reflux under N_2 for 24 h. After being cooled to room temperature, water (50 ml) was added and extracted with CH_2Cl_2 (50 ml x 3). The combined organic phases were washed with water (50 ml) and brine solution (50 ml), dried over anhydrous Na_2SO_4, filtered, and the solvents were removed to dryness. Purification by column chromatography over silica gel eluting with a mixture of CH_2Cl_2 and hexane (2:3) followed by recrystallization with a mixture of CH_2Cl_2 and methanol afforded 3',6'-di-*tert*-butyl-9-dodecyl-6-(4'-hexyl-[2,2'-bithiophen]-5-yl)-3,9'-bicarbazole (**2e**) (0.45 g, 93%) as white solid; $C_{58}H_{72}N_2S_2$; m.p. 129.130 °C; ^{1}H-NMR (300 MHz, $CDCl_3$) δ 8.28 (2H, s), 8.21 (2H, s), 7.78 (1H, dd, J = 7.6 Hz, J = 1.5 Hz), 7.63 (1H, dd, J = 8.5 Hz, J = 1.6 Hz), 7.57 (1H, d, J = 8.7 Hz), 7.51-7.45 (3H, m), 7.37 (2H, d, J = 8.7 Hz), 7.23 (1H, d, J = 3.6 Hz), 7.14 (1H, d, J = 3.9 Hz), 7.05 (1H, s), 6.80 (1H, s), 4.39 (2H, t, J = 6.7 Hz), 2.60 (2H, t, J = 7.6 Hz), 1.97 (2H, quin, J = 6.6 Hz), 1.67-1.28 (44H, m), and 0.89 (6H, t, J = 5.5 Hz) ppm; ^{13}C-NMR (75 MHz, $CDCl_3$) δ 144.11, 144.03, 142.47, 140.64, 140.28, 139.80, 137.28, 136.07, 129.74, 125.80, 125.36, 124.89, 124.72, 124.48, 124.33, 123.80, 123.65, 123.52, 123.10, 123.03, 122.62, 119.31, 118.70, 117.69, 116.20, 109.81, 109.41, 43.54, 34.76, 32.10, 31.93, 31.69, 30.56, 30.37, 29.65, 29.62, 29.55, 29.45, 29.36, 29.13, 29.01, 27.37, 22.71, 22.62, and 14.13 ppm; MS (MALDI-TOF) m/z = 860.3179 $[M]^{+\cdot}$, 860.5137 calcd for $C_{58}H_{72}N_2S_2$.

6-(5'-Bromo-4'-hexyl-[2,2'-bithiophen]-5-yl)-3',6'-di-*tert*-butyl-9-dodecyl-3,9'-bicarbazole (3e)

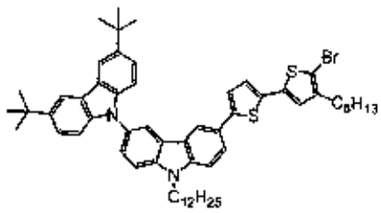

NBS (0.09 g, 0.53 mmol) was added in small portions to a stirred solution of 3',6'-di-*tert*-butyl-9-dodecyl-6-(4'-hexyl-[2,2'-bithiophen]-5-yl)-3,9'-bicarbazole (**2e**) (0.43 g, 0.50 mmol) in THF (20 ml). After being stirred at room temperature for 30 min, water was added.

The mixture was extracted with dichloromethane (30 ml x 3). The combined organic phase was washed with water (50 ml), brine solution (50 ml), dried over anhydrous sodium sulfate, filtered and the solvent was remove in vacuum. Purification by short column chromatography using silica gel eluting with hexane gave 6-(5'-bromo-4'-hexyl-[2,2'-bithiophen]-5-yl)-3',6'-di-*tert*-butyl-9-dodecyl-3,9'-bicarbazole (**3e**) as white solid (0.46 g, 99%); $C_{58}H_{71}BrN_2S_2$; m.p. 165-166 °C; ^{1}H-NMR (300 MHz, $CDCl_3$) δ 8.26 (2H, s), 8.20 (2H, s), 7.77 (1H, d, J =8.4 Hz), 7.61 (1H, d, J = 8.4 Hz), 7.56 (1H, d, J = 8.7 Hz), 7.50-7.44 (3H, m), 7.36 (2H, d, J = 8.7 Hz), 7.26 (1H, s), 7.19 (1H, s), 6.84 (1H, s), 4.38 (2H, t, J = 7.0 Hz), 2.63 (2H, t, J = 7.6 Hz), 1.97 (2H, quin, J = 6.7 Hz), 1.70-1.27 (44H, m), and 0.89 (6H, t, J = 6.7 Hz ppm; ^{13}C-NMR (75 MHz, $CDCl_3$) δ 145.00, 144.30, 142.43, 140.55, 140.30, 139.78, 129.60, 126.40, 125.26, 124.70, 123.71, 123.61, 123.48, 123.07, 122.94, 119.32, 118.42, 117.76, 116.18, 109.73, 109.25, 109.20, 43.52, 34.75, 32.09, 31.92, 31.72, 30.75, 30.45, 29.63, 29.60, 29.54, 29.44, 29.35, 29.12, 29.07, 27.37, 22.37, 22.69, 22.63, and 14.11 ppm; FT-IR (KBr) 3073, 3048, 3004, 2954, 2923, 2853, 1627, 1604, 1574, 1482, 1349, 1261, 873, 791, 750, 658, and 610 cm^{-1}; MS (MALDI-TOF) m/z = 938.1730 $[M]^{+\cdot}$, 938.4242 calcd for $C_{58}H_{71}BrN_2S_2$.

5''-(3',6'-Di-*tert*-butyl-9-dodecyl-[3,9'-bicarbazol]-6-yl)-3'-hexyl-[2,2':5',2''-terthiophene]-5-carbaldehyde (4e)

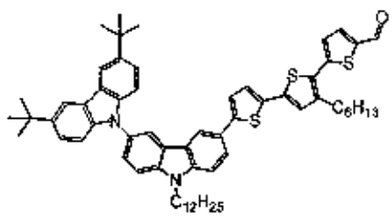

A mixture of **3e** (0.24 g, 2.25 mmol), (5-formylthiophen-2-yl)boronic acid (0.04 g, 0.28 mmol), $Pd(PPh_3)_4$ (0.006 g, 0.005 mmol), and 2 M Na_2CO_3 aqueous solution (3 ml, 5.55 mmol) in THF (20 ml) was degassed with N_2 for 5 min. The reaction mixture was stirred at reflux under N_2 for 24 h. After being cooled to room temperature, water (30 ml) was added and extracted with CH_2Cl_2 (30 ml x 3). The combined organic phases were washed with water (30 ml) and brine solution (30 ml), dried over anhydrous Na_2SO_4, filtered, and the solvents were removed to dryness. Purification by column chromatography over silica gel eluting with a mixture of CH_2Cl_2 and

hexane (2:3) followed by recrystallization with a mixture of CH_2Cl_2 and methanol afforded 5''-(3',6'-di-*tert*-butyl-9-dodecyl-[3,9'-bicarbazol]-6-yl)-3'-hexyl-[2,2':5',2''-terthiophene]-5-carbaldehyde (**4e**) (2.16 g, 99%) as orange solid; $C_{63}H_{74}N_2OS_3$; m.p. 122-123 °C; ^{1}H-NMR (300 MHz, $CDCl_3$) δ 9.88 (1H, s), 8.27 (1H, s), 8.20 (1H, s), 7.77 (1H, d, J = 8.7 Hz), 7.70 (1H, d, J = 3.9 Hz), 7.63 (1H, d, J = 8.7 Hz), 7.58 (1H, d, J = 8.7 Hz), 7.48 (3H, d, J = 7.5 Hz), 7.36 (2H, d, J = 8.7 Hz), 7.26-7.19 (3H, m), 7.06 (1H, s), 4.39 (2H, m), 2.81 (2H, t, J = 7.8 Hz), 2.34-2.29 (2H, m), 1.97-1.09 (44H, m), and 0.96-0.84 (6H, m) ppm; ^{13}C-NMR (75 MHz, $CDCl_3$) δ 182.50, 145.37, 143.12, 142.50, 142.00, 140.80, 140.24, 139.80, 137.70, 136.84, 134.57, 129.84, 126.58, 125.73, 125.44, 125.35, 124.45, 123.60, 123.50, 123.11, 123.07, 122.84, 119.29, 117.82, 116.21, 109.86, 109.47, 109.17, 43.56, 34.75, 32.77, 32.08, 31.94, 31.64, 30.17, 30.05, 29.96, 29.91, 29.71, 29.67, 29.63, 29.60, 29.54, 29.43, 29.37, 29.35, 29.25, 29.12, 27.36, 27.10, 26.76, 22.70, 22.58, 19.73, 14.11, and 14.06 ppm; FT-IR (KBr) 3072, 3042, 2957, 2921, 2852, 1749, 1668, 1486, 1449, 1376, 1262, 1231, 1053, 870, 819, 794, 752, 718, 656, and 611 cm^{-1}; MS (MALDI-TOF) m/z = 970.9969 $[M]^{+\cdot}$, 970.4963 calcd for $C_{63}H_{74}N_2OS_3$.

(*E*)-2-Cyano-3-(5''-(3',6'-di-*tert*-butyl-9-dodecyl-3,9'-bicarbazol]-6-yl)-3'-hexyl-[2,2':5',2''-terthiophen]-5-yl)acrylic acid (12)

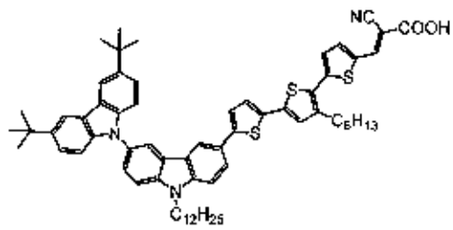

A mixture of **4e** (0.26 g, 0.27 mmol) and cyanoacetic acid (0.11 g, 1.34 mmol) was vacuum-dried and added piperidine (0.18 ml, 1.87 mmol) in $CHCl_3$ (20 ml). The solution was refluxed for 6 h. After cooling the solution, the organic layer was removed in vacuo. The pure product was obtained by column chromatography over silica gel eluting with a mixture of MeOH and EtOAc (1:9) followed by recrystallization with a mixture of CH_2Cl_2 and methanol afforded **12** (0.10 g, 36%) as dark red solid; $C_{66}H_{75}N_3O_2S_3$; m.p. 235-236 °C; ^{1}H-NMR (300 MHz, $CDCl_3$/DMSO-d6) δ 8.07-7.90 (5H, m), 7.38-7.35 (3H, m), 7.31-7.22 (4H, m), 7.13-7.04 (3H, m), 6.85-6.81 (3H, m), 6.71 (1H, s), 3.97 (2H, m), 2.48 (2H, m), 1.63 (2H, m), 1.48-1.03 (31H, m),

and 0.66-0.65 (6H, m) ppm; ^{13}C-NMR (75 MHz, $CDCl_3$/DMSO-d6) δ 168.00, 144.57, 143.88, 142.34, 142.26, 140.35, 139.91, 139.44, 136.93, 135.24, 134.38, 129.43, 128.15, 126.22, 125.17, 124.97, 124.09, 123.38, 123.32, 122.85, 122.61, 118.78, 117.17, 115.98, 43.13, 34.55, 31.92, 31.69, 31.45, 29.89, 29..79, 29.42, 29.40, 29.37, 29.32, 29.18, 29.12, 29.03, 28.83, 27.07, 22.47, 22.38, and 14.00 ppm; FT-IR (KBr) 3418, 3059, 2949, 2925, 2853, 2211, 1680, 1603, 1579, 1489, 1443, 1363, 1295, 1262, 1233, 1057, 873, 801, 741, and 654 cm^{-1}; MS (MALDI-TOF) m/z – 1037.4878 $[M]^{+\bullet}$, 1037.5021 calcd for $C_{66}H_{75}N_3O_2S_3$.

3',6'-Di-*tert*-butyl-6-(4',4''-dihexyl-[2,2':5',2''-terthiophen]-5-yl)-9-dodecyl-3,9'-bicarbazole (51)

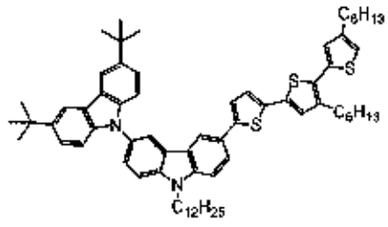

A mixture of **3e** (0.34 g, 0.36 mmol), 2-(4-hexylthiophen-2-yl)-4,4,5,5-tetramethyl-1,3,2-dioxaborolane (0.11 g, 0.36 mmol), $Pd(PPh_3)_4$ (0.02 g, 0.01 mmol), and 2 M K_2CO_3 aqueous solution (4 ml, 7.31 mmol) in THF (20 ml) was degassed with N_2 for 5 min. The reaction mixture was stirred at reflux under N_2 for 24 h. After being cooled to room temperature, water (50 ml) was added and extracted with CH_2Cl_2 (50 ml x 3). The combined organic phases were washed with water (50 ml) and brine solution (50 ml), dried over anhydrous Na_2SO_4, filtered, and the solvents were removed to dryness. Purification by column chromatography over silica gel eluting with hexane followed by recrystallization with a mixture of CH_2Cl_2 and methanol afforded 3',6'-di-*tert*-butyl-6-(4',4''-dihexyl-[2,2':5',2''-terthiophen]-5-yl)-9-dodecyl-3,9'-bicarbazole (**51**) (0.30 g, 82%) as white solid; $C_{68}H_{86}N_2S_3$; m.p. 122-123 °C; ^{1}H-NMR (300 MHz, $CDCl_3$) δ 8.27 (2H, s), 8.21 (2H, s), 7.78 (1H, d, J = 8.4 Hz), 7.63 (1H, dd, J = 7.9 Hz, J = 1.5 Hz), 7.57 (1H, d, J = 8.7 Hz), 7.50-7.45 (3H, m), 7.37 (2H, d, J = 8.7 Hz), 7.23 (1H, d, J = 3.6 Hz), 7.14 (1H, d, J = 3.6 Hz), 7.03 (1H, s), 6.97 (1H, s), 6.89 (1H, s), 4.39 (2H, t, J = 6.7 Hz), 2.74 (2H, t, J = 7.8 Hz), 2.61 (2H, t, J = 7.5 Hz), 1.97 (2H, quin, J = 6.4 Hz), 1.65 (4H, quin, J = 6.7 Hz), 1.56-1.27 (48H, m), and 0.91-0.84 (9H, m) ppm; ^{13}C-NMR (75 MHz, $CDCl_3$) δ 144.21, 143.65, 142.47, 140.66, 140.26, 140.05,

139.79, 135.65, 135.53, 135.05, 129.76, 127.11, 126.13, 125.73, 125.36, 124.46, 123.64, 123.51, 123.09, 123.03, 122.72, 119.30, 117.70, 116.19, 109.81, 109.42, 109.20, 43.55, 34.75, 32.09, 31.93, 31.70, 31.66, 30.51, 30.40, 29.63, 29.61, 29.54, 29.44, 29.39, 29.36, 29.25, 29.12, 29.02, 27.37, 22.70, 22.62, and 14.07 ppm; FT-IR (KBr) 3050, 2953, 2925, 2854, 1633, 1487, 1360, 1295, 1263, 1235, 1149, 1020, 873, 807, and 668 cm^{-1}; MS (MALDI-TOF) m/z = 1026.1387 $[M]^{+\cdot}$, 1026.5953 calcd for $C_{68}H_{86}N_2S_3$.

6-(5''-Bromo-4',4''-dihexyl-[2,2':5',2''-terthiophen]-5-yl)-3',6'-di-*tert*-butyl-9-dodecyl-3,9'-bicarbazole (52)

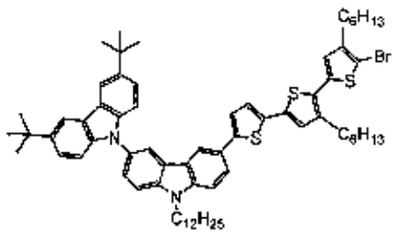

NBS (0.05 g, 0.29 mmol) was added in small portions to a stirred solution of 3',6'-di-*tert*-butyl-6-(4',4''-dihexyl-[2,2':5',2''-terthiophen]-5-yl)-9-dodecyl-3,9'-bicarbazole (**51**) (0.27 g, 0.27 mmol) in THF (20 ml). After being stirred at room temperature for 30 min, water was added. The mixture was extracted with dichloromethane (30 ml x 3). The combined organic phase was washed with water (50 ml), brine solution (50 ml), dried over anhydrous sodium sulfate, filtered and the solvent was remove in vacuum. Purification by short column chromatography using silica gel eluting with dichloromethane : hexane, 5:95 gave 6-(5''-bromo-4',4''-dihexyl-[2,2':5',2''-terthiophen]-5-yl)-3',6'-di-*tert*-butyl-9-dodecyl-3,9'-bicarbazole (**52**) as white solid (0.25 g, 84%); $C_{68}H_{85}BrN_2S_3$; m.p. 113-114 °C; ^{1}H-NMR (300 MHz, $CDCl_3$) δ 8.27 (2H, s), 8.20 (2H, s), 7.77 (1H, d, J = 8.7 Hz), 7.63 (1H, dd, J = 8.1 Hz, J = 1.2 Hz), 7.57 (1H, d, J = 8.4 Hz), 7.49-7.47 (3H, m), 7.36 (2H, d, J = 8.7 Hz), 7.23 (1H, d, J = 3.6 Hz), 7.14 (1H, d, J = 3.6 Hz), 7.01 (1H, s), 6.82 (1H, s), 4.39 (2H, t, J = 6.9 Hz), 2.69 (2H, t, J = 7.8 Hz), 2.56 (2H, t, J = 7.5 Hz), 1.97 (2H, quin, J = 6.6 Hz), 1.70-1.27 (52H, m), and 0.90-0.86 (9H, m) ppm; ^{13}C-NMR (75 MHz, $CDCl_3$) δ 144.49, 142.48, 140.70, 140.61, 140.26, 136.80, 135.60, 135.48, 135.24, 129.78, 128.68, 126.58, 126.05, 125.64, 125.39, 124.63, 124.45, 124.05, 123.63, 123.51, 123.09, 123.04, 122.74, 119.29, 117.73, 116.20, 109.83, 109.44, 109.19, 108.52, 43.56, 34.75, 32.08, 31.92, 31.64, 30.50, 29.63,

29.54, 29.43, 29.35, 29.21, 29.12, 28.91, 27.36, 22.69, 22.60, 14.11, and 14.08 ppm; FT-IR (KBr) 3059, 2954, 2925, 2848, 1619, 1486, 1362, 1294, 1261, 1121, 1092, 1019, 875, 807, 790, 665, and 613 cm^{-1}; MS (MALDI-TOF) m/z = 1104.8741 $[M]^{+\cdot}$, 1104.5058 calcd for $C_{68}H_{85}BrN_2S_3$.

5'''-(3',6'-Di-*tert*-butyl-9-dodecyl-3,9'-bicarbazol]-6-yl)-3',3''-dihexyl-[2,2':5',2'':5'',2'''-quaterthiophene]-5-carbaldehyde (53)

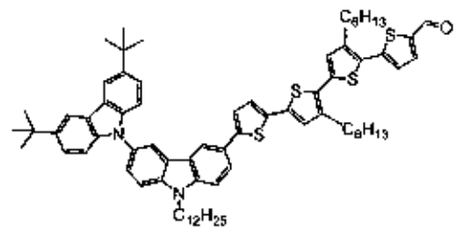

A mixture of **52** (0.46 g, 0.41 mmol), (5-formylthiophen-2-yl)boronic acid (0.07 g, 0.45 mmol), $Pd(PPh_3)_4$ (0.02 g, 0.02 mmol), and 2 M K_2CO_3 aqueous solution (4 ml, 8.26 mmol) in THF (30 ml) was degassed with N_2 for 5 min. The reaction mixture was stirred at reflux under N_2 for 24 h. After being cooled to room temperature, water (50 ml) was added and extracted with CH_2Cl_2 (50 ml x 3). The combined organic phases were washed with water (50 ml) and brine solution (50 ml), dried over anhydrous Na_2SO_4, filtered, and the solvents were removed to dryness. Purification by column chromatography over silica gel eluting with a mixture of CH_2Cl_2 and hexane (2:3) followed by recrystallization with a mixture of CH_2Cl_2 and methanol afforded 5'''-(3',6'-di-*tert*-butyl-9-dodecyl-[3,9'-bicarbazol]-6-yl)-3',3''-dihexyl-[2,2':5',2'':5'',2'''-quaterthiophene]-5-carbaldehyde **(53)** (0.13 g, 28%) as red solid; $C_{73}H_{88}N_2OS_4$; m.p. 121-122 °C; ^{1}H-NMR (300 MHz, $CDCl_3$) δ 9.80 (1H, s), 8.19 (2H, s), 8.12 (2H, s), 7.70 (1H, d, J = 8.7 Hz), 7.63 (1H, d, J = 3.6 Hz), 7.55 (1H, d, J = 8.7 Hz), 7.49 (1H, d, J = 8.4 Hz), 7.42-7.38 (3H, m), 7.28 (2H, d, J = 8.4 Hz), 7.18-7.15 (2H, m), 7.08 (1H, d, J = 3.6 Hz), 6.98-6.92 (2H, m), 4.13 (2H, t, J = 6.7 Hz), 2.77-2.70 (4H, m), 1.89 (2H, quin, J = 6.0 Hz), 1.62-1.57 (4H, m), 1.41-1.19 (51H, m), and 0.82-0.78 (6H, m) ppm; ^{13}C-NMR (75 MHz, $CDCl_3$) δ 182.87, 146.55, 144.98, 142.86, 142.76, 142.35, 141.44, 140.99, 140.50, 140.06, 137.18, 136.62, 136.27, 135.36, 130.04, 129.41, 129.10, 126.62, 126.07, 125.87, 125.84, 125.08, 124.71, 123.87, 123.79, 123.36, 123.31, 123.06, 119.56, 118.02, 116.48, 110.13, 109.73, 109.45, 43.83, 35.04, 32.36, 32.20, 31.94, 30.67, 30.50,

30.08, 29.99, 29.92, 29.82, 29.72, 29.63, 29.54, 29.40, 27.65, 22.98, 14.41, and 14.37 ppm; FT-IR (KBr) 3068, 3046, 2949, 2927, 2852, 1655, 1638, 1625, 1559, 1544, 1489, 1459, 1436, 1294, 1261, 1228, 1094, 1053, 1020, 876, 801, 669, and 614 cm^{-1}; MS (MALDI-TOF) m/z = 1136.9008 $[M]^{+\cdot}$, 1136.5779 calcd for $C_{73}H_{88}N_2OS_4$.

(*E*)-2-Cyano-3-(5'''-(3',6'-di-*tert*-butyl-9-dodecyl-3,9'-bicarbazol]-6-yl)-3',3''-dihexyl-[2,2':5',2'':5'',2'''-quaterthiophen]-5-yl)acrylic acid (13)

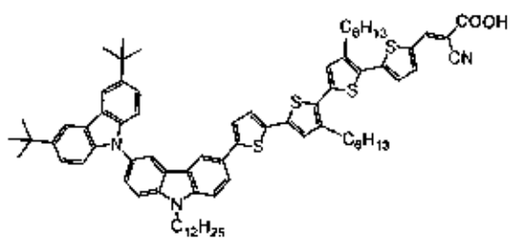

A mixture of **53** (0.11 g, 0.10 mmol) and cyanoacetic acid (0.04 g, 0.50 mmol) was vacuum-dried and added piperidine (0.07 ml, 0.70 mmol) in $CHCl_3$ (20 ml). The solution was refluxed for 6 h. After cooling the solution, the organic layer was removed in vacuo. The pure product was obtained by column chromatography over silica gel eluting with a mixture of MeOH and EtOAc (1:9) followed by recrystallization with a mixture of CH_2Cl_2 and methanol afforded **13** (0.05 g, 45%) as dark red solid; $C_{76}H_{89}N_3O_2S_4$; m.p. 87-88 °C; ^{1}H-NMR (500 MHz, $CDCl_3$/DMSO-d6) δ 8.22-8.18 (4H, m), 7.68-7.55 (3H, m), 7.46-7.45 (3H, m), 7.35-7.33 (3H, m), 7.20-7.16 (3H, m), 7.08-7.03 (2H, m), 6.99-6.92 (3H, m), 4.30 (2H, m), 3.66-3.59 (2H, m), 2.90-2.59 (4H, m), 2.41-2.26 (4H, m), 1.65-1.09 (56H, m), and 0.88-0.84 (9H, m) ppm; ^{13}C-NMR (125 MHz, $CDCl_3$/DMSO-d6) δ 176.07, 144.39, 142.44, 140.88, 140.55, 140.10, 139.65, 137.20, 136.86, 136.04, 135.67, 135.18, 134.98, 129.61, 129.42, 129.20, 128.73, 128.53, 127.65, 127.59, 127.55, 127.50, 126.17, 125.19, 124.63, 124.29, 123.89, 123.47, 122.98, 122.85, 122.65, 121.03, 120.88, 119.04, 117.45, 116.26, 116.11, 114.86, 114.74, 109.82, 109.38, 109.13, 47.86, 43.39, 37.41, 37.36, 37.01, 36.07, 34.67, 34.32, 34.16, 33.62, 33.00, 32.66, 32.02, 31.96, 31.84, 29.95, 29.61, 29.51, 29.45, 29.42, 29.33, 29.27, 29.26, 29.22, 29.20, 29.14, 29.07, 29.01, 27.25, 27.00, 24.92, 24.24, 22.61, 19.69, and 14.07 ppm; FT-IR (KBr) 3393, 3055, 2954, 2924, 2853, 2211, 1714, 1583, 1483, 1465, 1434, 1364, 1262, 1211, 972, 878, 810, 718, and 610 cm^{-1}; MS (MALDI-TOF) m/z = 1203.6244 $[M]^{+\cdot}$, 1203.5838 calcd for $C_{76}H_{89}N_3O_2S_4$.

Chapter 6:

5-(5-(3',6'-Di-*tert*-butyl-9-dodecyl-3,9'-bicarbazol]-6-yl)thiophen-2-yl)furan-2-carbaldehyde (56)

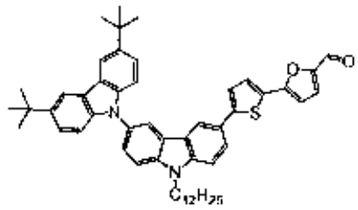

A mixture of **50** (0.54 g, 0.70 mmol), (5-formylfuran-2-yl)boronic acid (0.12 g, 0.83 mmol), $Pd(PPh_3)_4$ (0.03 g, 0.03 mmol), and 2 M Na_2CO_3 aqueous solution (7 ml, 14 mmol) in THF (20 ml) was degassed with N_2 for 5 min. The reaction mixture was stirred at reflux under N_2 for 24 h. After being cooled to room temperature, water (30 ml) was added and extracted with CH_2Cl_2 (30 ml x 3). The combined organic phases were washed with water (30 ml) and brine solution (30 ml), dried over anhydrous Na_2SO_4, filtered, and the solvents were removed to dryness. Purification by column chromatography over silica gel eluting with a mixture of CH_2Cl_2 and hexane (2:3) followed by recrystallization with a mixture of CH_2Cl_2 and methanol afforded **56** (0.35 g, 63%) as green solid; $C_{53}H_{60}N_2O_2S$; m.p. 209-210 °C; ^{1}H-NMR (300 MHz, $CDCl_3$) δ 9.60 (1H, s), 8.29 (1H, s), 8.26 (1H, s), 7.77 (1H, dd, J = 9.0 Hz, J = 1.6 Hz), 7.63 (1H, dd, J = 8.4 Hz, J = 1.8 Hz), 7.57 (1H, d, J = 8.7 Hz), 7.50-7.46 (4H, m), 7.36-7.25 (4H, m), 6.64 (1H, d, J = 3.9 Hz), 4.38 (2H, t, J = 6.9 Hz), 1.97 (2H, quin, J = 6.6 Hz), 1.54-1.26 (36H, m), and 0.87 (3H, t, J = 6.6 Hz) ppm; ^{13}C-NMR (75 MHz, $CDCl_3$) δ 176.92, 155.30, 151.72, 148.29, 142.82, 141.32, 140.52, 140.11, 130.25, 140.52, 14.11, 130.25, 129.69, 127.67, 125.83, 125.31, 124.87, 123.85, 123.79, 123.41, 123.38, 123.32, 119.56, 118.31, 116.48, 110.19, 109.84, 109.43, 107.41, 43.85, 35.02, 32.35, 32.18, 29.88, 28.85, 29.79, 29.68, 29.60, 29.37, 27.62, 22.95, and 14.36 ppm; FT-IR (KBr) 3055, 2957, 2922, 2847, 2812, 1662, 1586, 1538, 1480, 1361, 1290, 1262, 1023, 880, 806, 794, and 760 cm^{-1}; MS (MALDI-TOF) m/z = 788.6293 $[M]^{+\cdot}$, 788.4375 calcd for $C_{53}H_{60}N_2O_2S$.

(*E*)-2-Cyano-3-(5-(5-(3',6'-di-*tert*-butyl-9-dodecyl-3,9'-bicarbazol]-6-yl)thiophen-2-yl)furan-2-yl)acrylic acid (14)

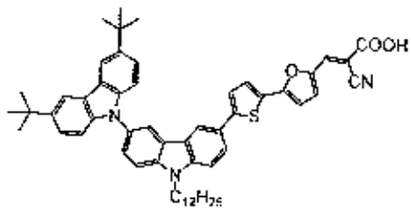

A mixture of **56** (0.18 g, 0.23 mmol) and cyanoacetic acid (0.10 g, 1.14 mmol) was vacuum-dried and added piperidine (0.14 ml, 1.60 mmol) in CHCl3 (20 ml). The solution was refluxed for 6 h. After cooling the solution, the organic layer was removed in vacuo. The pure product was obtained by column chromatography over silica gel eluting with a mixture of MeOH and EtOAc (1:9) followed by recrystallization with a mixture of CH_2Cl_2 and methanol afforded **14** (0.13 g, 65%) as red solid; $C_{56}H_{61}N_3O_3S$; ^{1}H-NMR (300 MHz, $CDCl_3$) δ 8.25 (2H, s), 8.19 (2H, s), 7.89 (1H, s), 7.75 (1H, d, J = 8.1 Hz), 7.63-7.52 (3H, m), 7.35-7.29 (4H, m), 7.68 (1H, d, J = 3.6 Hz), 5.42 (1H, s, br), 4.33 (2H, m), 1.93 (2H, m), 1.48-1.25 (36H, m), and 0.87-0.84 (3H, m) ppm; ^{13}C-NMR (75 MHz, $CDCl_3$) δ 176.44, 156.43, 149.34, 147.47, 142.82, 141.39, 140.52, 140.08, 130.26, 129.19, 129.04, 125.83, 125.16, 124.97, 123.80, 123.41, 123.33, 119.60, 118.29, 116.49, 116.03, 110.19, 109.84, 109.44, 43.82, 35.02, 32.35, 32.17, 29.88, 29.80, 29.68, 29.60, 29.35, 28.04, 27.61, 23.42, 22.94, and 14.36 ppm; FT-IR (KBr) 3411, 3046, 2953, 2924, 2852, 2219, 1693, 1604, 1557, 1487, 1434, 1387, 1363, 1293, 1258, 1234, 1191, 1026, 967, 921, 876, 801, 762, 742, 703, and 658 cm^{-1}; MS (MALDI-TOF) m/z = 855.4319 $[M]^{+\cdot}$, 855.4434 calcd for $C_{56}H_{61}N_3O_3S$.

3,6-Di-*tert*-butyl-9-(9-dodecyl-3-(5-(thiophen-2-yl)thiophen-2-yl)carbazol-6-yl) carbazole (54)

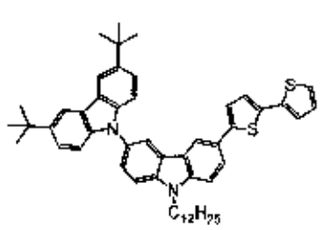

To a stirred solution of bromo compound (**50**) (2.87 g, 3.71 mmol) and $Pd(PPh_3)_4$ (0.10 g, 0.09 mmol) in tetrahydrofuran (55 mL) were added 2-thiophene-broronic acid (0.32 g, 2.47 mmol), and an aqueous Na_2CO_3 solution (7.87 g, 74.22 mmol). The mixture was refluxed for 48 h. After cooling the solution, H_2O (50 ml) was added to the solution and extracted by dichloromethane (50 ml x 3). The organic layer was separated and dried in Na_2SO_4. The solvent was removed in vacuo. The pure product was obtained by silica gel chromatography using a mixture of methylene chloride and *n*-hexane (1:4) as an eluent a pale yellow solids (2.31 g, 80%). mp: 142 C, ^{1}H NMR (300 MHz, $CDCl_3$): δ 8.27 (2H, s), 8.20 (2H, s), 7.78 (1H, d, J = 8.40 Hz), 7.60 (2H, q), 7.49-7.46 (3H, m), 7.36 (2H, d, J = 8.4 Hz), 7.27-7.16 (3H, m), 7.03 (1H, t, J = 3.9 Hz), 4.39 (2H, t, J = 7.20 Hz), 1.97 (2H, t, J = 6.90 Hz), 1.50-1.27 (36H, m) and 0.89 (3H, t, J = 6.90 Hz) ppm; ^{13}C NMR (300 MHz, $CDCl_3$) 144.35, 142.46, 140.68, 140.28, 139.81, 137.73, 135.62, 129.74, 127.81, 125.71, 125.39, 124.68, 124.50, 124.02, 123.64, 123.50, 123.29, 123.08, 123.03, 122.66, 119.34, 117.73, 116.19, 109.81, 109.41, 109.19, 43.55, 34.75, 32.08, 31.92, 29.63, 29.60, 29.54, 29.43, 29.35, 29.12, 27.36, 22.69 and 14.12 ppm; MS (APCI +MS) m/z = 777.4290 $[M+H]^+$, 776.4198 calcd for $C_{52}H_{60}N_2S_2$.

3,6-Di-*tert*-butyl-9-(3-(5-(5-bromothiophen-2-yl)thiophen-2-yl)-9-dodecyl-carbazol-6-yl)carbazole (55)

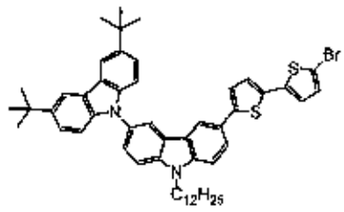

In a flask, covered with aluminum foil, stirred solution of 3,6-di-*tert*-butyl(9-dodecyl-3-(5-(thiophen-2-yl)thiophen-2-yl)carbazol-6-yl)carbazole (**54**) (2.29 g, 2.95 mmol) in THF (30 ml) was added NBS (0.55 g, 3.09 mmol), was added in small portions. The mixture was allowed to warm to room temperature for 3 h. Water (50 ml) was added and the mixture was extracted with methylene chloride (50 ml x 3). The organic layer was separated and dried in Na_2SO_4. The solvent was removed in vacuum. Purification by column chromatographyl over silica gel eluting with a mixture of methylene chloride and n-hexane (1:3) followed by recrystallization with a mixture of

methylene chloride and methanol afforded green solid (1.99 g, 79%). mp: 234 °C, ^{1}H NMR (300 MHz, $CDCl_3$): δ 8.24 (2H, s), 8.17 (2H, s), 7.74 (1H, d, J = 5.58 Hz), 7.59-7.57 (2H, m), 7.47 (3H, d, J = 8.60 Hz), 7.33 (3H, d, J = 8.60 Hz), 7.21-(1H, d, J = 3.72 Hz), 7.10 (1H, d, J = 3.72 Hz), 6.97-6.90 (2H, q), 4.37 (2H, t, J = 7.20 Hz), 1.98 (2H, t, J = 6.90 Hz), 1.57-1.27 (36H, m) and 0.85 (3H, t, J = 6.90 Hz) ppm; ^{13}C NMR (300 MHz, $CDCl_3$): 144.90, 142.48, 140.75, 140.26, 139.81, 139.22, 134.50, 130.64, 129.78, 125.45, 124.95, 124.50, 123.59, 123.50, 123.30, 123.08, 122.69, 119.34, 117.79, 116.21, 110.48, 109.85, 109.45, 109.17, 43.55, 34.75, 32.08, 31.92, 30.92, 29.63, 29.60, 29.54, 29.43, 29.35, 29.11, 27.36, 22.70 and 14.12. MS (APCI+MS) m/z = 855.3364 $[M+H]^+$, 854.3303 calcd for $C_{52}H_{59}BrN_2S_2$.

5-(5'-(3',6'-Di-*tert*-butyl-9-dodecyl-3,9'-bicarbazol]-6-yl)-[2,2'-bithiophen]-5-yl)furan-2-carbaldehyde (57)

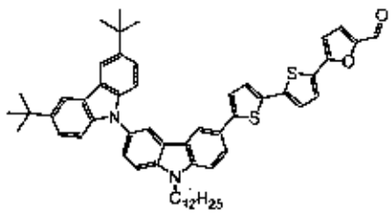

A mixture of **55** (0.93 g, 1.08 mmol), (5-formylfuran-2-yl)boronic acid (0.16 g, 1.17 mmol), $Pd(PPh_3)_4$ (0.05 g, 0.04 mmol), and 2 M Na_2CO_3 aqueous solution (11 ml, 22 mmol) in THF (30 ml) was degassed with N_2 for 5 min. The reaction mixture was stirred at reflux under N_2 for 24 h. After being cooled to room temperature, water (50 ml) was added and extracted with CH_2Cl_2 (50 ml x 3). The combined organic phases were washed with water (50 ml) and brine solution (70 ml), dried over anhydrous Na_2SO_4, filtered, and the solvents were removed to dryness. Purification by column chromatography over silica gel eluting with a mixture of CH_2Cl_2 and hexane (2:3) followed by recrystallization with a mixture of CH_2Cl_2 and methanol afforded **57** (0.67 g, 71%) as green solid; $C_{57}H_{62}N_2O_2S_2$; m.p. 164-165 °C; ^{1}H-NMR (300 MHz, $CDCl_3$) δ 9.70 (1H, s), 8.36 (2H, s), 8.29 (2H, s), 7.86 (1H, d, J = 5.0 Hz), 7.72 (1H, d, J = 10.0 Hz), 7.67 (1H, d, J = 10.0 Hz), 7.58-7.52 (4H, m), 7.45 (2H, d, J = 10.0 Hz), 7.38-7.36 (2H, m), 7.31 (1H, d, J = 5 Hz), 7.26 (1H, d, J = 2.5 Hz), 6.74 (1H, d, J = 5.0 Hz), 4.48 (2H, t, J = 7.5 Hz), 2.06 (2H, quin, J = 7.5 Hz), 1.67-1.36 (36H, m), and 0.97 (3H, t, J = 5.0 Hz) ppm; ^{13}C-NMR (75 MHz, $CDCl_3$) δ

176.71, 154.58, 151.52, 145.68, 142.51, 140.84, 140.26, 139.83, 127.14, 125.61, 124.52, 124.04, 123.53, 123.10, 122.93, 119.35, 116.24, 109.90, 109.52, 109.18, 107.52, 43.58, 34.77, 32.10, 31.94, 30.95, 29.65, 29.62, 29.56, 29.45, 29.37, 29.13, 27.38, 22.71, 20.72, 20.11, 17.67, 16.97, and 14.14 ppm; FT-IR (KBr) 3061, 2954, 2923, 2950, 1665, 1531, 1484, 1362, 1262, 1020, 879, 787, and 755 cm^{-1}; MS (MALDI-TOF) m/z = 870.7116 $[M]^{+}$, 870.4253 calcd for $C_{57}H_{62}N_2O_2S_2$.

(*E*)-2-Cyano-3-(5-(5'-(3',6'-di-*tert*-butyl-9-dodecyl-3,9'-bicarbazol]-6-yl)-[2,2'-bithiophen]-5-yl)furan-2-yl)acrylic acid (15)

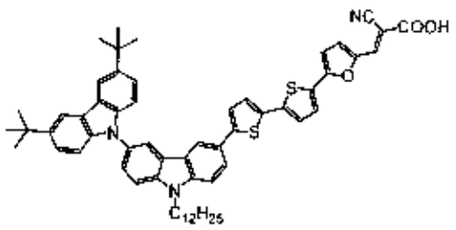

A mixture of **57** (0.25 g, 0.29 mmol) and cyanoacetic acid (1.22 g, 1.43 mmol) was vacuum-dried and added piperidine (0.20 ml, 2.01 mmol) in $CHCl_3$ (20 ml). The solution was refluxed for 6 h. After cooling the solution, the organic layer was removed in vacuo. The pure product was obtained by column chromatography over silica gel eluting with a mixture of MeOH and EtOAc (1:9) followed by recrystallization with a mixture of CH_2Cl_2 and methanol afforded **15** (0.15 g, 57%) as dark red solid; $C_{60}H_{63}N_3O_3S_2$; m.p. 176-177 °C; ^{1}H-NMR (300 MHz, $CDCl_3$) δ 8.23-8.19 (4H, m), 7.82 (1H, s), 7.69 (1H, d, J = 8.7 Hz), 7.59 (1H, dd, J = 8.4 Hz, J = 1.8 Hz), 7.52-7.45 (3H, m), 7.40-7.33 (4H, m), 7.25 (1H, s), 7.19-7.15 (2H, m), 7.08 (1H, d, J = 3.6 Hz), 6.60 (1H, d, J = 3.6 Hz), 4.28 (2H, t, J = 6.0 Hz), 3.61 (1H, s, br), 1.91 (2H, quin, J = 6.6 Hz), 1.48-1.24 (36H, m), and 0.86 (3H, t, J = 6.6 Hz) ppm; ^{13}C-NMR (75 MHz, $CDCl_3$) δ 167.63, 163.30, 155.51, 147.65, 146.03, 142.80, 141.03, 140.52, 140.01, 138.16, 134.63, 130.10, 129.20, 128.40, 126.05, 125.66, 125.54, 124.69, 124.50, 123.87, 123.40, 123.26, 123.12, 119.52, 117.90, 116.49, 116.16, 110.08, 109.70, 109.45, 96.07, 43.74, 35.02, 32.35, 32.17, 29.88, 29.80, 29.67, 29.60, 29.34, 27.60, 22.94, and 14.35 ppm; FT-IR (KBr) 3420, 3055, 2949, 2924, 2852, 2219, 1714, 1687, 1605, 1562, 1541, 1486, 1439, 1386, 1362, 1326, 1294, 1262, 1235, 1191, 1152, 1025, 922, 876,

788, 741, 692, and 658 cm^{-1}; MS (MALDI-TOF) *m/z* = 937.4232 $[M]^{+\cdot}$, 937.4311 calcd for $C_{60}H_{63}N_3O_3S_2$.

Chapter 7:

9-(7-(5-Bromothiophen-2-yl)-9,9-dihexylfluoren-2-yl)-3,6-di-*tert*-butylcarbazole (59)

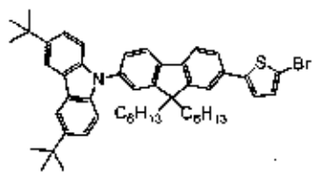

NBS (0.165 g, 0.927 mmol) was added in small portions to a stirred solution of 3,6-di-*tert*-butyl-9-(9,9-dihexyl-7-(thiophen-2-yl)fluoren-2-yl)carbazole (**58**) (0.63 g, 0.9mmol) in THF (20 ml). After being stirred at room temperature for 30 min, water was added. The mixture was extracted with dichloromethane (30 ml x 3). The combined organic phase was washed with water (50 ml), brine solution (50 ml), dried over anhydrous sodium sulfate, filtered and the solvent was remove in vacuum. Purification by short column chromatography using silica gel eluting with dichloromethane : hexane, 5:95 gave **59** as light yellow viscous (0.65 g, 94%); $C_{49}H_{58}BrNS$; m.p. 77-80 °C; ^{1}H-NMR (300 MHz, CDCl3) δ 8.18 (2H, s), 7.87 (1H, d, *J* = 8.7 Hz), 7.74 (1H, d, *J* = 7.8 Hz), 7.56-7.47 (6H, m), 7.39 (2H, d, *J* = 8.7 Hz), 7.15 (1H, d, *J* = 3.6 Hz), 7.07 (1H, d, *J* = 3.9 Hz), 2.04-21.98 (4H, m), 1.52 (18H, m), 1.19-1.11 (12H, m), and 0.82-0.77 (10H, m) ppm; ^{13}C-NMR (75 MHz, CDCl3) δ 152.64, 151.94, 146.54, 142.85, 140.41, 139.33, 139.22, 137.14, 132.63, 130.88, 125.44, 124.79, 123.56, 123.40, 123.09, 121.41, 120.81, 120.28, 119.91, 116.31, 111.14, 109.20, 55.50, 40.32, 34.75, 32.03, 31.51, 29.63, 23.88, 22.56, and 14.00 ppm; FT-IR (KBr) 3042, 2954, 2926, 2855, 1610, 1584, 1490, 1474, 1362, 1324, 1294, 1262, 1233, 1201, 877, 809, 790, 714, and 614 cm^{-1}; HRMS-ESI m/z = 772.3613 $[MH^+]$, 771.3473 calcd for $C_{49}H_{58}BrNS$.

4-(5-(7-(3,6-Di-*tert*-butylcarbazol-9-yl)-9,9-dihexylfluoren-2-yl)thiophen-2-yl)benzaldehyde (60)

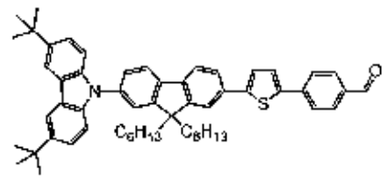

A mixture of **59** (0.40 g, 0.52 mmol), 4-formylphenylboronic acid (0.08 g, 0.56 mmol), $Pd(PPh_3)_4$ (0.01 g, 0.01 mmol), and 2 M Na_2CO_3 aqueous solution (5 ml, 10 mmol) in THF (50 ml) was degassed with N_2 for 5 min. The reaction mixture was stirred at reflux under N_2 for 24 h. After being cooled to room temperature, water (70 ml) was added and extracted with CH_2Cl_2 (70 ml x 3). The combined organic phases were washed with water (70 ml) and brine solution (70 ml), dried over anhydrous Na_2SO_4, filtered, and the solvents were removed to dryness. Purification by column chromatography over silica gel eluting with a mixture of CH_2Cl_2 and hexane (2:3) followed by recrystallization with a mixture of CH_2Cl_2 and methanol afforded **60** (0.22 g, 53%) as yellow solid; $C_{56}H_{63}NOS$; ^{1}H-NMR (300 MHz, $CDCl_3$) δ 10.02 (1H, s), 8.20 (1H, s), 8.17 (1H, s), 7.93 (3H, d, J = 7.8 Hz), 7.84-7.79 (2H, m), 7.72-7.65 (2H, m), 7.57-7.50 (3H, m), 7.45-7.41 (4H, m), 7.34-7.29 (2H, m), 2.08-2.03 (4H, m), 1.26-1.25 (22H, m), and 0.92-0.77 (18H, m) ppm; ^{13}C-NMR (75 MHz, $CDCl_3$) δ 191.36, 152.82, 152.00, 146.55, 141.53, 141.03, 140.48, 140.04, 139.74, 136.67, 135.07, 132.97, 130.54, 126.14, 125.93, 125.66, 125.00, 124.36, 123.42, 121.83, 120.96, 120.40, 120.07, 119.93, 66.68, 55.58, 40.32, 38.78, 34.43, 31.93, 31.50, 30.44, 29.70, 29.62, 29.36, 29.11, 28.94, 25.01, 23.91, 23.82, 22.98, 22.69, 22.54, 14.11, and 13.99 ppm; FT-IR (KBr) 3051, 2957, 2924, 2850, 2732, 1697, 1599, 1497, 1470, 1450, 13081230, 1167, 1118, 822, 800, 749, and 723 cm^{-1}.

(*E*)-2-Cyano-3-(4-(5-(7-(3,6-di-*tert*-butylcarbazol-9-yl)-9,9-dihexylfluoren-2-yl)thiophen-2-yl)phenyl)acrylic acid (16)

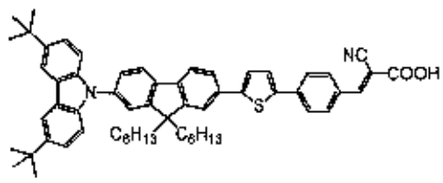

A mixture of **60** (0.22 g, 0.28 mmol) and cyanoacetic acid (0.12 g, 1.38 mmol) was vacuum-dried and added piperidine (0.19 ml, 1.93 mmol) in $CHCl_3$ (30 ml). The solution was refluxed for 6 h. After cooling the solution, the organic layer was removed in vacuo. The pure product was obtained by column chromatography over silica gel eluting with a mixture of MeOH and EtOAc (1:9) followed by recrystallization with a mixture of CH_2Cl_2 and methanol afforded **16** (0.11 g, 42%) as light orange solid; $C_{59}H_{64}N_2O_2S$; m.p. 224-225 °C; ^{1}H-NMR (300 MHz, $CDCl_3$/DMSO-d6) δ 8.04-7.97 (3H, m), 7.87-7.85 (2H, m), 7.77-7.74 (1H, m), 7.62 (3H, m), 7.53-7.47 (2H, m), 7.35 (3H, m), 7.26 (4H, m), 7.14-7.12 (2H, m), 1.88 (4H, m), and 1.07-0.93 (40H, m) ppm; ^{13}C-NMR (75 MHz, $CDCl_3$/DMSO-d6) δ 164.06, 153.28, 152.67, 151.80, 146.22, 141.33, 140.81, 140.28, 139.62, 138.48, 136.39, 132.80, 131.68, 130.30, 126.12, 125.85, 125.70, 125.55, 124.88, 124.40, 123.17, 121.56, 120.92, 120.36, 120.23, 119.16, 109.63, 102.80, 55.41, 40.79, 40.51, 40.23, 40.08, 39.96, 39.68, 39.40, 39.12, 31.30, 29.39, 23.73, 22.33, and 13.88 ppm; FT-IR (KBr) 3415, 3042, 2954, 2924, 2852, 2224, 1697, 1583, 1548, 1509,1496, 1473, 1451, 1421, 1334, 1281, 1231, 1186, 922, 803, 749, 723, and 678 cm^{-1}.

Chapter 8:

***N*-(4-Bromophenyl)-*N*-phenylnaphthalen-1-amine (62)**

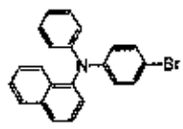

To a mixture of Cs_2CO_3 (45.62 g, 140.00 mmol), $Pd(OAc)_2$ (0.77 g, 3.42 mmol), PPh_3 (1.73 g, 6.61 mmol), and 1,4-dibromobenzene (8.07 g, 34.20 mmol) in toluene (60 mL) were added *N*-phenylnaphthalen-1-amine (**61**) (5 g, 22.80 mmol). The reaction mixture was stirred at 110 °C under nitrogen. After 24 h, water (100 ml) was added until the two phases mixed. The solution was extracted with CH_2Cl_2 (100 ml x 3), washed with water (100 ml), brine solution (100 ml) and dried with Na_2SO_4, filtered, and the solvents removed to dryness. After the solvent was evaporated. The crude product was purified by column chromatography on silica gel with hexane as eluent to yield *N*-(4-bromophenyl)-*N*-phenylnaphthalen-1-amine (**62**) (2.90 g, 34%) as light green viscous oil; $C_{22}H_{16}BrN$; ^{1}H-NMR (300 MHz, $CDCl_3$) δ 7.93 (2H, t, J = 7.9 Hz), 7.81

(1H, d, J = 8.1 Hz), 7.50 (2H, t, J = 7.8 Hz), 7.42-7.22 (6H, m), 7.09 (2H, d, J = 7.8 Hz), 7.00 (1H, t, J = 7.2 Hz), and 6.91 (2H, d, J = 8.7 Hz) ppm; ^{13}C-NMR (75 MHz, $CDCl_3$) δ 148.76, 143.88, 136.58, 132.33, 132.26, 132.02, 131.79, 131.58, 131.32, 131.28, 129.59, 129.34, 128.64, 127.66, 127.50, 127.21, 127.03, 126.88, 126.68, 126.60, 126.37, 124.71, 124.56, 124.31, 124.23, 124.22, 123.89, 122.94, 122.76, 122.64, 122.13, and 121.92 ppm; MS (MALDI-TOF) m/z = 373.2199 $[M]^{+\bullet}$, 373.0466 calcd for $C_{22}H_{16}BrN$.

5-(4-(Naphthalen-1-yl(phenyl)amino)phenyl)thiophene-2-carbaldehyde (63)

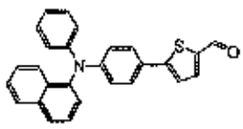

A mixture of **62** (0.10 g, 0.28 mmol), (5-formylthiophen-2-yl)boronic acid (0.05 g, 0.30 mmol), $Pd(PPh_3)_4$ (0.003 g, 0.003 mmol), and 2 M Na_2CO_3 aqueous solution (1.5 ml, 2.80 mmol) in THF (10 ml) was degassed with N_2 for 5 min. The reaction mixture was stirred at reflux under N_2 for 24 h. After being cooled to room temperature, water (70 ml) was added and extracted with CH_2Cl_2 (70 ml x 3). The combined organic phases were washed with water (70 ml) and brine solution (70 ml), dried over anhydrous Na_2SO_4, filtered, and the solvents were removed to dryness. Purification by column chromatography over silica gel eluting with a mixture of CH_2Cl_2 and hexane (2:3) followed by recrystallization with a mixture of CH_2Cl_2 and methanol afforded 5-(10-dodecylphenothiazin-3-yl)thiophene-2-carbaldehyde (**63**) (0.06 g, 50%) as green viscous oil; $C_{27}H_{19}NOS$; ^{1}H-NMR (300 MHz, $CDCl_3$) δ 9.34 (1H, s), 7.91 (2H, d, J = 8.7 Hz), 7.82 (1H, d, J = 8.0 Hz), 7.68 (1H, d, J = 3.9 Hz), 7.53-7.42 (4H, m), 7.41-7.35 (2H, m), 7.29-7.23 (3H, m), 7.15 (2H, d, J = 7.5 Hz), and 7.06-6.95 (3H, m) ppm; ^{13}C-NMR (75 MHz, $CDCl_3$) δ 182.88, 129.65, 128.82, 127.55, 126.65, 124.21, 123.60, 120.49, and 111.58 ppm; MS (MALDI-TOF) m/z = 405.3002 $[M]^{+\bullet}$, 405.1187 calcd for $C_{27}H_{19}NOS$.

(*E*)-2-Cyano-3-(5-(4-(naphthalen-1-yl(phenyl)amino)phenyl)thiophen-2-yl)acrylic acid (17)

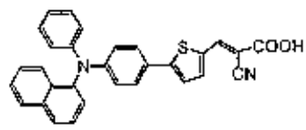

A mixture of **63** (0.27 g, 0.66 mmol) and cyanoacetic acid (0.14 g, 1.66 mmol) was vacuum-dried and added piperidine (0.20 ml, 1.99 mmol) in $CHCl_3$ (20 ml). The solution was refluxed for 6 h. After cooling the solution, the organic layer was removed in vacuo. The pure product was obtained by column chromatography over silica gel eluting with a mixture of MeOH and EtOAc (1:9) followed by recrystallization with a mixture of CH_2Cl_2 and methanol afforded **17** (0.14 g, 45%) as light orange solid; $C_{30}H_{20}N_2O_2S$; m.p. 257-258 °C; ^{1}H-NMR (500 MHz, $CDCl_3$/DMSO-d6) δ 8.25 (1H, s), 7.80-7.75 (2H, m), 7.69 (1H, m), 7.45 (1H, s), 7.40-7.35 (3H, m), 7.23-7.12 (6H, m), 6.97-6.92 (3H, m), 6.86 (1H, s), and 6.72 (2H, s) ppm; ^{13}C-NMR (125 MHz, $CDCl_3$/DMSO-d6) δ 163.32, 151.51, 148.78, 147.28, 144.81, 142.60, 137.67, 135.13, 134.67, 131.91, 130.87, 130.42, 129.18, 128.40, 127.16, 126.86, 126.86, 126.79, 126.50, 126.27, 126.18, 125.97, 125.68, 123.83, 122.80, 122.71, 122.62, 122.35, 120.34, 118.70, and 103.17 ppm; FT-IR (KBr) 3422, 3042, 2949, 2919, 2848, 2211, 1591, 1492, 1440, 1391, 1311, 935, 799, 774, 753, and 695 cm^{-1}; MS (MALDI-TOF) m/z = 472.3404 $[M]^{+\bullet}$, 472.1245 calcd for $C_{30}H_{20}N_2O_2S$.

2-Iodo-9,9-dioctylfluorene (1f)

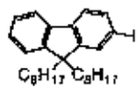

To a mixture of 2-iodofluorene (**34**) (10 g, 34.23 mmol) and tetrabutyl ammonium bromide(1g) in DMSO (100 ml) was added an aqueous NaOH solution (50% W/V, 6 ml) follow by 1-bromooctane (17 ml). After being stirred at room temperature for 3 h, the reaction mixture was extracted with ethyl acetate (100 mlx3). The combined organic phase was washed with water(100 ml), HCl solution(1 M, 50 ml), brine solution(100 ml), dried over sodium sulfate anhydrous, filtered and the organic phase was removed in vacuum. Purification by column chromatography using siliga gel eluent with hexane gave 2,7-dibromo-9,9-dioctylfluorene (**1f**) (14

g, 80%) as colourless viscous; $C_{29}H_{41}I$; ^{1}H-NMR (300 MHz, $CDCl_3$) δ 7.65 (3H, s), 7.44-7.31 (4H, m), 1.92 (4H, t, J = 5.7 Hz), 1.10-1.04 (21H, m), 0.84-0.80 (6H, m), and 0.59 (3H, s) ppm; ^{13}C-NMR (75 MHz, $CDCl_3$) δ 153.44, 150.38, 141.05, 140.36, 136.04, 132.31, 127.91, 127.17, 123.10, 121.67, 120.06, 92.74, 55.58, 40.50, 30.06, 20.22, 29.48, 23.94, 22.89, and 14.38 ppm; MS (MALDI-TOF) m/z = 516.4175 $[M]^{+\bullet}$, 516.2253 calcd for $C_{29}H_{41}I$.

_N_-(Naphthalen-1-yl)-9,9-dioctyl-_N_-phenylfluoren-2-amine (2f)

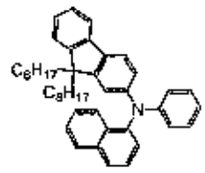

To a mixture of CuI (0.27 g, 1.44 mmol), KO^{t}Bu (0.48 g, 4.31 mmol), and 2-iodo-9,9-dioctylfluorene (**1f**) (1.86 g, 3.59 mmol) in toluene (50 mL) were added N-phenylnaphthalen-1-amine (0.63 g, 2.87 mmol) and (±)-*trans*-1,2-diaminocyclohexane (0.20 g, 1.72 mmol). The reaction mixture was stirred at 110 °C under nitrogen. After 24 h, water (100 ml) was added until the two phases mixed. The solution was extracted with CH_2Cl_2 (100 ml x 3), washed with water (100 ml), brine solution (100 ml) and dried with Na_2SO_4, filtered, and the solvents removed to dryness. After the solvent was evaporated. The crude product was purified by column chromatography on silica gel with hexane as eluent to yield *N*-(naphthalen-1-yl)-9,9-dioctyl-*N*-phenylfluoren-2-amine (**2f**) (1.13 g, 65%) as light white viscous oil; $C_{45}H_{53}N$; ^{1}H-NMR (300 MHz, $CDCl_3$) δ 8.00 (1H, d, J = 8.4 Hz), 7.93 (1H, d, J = 8.1 Hz), 7.81 (1H, d, J = 8.1 Hz), 7.62 (1H, d, J = 7.5 Hz), 7.55-7.45 (3H, m), 7.41-7.23 (5H, m), 7.17-7.10 (3H, m), 7.01-6.97 (2H, m), 1.96-1.77 (4H, m), 1.31-1.08 (20H, m), 0.91 (6H, t, J = 6.9 Hz), and 0.68 (4H, m) ppm; ^{13}C-NMR (75 MHz, $CDCl_3$) δ 152.05, 150.60, 149.04, 147.96, 144.05, 141.10, 135.57, 135.43, 131.08, 129.13, 128.46, 126.78, 126.36, 126.24, 126.17, 126.11, 124.54, 122.69, 121.74, 121.56, 121.47, 120.35, 119.04, 117.33, 55.03, 40.37, 31.94, 30.11, 30.01, 29.37, 23.90, 22.74, and 14.23 ppm; FT-IR (KBr) 3058, 3010, 2957, 2924, 2854, 1594, 1490, 1450, 1392, 1275, 771, 739, and 694 cm^{-1}; MS (MALDI-TOF) m/z = 607.5945 $[M]^{+\bullet}$, 607.4178 calcd for $C_{45}H_{53}N$.

_N_-(4-Bromophenyl)-_N_-(naphthalen-1-yl)-9,9-dioctylfluoren-2-amine (3f)

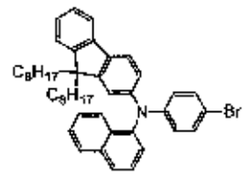

NBS (0.14 g, 0.81 mmol) was added in small portions to a stirred solution of _N_-(naphthalen-1-yl)-9,9-dioctyl-_N_-phenylfluoren-2-amine (**2f**) (0.50 g, 0.82 mmol) in THF (20 ml). After being stirred at 0°C for 30 min, water was added. The mixture was extracted with dichloromethane (30 ml x 3). The combined organic phase was washed with water (50 ml), brine solution (50 ml), dried over anhydrous sodium sulfate, filtered and the solvent was remove in vacuum. Purification by short column chromatography using silica gel eluting with dichloromethane : hexane, 5:95 gave **3f** as light white viscous (0.38 g, 67%); $C_{45}H_{52}BrN$; ^{1}H-NMR (300 MHz, $CDCl_3$) δ 8.26 (1H, d, J = 8.7 Hz), 7.97 (1H, d, J = 8.4 Hz), 7.75 (1H, d, J = 7.8 Hz), 7.58-7.47 (3H, m), 6.92 (1H, dd, J = 8.1 Hz, J = 1.8 Hz), 1.89-1.70 (4H, m), 1.26-1.01 (10H, m), 0.84 (6H, t, J = 6.9 Hz), and 0.62-0.59 (4H, m) ppm; ^{13}C-NMR (75 MHz, $CDCl_3$) δ 152.43, 150.83, 149.07, 147.93, 144.41, 141.18, 136.11, 133.80, 132.42, 130.62, 129.44, 128.06, 127.75, 127.27, 127.15, 127.01, 126.51, 125.29, 122.95, 122.21, 122.12, 121.84, 120.61, 120.26, 119.31, 117.63, 55.30, 40.53, 32.14, 30.29, 30.01, 29.56, 24.11, 22.34, and 14.40 ppm; MS (MALDI-TOF) m/z = 685.4203 $[M]^{+\cdot}$, 685.3283 calcd for $C_{45}H_{52}BrN$.

5-(4-((9,9-Dioctylfluoren-2-yl)(naphthalen-1-yl)amino)phenyl)thiophene-2-carbaldehyde (4f)

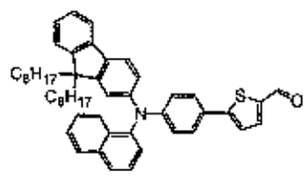

A mixture of **3f** (0.40 g, 0.58 mmol), (5-formylthiophen-2-yl)boronic acid (0.06 g, 0.39 mmol), $Pd(PPh_3)_4$ (0.004 g, 0.004 mmol), and 2 M Na_2CO_3 aqueous solution (4 ml, 7.76 mmol) in THF (50 ml) was degassed with N_2 for 5 min. The reaction mixture was stirred at reflux

under N_2 for 24 h. After being cooled to room temperature, water (70 ml) was added and extracted with CH_2Cl_2 (70 ml x 3). The combined organic phases were washed with water (70 ml) and brine solution (70 ml), dried over anhydrous Na_2SO_4, filtered, and the solvents were removed to dryness. Purification by column chromatography over silica gel eluting with a mixture of CH_2Cl_2 and hexane (2:3) followed by recrystallization with a mixture of CH_2Cl_2 and methanol afforded 5-(4-((9,9-dioctylfluoren-2-yl)(naphthalen-1-yl)amino)phenyl)thiophene-2-carbaldehyde **(4f)** (0.25 g, 60%) as yellow viscous; $C_{50}H_{55}NOS$; ^{1}H-NMR (300 MHz, $CDCl_3$) δ 9.84 (1H, s), 7.91 (2H, d, J = 8.7 Hz), 7.82 (1H, d, J = 6.9 Hz), and 0.63-0.61 (4H, m) ppm; ^{13}C-NMR (75 MHz, $CDCl_3$) δ 182.83, 155.08, 152.44, 150.87, 150.30, 146.80, 143.16, 141.34, 138.01, 137.01, 128.81, 127.50, 127.20, 127.03, 126.74, 126.58, 126.53, 124.31, 122.96, 122.84, 120.76, 120.54, 55.31, 40.46, 32.12, 30.24, 29.97, 29.54, 24.09, 22.91, and 14.38 ppm; MS (MALDI-TOF) m/z = 717.4633 $[M]^{+\cdot}$, 717.4004 calcd for $C_{50}H_{55}NOS$.

(*E*)-2-Cyano-3-(5-(4-((9,9-dioctylfluoren-2-yl)(naphthalen-1-yl)amino)phenyl) thiophen-2-yl)acrylic acid (18)

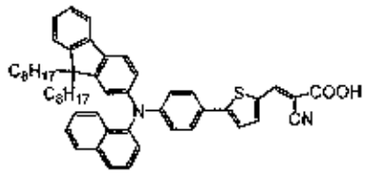

A mixture of **4f** (0.10 g, 0.15 mmol) and cyanoacetic acid (0.02 g, 0.29 mmol) was vacuum-dried and added piperidine (0.044 ml, 0.44 mmol) in $CHCl_3$ (20 ml). The solution was refluxed for 6 h. After cooling the solution, the organic layer was removed in vacuo. The pure product was obtained by column chromatography over silica gel eluting with a mixture of MeOH and EtOAc (1:9) followed by recrystallization with a mixture of CH_2Cl_2 and methanol afforded **18** (0.06 g, 56%) as dark orange solid; $C_{53}H_{56}N_2O_2S$; m.p. 238-239 °C; ^{1}H-NMR (300 MHz, $CDCl_3$/DMSO-d6) δ 8.47 (1H, s), 8.25-8.06 (1H, m), 7.92-7.89 (1H, m), 7.72-7.69 (1H, m), 7.44-6.71 (16H, m), 2.38 (1H, m), 1.77 (4H, m), and 1.26-0.60 (30H, m) ppm; ^{13}C-NMR (75 MHz, $CDCl_3$/DMSO-d6) δ 166.82, 152.88, 152.30, 151.72, 150.75, 149.09, 148.71, 148.48, 147.81, 147.15, 145.44, 144.14, 142.42, 141.14, 136.86, 136.07, 135.36, 134.83, 133.78, 133.16, 132.37, 131.21, 130.57, 129.44, 129.33, 129.12, 128.07, 127.73, 127.27, 126.95, 126.40, 125.81, 125.13,

122.88, 122.41, 122.15, 121.99, 120.61, 120.41, 119.28, 117.59, 103.50, 40.48, 31.99, 30.08, 29.47, 24.10, 22.80, and 14.26 ppm; FT-IR (KBr) 3428, 3039, 3024, 2949, 2924, 2853, 2207, 1715, 1610, 1594, 1584, 1492, 1450, 1377, 1338, 1272, 1246, 935, 808, 760, 740, and 695 cm^{-1}; MS (MALDI-TOF) m/z = 784.2891 $[M]^{+\cdot}$, 784.4062 calcd for $C_{53}H_{56}N_2O_2S$.

3-Iodo-9-octylcarbazole (1g)

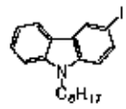

To a solution of 3-iodocarbazole (**26**) (16.10 g, 54.33 mmol) in DMF (100 ml) was added followed by NaH (2.64 g, 109.86 mmol). 1-Bromooctane (13.79 g, 71.41 mmol) was added. The reaction mixture was stirred at room temperature for 3 h. Water (100 ml) was added and the mixture was extracted with methylene chloride (100 ml x 3). The combined organic phases were washed with a dilute HCl solution (100 ml x 2), water (100 ml), and brine solution (100 ml), dried over anhydrous Na_2SO_4, filtered and the solvents were removed to dryness. Purification by column chromatography over silica gel eluting with hexane gave a colorless viscous oil (17.60 g, 80%); $C_{20}H_{24}IN$; ^{1}H-NMR (300 MHz, $CDCl_3$) δ 8.38 (1H, s), 8.01 (2H, d, J = 7.2 Hz), 7.68 (2H, d, J = 8.4 Hz), 7.46 (1H, t, J = 7.2 Hz), 7.37 (1H, d, J = 8.1 Hz), 7.23 (1H, d, J = 5.7 Hz), 7.17 (1H, t, J = 7.0 Hz), 4.23 (2H, t, J = 7.0 Hz), 1.82 (2H, t, J = 5.7 Hz), 1.30-1.23 (10H, m), and 0.85 (3H, t, J = 5.4 Hz) ppm; ^{13}C-NMR (75 MHz, $CDCl_3$) δ 134.02, 129.46, 126.57, 120.77, 119.53, 111.00, 109.13, 43.44, 32.04, 29.61, 29.42, 29.16, 27.54, 22.87, and 14.33 ppm; MS (MALDI-TOF) m/z = 405.3305 $[M]^{+\cdot}$, 405.0953 calcd for $C_{20}H_{24}IN$.

***N*-(Naphthalen-1-yl)-9-octyl-*N*-phenylcarbazol-3-amine (2g)**

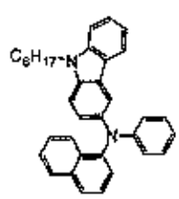

To a mixture of CuI (0.77 g, 4.07 mmol), KO^{t}Bu (1.37 g, 12.22 mmol), and 3-iodo-9-octylcarbazole (**1g**) (4.51 g, 10.18 mmol) in toluene (60 mL) were added *N*-phenylnaphthalen-1-amine (1.79 g, 8.14 mmol) and (±)-*trans*-1,2-diaminocyclohexane (0.65 ml, 4.89 mmol). The reaction mixture was stirred at 110 °C under nitrogen. After 24 h, water (100 ml) was added until the two phases mixed. The solution was extracted with CH_2Cl_2 (100 ml x 3), washed with water (100 ml), brine solution (100 ml) and dried with Na_2SO_4, filtered, and the solvents removed to dryness. After the solvent was evaporated. The crude product was purified by column chromatography on silica gel with hexane as eluent to yield *N*-(naphthalen-1-yl)-9-octyl-*N*-phenylcarbazol-3-amine (**2g**) (3.08 g, 61%) as colorless viscous; $C_{36}H_{36}N_2$; ^{1}H-NMR (300 MHz, $CDCl_3$) δ 8.09 (1H, d, J = 8.1 Hz), 7.92-7.83 (3H, m), 7.70 (1H, d, J = 7.5 Hz), 7.44-7.10 (11H, m), 6.89-6.82 (3H, m), 4.20 (2H, t, J = 7.0 Hz), 1.83 (2H, quin, J = 6.4 Hz), 1.32-1.23 (10H, m), and 0.89-0.83 (3H, m) ppm; ^{13}C-NMR (75 MHz, $CDCl_3$) δ 150.49, 144.83, 141.29, 140.82, 137.62, 135.65, 131.50, 129.09, 126.02, 124.99, 124.26, 123.86, 122.87, 120.84, 120.14, 119.83, 118.89, 117.13, 43.51, 32.11, 29.68, 29.48, 29.35, 27.64, 22.92, and 14.38 ppm; MS (MALDI-TOF) m/z = 496.4930 $[M]^{+\cdot}$, 496.2878 calcd for $C_{36}H_{36}N_2$.

_N_-(4-Bromophenyl)-_N_-(naphthalen-1-yl)-9-octylcarbazol-3-amine (3g)

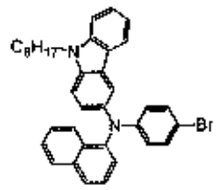

NBS (0.10 g, 0.56 mmol) was added in small portions to a stirred solution of *N*-(naphthalen-1-yl)-9-octyl-*N*-phenylcarbazol-3-amine (**2g**) (0.28 g, 0.56 mmol) in THF (20 ml). After being stirred at room temperature for 30 min, water was added. The mixture was extracted with dichloromethane (30 ml x 3). The combined organic phase was washed with water (50 ml), brine solution (50 ml), dried over anhydrous sodium sulfate, filtered and the solvent was remove in vacuum. Purification by short column chromatography using silica gel eluting with dichloromethane : hexane, 5:95 gave **3g** as light yellow viscous (0.20 g, 63%); $C_{36}H_{35}BrN_2$; ^{1}H-NMR (300 MHz, $CDCl_3$) δ 8.27-8.03 (2H, m), 7.90-7.85 (2H, m), 7.72 (1H, d, J =7.8 Hz),

7.55-7.09 (11H, m), 6.87 (1H, d, J = 7.5 Hz), 6.71 (1H, dd, J = 8.1 Hz, J = 1.8 Hz), 4.21 (2H, t, J = 6.7 Hz), 1.83 (2H, quin, J = 5.7 Hz), 1.33-1.24 (10H, m), and 0.85 (3H, t, J = 6.3 Hz) ppm; ^{13}C-NMR (75 MHz, $CDCl_3$) δ 150.23, 149.51, 144.16, 141.27, 140.11, 137.83, 132.05, 130.72, 129.32, 127.25, 127.04, 126.72, 126.47, 126.16, 125.51, 124.71, 124.25, 123.87, 120.94, 120.84, 120.15, 119.01, 117.35, 111.99, 109.76, 109.10, 43.52, 32.11, 29.69, 29.49, 29.35, 27.64, 22.93, and 14.41 ppm; MS (MALDI-TOF) m/z = 574.3701 $[M]^{+\cdot}$, 574.1984 calcd for $C_{36}H_{35}BrN_2$.

5-(4-(Naphthalen-1-yl(9-octylcarbazol-3-yl)amino)phenyl)thiophene-2-carbaldehyde (4g)

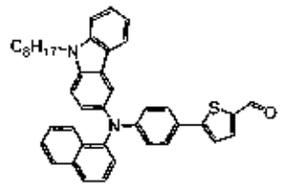

A mixture of **3g** (1.00 g, 1.74 mmol), (5-formylthiophen-2-yl)boronic acid (0.27 g, 1.74 mmol), $Pd(PPh_3)_4$ (0.02 g, 0.02 mmol), and 2 M Na_2CO_3 aqueous solution (17 ml, 34 mmol) in THF (50 ml) was degassed with N_2 for 5 min. The reaction mixture was stirred at reflux under N_2 for 24 h. After being cooled to room temperature, water (70 ml) was added and extracted with CH_2Cl_2 (70 ml x 3). The combined organic phases were washed with water (70 ml) and brine solution (70 ml), dried over anhydrous Na_2SO_4, filtered, and the solvents were removed to dryness. Purification by column chromatography over silica gel eluting with a mixture of CH_2Cl_2 and hexane (2:3) followed by recrystallization with a mixture of CH_2Cl_2 and methanol afforded 5-(4-(naphthalen-1-yl(9-octylcarbazol-3-yl)amino)phenyl)thiophene-2-carbaldehyde (**4g**) (0.65 g, 62%) as yellow viscous oil; $C_{41}H_{38}N_2OS$; ^{1}H-NMR (300 MHz, $CDCl_3$) δ 9.96 (1H, s), 8.19 (2H, d, J = 8.4 Hz), 7.93 (2H, d, J = 6.3 Hz), 7.84 (1H, t, J = 3.6 Hz), 7.57-7.31 (9H, m), 7.21-7.12 (3H, m), 6.94-6.87 (3H, m), 4.26 (2H, t, J = 7.3 Hz), 1.86 (2H, quin, J = 7.0 Hz), 1.35-1.26 (10H, m), and 0.86 (3H, t, J = 6.4 Hz) ppm; ^{13}C-NMR (75 MHz, $CDCl_3$) δ 183.09, 152.90, 150.28, 146.58, 143.71, 141.50, 140.65, 137.80, 136.83, 133.24, 131.35, 129.30, 128.91, 127.32, 126.72, 126.11, 125.94, 125.84, 125.69, 124.36, 123.93, 122.76, 120.83, 120.60, 118.96, 117.43, 109.71, 109.07, 43.53, 32.05, 29.98, 29.64, 29.45, 29.32, 27.62, 22.88, and 14.33 ppm; MS (MALDI-TOF) m/z = 606.4253 $[M]^{+\cdot}$, 606.2705 calcd for $C_{41}H_{38}N_2OS$.

(*E*)-2-Cyano-3-(5-(4-(naphthalen-1-yl(9-octylcarbazol-3-yl)amino)phenyl) thiaphen-2-yl)acrylic acid (19)

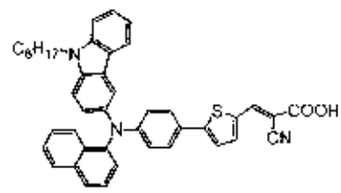

A mixture of **4g** (0.15 g, 0.25 mmol) and cyanoacetic acid (0.10 g, 1.24 mmol) was vacuum-dried and added piperidine (0.15 ml, 1.73 mmol) in $CHCl_3$ (20 ml). The solution was refluxed for 6 h. After cooling the solution, the organic layer was removed in vacuo. The pure product was obtained by column chromatography over silica gel eluting with a mixture of MeOH and EtOAc (1:9) followed by recrystallization with a mixture of CH_2Cl_2 and methanol afforded **19** (0.10 g, 60%) as light green solid; $C_{44}H_{39}N_3O_2S$; m.p. 149-150 °C; ^{1}H-NMR (300 MHz, $CDCl_3$/DMSO-d6) δ 8.46 (1H, s), 8.05-7.98 (2H, m), 7.79-7.71 (2H, m), 7.34-7.22 (3H, m), 7.10-7.02 (10H, m), 6.78 (3H, d, J = 7.8 Hz), 4.12 (2H, m), 1.76 (2H, m), 1.26-1.20 (10H, m), and 0.82 (3H, m) ppm; ^{13}C-NMR (75 MHz, $CDCl_3$/DMSO-d6) δ 169.49, 150.12, 149.65, 145.84, 141.18, 140.56, 137.54, 137.09, 133.11, 131.17, 129.15, 128.75, 128.61, 127.08, 126.42, 126.04, 125.92, 125.72, 124.07, 123.74, 122.69, 120.73, 120.48, 118.83, 116.92, 109.56, 108.90, 43.34, 40.88, 40.60, 40.32, 40.04, 39.77, 31.92, 29.85, 29.49, 29.30, 29.16, 27.45, 22.73, and 14.19 ppm; FT-IR (KBr) 3421, 3046, 2922, 2848, 2210, 1597, 1573, 1489, 1463, 1445, 1318, 1274, 1226, 930, 875, 691, 764, and 745 cm^{-1}; MS (MALDI-TOF) m/z = 673.3036 $[M]^{+\cdot}$, 673.2763 calcd for $C_{44}H_{39}N_3O_2S$.

10-Octylphenothiazine (64)

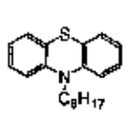

To a mixture of phenothiazine (**35**) (10 g, 50.18 mmol) and tetrabutyl ammonium bromide (1g) in DMSO (100 ml) was added an aqueous NaOH solution (50% W/V, 6 ml) follow by 1-bromooctane (10 ml). After being stirred at room temperature for 3 h, the reaction mixture

was extracted with ethyl acetate (100 mlx3). The combined organic phase was washed with water(100 ml), HCl solution(1 M, 50 ml), brine solution(100 ml), dried over sodium sulfate anhydrous, filtered and the organic phase was removed in vacuum. Purification by column chromatography using siliga gel eluent with hexane gave 10-octylphenothiazine (**64**) (14 g, 90%) as colourless viscous; $C_{20}H_{25}NS$; ^{1}H-NMR (300 MHz, $CDCl_3$) δ 7.18-7.09 (4H, m), 6.90-6.82 (4H, m), 3.81 (2H, t, J = 7.0 Hz), 1.78 (2H, quin, J = 6.8 Hz), 1.41-1.26 (10H, m), and 0.86 (3H, t, J = 6.4 Hz) ppm; ^{13}C-NMR (75 MHz, $CDCl_3$) δ 145.63, 127.69, 127.43, 125.23, 122.57, 115.66, 47.72, 32.04, 29.51, 27.26, 22.91, and 14.37 ppm.

3-Iodo-10-octylphenothiazine (1h)

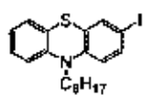

Two-necked flask equipped with a reflux condenser and a magnetic stirring bar is charged with (15.55 g, 47.77 mmol) of 10-octylphenothiazine (**64**), (2.32 g, 10.16 mmol) of periodic acid dehydrate and (20.33 g, 5.16 mmol) of iodine. A solution of H_2SO_4 conc. (5 ml) and 20% HOAc (155 ml) is added to this mixture. The resulting purple solution is heated at 65-70 °C with stirring for approximately 1 h, the reaction mixture was extracted with CH_2Cl_2 (100 ml x 3). The combined organic phase was washed with water (100 ml), brine solution (100 ml), dried over sodium sulfate anhydrous. Purification by column chromatography using silica gel eluent with hexane gave 3-iodo-10-octylphenothiazine (**1h**) (12 g, 60%) as purple viscous oil; $C_{20}H_{24}INS$; ^{1}H-NMR (300 MHz, $CDCl_3$) δ 8.37 (1H, s), 8.00 (1H, d, J = 7.5 Hz), 7.67 (1H, d, J = 8.4 Hz), 7.48-7.35 (2H, m), 7.24-7.10 (2H, m), 4.20 (2H, t, J = 6.9 Hz), 1.81 (2H, s), 1.29-1.22 (10H, m), and 0.85 (3H, t, J = 5.1 Hz) ppm; ^{13}C-NMR (75 MHz, $CDCl_3$) δ 140.67, 139.34, 134.77, 134.03, 129.62, 129.45, 126.59, 125.63, 121.84, 120.79, 119.54, 111.18, 111.03, 109.16, 81.42, 43.43, 32.08, 29.46, 29.45, 29.18, 27.57, 22.91, and 14.39 ppm; MS (MALDI-TOF) m/z = 437.2769 $[M]^{+\cdot}$, 437.0674 calcd for $C_{20}H_{24}INS$.

_N_-(Naphthalen-1-yl)-10-octyl-_N_-phenylphenothiazin-3-amine (2h)

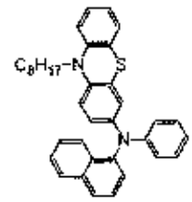

To a mixture of CuI (0.09 g, 0.46 mmol), KO^{t}Bu (0.15 g, 1.37 mmol), and 3-iodo-10-octyl-10H-phenothiazine (**1h**) (0.51 g, 1.14 mmol) in toluene (60 mL) were added N-phenylnaphthalen-1-amine (0.20 g, 0.91 mmol) and (±)-*trans*-1,2-diaminocyclohexane (0.06 g, 0.55 mmol). The reaction mixture was stirred at 110 °C under nitrogen. After 24 h, water (100 ml) was added until the two phases mixed. The solution was extracted with CH_2Cl_2 (100 ml x 3), washed with water (100 ml), brine solution (100 ml) and dried with Na_2SO_4, filtered, and the solvents removed to dryness. After the solvent was evaporated. The crude product was purified by column chromatography on silica gel with hexane as eluent to yield *N*-(naphthalen-1-yl)-9-octyl-*N*-phenylcarbazol-3-amine (**2h**) (0.20 g, 41%) as dark green viscous oil; $C_{36}H_{36}N_2S$; ^{1}H-NMR (300 MHz, $CDCl_3$) δ 7.97-7.87 (2H, m), 7.76 (1H, d, J = 8.1 Hz), 7.46 (2H, t, J = 7.6 Hz), 7.39-7.26 (2H, m), 7.20-7.08 (4H, m), 6.95-6.83 (7H, m), 6.72-6.66 (1H, m), 3.81-3.70 (2H, m), 1.83-1.78 (2H, m), 1.47-1.29 (10H, m), and 0.91-0.87 (3H, m) ppm; ^{13}C-NMR (75 MHz, $CDCl_3$) δ 145.52, 145.22, 136.07, 135.56, 127.78, 127.68, 127.43, 124.51, 122.94, 122.57, 117.34, 115.81, 115.65, 84.40, 47.70, 32.01, 29.47, 27.26, 27.16, 27.02, 22.91, and 14.39 ppm; MS (MALDI-TOF) m/z = 528.4290 $[M]^{+\cdot}$, 528.2599 calcd for $C_{36}H_{36}N_2S$.

_N_-(4-Bromophenyl)-_N_-(naphthalen-1-yl)-10-octylphenothiazin-3-amine (3h)

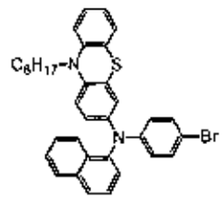

NBS (0.05 g, 0.27 mmol) was added in small portions to a stirred solution of *N*-(naphthalen-1-yl)-10-octyl-*N*-phenylphenothiazin-3-amine (**2h**) (0.14 g, 0.27 mmol) in THF (20

ml). After being stirred at room temperature for 30 min, water was added. The mixture was extracted with dichloromethane (30 ml x 3). The combined organic phase was washed with water (50 ml), brine solution (50 ml), dried over anhydrous sodium sulfate, filtered and the solvent was remove in vacuum. Purification by short column chromatography using silica gel eluting with dichloromethane : hexane, 5:95 gave **3h** as dark green viscous oil (0.11 g, 65%); $C_{36}H_{35}BrN_2S$; ^{1}H-NMR (500 MHz, $CDCl_3$) δ 8.03 (1H, d, J = 5.1 Hz), 7.99 (1H, d, J = 4.8 Hz), 7.94 (1H, d, J = 4.5 Hz), 7.89 (1H, d, J = 4.8 Hz), 7.69-7.67 (1H, m), 7.59-7.54 (2H, m), 7.47-7.43 (3H, m), 7.36-7.34 (3H, m), 7.32-7.25 (3H, m), 7.12 (1H, d, J = 4.8 Hz), 7.05 (1H, d, J = 4.3 Hz), 4.25 (2H, m), 1.68-1.66 (2H, m), 1.43-1.30 (10H, m), and 0.98-0.91 (3H, m) ppm; ^{13}C-NMR (125 MHz, $CDCl_3$) δ 148.12, 142.98, 142.92, 136.38, 135.36, 133.07, 132.81, 131.76, 131.08, 129.44, 129.34, 128.50, 127.29, 127.15, 127.00, 126.81, 126.67, 126.42, 126.29, 124.05, 123.59, 121.96, 121.39, 121.19, 116.67, 115.42, 48.24, 45.37, 37.13, 31.76, 30.06, 29.73, 26.89, 22.70, 21.38, and 14.09 ppm.

5-(4-(Naphthalen-1-yl(10-octylphenothiazin-3-yl)amino)phenyl)thiophene-2-carbaldehyde (4h)

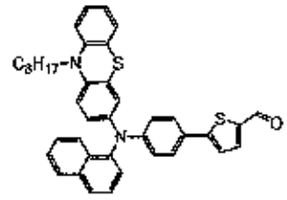

A mixture of **3h** (0.50 g, 0.82 mmol), (5-formylthiophen-2-yl)boronic acid (0.13 g, 0.82 mmol), $Pd(PPh_3)_4$ (0.09 g, 0.08 mmol), and 2 M Na_2CO_3 aqueous solution (8 ml, 16 mmol) in THF (30 ml) was degassed with N_2 for 5 min. The reaction mixture was stirred at reflux under N_2 for 24 h. After being cooled to room temperature, water (70 ml) was added and extracted with CH_2Cl_2 (70 ml x 3). The combined organic phases were washed with water (70 ml) and brine solution (70 ml), dried over anhydrous Na_2SO_4, filtered, and the solvents were removed to dryness. Purification by column chromatography over silica gel eluting with a mixture of CH_2Cl_2 and hexane (2:3) followed by recrystallization with a mixture of CH_2Cl_2 and methanol afforded 5-(4-(naphthalen-1-yl(10-octylphenothiazin-3-yl)amino)phenyl)thiophene-2-carbaldehyde **(4h)** (0.16 g, 30%) as dark yellow viscous oil; $C_{41}H_{38}N_2OS_2$; ^{1}H-NMR (300 MHz, $CDCl_3$) δ 9.94 (1H,

s), 8.16-7.83 (4H, m), 7.48-7.26 (10H, m), 6.92-6.71 (6H, m), 4.20 (2H, m), 1.55-1.26 (12H, m), and 0.86 (3H, m) ppm; MS (MALDI-TOF) m/z - 638.3040 $[M]^{-\cdot}$, 638.2426 calcd for $C_{41}H_{38}N_2OS_2$.

(*E*)-2-Cyano-3-(5-(4-(naphthalen-1-yl(10-octylphenothiazin-3-yl)amino)phenyl) thiophen-2-yl)acrylic acid (20)

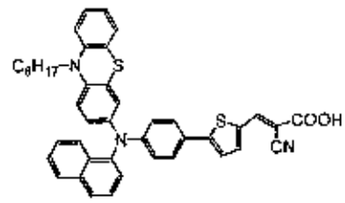

A mixture of **4h** (0.17 g, 0.27 mmol) and cyanoacetic acid (0.11 g, 1.35 mmol) was vacuum-dried and added piperidine (0.19 ml, 1.90 mmol) in $CHCl_3$ (20 ml). The solution was refluxed for 6 h. After cooling the solution, the organic layer was removed in vacuo. The pure product was obtained by column chromatography over silica gel eluting with a mixture of MeOH and EtOAc (1:9) followed by recrystallization with a mixture of CH_2Cl_2 and methanol afforded **20** (0.12 g, 64%) as dark orange solid; $C_{44}H_{39}N_3O_2S_2$; m.p. 168-169 °C; ^{1}H-NMR (300 MHz, $CDCl_3$/DMSO) δ 8.47 (1H, s), 7.99 (1H, d, J = 8.1 Hz), 7.86-7.83 (1H, m), 7.71 (1H, m), 7.29-6.94 (9H, m), 6.86-6.65 (7H, m), 6.56-6.53 (1H, m), 4.18 (1H, s, br), 3.69-3.54 (2H, m), 1.70-1.68 (2H, m), 1.34-1.21 (10H, m), and 0.82-0.81 (3H, m) ppm; ^{13}C-NMR (125 MHz, $CDCl_3$/DMSO) δ 169.62, 149.20, 148.48, 145.21, 144.46, 143.13, 140.51, 136.83, 132.71, 130.38, 129.07, 129.01, 128.78, 128.41, 127.34, 127.18, 126.98, 126.88, 126.47, 126.34, 126.31, 125.97, 125.82, 125.64, 124.61, 124.20, 124.14, 122.15, 122.05, 121.37, 121.15, 120.78, 118.80, 115.66, 115.18, 47.47, 31.69, 29.17, 29.16, 26.94, 26.85, 22.57, and 14.09 ppm; FT-IR (KBr) 3394, 3059, 3024, 2922, 2852, 2213, 1719, 1610, 1575, 1492, 1463, 1443, 1379, 1248, 1228, 939, 806, 764, 746, and 694 cm^{-1}; MS (MALDI-TOF) m/z = 705.2441 $[M]^{+\cdot}$, 705.2484 calcd for $C_{44}H_{39}N_3O_2S_2$.

Chapter 9:

3,6-Dibromo-9-dodecylcarbazole (66)

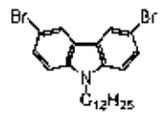

NBS (0.56 g, 3.13 mmol) was added in small portions to a stirred solution of 9-dodecylcarbazole (65) (0.50 g, 1.49 mmol) in THF (20 ml). After being stirred at room temperature for 30 min, water was added. The mixture was extracted with dichloromethane (30 ml x 3). The combined organic phase was washed with water (50 ml), brine solution (50 ml), dried over anhydrous sodium sulfate, filtered and the solvent was remove in vacuum. Purification by short column chromatography using silica gel eluting with hexane, gave **66** as light white viscous (0.69 g, 94%); $C_{24}H_{31}Br_2N$; mp: 50 °C; ^{1}H NMR (300 MHz, $CDCl_3$) δ 8.15 (2H, d, J = 1.50 Hz), 7.56 (2H, d, J = 0.60 Hz), 7.26 (2H, d, J = 0.90 Hz), 4.24 (2H, t, J = 0.90 Hz), 1.82 (2H, t, J = 0.90 Hz), 1.43 (18H, m), and 0.87 (3H, t, J = 2.10 Hz) ppm; ^{13}C NMR (75 MHz, $CDCl_3$) δ 139.32, 129.00, 128.18, 123.45, 123.24, 111.94, 110.38, 108.93, 43.35, 31.90, 29.58, 29.52, 29.44, 29.32, 28.83, 27.20, 22.68, and 14.11 ppm.

4,4'-(9-Dodecylcarbazole-3,6-diyl)bis(*N*,*N*-diphenylaniline) (T2C)

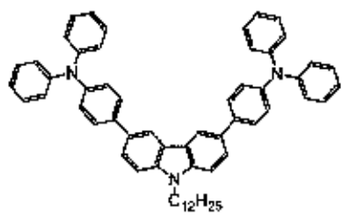

A mixture of **66** (0.10 g, 0.20 mmol), 4-(diphenylamino)phenyl boronic acid (0.15 g, 0.51 mmol), $Pd(PPh_3)_4$ (0.01 g, 0.01 mmol), and 2 M Na_2CO_3 aqueous solution (2 ml, 4.05 mmol) in THF (30 ml) was degassed with N_2 for 5 min. The reaction mixture was stirred at reflux under N_2 for 24 h. After being cooled to room temperature, water (70 ml) was added and extracted with CH_2Cl_2 (70 ml x 3). The combined organic phases were washed with water (70 ml) and brine solution (70 ml), dried over anhydrous Na_2SO_4, filtered, and the solvents were removed to dryness. Purification by column chromatography over silica gel eluting with a mixture of CH_2Cl_2 and

hexane (1:4) followed by recrystallization with a mixture of CH_2Cl_2 and methanol afforded T2C (0.12 g, 75%) as white solid; $C_{60}H_{59}N_3$; mp: 170-172 °C; ^{1}H NMR (300 MHz, $CDCl_3$) δ 8.35 (2H, s), 7.72 (2H, d, J = 12.0 Hz), 7.63 (4H, d, J = 8.7 Hz), 7.46 (2H, d, J = 8.4 Hz), 7.30 (8H, t, J = 8.4 Hz, J = 7.5 Hz), 7.20 (12H, t, J = 9.3 Hz, J = 7.8 Hz), 7.05 (4H, t, J = 7.5 Hz, J = 7.2 Hz), 4.34 (2H, t, J = 6.6 Hz, J = 6.9 Hz), 1.93 (2H, t, J = 6.6 Hz, J = 6.9 Hz), 1.27-1.49 (18H, m), and 0.90 (3H, t, J = 6.3 Hz, J = 6.9 Hz) ppm; ^{13}C NMR (75 MHz, CDCl3) δ 147.87, 146.39, 140.20, 136.47, 131.90, 129.24, 127.88, 124.96, 124.50, 124.18, 123.50, 122.67, 118.45, 109.03, 43.36, 31.91, 29.61, 29.52, 29.43, 29.33, 29.08, 27.34, 22.69, and 14.12 ppm; HRMS m/z = 822.5430 [MH^+], 821.4709 calcd for $C_{60}H_{59}N_3$.

1,3,6-Tribromo-9-dodecylcarbazole (67)

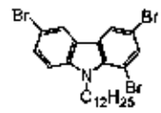

NBS (1.44 g, 8.11 mmol) was added in small portions to a stirred solution of 9-dodecylcarbazole (**65**) (0.50 g, 1.01 mmol) in THF (20 ml). After being stirred at room temperature for 30 min, water was added. The mixture was extracted with dichloromethane (30 ml x 3). The combined organic phase was washed with water (50 ml), brine solution (50 ml), dried over anhydrous sodium sulfate, filtered and the solvent was remove in vacuum. Purification by short column chromatography using silica gel eluting with hexane, gave **67** as light white viscous (0.43 g, 75%); $C_{24}H_{30}Br_3N$; mp: 54 °C; ^{1}H NMR (300 MHz, $CDCl_3$) δ 8.05 (1H, d, J = 1.80 Hz), 7.99 (1H, d, J = 1.50 Hz), 7.61 (1H, d, J = 1.20 Hz), 7.52 (1H, d, J = 9.00 Hz), 7.23 (1H, d, J = 9.00 Hz), 4.56 (2H, t, J = 7.20 Hz), 1.30 (18H, m), 1.78 (2H, m) and 1.29 (3H, t, J = 6.90 Hz) ppm; ^{13}C NMR (75 MHz, $CDCl_3$) δ 140.24, 135.68, 133.43, 129.80, 126.16, 122.87, 122.17, 111.75, 111.73, 110.87, 103.36, 44.34, 31.93, 30.50, 29.72, 29.63, 29.55, 29.52, 29.34, 29.32, 26.74, 22.71, and 14.14 ppm.

4,4',4''-(9-Dodecylcarbazole-1,3,6-triyl)tris(*N*,*N*-diphenylaniline) (T3C)

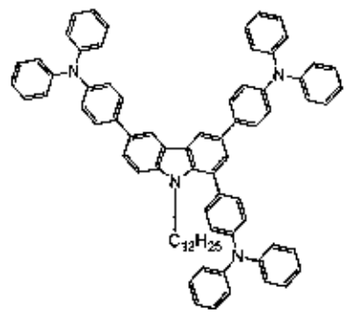

A mixture of **67** (0.10 g, 0.17 mmol), 4-(diphenylamino)phenyl boronic acid (0.18 g, 0.61 mmol), $Pd(PPh_3)_4$ (0.01 g, 0.01 mmol), and 2 M Na_2CO_3 aqueous solution (2 ml, 3.50 mmol) in THF (30 ml) was degassed with N_2 for 5 min. The reaction mixture was stirred at reflux under N_2 for 24 h. After being cooled to room temperature, water (70 ml) was added and extracted with CH_2Cl_2 (70 ml x 3). The combined organic phases were washed with water (70 ml) and brine solution (70 ml), dried over anhydrous Na_2SO_4, filtered, and the solvents were removed to dryness. Purification by column chromatography over silica gel eluting with a mixture of CH_2Cl_2 and hexane (1:4) followed by recrystallization with a mixture of CH_2Cl_2 and methanol afforded T3C (0.17 g, 92%) as white solid; $C_{78}H_{72}N_4$; mp: 120-122 °C; ^{1}H NMR (300 MHz, CDCl3) δ 8.35 (2H, d, J = 6.3 Hz), 7.61-7.72 (5H,m), 7.54 (1H, s), 7.42 (3H, d, J = 8.4 Hz), 7.18-7.33 (29H, m), 7.06 (7H, t, J = 9.9 Hz), 4.00 (2H, s), 1.04-1.23 (20H, m), and 0.87 (3H, m) ppm; ^{13}C NMR (75 MHz, CDCl3) δ 147.77, 147.28, 146.46, 130.66, 129.36, 129.24, 127.91, 126.11, 125.09, 124.53, 124.47, 124.19, 124.14, 123.05, 122.68, 118.20, 117.16, 109.54, 31.92, 29.68, 29.62, 29.34, 26.89, 22.70, and 14.16 ppm; HRMS m/z = 1065.7021 [MH^+], 1064.5757 calcd for $C_{78}H_{72}N_4$.

1,3,6,8-Tetrabromo-9-dodecylcarbazole (68)

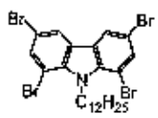

NBS (1.87 g, 10.49 mmol) was added in small portions to a stirred solution of 9-dodecylcarbazole (**65**) (0.50 g, 0.87 mmol mmol) in THF (20 ml). After being stirred at room temperature for 30 min, water was added. The mixture was extracted with dichloromethane (30 ml

x 3). The combined organic phase was washed with water (50 ml), brine solution (50 ml), dried over anhydrous sodium sulfate, filtered and the solvent was remove in vacuum. Purification by short column chromatography using silica gel eluting with hexane, gave **68** as light white viscous (0.44 g, 77%): $C_{24}H_{29}Br_4N$; mp: 90 °C; ^{1}H-NMR (300 MHz, $CDCl_3$) δ 7.99 (2H, s), 7.76 (2H, s), 5.04 (2H, t, J = 8.10 Hz), 1.26 (18H, m), 1.76 (2H, m), and 0.88 (3H, t, J = 7.20 Hz) ppm; ^{13}C NMR (75 MHz, $CDCl_3$) δ 137.01, 134.94, 126.21, 122.08, 112.77, 104.20, 44.74, 31.91, 31.78, 29.63, 29.51, 29.33, 29.23, 26.05, 22.69, and 14.12 ppm.

4,4',4'',4'''-(9-Dodecylcarbazole-1,3,6,8-tetrayl)tetrakis(*N*,*N*-diphenylaniline) (T4C)

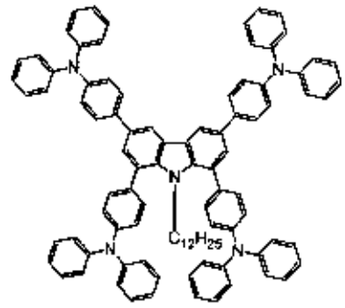

A mixture of **68** (0.10 g, 0.15 mmol), 4-(diphenylamino)phenyl boronic acid (0.20 g, 0.69 mmol), $Pd(PPh_3)_4$ (0.01 g, 0.01 mmol), and 2 M Na_2CO_3 aqueous solution (1.5 ml, 3.07 mmol) in THF (30 ml) was degassed with N_2 for 5 min. The reaction mixture was stirred at reflux under N_2 for 24 h. After being cooled to room temperature, water (70 ml) was added and extracted with CH_2Cl_2 (70 ml x 3). The combined organic phases were washed with water (70 ml) and brine solution (70 ml), dried over anhydrous Na_2SO_4, filtered, and the solvents were removed to dryness. Purification by column chromatography over silica gel eluting with a mixture of CH_2Cl_2 and hexane (1:4) followed by recrystallization with a mixture of CH_2Cl_2 and methanol afforded **T4C** (0.17 g, 86%) as white solid; mp: 128-130 °C; ^{1}H NMR (300 MHz, CDCl3) δ 8.34 (2H, s), 7.65 (4H, d, J = 8.4 Hz), 7.54(2H, d, J = 1.5 Hz), 7.43 (4H, d, J = 8.4 Hz), 7.25-7.32 (18H,m), 7.16 (21H, t, J = 4.5 Hz, J = 3.9 Hz), 7.00-7.08 (9H, m), 3.70 (2H, d, J = 7.2 Hz), 0.83-1.26 (20H, m), and 0.53 (3H, t, J = 6.9 Hz, J = 6.3 Hz) ppm; ^{13}C NMR (75 MHz, CDCl3) δ 147.76, 147.10, 146.51, 139.04, 136.01, 134.64, 132.37, 130.98, 130.28, 129.33, 129.23, 128.24, 127.91, 126.88,

126.55, 126.07, 124.53, 124.42, 124.16, 123.33, 122.99, 122.69, 116.89, 45.57, 31.88, 29.71, 29.60, 29.50, 29.34, 29.01, 28.63, 26.23, 22.66, and 14.13 ppm; HRMS m/z = 1308.9110 [M^+], 1308.6839 calcd for $C_{99}H_{88}N_4$.

REFERENCES

REFERENCES

[1] K. Staub and et al. (2003). "Synthesis and stability studies of conformationally locked 4-(diarylamino)aryl-and 4-(dialkylamino)phenyl-substituted second-order nonlinear optical polyene chromophores", J. Mater. Chem. 13(1): 825-833.

[2] Y.H. Zhou and et al. (2007). "Novel donor- acceptor molecules as donors for bulk heterojunction solar cells", Synth. Met. 157(13-15): 502-507.

[3] X.H. Li and et al. (2008). "A new carbazole-based phenanthrenyl ruthenium complex as sensitizer for a dye-sensitized solar cell", Inorg. Chim. Acta. 361(9-10): 2835–2840.

[4] T.-Y. Wu and et al. (2010). "Synthesis and Characterization of Organic Dyes Containing Various Donors and Acceptors", Int. J. Mol. Sci. 11(1): 329-353.

[5] M. Gratzel. (2005). "Mesoscopic solar cells for electricity and hydrogen production from sunlight", Chem. Lett. 34(1): 8-13.

[6] B. O'Regan and M. Gratzel. (1991). "A low-cost, high-efficiency solar cell based on dye sensitized colloidal TiO_2 films", Nature. 353(6346): 737-740.

[7] A. J. Bard. (1982). "Design of semiconductor photoelectrochemical systems for solar energy conversion", J. Phys. Chem. 86(2): 172-177.

[8] C. A. Bignozzi and et al. (2000). "Molecular and supramolecular sensitization of nanocrystalline wide band-gap semiconductors with mononuclear and polynuclear metal complexes", Chem. Soc. Rev. 29(2): 87-96.

[9] M. Matsumura and et al. (1980). "Dye Sensitization and Surface Structures of Semiconductor Electrodes", Ind. Eng. Chem. Prod. Res. Dev. 19(3): 415-421.

[10] M. Gratzel. (2005). "Solar energy conversion by dye-sensitized photovoltaic cells", Inorg. Chem. 44(20): 6841-6851.

[11] D. Hagberg. (2008). Synthesis of Organic Chromophores for Dye-Sensitized Solar Cells. Doctoral Thesis: Rutgers University.

[12] M. Gratzel and et al. (2003). "Dye-sensitized solar cells", Photochem. Photobiol. C. 4(2): 145-153.

[13] X. Li and et al. (2008). "A new carbazole-based phenanthrenyl ruthenium complex as sensitizer for a dye-sensitized solar cell", Inorg. Chim. Acta. 361(9-10): 2835-2840.

REFERENCES (CONTINUED)

[14] K. Hara and et al. (2003). "Dye-sensitized nanocrystalline TiO_2 solar cells based on novel coumarin dyes", Sol. Energ. Mat. Sol. C. 77(1): 89-103.

[15] K. Hara and et al. (2005). "Oligothiophene-Containing Coumarin Dyes for Efficient Dye-Sensitized Solar Cells", J. Phys. Chem. B. 109(32): 15476-15482.

[16] S. Ito and et al. (2006). "High-Efficiency Organic-Dye- Sensitized Solar Cells Controlled by Nanocrystalline-TiO_2 Electrode Thickness", Adv. Mater. 18(9): 1202-1205.

[17] N. Koumura and et al. (2006). "Alkyl-Functionalized Organic Dyes for Efficient Molecular Photovoltaics", J. Am. Chem. Soc. 128(44): 14256-14257.

[18] D. Kim and et al. (2007). "Molecular engineering of organic dyes containing *N*-aryl carbazole moiety for solar cell", Tetrahedron. 63(9): 1913-1922.

[19] Y. J. Chang and et al. (2009). "Dye-sensitized solar cell utilizing organic dyads containing triarylene conjugates", Tetrahedron. 65(24): 4726-4734.

[20] Z. Wanand et al. (2012). "Influence of different arylamine electron donors in organic sensitizers for dye-sensitized solar cells", Dyes Pigments. 95(1): 41-46.

[21] Freie University of Berlin. "Dye-sensitized solar cell", http://www.diss.fuberlin.de/diss/servlets/MCRFileNodeServlet/FUDISS_derivate_000000002568/02_2.pdf. July, 2007.

[22] W. M. Capbell and et al. (2004). "Porphyrins as light harvesters in the dye-sensitised TiO_2 solar cell", Coordin. Chem. Rev. 248(13–14): 1363-1379.

[23] Wikipedia The Free Encyclopedia. "Organic light-emitting diode", http://en.wikipedia.org/wiki/Organic_light-emitting_diode. April, 2013.

[24] L. J. Rothberg and A. J. Lovinger. (1996). "Electrically Active Organic and. Polymeric Materials for Thin-Film-Transistor Technologies", J. Mater. Res. 11(6): 1581-1592.

[25] Sheats, J. R. and et al. (1996). "Organic Electroluminescent Devices", Science. 273(5277): 884-888.

[26] D. D. C. Bradley. (1992). "Electroluminescence: a bright future for conjugated polymers", Adv. Mater. 4(11): 756-758.

REFERENCES (CONTINUED)

[27] S. R. Forrest and et al. (1997). "Organic electroluminescent elements", El. Mater. Dev. 52(4): 415-458.

[28] M. Deussen and H. Bässler. (1997). "Organic light emitting diodes", Chimz. 31(2): 76-86.

[29] M. Sonntag. (2005). New Carbazole Based Materials for Optoelectronic Applications. Doctor of Natural Science: University of Bayreuth.

[30] Y. Shirota and et al. (2005). "Amorphous electron-accepting materials for organic optoelectronics", J. Mater. Chem. 15(1): 75-93.

[31] Y. Kishigami and et al. (2005). "Conjugated polymers: theory, synthesis, properties, and characterization", Synth. Met. 153(1–3): 241-244.

[32] D.D.C. Bradley. (1990). "Light-emitting diodes based on conjugated polymers", Nature. 347(6293): 539- 541.

[33] D. Meunmart and et al. (2012). "Bis(4-diphenylaminophenyl)carbazole end-capped fluorene as solution-processed deep-blue light-emitting and hole-transporting materials for electroluminescent devices", Tetrahedron Lett. 53(28): 3615–3618.

[34] S. Pansay. (2011). Synthesis and characterization of carbazole derivatives for optoelectronic devices. Master Thesis: Ubon ratchathani university.

[35] P. Kanapan. (2012). Synthesis and characterization of phenothiazine derivatives for dye sensitized solar cell. bachelor Thesis: Ubon ratchathani university.

[36] C. Y. Chen and et al. (2006). "A Ruthenium Complex with Superhigh Light Harvesting Capacity for Dye-Sensitized Solar Cells", Angew. Chem. Int. Ed. 45(35): 5822-5825.

[37] Z. S. Wang and et al. (2000). "Photoelectric conversion properties of nanocrstalline TiO_2 electrode sensitized with hemicyanine derivatives", J. Phys. Chem. B. 104(41): 9676-9682.

[38] X. Li and et al. (2008). "a new carbazole-based phenanthrenyl ruthenium complex as sensitizer for a dye-sensitized solar cell", Inorg. Chim. Acta. 361(9): 2835–2840.

[39] V. Promarak and et al. (2007). "Synthesis and characterization of *N*-carbazole end-capped oligofluorene-thiophenes", Tetrahedron. 63(36): 8881-8890.

[40] K. Hara and et al. (2003). "Design of new coumarin dyes having thiophene moieties for highly efficient organic-dye-sensitized solar cells", New J. Chem. 27(5): 783-785.

REFERENCES (CONTINUED)

[41] J. R. Mann and et al. (2008). "Optimizing the Photocurrent Efficiency of Dye-Sensitized Solar Cells through the Controlled Aggregation of Chalcogenoxanthylium Dyes on Nanocrystalline Titania Films", J. Phys. Chem. C. 112(34): 13057-13061.

[42] B. Hemmateenejad and et al. (2012). "Effects of solvent and substituent on the electronic absorption spectra of some substituted Schiff bases: A chemometrics study", Spectrochim. Acta Mol. Biomol. Spectros. 91(0): 198-205.

[43] H. Meng and et al. (2001). "A Robust Low Band Gap Processable *n*-Type Conducting Polymer Based on Poly(isothianaphthene)", Macromolecules. 34(6): 1810-1816.

[44] J. Bäckvall. (2010). "Paladium-catalyzed cross couplings in organic synthesis", The Royal Swedish Academy of Sciences. http://www.kva.se/Documents/Priser/Nobel/2010/Kemi/sciback_ke_10.pdf. May, 2013.

[45] N. Koumura and et al. (2006). "Alkyl-Functionalized Organic Dyes for Efficient Molecular Photovoltaics", J. Am. Chem. Soc. 128(44): 14256-14257.

[46] Z.-S. Wang and et al. (2008). "Long-term stability of organic–dye-sensitized solar cells based on an alkyl-functionalized carbazole dye", Chem. Mater. 20: 3993- 4003.

[47] S. Kim and et al. (2007). "Synthesis of conjugated organic dyes containing alkyl substituted thiophene for solar cell", Tetrahedron. 63(46): 11436-11443.

[48] X. Lu and (2012). "Molecular Engineering of Quinoxaline-Based Organic Sensitizers for Highly Efficient and Stable Dye-Sensitized Solar Cells", Chem. Mater. 24(16): 3179-3187.

[49] D. Deng et al. (2011). "Triphenylamine-containing linear D-A-D molecules with benzothiadiazole as acceptor unit for bulk-heterojunction organic solar cells", Organic Electronics. 12(4): 614-622.

[50] D. Hagberg. (2009). "Synthesis of Organic Chromophores for Dye-Sensitized Solar Cells", Doctoral Thesis: Univesity of Stockholm.

[51] S. Roquet and et al. (2006). "Triphenylamine-thienylenevinylenes Hybrid Systems with Internal Charge-transfer as Donor Material for Hetero-junction Solar Cells", J. Am. Chem. Soc. 128(10): 3459-3466.

REFERENCES (CONTINUED)

[52] P. Shen and et al. (2011). "Effects of aromatic π-conjugated bridges on optical and photovoltaic properties of *N*,*N*-diphenylhydrazone-based metal-free organic dyes", Organic Electronics. 12(12): 1992-2002.

[53] T. Sudyoadsuk and et al. (2013). "An organic dye using *N*-dodecyl-3-(3,6-di-*tert*-butylcarbazol-*N*-yl)carbazol-6-yl as a donor moiety for efficient dye-sensitized solar cells", Tetrahedron Lett. 54(36): 4903-4907.

[54] C. W. Tang and S. A. VanSlyke (1987). "Organic electroluminescent diodes," Appl. Phys. Lett. 51(12): 913-915.

[55] C. C. Wu and et al. (2005). "Advanced organic light-emitting devices for enhancing display performances", J. Dis. Tech. 1(2): 248–266.

[56] A. Thangtong and et al. (2011). "Bifunctional anthracene derivatives as non-doped blue mitters and hole-transporters for electroluminescent devices, Chemical Communications", Chem. Commun. 47(25): 7122-7124.

[57] T. W. Kelley and et al. (2004). "Recent progress in organic electronics: materials, devices and processes", Chem. Mater. 16(23): 4413-4422.

[58] C.W Tang. (1987). "Organic electroluminescent Diodes", Appl. Phys. Lett. 51(12): 913-915.

[59] P. Kochapradist and et al. (2012). "Multi-triphenylamine-substituted carbazoles: synthesis, characterization, properties, and applications as hole-transporting materials", Tetrahedron Lett. 54(28): 3683-3687.

APPENDIX

C3_C0089

SYNTHESIS AND CHARACTERIZATION OF NOVEL DONOR-π-ACCEPTOR ORGANIC DYES FOR DYE-SENSITIZED SOLAR CELLS (DSSCS)

Palita Kochpradist, Tinnagorn Keawin, Siriporn Jungsuttiwong, Taweesak Sudyoadsuk, Vinich Promarak*
Center for Organic Electronic and Alternative Energy, Department of Chemistry and Center of Excellence for Innovation in Chemistry, Faculty of Science, Ubon Ratchathani University, Warinchumrap, Ubon Ratchathani 34190, Thailand
*e-mail: pvinich@gmail.com

Abstract: Novel D-π-A organic dyes containing different linker and acceptor units for dye-sensitized solar cells (DSSCs) were successfully synthesized and characterized. Different numbers of phenyl units are introduced to the molecule as linkers. The electron-withdrawing groups are acrylic acid, cyanoacrylic acid and cyanoacrylamide groups. The target molecules were characterized by NMR, IR, UV-vis and fluorescence techniques. They are soluble in chlorinated solvents, tetrahydrofuran and acetone. Their optical properties exhibit absorption band covering UV and visible regions.

Introduction: Dye sensitized-solar cells (DSSCs) have been intensively investigated since the report of highly efficient ruthenium complex-sensitized TiO_2 solar cells by the Swiss scientists. To date, overall conversion efficiencies of up to 12% were achieved from the ruthenium complex device. However, pure organic dyes exhibit not only higher extinction coefficient, but simple preparation and purification procedure with a low cost. Recently, enormous progress has been made in this field and the highest overall photoelectric conversion efficiency of solar cells sensitized by organic dyes containing an electron donor (D) and an electron acceptor (A), separated by a π-conjugation bridge (π) has reached 9.8%. This indicates the promising perspective of metal-free organic dyes.

In this work, we synthesized six carbazole-fluorene based D-π-A organic dyes for DSSCs. It is well known that changes in molecular structure and conjugation system can induce very different optical and physical properties of the compounds. Fluorene bearing alkyl groups at the C-9 position is introduced to increase the solubility property and to prevent the recombination of the electrons from the semiconductor to the electrolyte. Different numbers of electron spacers are phenyl moieties, which are considered to be the ideal constructional unit in dye sensitizer engineering, adopted for expansion of the π-conjugating backbone and adjusting the absorption spectra. Dyes **1** and **2** have a cyanoacrylic acid group as electron-withdrawing part and for anchoring onto the TiO_2 surface. Dyes **3** and **4** have an acrylic acid group while dyes **5** and **6** contain a cyanoacrylamide group.

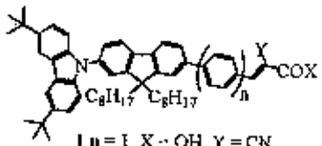

1 n = 1, X = OH, Y = CN
2 n = 2, X = OH, Y = CN
3 n = 1, X = OH, Y = H
4 n = 2, X = OH, Y = H
5 n = 1, X = NH_2, Y = CN
6 n = 2, X = NH_2, Y = CN

Figure 1. Chemical structures of the designed dyes.

Methodology: All reagents were purchased from Aldrich, Acros or Fluka and used without further purification. All solvents were supplied by Thai companies and used without further distillation. THF was refluxed with sodium and benzophenone, and freshly distilled prior to use. ^{1}H and ^{13}C NMR spectra were recorded on a Bruker AVANCE 300 MHz spectrometer. Infrared (IR) spectra were measured on a Perkin-Elmer FTIR spectroscopy Spectrum RXI spectrometer. Ultraviolet-visible (UV-Vis) spectra were recorded on a Perkin-Elmer UV Lambda 25 spectrometer and photoluminescence spectra were recorded with a Perkin-Elmer LS 50B Luminescence Spectrometer as dilute CH_2Cl_2 solution.

Results, Discussion and Conclusion: In the synthesis of dyes **1-6**, fluorene (**7**) was firstly brominated with bromine in chloroform to provide 2,7-dibromofluorene (**8**) as a white solid in 80% yield. Alkylation of **8** with bromooctane by using tetrabutylammonium bromide as a phase transfer catalyst and 50% sodium hydroxide as a base in dimethyl sulfoxide gave the dialkylated product 2,7-dibromo-9,9-dioctylfluorene (**9**) in 89% yield. Subsequently, the key intermediate *N*-carbazole fluorene **11** was synthesized by using Ullmann coupling reaction of **9** with 3,6-di-*tert*-butylcarbazole (**10**) in the presence of copper iodide as a catalyst, (±)-*trans*-1,2-diaminocyclohexane as a co-catalyst, and potassium phosphate as a base in refluxing toluene and obtained as a light yellow viscous oil in 73% yield. The Suzuki coupling reaction was performed with the **11** and 4-formylphenylboronic acid in the presence of $Pd(PPh_3)_4$ as a catalyst and Na_2CO_3 as a base in THF as a solvent to yield the aldehyde **12** as yellow solid in 87% yield. The dye possessing cyanoacrylic acid as an acceptor was next synthesized. Knoevenagel condensation reaction of **12** with cyanoacetic acid in the presence of piperidine as a catalytic base in mixture of THF and acetonitrile as the solvent at refluxing temperature gave dye **1** as light green solid in 66% yield. Dye **3** having acrylic acid as an acceptor was prepared from reaction of **12** with malonic acid under similar reaction conditions to those for preparation of dye **1**, affording dye **3** as a light green solid in 81% yield. Condensation reaction of **12** with 2-cyanoacetamide in the presence of acetic acid as a catalyst and ammonium acetate as a co-catalyst gave dye **5** bearing cyanoacrylamide as an acceptor in good yield.

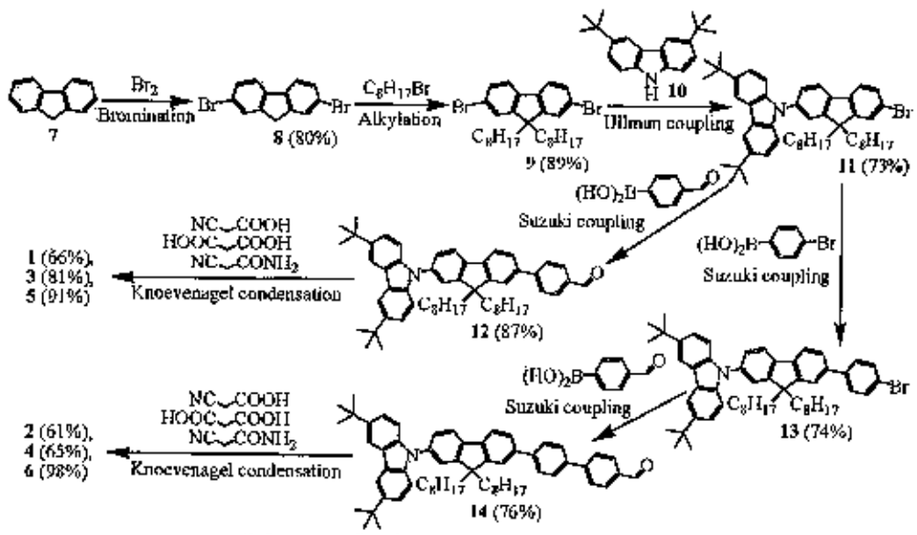

Scheme 1. Synthetic route to the target dyes.

Dyes **2**, **4** and **6** having biphenyl in the π-spacer were synthesized by Suzuki coupling reaction of excess amount of **11** with 4-bromophenylboronic acid to give compound **13** as a white solid in 74% yield. The aldehyde **14** was then prepared in the same manner as for the preparation of **12** and was obtained as green solid in 76% yield. Dyes **2**, **4** and **6** were finally prepared using Knoevenagel condensation and were obtained in moderate to good yield. Their chemical structures were characterized unambiguously using FTIR, ^{1}H-NMR, ^{13}C-NMR spectroscopy as well as high resolution mass spectrometry. These compounds showed good solubility in most organic solvents, resulting probably from their bulkiness, and *tert*-butyl and octyl substituents on the carbazole and fluorene rings, respectively.

The UV-vis and fluorescence spectra of dyes **1-6** in CH_2Cl_2 are shown in Figure 2. All the dyes display two major absorption bands appearing at 297-300 and 320-450 nm, respectively.[1] The first absorption band is attributed to a localized π-π^* transitions of the end-capped carbazole-fluorene donor unit. The latter broader band is ascribed to the intramolecular charge transfer (ICT) transitions from the 3,6-di-tert-butylcarbazole-9,9-dioctyl-fluorene electron donor to the electron acceptor moiety. Dyes **1** and **2** showed nearly the same absorption onset indicating similar π-conjugation length. This is due to arrangement of biphenyl unit capable of inducing the non-planar structure. This result was also observed in the cases of dyes **3** and **4** and dyes **5** and **6**. Dyes **2**, **4** and **6** having biphenyl unit as π-spacer showed larger molar extinction coefficients (ε) compared to those dyes **1**, **3** and **5** having phenyl unit as π-spacer. This result indicates that the presence of biphenyl unit in photosensitizer can increase the light harvesting efficiency. In addition, change in the electron acceptor part has a small effect on the absorption feature. The energy band gaps of dyes **1**, **2**, **3**, **4**, **5** and **6** dyes were estimated to be 2.79, 2.91, 3.08, 3.15, 2.73 and 2.85 eV, respectively, from the absorption edge of the solution spectra.

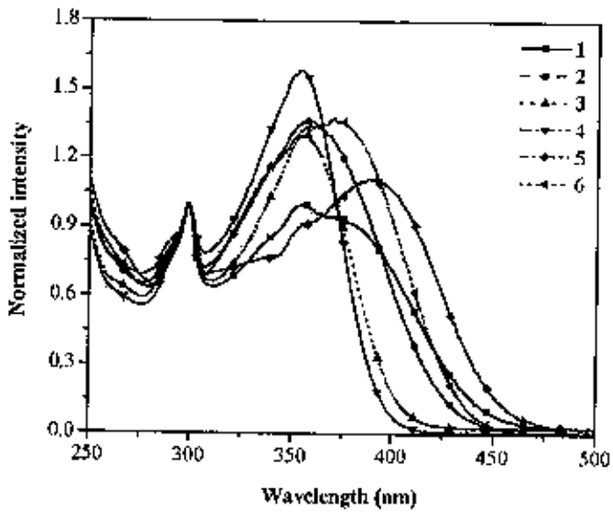

Figure 2. Absorption spectra in CH_2Cl_2 of **1-6**.

References:

1. Vinich P, Musubu I, Taweesak S, Sayant S, Siriporn J, Tinnagon K. Synthetic Met 2007;157:17–22.

Acknowledgements: PERCH-CIC, TRF (MRU5080052), UBU, CHE.

Keywords: donor, acceptor, π-conjugate, dye solar cells

Tetrahedron Letters 54 (2013) 3683–3687

Contents lists available at SciVerse ScienceDirect

Tetrahedron Letters

journal homepage: www.elsevier.com/locate/tetlet

Multi-triphenylamine-substituted carbazoles: synthesis, characterization, properties, and applications as hole-transporting materials

Palita Kochapradist [a], Narid Prachumrak [a], Ruangchai Tarsang [a], Tinnagon Keawin [a], Siriporn Jungsuttiwong [a], Taweesak Sudyoadsuk [b], Vinich Promarak [b,*]

[a] Department of Chemistry and Center of Excellence for Innovation in Chemistry, Faculty of Science, Ubon Ratchathani University, Ubon Ratchathani 34190, Thailand
[b] School of Chemistry and Center of Excellence for Innovation in Chemistry, Institute of Science, Suranaree University of Technology, Muang District, Nakhon Ratchasima 30000, Thailand

ARTICLE INFO

Article history:
Received 15 February 2013
Revised 22 April 2013
Accepted 3 May 2013
Available online 13 May 2013

Keywords:
Carbazole
Triphenylamine
Bromination
Hole-transporting material
Organic light-emitting diode

ABSTRACT

A series of triphenylamine-substituted carbazoles, namely TnC (n = 2–4), are synthesized and characterized. By increasing the number of triphenylamine substituents, we are able to reduce the crystallization and improve the thermal stability of the molecule. Their thermal properties and abilities as hole-transporting layers in Alq3-based OLED, especially T4C having four triphenylamine substituents, are greater than both the common hole-transporters, *N,N'*-diphenyl-*N,N'*-bis(1-naphthyl)-(1,1'-biphenyl)-4,4'-diamine (NPB) and *N,N'*-bis(3-methylphenyl)-*N,N'*-bis(phenyl)benzidine (TPD). A green light-emitting device with a luminance efficiency as high as 5.07 cd/A is achieved.

Since the pioneering work on the first organic light-emitting diodes (OLEDs) by Tang in 1987,[1] OLEDs have attracted significant attention from the scientific community due to their potential for future flat-panel displays and lighting applications.[2] The past decade has seen great progress in both device fabrication techniques and material development.[3,4] One of the key developments is the use of hole-transporting layers (HTLs) for hole injection from the anode into the light-emitting layer providing significant improvements in the performance of devices.[5] As a result, many new hole-transporting materials (HTMs) have been developed.[6–8] In particular, low-molecular weight amorphous materials have received interest as HTM candidates due to their easy purification by vapor deposition or column chromatographic techniques, and uniformly thin films can be processed simply by coating techniques. The most commonly used amorphous hole-transporting materials (AHTMs) are triarylamine derivatives such as *N,N'*-diphenyl-*N,N'*-bis(1-naphthyl)-(1,1'-biphenyl)-4,4'-diamine (NPB) and *N,N'*-bis(3-methylphenyl)-*N,N'*-bis(phenyl)benzidine (TPD), which demonstrate excellent hole-transporting properties. However, their low thermal and morphological stability usually leads to their degradation.[9] In order to achieve highly efficient and long lifetime devices, an AHTM with high mobility, a high glass transition temperature (T_g), a stable amorphous state, and good thin film forming ability are desirable. To optimize all these requirements, many efforts have been devoted to the synthesis of new AHTMs.[6,10] Carbazole derivatives containing a peripheral diarylamine,[11] additional carbazole,[12] bis[4-(*tert*-butylphenyl)]carbazole,[13] and dipyrenyl units[14] were also reported to exhibit good thermal and morphological stability. Recently, we synthesized a series of aromatic compounds with peripheral triphenylamine–carbazole units possessing high T_g (121–185 °C) values, and found that the OLED devices based on the resulting carbazole compounds were promising in terms of device performance and stability.[15] Undoubtedly, it is very attractive to explore and develop new carbazole derivatives that meet the requirements as AHTMs for OLEDs, and which can be synthesized using simple and low-cost methods. Our design involved multiple substitution of the carbazole ring with triphenylamine moieties. With this molecular architecture, compounds should exhibit amorphous hole-transporting ability.

Herein, we report on a simple synthesis of multi-triphenylamine substituted carbazoles (TnC, n = 2–4), and their physical and photophysical properties. Investigations on their abilities to act as hole-transporting layers in OLEDs are also reported. Scheme 1 outlines the synthesis of the triphenylamine functionalized carbazoles. We began with the synthesis of 3,6-dibromo-*N*-dodecylcarbazole (2),

* Corresponding author. Tel.: +66 44 224 277; fax: +66 44 224 643.
E-mail address: pvinich@sut.ac.th (V. Promarak).

0040-4039/$ - see front matter
http://dx.doi.org/10.1016/j.tetlet.2013.05.007

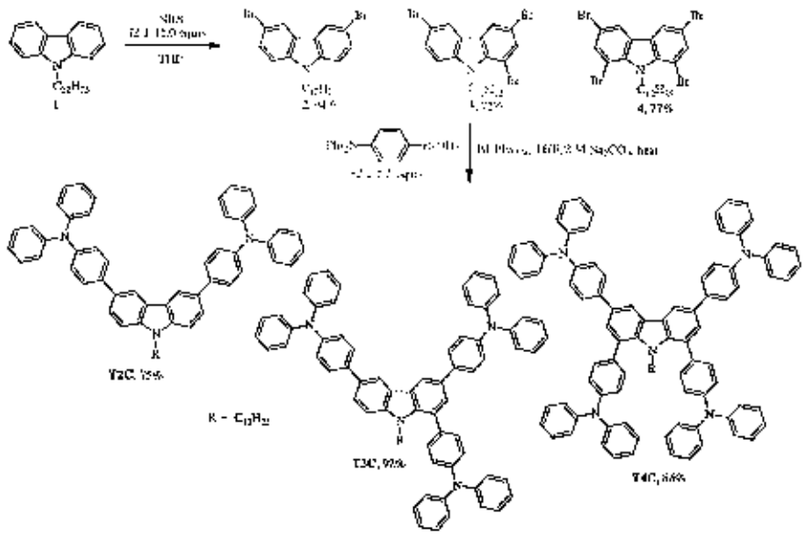

Scheme 1. Synthesis of triphenylamine substituted carbazoles TnC.

1,3,6-tribromo-*N*-dodecylcarbazole (3), and 1,3,6,8-tetrabromo-*N*-dodecylcarbazole (4) by bromination of *N*-dodecylcarbazole (1) with NBS.[16] A solution of 2 in THF was treated with NBS (2.1–15.0 equiv) in small portions in the absence of light to yield bromides 2–4 in moderate to good yields (75–94%). Subsequently, coupling of these multibromo-*N*-dodecylcarbazoles 2–4 with 4-(diphenylamino)phenylboronic acid (2.2–5.5 equiv) in the presence of $Pd(PPh_3)_4$ as the catalyst and aqueous Na_2CO_3 as the base in THF at reflux afforded 3,6-bis[4-(diphenylamino)phenyl]-*N*-dodecylcarbazole (T2C), 1,3,6-tri[4-(diphenylamino)phenyl]-*N*-dodecylcarbazole (T3C), and 1,3,6,8-tetrakis(4-[diphenylamino]phenyl)-*N*-dodecylcarbazole (T4C) as white solids in good yields (75–93%). The structures of the products were characterized unambiguously by ^1H NMR and ^{13}C NMR spectroscopy as well as high-resolution mass spectrometry.[17] Noticeably, the ^1H NMR spectra of TnC showed that the chemical shifts of the dodecyl protons were shifted to low frequency as the number of triphenylamine substituents on the carbazole increased. This is due to a shielding effect resulting from the ring current produced by the surrounding 1- and 8-triphenylamine substituents. For example, the chemical shift of $-NCH_2-$ protons of T2C (4.34 ppm) was shifted to 4.00 and 3.70 ppm in T3C and T4C, respectively. These compounds showed good solubility in most organic solvents.

To gain insight into the geometrical and electronic properties of these multisubstituted carbazoles, quantum chemistry calculations were performed using the TDDFT/B3LYP/6-31G(d) method.[18] The optimized structures of the TnCs revealed that the phenyl rings attached to the carbazole of each triphenylamine were twisted out of the plane of the carbazole, forming bulky substituents around the carbazole, especially in T4C (Fig. 1). This would facilitate the formation of amorphous materials. In all cases, π-electrons in the HOMO orbitals were delocalized only over the carbazole and two triphenylamine substituents at the 3- and 6-positions [3,6-bis[4-(diphenylamino)phenyl]carbazole backbone], and no electrons at the triphenylamine moieties at the 1 and 8-positions. In the LUMO orbitals, the excited electrons were delocalized over the carbazole plane and the phenyl ring of the triphenylamine substituents at the 1,8-positions. This suggests that substitution of the carbazole at the 1- or 8-positions with triphenylamine only affected the LUMO of the molecule, while the HOMO remained nearly untouched.

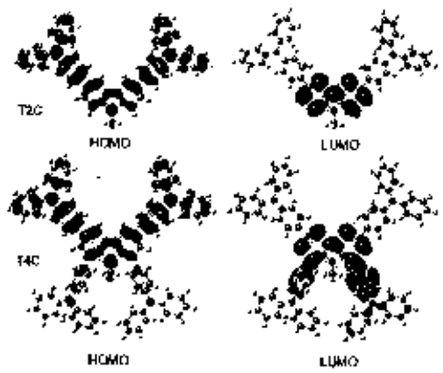

Figure 1. HOMO and LUMO orbitals of T2C and T4C calculated by the TDDFT/B3LYP/6-31G(d) method.

The solution UV–vis absorption spectra of TnC showed absorption bands at 320–328 nm corresponding to the π–π* electronic transition of the π-conjugated 3,6-bis[4-(diphenylamino)phenyl] carbazole backbone (Fig. 2a). With T3C and T4C, absorption bands at lower wavelengths (284–296 nm) were observed, which were identical to the absorption peak of a triphenylamine

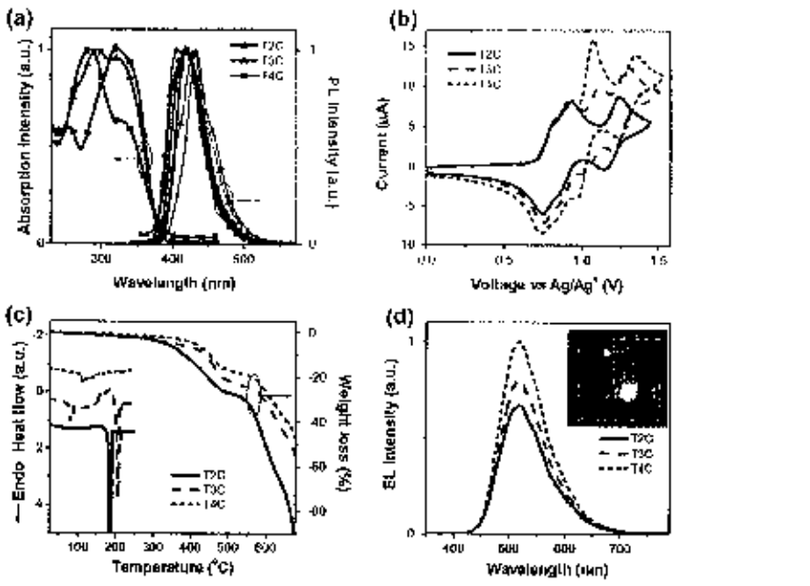

Figure 2. (a) UV–vis absorption and PL spectra in CH_2Cl_2 solution (thick line) and thin films (dash line). (b) CV curves measured in CH_2Cl_2 at a scan rate of 50 mV/s. (c) DSC and TGA curves measured with a heating rate of 10 °C/min under N_2. (d) EL spectra of the OLEDs.

chromophore.[19] This absorption band can be assigned to the π–π* electron transition of the isolated triphenylamine substituents at the 1- or 8-positions. The intensity of this peak was stronger in **T4C** as it has two triphenylamine moieties (1,8-positions). This outcome agrees with the quantum chemistry calculation results. The solution photoluminescence (PL) spectra of **TnC** displayed an emission band in the blue-purple region (λ_{max} = 415–419 nm). The PL spectra of their thin films were similar to those in solution with a ~10 nm red shift. This indicates the presence of certain intermolecular electronic interactions. Nevertheless, the degree of the red shift is considerably smaller than those observed with π–conjugated compounds that adopt face-to-face stacking.[20] These materials show slight Stoke shifts (91–95 nm) suggesting reduced energy loss during the relaxation process.

The CV curves of the **TnCs** measured in CH_2Cl_2 containing *n*-Bu_4NF_6 as the supporting electrolyte exhibited multiple quasi-reversible oxidation processes (Fig. 2b, Table 1). Under these experimental conditions; no reduction was observed in all cases. The first two oxidation waves at 0.78 and 0.89 V in all the compounds appeared at the same potential and could be assigned to the removal of electrons from the conjugated 3,6-bis[4-(diphenylamino)phenyl]carbazole backbone resulting in a radical cation and dication, respectively. The oxidation waves at 1.03–1.07 V in both **T3C** and **T4C** matched with the oxidation potential of a triphenylamine (E_{ox} = 0.98 V vs SCE), and therefore can be assigned to oxidation of the isolated triphenylamine substituent at the 1,8-positions, consistent with both the optical and the quantum chemistry calculation results. The oxidation waves at higher potential

Table 1
Physical data of the **TnCs** and their OLED device characteristics

Compd	Abs[a] (nm)	Em[a] (nm)	T_g/T_m/T_{dec}[b] (°C)	$E^{ox}_{1/2}$ versus Ag/Ag+[c] (V)	E_g (eV)[d]	HOMO/LUMO[d] (eV)	V_{on}/V_{1000} (V)[e]	λ_{max} (nm)	L_{max} (cd/m²)	η (cd/A)	EQE (%)[f]
T2C	320	415	—/189/334	0.78, 0.89, 1.20	3.28	−5.15/−1.85	2.4/3.0	518	28781	4.97	0.24
T3C	296, 325	417	78/207/372	0.78, 0.89, 1.07, 1.25	3.26	−5.16/−1.90	2.4/3.4	518	29052	5.00	0.24
T4C	284, 328	419	122/—/419	0.78, 0.89, 1.03, 1.29	3.24	−5.15/−1.91	2.5/3.4	518	22411	5.07	0.25
NPB	339	450	100/—/—	—	—	−5.50/−2.40	2.5/3.6	519	31857	4.45	0.22
TPD	352	398	63/—/—	—	—	−5.50/−2.30	2.5/3.7	516	22339	4.05	0.20

[a] Measured in CH_2Cl_2 solution.
[b] Measured by DSC and TGA.
[c] Measured by CV using a glassy carbon working electrode, a Pt counter electrode, and an Ag/Ag+ reference electrode with 0.1 M *n*-Bu_4NPF_6 as the supporting electrolyte in CH_2Cl_2.
[d] Calculated from: E_g = 1240/λ_{onset}; HOMO = −(4.44 + $E^{ox}_{1/2}$); LUMO = E_g + HOMO.
[e] Voltage at a luminance of 1 and 100 cd/m².
[f] External quantum efficiency.

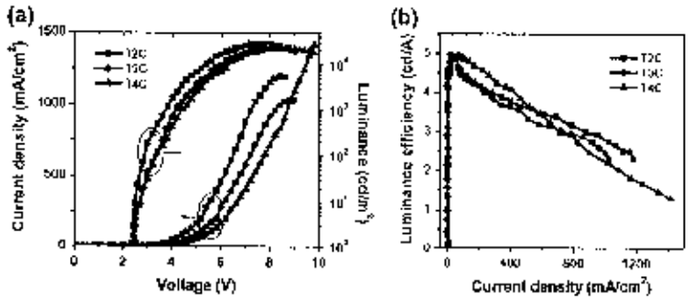

Figure 3. (a) J–V–L and (b) η–J characteristics of the fabricated OLEDs.

(1.20–1.29 V) of all cases correspond to the removal of electrons from the interior of the carbazole moiety. Multiple CV scans (7 scans) revealed identical CV curves with no additional peak at lower potentials on the cathodic scan (E_{pc}) being observed. This suggests no electrochemical coupling at either the carbazole or triphenylamine peripheries, indicating electrochemically stable molecules. Usually, this type of electrochemical coupling reaction is detected in most triphenylamine derivatives with unsubstituted *p*-positions on the phenyl ring, such as in the case of 7-(pyren-1-yl)-2,9,9-tris[4-diphenylaminophenyl]fluorene.[21] The steric hindrance effect and stability from electron delocalization might play an important role in protecting the triphenylamine moieties particularly in such electrochemical reactions in all compounds. The HOMO and LUMO energy levels of the TnCs were calculated from the oxidation onset potentials (E_{onset}) and energy gaps (E_g), and the results are summarized in Table 1. All the compounds had identical HOMO levels of −5.15 V, while their LUMO levels are varied from −1.86 to −1.91 V.

The thermal properties of the TnCs were determined by differential scanning calorimetry (DSC) and thermogravimetric analysis (TGA) and the results are shown in Figure 2c and Table 1. T2C is a crystalline material as its DSC trace reveals only an endothermic peak due to the melting point at 189 °C, while the thermogram of T4C showed only an endothermic baseline shift due to glass transitions (T_g) at 122 °C, indicating an amorphous material. When the crystalline sample of T3C was subjected to a DSC heating scan, an endothermic baseline shift at 78 °C followed by an exothermic peak due to crystallization and an endothermic melting peak at 163 and 207 °C, respectively, were observed, indicating a semi-crystalline material. The T_g value of amorphous T4C was higher than those of the most widely used HTMs, NPB (T_g = 100 °C), and TPD (T_g = 63 °C).[22] The thermal stabilities of TnC were further confirmed by TGA measurements showing an increasing 5% weight loss temperature (T_{5d}) from 334 °C for T2C to 415 °C for T4C as the number the triphenylamines in the molecule increased. These results suggest that the presence of multiple triphenylamines in the molecule not only improves its thermal stability, but also induces the formation of an amorphous form, which in turn could increase the service time in device operation and enhance the morphological stability of the thin film. Moreover, the ability to form a molecular glass with the possibility to prepare good thin films by both evaporation and solution-casting processes is highly desirable for applications in electroluminescent devices.

According to the above discussed excellent properties, the ability of these TnCs as a hole-transporting layer (HTL) in OLEDs was investigated. Alq3-based green OLEDs with the following structure of ITO/PEDOT:PSS/TnC (spin-coating)/Alq3 (50 nm)/LiF (0.5 nm)/Al (200 nm) were fabricated, where Alq3 is the green light-emitting and electron transporting layer (EML). Under the applied voltage, all the devices exhibited a bright green emission with peaks centered at 517–518 nm and the Commission Internationale de l'Eclairage (*CIE*) coordinates of (0.29, 0.53) (Fig. 2d). The electroluminescence (EL) spectra of these diodes were identical, and matched with the PL spectrum of Alq3, the EL of the reference devices (NPB and TPD as HTL), and also other reported EL spectra of Alq3-based devices.[23] No emission at a longer wavelength owing to exciplex species formed at the interface of TnC and Alq3, which often occurs in the devices fabricated with planar molecules, was detected.[24] From these results, and in view of the fact that the barrier for electron migration at the Alq3/TnC interface (~2.10 eV) was significantly higher than those for hole-migration at the TnC/Alq3 interface (~0.36 eV); hence, under the present device configuration, TnCs would act only as HTL, and Alq3 would act preferably as an electron blocker more than as a hole blocker with charge recombination thus confined to Alq3 layer. A stable emission was observed in all diodes with the EL spectra and CIE coordinates remaining unchanged over a range of operating voltages. The TnC-based devices exhibited turn-on voltages in the range of 2.4–2.5 V and operating voltages at 100 cd/m² in the range of 3.0–3.4 V, indicating good device performance (Fig. 3 and Table 1). The device with T4C as the HTL displayed the best performance with a high maximum brightness (L_{max}) of 22411 cd/m² at 8.4 V, a low turn-on voltage (V_{on}) of 2.5 V and a maximum luminous efficiency (η) of 5.07 cd/A. A comparable device performance was observed from the T3C-based device showing L_{max} of 25052 cd/m² at 8.0 V, V_{on} of 2.4 V and a maximum η of 5.00 cd/A, while the T2C-based device showed slightly lower device performance. In comparison with the NPB- and TPD-based devices (Table 1), the use of TnCs as HTLs clearly improves the device performance, indicating the ability of the TnCs as HTMs was superior than NPB and TPD.

In summary, we have demonstrated the simple design strategy, synthesis, and characterization of multi-triphenylamine-substituted carbazoles. Increasing the number of triphenylamine substituents in the molecule not only improved the thermal stability, but also induced the formation of an amorphous form in the material. They are electrochemically and thermally stable materials with reasonably high glass transition temperatures. These materials show excellent hole-transporting properties for Alq3-based green OLEDs with device luminance efficiencies as high as 5.07 cd/A being achieved.

Acknowledgements

This work was financially supported by the SUT Research and Development Fund. We acknowledge the support from the Thailand Research Fund (RMUS080052), Center for Innovation in

Chemistry, the Science Achievement Scholarship of Thailand (SAST) and Precise Green Technology and Service Ltd.

References and notes

1. Tang, C. W.; VanSlyke, S. A. *Appl. Phys. Lett.* **1987**, *51*, 913–915.
2. (a) Wu, C.-C.; Chen, C.-W.; Lin, C.-L.; Yang, C.-J. *J. Display Technol.* **2005**, *1*, 248–266; (b) So, F.; Kido, J.; Burrows, P. *MRS Bull.* **2008**, *33*, 663–669.
3. Kelley, T. W.; Baude, P. F.; Gerlach, C.; Ender, D. E.; Muyres, D.; Haase, M. A.; Vogel, D. E.; Theiss, S. D. *Chem. Mater.* **2004**, *16*, 4413–4422.
4. Thangthong, A.; Meunmart, D.; Prachumrak, N.; Jungsuttiwong, S.; Keawin, T.; Sudyoadsuk, T.; Promarak, V. *Chem. Commun.* **2011**, *47*, 7128–7130.
5. Promarak, V.; Ichikawa, M.; Sudyoadsuk, T.; Saengsuwan, S.; Keawin, T. *Synth. Met.* **2007**, *157*, 17–22.
6. Shirota, Y. *J. Mater. Chem.* **2000**, *10*, 1–25.
7. Balaji, G.; Perumiswaran, M.; Jin, T. M.; Vijaya, C.; Kurong, C.; Valiyaveettil, S. *J. Phys. Chem. C* **2010**, *114*, 4628–4635.
8. So, W.-Y.; Chen, Y. *Polymer* **2011**, *52*, 77–85.
9. Azzi, H.; Papovic, Z. D.; Hu, N.-X.; Hor, A.-M.; Xu, G. *Science* **1990**, *363*, 1900–1902.
10. (a) Katsuma, K.; Shirota, Y. *Adv. Mater.* **1998**, *10*, 223–226; (b) Mouanzin, F.; Prachumrak, N.; Rattanawan, R.; Keawin, T.; Jungsuttiwong, S.; Sudyoadsuk, T.; Promarak, V. *Chem. Commun.* **2012**, 3382–3384.
11. Thomas, K. R. J.; Lin, J. T.; Tao, Y.-T.; Ko, C. W. *J. Am. Chem. Soc.* **2001**, *123*, 9404–9411.
12. Promarak, V.; Ichikawa, M.; Sudyoadsuk, T.; Saengsuwan, S.; Jungsuttiwong, S.; Keawin, T. *Thin Solid Films* **2006**, *516*, 2881–2888.
13. Cha, S. W.; Jin, J.-I. *Synth. Met.* **2006**, *149*, 97–101.
14. Kumchoo, T.; Promarak, V.; Sudyoadsuk, T.; Sukwattanasinitt, M.; Rashatasakhon, P. *Chem. Asian J.* **2010**, *5*, 2162–2167.
15. Promarak, V.; Ichikawa, M.; Meunmart, D.; Sudyoadsuk, T.; Saengsuwan, S.; Keawin, T. *Tetrahedron Lett.* **2006**, *47*, 8949–8952.
16. Paesaya, S.; Prachumrak, N.; Jungsuttiwong, S.; Keawin, T.; Sudyoadsuk, T.; Promarak, V. *Tetrahedron Lett.* **2012**, *53*, 4568–4572.
17. Characterization data for **TBC**: mp 170–172 °C; ^{1}H NMR (300 MHz, $CDCl_3$): δ 0.90 (3H, t, J = 6.9 Hz), 1.27–1.49 (18H, m), 1.93 (2H, t, J = 6.9 Hz), 4.34 (2H, t, J = 6.6 Hz), 7.05 (4H, t, J = 7.5 Hz), 7.20 (12H, t, J = 9.3 Hz), 7.30 (8H, t, J = 8.4 Hz), 7.45 (2H, d, J = 8.4 Hz), 7.63 (4H, d, J = 8.7 Hz), 7.92 (2H, d, J = 12.0 Hz), 8.35 (2H, s); ^{13}C NMR (75 MHz, $CDCl_3$): δ 14.12, 22.69, 27.34, 29.08, 29.33, 29.43, 29.52, 29.61, 31.91, 43.36, 108.13, 118.45, 122.67, 123.50, 124.38, 124.51, 124.96, 127.68, 129.24, 131.90, 136.47, 140.20, 146.38, 147.57; HRMS calcd for $C_{68}H_{69}N_3$, m/z: 921.4709; found: 922.5480 [MH$^+$].
Characterization data for **TBC**: mp 120–122 °C; ^{1}H NMR (300 MHz, $CDCl_3$): δ 0.87 (3H, m), 1.04–1.25 (20H, m), 4.00 (2H, s), 7.06 (7H, t, J = 9.9 Hz), 7.18–7.33 (29H, m), 7.42 (3H, d, J = 8.4 Hz), 7.54 (1H, s), 7.61–7.72 (5H, m), 8.35 (2H, d, J = 6.3 Hz); ^{13}C NMR (75 MHz, $CDCl_3$): δ 14.16, 22.70, 26.89, 29.34, 29.62, 29.68, 31.92, 109.54, 117.15, 118.20, 122.68, 123.06, 124.14, 124.19, 124.47, 124.53, 125.09, 126.11, 127.91, 129.24, 129.36, 130.06, 136.46, 147.28, 147.77. HRMS calcd for $C_{79}H_{73}N_3$, m/z: 1064.5757; found: 1065.7021 [MH$^+$].
Characterization data for **TPC**: mp 168–170 °C; ^{1}H NMR (300 MHz, $CDCl_3$): δ 0.53 (3H, t, J = 6.9 Hz), 0.83–1.26 (20H, m), 3.90 (2H, s), 7.00–7.08 (9H, m), 7.16 (21H, t, J = 4.8 Hz), 7.25–7.32 (10H, m), 7.43 (4H, d, J = 8.4 Hz), 7.54 (2H, d, J = 1.5 Hz), 7.65 (4H, d, J = 8.4 Hz), 8.34 (2H, s); ^{13}C NMR (75 MHz, $CDCl_3$): δ 14.13, 22.66, 26.23, 28.63, 29.01, 29.34, 29.58, 29.60, 29.73, 31.88, 45.47, 116.89, 122.68, 122.99, 123.33, 124.16, 124.42, 124.53, 126.07, 126.55, 126.88, 127.01, 128.34, 129.23, 129.93, 130.28, 130.98, 132.32, 134.64, 136.01, 139.04, 140.51, 147.10, 147.30; HRMS calcd for $C_{81}H_{85}N_3$ m/z: 1108.6839; found: 1108.6110 [MH$^+$].
18. Frisch, M. J.; Trucks, G. W.; Schlegel, H. B.; Scuseria, G. E.; Robb, M. A.; Cheeseman, J. R.; Scalmani, G.; Barone, V.; Mennucci, B.; Petersson, G. A.; Nakatsuji, H.; Caricato, M.; Li, X.; Hratchian, H. P.; Izmaylov, A. F.; Bloino, J.; Zheng, G.; Sonnenberg, J. L.; Hada, M.; Ehara, M.; Toyota, K.; Fukuda, R.; Hasegawa, J.; Ishida, M.; Nakajima, T.; Honda, Y.; Kitao, O.; Nakai, H.; Vreven, T.; Montgomery, J. A., Jr.; Peralta, J. E.; Ogliaro, F.; Bearpark, M.; Heyd, J. J.; Brothers, E.; Kudin, K. N.; Staroverov, V. N.; Kobayashi, R.; Normand, J.; Raghavachari, K.; Rendell, A.; Burant, J. C.; Iyengar, S. S.; Tomasi, J.; Cossi, M.; Rega, N.; Millam, J. M.; Klene, M.; Knox, J. E.; Cross, J. B.; Bakken, V.; Adamo, C.; Jaramillo, J.; Gomperts, R.; Stratmann, R. E.; Yazyev, O.; Austin, A. J.; Cammi, R.; Pomelli, C.; Ochterski, J. W.; Martin, R. L.; Morokuma, K.; Zakrzewski, V. G.; Voth, G. A.; Salvador, P.; Dannenberg, J. J.; Dapprich, S.; Daniels, A. D.; Farkas, Ö.; Foresman, J. B.; Ortiz, J. V.; Cioslowski, J.; Fox, D. J. *Gaussian 09, Revision A.1*; Gaussian, Inc.: Wallingford CT, 2009.
19. Li, Z.; Chen, Y.; Du, Y.; Wang, X.; Yang, P.; Zheng, J. *Int. J. Hydrogen Energy* **2012**, *37*, 4880–4888.
20. Berrios, M. T.; Arbeteta, M.; O'Brien, J.; Wu, W. *Adv. Mater.* **2008**, *32*, 3737–3740.
21. (a) Thangthong, A.; Prachumrak, N.; Tarsang, R.; Keawin, T.; Jungsuttiwong, S.; Sudyoadsuk, T.; Promarak, V. *J. Mater. Chem.* **2012**, *22*, 6869–6877; (b) Kamtekar, K. T.; Wang, C. S.; Bettington, S.; Batsanov, A. S.; Perepichka, I. F.; Bryce, M. R.; Ahn, J. H.; Rabinal, M.; Petty, M. C. *J. Mater. Chem.* **2006**, *16*, 3823–3835.
22. Koetz, B. E.; Loy, D. E.; Thompson, M. E. *Chem. Mater.* **1998**, *10*, 2235–2250.
23. (a) Kim, Y. K.; Hwang, S.-H. *Synth. Met.* **2006**, *156*, 1028–1035; (b) Thangthong, A.; Saengsuwan, S.; Jungsuttiwong, S.; Keawin, T.; Sudyoadsuk, T.; Promarak, V. *Tetrahedron Lett.* **2011**, *52*, 4749–4752.
24. Kim, D. Y.; Cho, H. N.; Kim, C. Y. *Prog. Polym. Sci.* **2000**, *25*, 1089–1139.

Journal of
Materials Chemistry C

RSC Publishing

PAPER

Cite this: J. Mater. Chem. C, 2013, 1, 4916

Pyrene-functionalized carbazole derivatives as non-doped blue emitters for highly efficient blue organic light-emitting diodes†

Palita Kotchapradist,[a] Narid Prachumrak,[b] Ruangchai Tarsang,[b] Siriporn Jungsuttiwong,[b] Tinnagon Keawin,[a] Taweesak Sudyoadsuk[b] and Vinich Promarak*[b]

A series of pyrene-functionalized carbazole derivatives, namely *N*-dodecyl-3,6-di(pyren-1-yl)carbazole (**CP2**), *N*-dodecyl-1,3,6-tri(pyren-1-yl)carbazole (**CP3**) and *N*-dodecyl-1,3,6,8-tetra(pyren-1-yl)carbazole (**CP4**), are synthesized and characterized as simple non-doped solution processed blue emitters for OLEDs. By multiple substitution of pyrene on the carbazole ring, we are able to retain the high blue emissive ability of pyrene in the solid as well as improve the amorphous stability and solubility of the material. These materials show high solution fluorescence quantum efficiencies (up to 94%) and can form morphologically stable amorphous thin films with T_g as high as 170 °C. Solution processed double-layer OLEDs using these materials as non-doped blue emitters exhibit good device performance with luminance efficiencies up to 2.53 cd A^{-1}. Their multi-layer devices exhibit outstanding performances. The **CP2**-based device shows a low turn-on voltage (down to 2.6 V) with an excellent blue emission color (λ_{em} = 436 nm) and CIE coordinates of (0.16, 0.14), while the **CP3** and **CP4**-based blue devices also display low turn-on voltages (down to 2.7 V) with high luminance (up to 24429 cd m^{-2}) and luminance efficiencies (up to 6.92 cd A^{-1}).

Received 18th April 2013
Accepted 7th June 2013

DOI: 10.1039/c3tc30719k

www.rsc.org/MaterialsC

Introduction

Since the innovative works on the first organic light-emitting diodes [OLEDs] by C. W. Tang in 1987,[1] OLEDs and displays made from these devices have received tremendous interest due to their excellent technological aspects such as low costs, the ease of fabrication using standard techniques (*e.g.* vacuum deposition or solution processing), the possibility of realizing flexible or large-area displays and their use in lighting applications.[2] In today's developments of OLED technologies, the trends of OLEDs are mainly focusing both on optimizations of device structures and on developing new emitting materials. Clearly the key point of OLEDs development for full color-flat display is to find materials emitting pure colors of red, green and blue (RGB) with excellent emission efficiency and high stability. The performance of blue OLEDs is usually inferior to that of green and red OLEDs due to poor carrier injection into the emitters,[3] and hence the electroluminescent (EL) properties of the blue ones need to be improved. Therefore, one area of continuing research in this field is the pursuit of a stable-blue emitting material.[4] Although many fluorescent blue emitters have been reported, such as anthracene derivatives,[5] phenylene derivatives,[6] pyrene derivatives,[7] fluorene derivatives,[8] carbazole derivatives,[9] aromatic hydrocarbon,[10] triarylamine derivatives,[11] and phosphorescent iridium complexes,[12] there is still a clear need for further developments in terms of efficiency and colour purity compared to red and green emitters.

Pyrene is a flat electron-rich polycyclic aromatic hydrocarbon (PAH) with strong blue fluorescence which is suitable for developing blue emitters for OLEDs applications. However, the use of pyrene molecules is limited, because pyrene molecules easily formed aggregates/excimers leading to an additional emission band at long wavelength and the quenching of fluorescence, resulting in low solid-state fluorescence quantum yields. However, in rare cases, the aggregates between the pyrene rings make the molecules highly emissive in the solid state *via* an aggregation-enhanced excimer emission.[13] Several molecular designs therefore have been developed to solve this problem and various pyrene based light-emitting materials have been reported in recent literature including functionalized pyrene-based light-emitting molecules,[14] functionalized pyrene-based light emitting dendrimers,[15] and functionalized

[a]Department of Chemistry, Faculty of Science, Ubon Ratchathani University, Ubon Ratchathani, 34190, Thailand

[b]School of Chemistry and Center of Excellence for Innovation in Chemistry, Institute of Science, Suranaree University of Technology, Muang District, Nakhon Ratchasima, 30000, Thailand. E-mail: prarich@sut.ac.th; Fax: +66 4422 4377; Tel: +66 4422 4648

† Electronic supplementary information (ESI) available: AFM images, quantum chemical calculation data, repeated CV scan plot, OLED device data and NMR spectra. See DOI: 10.1039/c3tc30719k

pyrene-based light-emitting oligomers and polymers.[9] To date, many kinds of pyrene-based materials have been synthesized and considered for several applications,[10] and some of them were proven to be promising blue emitters for OLEDs.[11] Recently, we have reported on pyrene derivatives with the combined characteristics of blue light-emitting and hole transporting materials.[12] Non-doped blue OLEDs with maximum efficiencies up to 2.06 cd A^{-1} were attained. However, new classes of pyrene-based blue light-emitters with improvements in terms of efficiency and colour purity remain to be explored.

In this work, we report on the design, synthesis and properties of simple pyrene-functionalized carbazole derivatives, namely *N*-dodecyl-3,6-di(pyren-1-yl)carbazole (CP2), *N*-dodecyl-1,3,6-tri(pyren-1-yl)carbazole (CP3) and *N*-dodecyl-1,3,6,8-tetra(pyren-1-yl)carbazole (CP4), as solution processed blue emitters for OLEDs. In our design, the use of *N*-dodecylcarbazole as a core will improve the hole transporting capability of pyrene as well as thermal stability and solubility of the molecule, while multiple functionalization with pyrene moiety will effectively retain the high blue emissive ability of pyrene in the solid state, which significantly impacts on the emission behavior of materials and devices. Owing to its excellent hole-transporting ability, high charge carrier mobility, high thermal, morphological and photochemical stability, and ease to be functionalized, carbazole has been used as a building block to form many amorphous hole-transporting materials.[13] With this design therefore a simple solution processed hole-transporting non-doped blue emitter can be attained and a simple structure non-doped blue OLED can be fabricated. Investigations on OLED device fabrication and characterization of these materials are also established.

Experimental section

General procedure

^{1}H and ^{13}C nuclear magnetic resonance (NMR) spectra were recorded on a Brüker AVANCE 300 MHz spectrometer with TMS as the internal reference using $CDCl_3$ as solvent in all cases. Infrared (IR) spectra were measured on a Perkin-Elmer FTIR spectroscopy spectrum BXI spectrometer as potassium bromide (KBr) disc. Ultraviolet-visible (UV-Vis) spectra were recorded as a dilute solution in CH_2Cl_2 on a Perkin-Elmer UV Lambda 25 spectrometer. Photoluminescence spectra and the fluorescence quantum yields (Φ_F) were recorded with a Perkin-Elmer LS 50B Luminescence Spectrometer as a dilute solution in CH_2Cl_2 and thin film obtained by thermal evaporation. Quinine sulfate solution in 0.01 M H_2SO_4 ($\Phi_F = 0.54$) was used as a reference standard.[14] Differential scanning calorimetry (DSC) and thermal gravimetric analysis (TGA) were performed on a METTLER DSC823e thermal analyzer and a Rigaku TG-DTA 8120 thermal analyzer, respectively, with heating rate of 10 °C min^{-1} under nitrogen atmosphere. Cyclic voltammetry (CV) was carried out on an Autolab potentiostat PGSTAT 12 with a three electrode system (platinum counter electrode, glassy carbon working electrode and Ag/Ag$^+$ reference electrode) at a scan rate of 50 mV s^{-1} in the presence of *n*-Bu_4NPF_6 as a supporting electrolyte in CH_2Cl_2 under argon atmosphere. Melting points were measured using an Electrothermal IA 9100 series of digital melting point instrument and are uncorrected. High resolution mass spectrometry (HRMS) analysis was performed by a Mass Spectrometry Unit, Mahidol University, Thailand.

Synthesis

Suzuki coupling conditions: A mixture of multibromo-9-dodecyl carbazole (2 **4**) (0.2 mmol), pyren-1-boronic acid (0.5–0.92 mmol), $Pd(PPh_3)_4$ (0.33 g, 0.29 mmol), and 2 M Na_2CO_3 (aq.) (25 ml) in THF (30 ml) was degassed with N_2 for 5 min. The reaction mixture was stirred at reflux under N_2 atmosphere for 18 h. Water (50 ml) was added, the mixture was extracted with CH_2Cl_2 (2 × 50 ml). The combined organic layer was washed with water (50 ml), brine solution (50 ml), dried over anhydrous Na_2SO_4, filtered and evaporated to dryness. The crude product was purified by column chromatography over silica gel eluting with CH_2Cl_2 : hexane (1 : 4) followed by recrystallisation with a mixture of CH_2Cl_2 and methanol.

N-**Dodecyl 3,6-di(pyren-1-yl)carbazole (CP2)** yellowish solid, 88%; mp 165–167 °C; ^{1}H NMR (300 MHz, $CDCl_3$, δ): 0.88 (3H, t, J = 6.9 Hz), 1.29–1.57 (18H, m), 2.03–2.12 (2H, m), 4.50 (2H, t, J = 7.0 Hz), 7.65 (2H, d, J = 8.1 Hz), 7.80 (2H, d, J = 8.1 Hz), 8.01 (4H, d, J = 8.7 Hz), 8.10–8.20 (10H, m), 8.25 (2H, d, J = 7.5 Hz), 8.32 (2H, d, J = 9.3 Hz), 8.40 (2H, s); ^{13}C NMR (75 MHz, $CDCl_3$, δ): 14.12, 22.70, 27.49, 29.24, 29.54, 29.62, 29.66, 31.94, 43.56, 108.70, 122.46, 123.10, 124.92, 125.05, 125.09, 125.72, 125.93, 127.06, 127.30, 127.50, 128.23, 128.74, 128.88, 130.29, 131.09, 131.57, 132.09, 138.57, 140.31; HRMS-ESI calcd for $C_{56}H_{49}N$: *m/z* 735.3865; found: *m/z* 736.3885 [MH$^+$].

N-**Dodecyl-1,3,6-tri(pyren-1-yl)carbazole (CP3)** yellowish solid, 69%; mp 172–174 °C; ^{1}H NMR (300 MHz, $CDCl_3$, δ): 0.40–0.50 (3H, m), 0.62–1.34 (20H, m), 2.50–2.66 (2H, m), 7.52 (1H, d, J = 8.4 Hz), 7.77–7.85 (2H, m), 7.95–8.10 (12H, m), 8.15–8.28 (11H, m), 8.35 (3H, t, J = 9.3 Hz), 8.53 (2H, d, J = 9.0 Hz), 8.59 (1H, s); ^{13}C NMR (75 MHz, $CDCl_3$, δ): 14.16, 22.73, 26.53, 26.93, 28.80, 29.22, 29.35, 29.50, 29.57, 31.97, 44.85, 109.17, 121.89, 122.39, 123.29, 124.04, 124.29, 124.36, 124.67, 124.81, 124.94, 125.03, 125.13, 125.29, 125.43, 125.63, 125.71, 125.90, 125.94, 126.24, 127.18, 127.34, 127.47, 127.77, 128.08, 128.23, 128.32, 128.83, 128.95, 130.23, 130.41, 131.07, 131.54, 131.88, 132.46, 134.98, 138.14, 138.37, 138.61, 141.04; HRMS-ESI calcd for $C_{72}H_{53}N$: *m/z* 935.4191; found: *m/z* 936.2080 [MH$^+$].

N-**Dodecyl-1,3,6,8-tetra(pyren-1-yl)carbazole (CP4)** yellowish solid, 63%; mp 182–184 °C; ^{1}H NMR (300 MHz, $CDCl_3$, δ): 0.24 (3H, m), 0.10–1.32 (20H, m), 2.66–2.79 (2H, m), 7.82 (2H, s), 7.91–8.20 (12H, m), 8.26 (4H, s), 8.56 (2H, d, J = 9.3 Hz), 8.72 (2H, s); ^{13}C NMR (75 MHz, $CDCl_3$, δ): 28.08, 28.25, 28.73, 28.82, 28.87, 28.95, 29.29, 29.36, 29.43, 29.52, 29.82, 30.05, 31.95, 45.48, 45.80, 121.70, 124.21, 124.24, 124.52, 124.61, 124.69, 124.72, 124.96, 125.03, 125.16, 125.28, 125.37, 125.55, 125.63, 125.93, 125.99, 126.10, 127.22, 127.28, 127.52, 127.77, 127.85, 128.01, 128.31, 128.85, 129.91, 129.94, 130.39, 130.80, 130.83, 130.90, 131.00, 131.07, 131.33, 131.43, 131.55, 132.43, 132.61, 133.12, 133.17, 134.97, 135.03, 138.07, 138.10, 139.47, 139.54; HRMS-ESI calcd for $C_{92}H_{61}N$: *m/z* 1135.5117; found: *m/z* 1136.5524 [MH$^+$].

Quantum calculation

The ground state geometries of all molecules were fully optimized using density functional theory (DFT) at the B3LYP/6-31G(d,p) level, as implemented in Gaussian 03.[32] TDDFT/B3LYP calculations of lowest excitation energies were performed at the optimized geometries of the ground states.

Device fabrication and testing

Blue OLED devices using CPn as EML with the device configurations of ITO/PEDOT:PSS/CPn(spin-coating)/BCP (40 nm)/LiF (0.5 nm)/Al (150 nm) and ITO/PEDOT:PSS/TPD (30 nm)/CPn(evaporating)/BCP (40 nm)/LiF (0.5 nm)/Al (150 nm) were fabricated and characterized as follows. The patterned indium tin oxide (ITO) glass substrate with a sheet resistance of 14 ohm sq^{-1} (purchased from Kintec Company) was cleaned and dried at 60 °C in a vacuum oven. A 50 nm thick PEDOT:PSS layer was spin-coated on top of ITO from a 0.75 wt% dispersion in water at a spin speed of 3000 rpm for 20 s and dried at 200 °C for 15 min under vacuum. A 30 nm thick TPD layer was deposited by evaporation from resistively heated alumina crucibles at an evaporation rate of 0.5–1.0 nm s^{-1} in vacuum evaporator deposition (ES280, ANS Technology) under a base pressure of ~10–5 mbar. The film thickness was monitored and recorded by a quartz oscillator thickness meter (TM-350, MAXTEK). Thin films of CPn were deposited on top of the PEDOT:PSS layer by either spin-coating a $CHCl_3$: toluene solution (1 : 1) of CPn (1.5% w/v) at a spin speed of 3000 rpm for 30 seconds to get a 30–40 nm thick film or evaporating from resistively heated alumina crucibles at an evaporation rate of 0.5–1.0 nm s^{-1} under a base pressure of ~10–5 mbar. The film thickness was measured by using a Tencor Alpha Step 500 surface profiler. A 40 nm thick layer of BCP was then deposited on the organic EML without breaking the vacuum chamber. The chamber was vented with dry-air to load the cathode materials and pumped back; a 0.5 nm thick LiF and a 150 nm thick aluminium layers were then subsequently deposited through a shadow mask on the top of the EML/HTL film without braking the vacuum to form active diode areas of 4 mm^2. The measurement of device efficiency was performed according to M. E. Thomson's protocol and the device external quantum efficiencies were calculated using the procedure reported previously.[33] Current density–voltage–luminescence (*J*–*V*–*L*) characteristics were measured simultaneously by the use of a Keithley 2400 source meter and a Newport 1835C power meter equipped with a Newport 818-UV/CM calibrated silicon photodiode. The EL spectra were acquired by an Ocean Optics USB4000 multichannel spectrometer. All the measurements were performed under ambient atmosphere at room temperature.

Results and discussion

Synthesis

Scheme 1 outlines the synthesis of the pyrene functionalized carbazoles (CPn). We began with the synthesis of 3,6-dibromo-*N*-dodecylcarbazole (2), 1,3,6-tribromo-*N*-dodecyl carbazole (3) and 1,3,6,8-tetrabromo-*N*-dodecylcarbazole (4) by bromination of *N*-dodecylcarbazole (1) with NBS (2.1–15.0 equiv.) in THF.[34] Subsequently coupling of the bromo 2–4 with 1-(pyrene)boronic acid (2.2–5.5 equiv.) catalyzed by $Pd(PPh_3)_4/Na_2CO_3$ (aq.) in THF at reflux afforded *N*-dodecyl-3,6-di(pyren-1-yl)carbazole (CP2), *N*-dodecyl-1,3,6-tri(pyren-1-yl)carbazole (CP3) and *N*-dodecyl-1,3,6,8-tetra(pyren-1-yl)carbazole (CP4) as yellowish solids in good yields (61–88%).

The structures of all molecules were characterized unambiguously with ^{1}H NMR and ^{13}C NMR spectroscopy as well as high resolution mass spectrometry. Noticeably, the ^{1}H NMR spectra of CPn show the chemical shifts of the dodecyl protons being shifted to low frequency as the number of the pyrene substituents on a carbazole increased. This is due to a shielding effect resulting from a ring current produced by the surrounding 1- and 8-pyrene substituents. For example, the chemical shift of $-NCH_2-$ protons of CP2 (4.30 ppm) shifts to 3.50 and 2.75 ppm in CP3 and CP4, respectively. These materials show high solubility in most organic solvents allowing their thin films to be fabricated by spin coating process. The morphology of their spin coated films, which is another key factor for OLEDs fabrication, was investigated by atomic force microscopy (AFM). All thin films spin-coated from $CHCl_3$: toluene solution have a fairly smooth and pinhole-free surface indicating good film-forming property, allowing OLED devices to be fabricated by low cost solution processes (Fig. 1 and S1, ESI†).

Quantum calculation and physical properties

To gain insights into the geometrical and electronic properties of these multiple substituted carbazoles, quantum chemistry calculations were performed using the TDDFT/B3LYP/6-31G(d,p) method.[35] The optimized structures of CPn reveal that the attached pyrene units twist out of the plane of the carbazole forming bulky substituents around the carbazole, especially in CP4 (Fig. 2 and S2, ESI†). This would facilitate the formation of amorphous materials. In all cases, π-electrons in the HOMO orbitals delocalize only over the carbazole and two pyrene substituents at the 3,6-positions (3,6-bis(pyren-1-yl)carbazole backbone), and no electrons at pyrene moieties at the 1,8-positions. In the LUMO orbitals, the excited electrons are delocalized largely over the pyrene plane. This suggests that substitution of a carbazole at the 1- or/and 8-positions with pyrene has no or little if any effect on the HOMO of these molecules. The HOMO–LUMO energy gaps (E_g cal.) of CPn were calculated and the values (3.09–3.15 eV) match well with those estimated from the absorption onset (3.07–3.12 eV) (Table 1).

The optical properties of CPn were investigated in CH_2Cl_2 solution and thin film coated on quartz substrates. The results are presented Fig. 3 and summarized in Table 1. Their UV-Vis spectra show two absorption bands, which are assigned in terms of the absorption band at 279 nm corresponding to the π–π* local electron transition of the carbazole ring, and the absorption band at longer wavelengths (347 nm) attributed to the π–π* electron transition of the 3,6-bis(pyren-1-yl)carbazole backbone. These compounds in solution fluoresce in the blue region (430–439 nm) with featureless photoluminescence (PL) spectra. The spectra are slightly red shifted as the number of